Aus der Medizinischen Klinik und Poliklinik III

Klinikum Großhadern / Ludwig-Maximilians-Universität München

Vorstand: Prof. Dr. med. Wolfgang Hiddemann

Studie über das leukämogene Potential der Hoxb4-ΔProlin Mutante in einem murinen Knochenmarkstransplantationsmodell und den Effekt der Hemmung von Histondeacetylasen *in vitro* und *in vivo*

Dissertation
zum Erwerb des Doktorgrades der Medizin
an der Medizinischen Fakultät der
Ludwig-Maximilians-Universität in München

vorgelegt von

Monica Cusan

aus

Portogruaro, Italien

Jahr

2012

Mit Genehmigung der Medizinischen Fakultät
der Universität München

Berichterstatter:	Prof. Dr. med. Christian Buske
Mitberichterstatter:	Priv. Doz. Dr. Irmela Jeremias Priv. Doz. Dr. Michael Albert Prof. Dr. Christian P. Sommerhoff Prof. Dr. Stefan Endres
Dekan:	Prof. Dr. med. Dr. h.c. M. Reiser, FACR, FRCR

Tag der mündlichen Prüfung: 04.10.2012

From the Department of Medicine III

University Hospital Großhadern, Ludwig-Maximilians-University Munich

Director: Prof. Dr. med. Wolfgang Hiddemann

Investigation of the leukemogenic potential of the Hoxb4-ΔProline mutant in a murine bone marrow transplantation model and the effect of the histonedeacetylase inhibition *in vitro* and *in vivo*

Thesis Submitted for a Doctoral Degree in Human Medicine
at the Faculty of Medicine,
Ludwig-Maximilians-University in Munich

submitted by

Monica Cusan

from

Portogruaro, Italy

Year

2012

With permission from the Faculty of Medicine
University of Munich

Supervisor/Examiner:	Prof. Dr. med. Christian Buske
Co-Examiner:	Priv. Doz. Dr. Irmela Jeremias Priv. Doz. Dr. Michael Albert Prof. Dr. Christian P. Sommerhoff Prof. Dr. Stefan Endres
Dean:	Prof. Dr. med. Dr. hc. M. Reiser, FACR, FRCR

Date of Oral Exam: 04.10.2012

Introduction

1.1 Hematopoiesis

1.1.1 The hematopoiesis

The term hematopoiesis indicates the controlled production of the blood cells. The blood cells, leukocytes, erythrocytes and platelets, are continuously produced and released from the bone marrow on a daily base to replace altered cells and to enrich the pool of necessary cells in response to increased demand, like in case of injury, bleeding or disease. The control of the blood cells production undergoes homeostatic mechanisms, which are modifying their turnover and re-establishing the steady state after the stress situation is resolved. The first site of primitive hematopoiesis is the yolk sac in the first few weeks of gestation. In this first time of blood cell production putative hemangioblasts, which correspond to the common mesodermal precursors of endothelial and hematopoietic lineages, give rise to a temporary embryonic hematopoietic system. During the gestational development these precursors are believed to migrate to the fetal liver, and from this to the spleen and bone marrow (Weissman 2000, Morrison 1995a). This migration is due to molecular changes as well as to modifications of cell surface adhesion molecules (Hirsch 1996). From 6 weeks until 6-7 months of fetal life liver and spleen are the major hematopoietic organs, which continue to produce blood cells until about 2 weeks after birth. The bone marrow becomes the major hematopoietic organ from 6 to 7 months of fetal life. The adult multilineage blood system is maintained by pluripotent hematopoietic stem cells (HSC), which have the capacity to self-renew, to differentiate hierarchically giving rise to all the different mature progeny cells of the blood, and can long-term repopulate myeloablated recipients. By performing *in vitro* clonogenic and *in vivo* transplantation assays at least five classes of partially independent hematopoietic cells in the murine embryo/fetus have been defined: the primitive present in the yolk sac, the pro-definitive (myeloid progenitors), the meso-definitive (lymphoid-myeloid progenitors), the meta-definitive (neonatal repopulating HSCs and CFU-S) (these tree classes located in the para-aortic splanchnopleura), and adult-definitive (adult definitive repopulating HSCs), which appear in the aorta-gonad mesonephros (AGM) region, in the liver, thymus, spleen and bone marrow (Dzierzak 2003, Dzierzak 2008).

Based on many reports the human embryonic development seems to significantly parallel the mouse development (Fig 1.1.1). Adult HSCs can divide asymmetrically into one daughter HSC and a committed progenitor, and the fate determination depends on a number of essential hematopoietic transcription factors. For example, PU.1 drives the cell into myeloid lineage, while GATA-1 induces erythropoietic and megakaryocytic differentiation. Moreover, the lineage differentiation can also be influenced by several exogenous factors, like the growth factors IL-3, SCF, IL-6 and G-CSF.

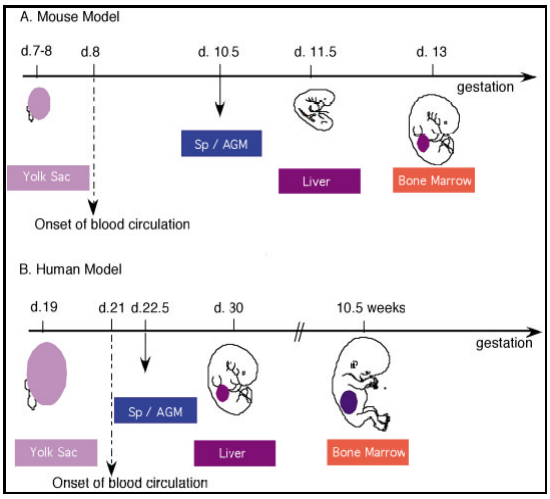

Fig 1.1.1. Development of the hematopoietic system (Bonnet 2003).

1.1.2 The hematopoietic hierarchy

The cells of mature hematopoietic progeny derive from a limited number of committed hematopoietic progenitors, which arise from even more rare hematopoietic stem cells (HSCs) (Weissman 2000). The self-renewing HSCs are termed long-term repopulating HSCs (LT-HCSs) for their ability to confer long-term engraftment on lethally irradiated recipients, and they generate the short-term repopulating HSCs (ST-HSCs) with limited self-renewal and increased proliferation capacity. ST-HSCs subsequently give rise to multipotent progenitors (MPPs) that generate committed progenitors of different lineages: the common myeloid progenitor (CMP) for the myeloid-erythroid lineage, and the common lymphoid progenitor (CLP) for the lymphoid lineage. The CMP in turn gives rise to the granulocyte-macrophage progenitors (GMPs) and the megakaryocyte-erythrocyte progenitors (MEPs) that are restricted to churning out mature granulocytes, macrophages or mast cells and megakaryocytes or erythrocytes, respectively. The CLPs generate all mature lymphoid cell types including B and T

lineage cells, dendritic and NK cells. Dendritic cells can be generated from both CLPs as well as CMPs. Thus the hematopoietic hierarchy is composed of the stem cells, the committed progenitors and their progeny, the mature blood cells of all lineages. The first level where we can observe a profound homeostatic control of the high turnover rate of the hematopoietic system is within the HSCs compartment. Moreover, a significant homeostatic control is also necessary at the level of more committed multipotent, oligopotent, and lineage-restricted progenitor cells, if one considers the even larger proliferative and developmental capacity of these progenitors (Bryder 2006) (Fig. 1.1.2).

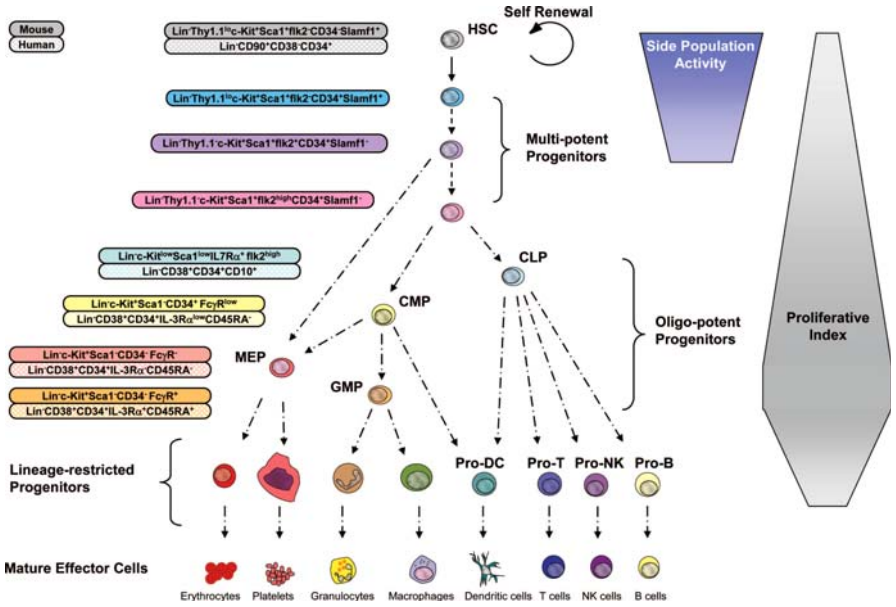

Fig. 1.1.2. A representative scheme of the hematopoietic developmental hierarchy. The cell surface markers of many of these cells types are known for the murine and human system. However, many markers have been described only for few mouse strains, while the absolute lineage potential and developmental relationship of some of the subsets indicated have not been yet completely characterized. The differentiation of HSCs into multipotent, oligopotent, and lineage-specific progenitors is generally associated with increased proliferative index, although this characteristic is not absolute and has not been resolved for all stages of development. The side population activity represents the capacity of efflux dyes, and it is restricted to HSCs and their immediate downstream multipotent progenitors. Of note is that the different multipotent progenitor subsets in human system have not been functionally resolved to a significant degree like for the murine hematopoiesis (Bryder 2006).

1.1.3 Stem cells and hematopoietic stem cells

Stem cells can be classified into two main categories, embryonic and adult stem cells. Stem cells are clonogenic cells capable of both self-renewal and multilineage differentiation. Some adult tissues like blood, skin, gut etc. need a constant turnover of cells for tissue renewal. Tissue stem cells, which are adult stem cells, respond to this need as they consist of multipotent progenitors. After

the observation that cellular recovery can be achieved following lethal irradiation by transplanting bone marrow, it was defined that the ability of such transplants to reconstitute hematopoiesis can be attribute to a few extremely rare stem cells found predominantly in the bone marrow but capable of mobilization into peripheral tissues via the blood vascular system. Since then, HSCs have been the best characterized stem cells at the phenotypic and functional level, and the hematopoietic system has been the proving ground for most of the experimental procedures and conceptual paradigms for the stem cells biology in general. HSCs and indeed most stem cells can be defined by certain unique properties, sometimes referred as “stemness”, the most prominent of which are self-renewal, multipotency, and quiescence. During their lifespan, humans produce approximately 10^{16} blood cells of different types. The hallmark properties of the HSCs were defined in 1963 by Till and McCulloch. In a mouse model they have identified a population of clonogenic BM cells able to generate myeloid-erythroid colonies in the spleen of lethally irradiated hosts. These clonogenic cells in some cases gave rise to cells that also could be transferred to secondary hosts and there reconstitute all blood lineages (Till & McCulloch 1961; Siminovich 1963). With the development of clonal assays for all major hematopoietic cell lineages, cell sorted-based separation of monoclonal antibody- or dye-stained BM subsets led to the isolation of candidate stem cell populations (Osawa 1996). *In vivo* limiting dilution analysis of these cells allowed the characterization of at least 2 classes of multipotent cells, long-term (LT-HSC) and short-term repopulating hematopoietic stem cells (ST-HSC), the last ones able to self-renew for a definite interval (≈8 weeks in mice) (Passagué 2003, Morrison 1995). Stem cells have the ability to self-renew, and are able to persist in recipients for long period of time after transplantation, continuously replenishing the blood with mature differentiated cells or remaining quiescent. The competitive repopulating units (CRUs) represent a functionally defined class of very primitive HSCs with the potential of long-term reconstitution of all hematopoietic lineages in recipient animals. The CRU-assay allows not only the quantification of these primitive HSCs, but also allows establishing a competitive pressure on the HSCs originating from the compromised irradiated host, from the transduced HSCs and the cotransplanted competitor HSCs (Szilvassy 1990, Miller 1997).

Self-renewal. Self-renewal is the property of a stem cell to generate progeny with exact stem cell properties of the parental cell. A stem cell can divide symmetrically to give rise to two daughter stem cells, each possessing stem cells properties, or alternatively, asymmetrically, wherein one daughter cell is a stem cell and the other is a rapidly cycling downstream progenitor with a reduced capacity of self-renewal (Warner 2004). The downstream progenitor of an HSC displays a partially increased proliferation capability and it leads to clonal expansion and production of numerous committed progenitors and more differentiated hematopoietic cells. The short-term repopulating stem cell gives rise to the non-self-renewing oligolineage progenitors which in turn give rise to progeny that are more restricted in their differentiation potential, and finally to functionally mature cells. In a steady state bone marrow HSCs divide rarely but mostly asymmetrically to retain their original pool numbers as well as to produce the entire complement of cells necessary for normal hematopoiesis, which is the result of a sophisticated equilibrium between self-renewal and differentiation. The mechanisms regulating the fate decision are poorly understood. However, many gene families have been associated to this process, like the Hox genes family (Antonchuk 2001, Buske 2002), the Wnt family (Reya 2003), and the Polycomb group (Lessard 2003). Other factors have been reported to play a role in the maintenance of quiescence as well as in the activation of HSCs, like Notch (Karanu 2000) and Hedgehog (Bhardwaj 2001), in particular in relation to the function of the stem cell niche in the bones.

Multipotency. The adult stem cells are multipotent, i.e. are able to give rise to all the cells of a given tissue, while the embryonic stem cells are able to give rise to all the cells of every tissue of an organism, which is called totipotency. The HSCs are multipotent cells capable to long-term repopulate both the lymphoid and myeloid hematopoietic compartments via differentiation into committed progenitors, which can proliferate extensively but have increasingly limited differentiation potential (Orlic 1994). In leukemias the HSCs undergo a loss of multipotency in form of block of differentiation and/or dysregulation of certain lineage specific transcription factors.

Plasticity and heterogeneity. In the recent years many efforts have been done in order to investigate the possibility that adult mammalian stem cells may differentiate across tissue lineage borders, which could represent an

extraordinary tool to establish new therapeutic issues as tissue regeneration. The first studies using BM cells or HSCs to regenerate other tissues have been controversial (Goodell 2003, Raff 2003). The more promising results were obtained in an effort to define the capacity of enriched BM populations to restore myocardial function in infarct models (Orlic 2001). In a number of reports BM cells have been described to repopulate renal, neuronal, cardiac and liver tissues in response to certain injuries, but the significance of these results still remains to be clarified. Interestingly, some authors have suggested that tissue-committed stem cells (TCSCs), which express mRNA/protein for different markers, could be normally present in the adult BM compartment (Kucia 2005).

An opposite concept that has been developed is the heterogeneity of HSCs. Although a relatively simple surface phenotype may be ascribed to HSCs (for example, $Thy1.1^{+}Lin^{-}Sca^{+}ckit^{+}$) (Morrison 1994) and is of enormous value in their prospective enrichment, it is also evident that even highly purified HSC populations are heterogeneous, either with respect to other surface markers or functions (Weissman 2000b, Morrison 1995b). Whereas a model invoking stem cell heterogeneity may account for the majority of recent findings, reprogramming of HSCs, albeit at a low rate, may best explain the contribution of purified HSCs to liver, as shown by the experiments of Lagasse et al (Lagasse 2000), where purified HSCs seemed to differentiate into hepatocytes *in vivo* (Orkin 2002).

Quiescence. Quiescence or the relatively slow cycling of HSCs, in contrast to the rapidly proliferation of the downstream progenitors, is necessary to protect the stem cell compartment from toxic and oxidative stress and to prevent consumption of the regenerative cell pool, an occurrence known as stem cell exhaustion (Cheng 2000). Bonnet et al have calculated the frequency of HSCs to be 1 in 10,000 to 100,000 cells in peripheral blood. The HSCs occupy in relatively larger number well defined “stem cell niches” in adult BM where they are normally in an inactive state (Bonnet 2002). It was demonstrated by 5-bromo-2´-deoxy-uridine (BrdU) incorporation studies (for the measurement of cell proliferation) in mice, that approximately 75% of long-term repopulating HSCs were in the G_0 phase/quiescence at any given time in steady state BM (Cheshier 1999). LT-HSCs divide very rarely and give rise to the more proliferative ST-HSCs which in turn give origin to the non-self-renewing lineage committed progenitors. HSCs can however proliferate rapidly symmetrically in response to myelosuppressive

chemotherapy or irradiation prior BM transplantation to give rise to committed progenitors as well as copies of more HSCs, which then return to the quiescent state (Dixon 1981). The control of the quiescent state is especially crucial in conditions of stress, such as myelotoxic injury, to prevent hematopoietic death. There is little information about the molecular events that promote this process, though the BM microenvironment or the “stem cell niche” is believed to play an important role generating signals that regulate the self-renewal and the differentiation of normal stem cells (Lemischka 1997).

1.2 Leukemia

1.2.1 Acute leukemia

The leukemias are a group of diseases in which the common manifestation is a malignant, unregulated proliferation of cells originating from the bone marrow. Leukemia may involve any of the blood-forming cells or their precursors and may be found throughout the body, including brain, liver, spleen, and lymph nodes. Although each type of leukemia progresses differently, the unregulated proliferating cells (1) usually displace normal BM cells, (2) can interfere with normal marrow function, (3) may colonize other organs, and (4) eventually lead to death if not treated. Based on the progress, leukemias are distinguished into chronic (first described in 1845 by Bennet and Virchow, Bennet 1845, Virchow 1846) and acute leukemias, which were described 25 years later when patients with “white blood” were observed to die rapidly after a short debilitating illness (Friedrich 1857, Ebstein 1889). Acute and chronic leukemias can be distinguished based on their presenting signs and symptoms, and the cell type involved. Acute leukemias are characterized by rapid onset of clinical signs (e.g., infection, haemorrhage, and pallor) and symptoms (e.g., fatigue, weakness, bone and joint pain), by the detection of normocytic anemia, neutropenia and/or thrombocytopenia, and death occurs within months if treatment is not initiated. In 1976 the FAB (French-American-British) classification of leukemias was introduced, which was based on the number of blasts (immature cells of myeloid or lymphoid origin) of at least 30% of all nucleated bone marrow cells, and on the morphology of these cells. The proposed World Health Organization classification has modified the percentage of blasts to 20% in either peripheral blood or bone marrow (Brunning 1999). The diagnosis of acute myeloid leukemia can be based

also on the presence of less than 20% of blasts in the bone marrow, if typical chromosomal aberrations are detected. Overall, peripheral blood white cell counts can be increased, decreased, or within reference range, although they are typically increased. The use of light microscopy is the initial step in the diagnosis of acute leukemias, which are classified cytomorphologically into acute myeloid (AML) and acute lymphoblastic leukemia (ALL) on the basis of the blasts' morphologic similarity to myeloblasts or lymphoblasts. For example, Auer rods (spindle-shaped pink-red inclusions composed of azurophilic granule derivatives) may be seen in the cytoplasm of any subtype of human AML. The old FAB classification system used a combination of Romanowsky-based stains and cytochemical reactions, including staining for myeloperoxidase, chloracetate esterase, non-specific esterase, and stains with Sudan black B, periodic acid Shiff and TdT. In 2008 the World Health Organization has published the 4th revision of the classification of tumors of hematopoietic and lymphoid tissues (Figure 1.2.1). The guidelines presented there include the analysis of PB and BM specimens, the assessment of blasts and blast lineage by morphological, immunophenotypical and cytochemical analyses, as well as the evaluation of genetic features, like the karyotype (for the detection of chromosomal alterations), and point mutations (like NPM1, CEBPA, FLT3, and RUNX1), which have been demonstrated to be significantly associated with different prognosis. Chromosomal alterations have been seen consistently in leukemic cells. Using standardized banding high-resolution techniques, almost all leukemic cells will present a clonal cytogenetic abnormality of one type or another. These abnormalities can be of number (ploidy) or of structure (translocations, deletions, and rearrangements). The follow up of these molecular markers in patients showing morphological remission enable to detect groups of patient at high risk of relapse. The persistence of these markers is defined as minimal residual disease (MRD).

Myeloproliferative neoplasms (MPN)	**Myeloid and lymphoid neoplasm associated with eosinophilia and abnormalities of PDGFRA, PDGFRB, or FGFR1**
• Chronic myelogenous leukemia, BCR-ABL1 positive • Polycythemia vera • Essential thrombocythemia • Chronic eosinophilic leukemia, n.o.s. • Chronic neutrophilic leukemia • Primary myelofibrosis • Mastocytosis • Myeloproliferative neoplasm, unclassifiable	• Myeloid and lymphoid neoplasms associated with PDGFRA rearrangement • Myeloid neoplasms associated with PDGFRB rearrangement • Myeloid and lymphoid neoplasms associated with FGFR1 abnormalities
Myelodysplastic/myeloproliferative neoplasms (MDS/MPN)	**Myelodysplastic syndromes (MDS)**

• Chronic myelocytic leukemia • Atypical chronic myeloid leukemia, BCR-ABL1 negative • Juvenile myelomonocytic leukemia • Myelodysplastic/myeloproliferative neoplasms, unclassifiable *Provisional entity: refractory anemia with ringsideroblasts and thrombocytosis*	• Refractory cytopenia with unilineage dysplasia - Refractory anemia - Refractory neutropenia - Refractory thrombocytopenia • Refractory anemia with ring sideroblasts • Refractory cytopenia with multilineage dysplasia • Refractory anemia with excess blasts • Myelodysplastic syndrome with isolated del(5q) • Myelodysplastic syndrome, unclassifiable • Childhood myelodysplastic syndrome *Provisional entity: refractory cytopenia of childhood*
Acute myeloid leukemia and related neoplasms	**Acute leukemia of ambiguous lineage**
• Acute myeloid leukemia with recurrent genetic abnormalities - AML with t(8;21)(q22;q22); *RUNX1-RUNX1T1* - AML with inv(16)(p13.1q22) or t(16;16)(p13.1;q22); *CBFB-MYH11* - APL with t(15;17)(q22;q12); *PML-RARA* - AML with t(9;11)(p22;q23); *MLLT3-MLL* - AML with t(6;9)(p23;q24); *DEK-NUP214* - AML with inv(3)(q21;q26.2) or t(3;3)(q21;q26.2); *RPN1-EVI1* - AML (megakaryoblastic) with t(1;22)(p13;q13); *RBM15-MKL1* *Provisional entity: AML with mutated NPM1* *Provisional entity: AML with mutated CEBPA* • Acute myeloid leukemia with myelodysplasia-related changes • Therapy-related myeloid neoplasms • Acute myeloid leukemia, n.o.s. - AML with minimal differentiation - AML without maturation - AML with maturation - Acute myelomonocytic leukemia - Acute monoblastic/monocytic leukemia - Acute erythroid leukemia Pure erythroid leukemia Erythroleukemia, erythroid/myeloid - Acute megakaryoblastic leukemia - Acute basophilic leukemia - Acute panmyelosis with myelofibrosis • Myeloid sarcoma • Myeloid proliferations related to Down syndrome - Transient abnormal myelopoiesis - Myeloid leukemia associated with Down syndrome • Blastic plasmacytoid dendritic cell neoplasm	• Acute undifferentiated leukemia • Mixed phenotype acute leukemia with t(9;22)(q34;q11.2); *BCR-ABL1* • Mixed phenotype acute leukemia with t(v;11q23); *MLL* rearranged • Mixed phenotype acute leukemia, B-myeloid, n.o.s. • Mixed phenotype acute leukemia, T-myeloid, n.o.s. *Provisional entity: natural killer (NK) cell lymphoblastic leukemia/lymphoma*
	Precursors lymphoid neoplasms
	B lymphoblastic leukemia/lymphoma • B lymphoblastic leukemia/lymphoma, n.o.s. • B lymphoblastic leukemia/lymphoma with recurrent genetic abnormalities - B lymphoblastic leukemia/lymphoma with t(9;22)(q32;q11.2); *BCR-ABL1* - B lymphoblastic leukemia/lymphoma with t(v;11q23); MLL rearranged - B lymphoblastic leukemia/lymphoma with t(12;21)(p13;q22); *TEL-AML1 (ETV6-RUNX1)* - B lymphoblastic leukemia/lymphoma with hyperdiploidy - B lymphoblastic leukemia/lymphoma with hypodiploidy - B lymphoblastic leukemia/lymphoma with t(5;14)(q31;q32); *IL3-IGH* - B lymphoblastic leukemia/lymphoma with t(1;19)(q23;p13.3); *TCF3-PBX1* **T lymphoblastic leukemia/lymphoma**
Mature B-cell neoplasms	**Mature T-cell and NK-cell neoplasms**
• Chronic lymphocytic leuekemia/small lymphocytic lymphoma • B-cell prolymphocytic leukemia • Splenic B-cell marginal zone lymphoma • Hairy cell leukemia - Splenic B-cell lymphoma/leukemia, unclassifiable - Splenic diffuse red pulp small B-cell lymphoma - Hairy cell leukemia variant • Lymphoplasmacytic lymphoma - Waldenström macroglobulinemia • Heavy chain diseases - Alpha heavy chain disease - Gamma heavy chain disease - Mu heavy chain disease • Plasma cell lymphoma • Solitary plasmocytoma of bone • Extraosseous plasmocytoma • Extranodal marginal zone lymphoma of mucosa-associated lymphoid tissue (MALT lymphoma) • Nodal marginal zone lymphoma • *Paedriatic nodal marginal zone lymphoma* • Follicular lymphoma • *Paedriatic follicular lymphoma* • Primary cutaneous follicle centre lymphoma • Mantle cell lymphoma • Diffuse large cell lymphoma (DLBCL), n.o.s. - T-cell/hystiocyte rich large B-cell lymphoma - Primary DLBCL of the CNS - Primary cutaneous DLBCL, leg-type - *EBV positive DLBCL of the elderly*	• T-cell prolymphocytic leukemia • T-cell large granular lymphocytic leukemia • *Chronic lymphoproliferative disorder of Nk-cells* • Aggressive NK-cell leukemia • Systemic EBV positive T-cell lymphoproliferative disease of childhood • Hydroa vacciniforme-like lymphoma • Adult T-cell leukemia/lymphoma • Extranodal NK/T-cell lymphoma, nasal type • Enteropathy-associated T-cell lymphoma • Hepatosplenic T-cell lymphoma • Subcutaneous panniculitis-likeT-cell lymphoma • Mycosis fungoides • Sézary syndrome
	Primary cutaneous T-cell disorders
	• Primary cutaneous CD30 positive T-cell lymphoproliferative dosirders - Lymphomatoid papulomatosis - Primary cutaneous anaplastic large cell lymphoma • Primary cutaneous gamma-delta T-cell lymphoma • *Primary cutaneous CD8 positve aggressive epidermotropic cytotoxic T-cell lymphoma* • *Primary cutaneous CD4 positive small/medium T-cell lymphoma*
	Peripheral T-cell lymphoma, n.o.s. **Angioimmunoblastic T-cell lymphoma** **Anaplastic large cell lymphoma, ALK positive**

• DLBCL associated with chronic inflammation • Lymphomatoid granulomatosis • Primary mediastinal (thymic) large B-cell lymphoma • Intravascular large B-cell lymphoma • ALK positive large B-cell lymphoma • Plasmablastic lymphoma • Large B-cell lymphoma arising in HHV8-associated multicentric Castleman disease • Primary effusion lymphoma • Burkitt lymphoma • B-cell lymphoma, unclassifiable, with features intermediate between DLBCL and Burkitt lymphoma • B-cell lymphoma, unclassifiable, with features intermediate between DLBCL and classical Hodgkin lymphoma	***Anaplastic large cell lymphoma, ALK negative***
Post-transplantation lymphoproliferative disorders (PTLD)	**Hodgkin lymphoma**
• Early lesions - Plasmacytic hyperplasia - Infectious mononucleosis-like PTLD • Polymorphic PTLD • Monomorphic PTLD (B- and T/NK-cell types) • Classical Hodgkin lymphoma type PTLD	• Nodular lymphocyte predominant Hodgkin lymphoma • classical Hodgkin lymphoma - Nodular sclerosis classical Hodgkin lymphoma - Mixed cellularity classical Hodgkin lymphoma - Lymphocyte-depleted classical Hodgkin lymphoma
	Histiocytic and dendritic cell neoplasms
	• Histiocytic sarcoma • Langerhnas cell histiocytosis • Langerhans cell sarcoma • Interdigitating dendritic cell sarcoma • Follicular dendritic cell sarcoma • Fibroblastic reticular cell tumor • Indeterminate dendritic cell tumor • Disseminated juvenile xanthogranuloma

Fig 1.2.1. WHO classification of hematopoietic and lymphoid neoplasms (Vardiman 2009, Vardiman 2010). n.o.s.: not otherwise specified.

1.2.2 Leukemic stem cells

The cells within a certain cancer are heterogeneous and a growing amount of evidences suggest that cancers originate from a rare population of cancer stem cells (CSCs) with unlimited proliferation potential, which induce the generation and growth of a tumor (Bonnet 1997, Reya 2001). This can explain the treatment failure of therapies currently in use, which are cytotoxic to the tumor bulk, but are not able to exhaust the cancer stem cells. The blood-related cancer leukemias were the first diseases for which human cancer stem cells, or leukemic stem cells (LSCs), were isolated through the ground breaking work of Bonnet and Dick (Bonnet 1997, Dick 2003). Most of the therapies currently used for acute leukemias have been designed to target the high proliferating malignant blasts. However, one hallmark of the human LSCs studied so far is the quiescence, which is protecting them from the toxicity of the common chemotherapeutic agents (Holyoake 1999). Nowadays, the characterization of the LSCs is based on the immunophenotype analysis together with functional assays *in vivo* like the xenotransplantation of primary human AML cells in immunodeficient NOD-SCID mice. It has been shown that the LSCs reside in the $CD34^+CD38^-$ or $CD34^+/CD38^+$ subpopulation, which match with the phenotype of the normal HSCs, but the LSCs differentially express also other markers, like CD123/IL3-Rα or CD33 (Jordan 2000, Taussig 2005). This allowed the design of a promising therapeutic approach with the administration of an IL3/diphteria toxin fusion protein to transplanted animals (Feuring-Buske 2002). This treatment schedule

has been used for a phase I clinical study for patients with chemo-refractory AML. Another intriguing aspect of the LSCs is that they can arise from both self-renewing HSC and non-self-renewing progenitor populations which are supposed to re-aquire HSCs specific features (Goardon 2011). This could allow the development of more effective drugs targeting e.g. common leukemogenic self-renewal pathways displayed by all the different LSCs, which could be used in combination with conventional therapies (e.g. imatinib, chemotherapy) (Passegué 2005).

1.2.3. Molecular pathways leading to leukemia

The carcinogenesis is a multistep process where the cancer cell acquires increasing numbers of somatic mutations leading to disruption of determinant biological pathways. In details, the cancer cells can gain and lose important functions: initially a clonal event causes increased proliferation, while further mutations drive to block of differentiation, leading to malignant transformation. This is characterized by self-sufficiency in growth signals, resistance to antigrowth and apoptotic signals, capacity to change the microenvironment and to induce angiogenesis and metastasis (Hanahan 2000). The genetic alterations lead in most of the cases to the activation of an oncogene and to the inactivation of a tumor suppressor gene. In general many genetic alterations and leukemic-associated fusion genes are perturbing the normal hematopoietic differentiation programs, but in most of the cases further cooperative mutations are necessary to allow a full malignant transformation, as supported by murine transplantation models (Kelly and Gilliland 2002). Additional supports to this hypothesis are coming from the observations that there are inherited gene mutations predisposing to the development of leukemia and that in many sporadic AMLs more than one mutation can be detected. A significant group of genes that are altered in the leukemogenesis are the proto-oncogenes as shown in the Fig. 1.2.3a (Domen 2000, Fröhling 2005). In detail, the genetic mutations observed in acute leukemia can be classified in three groups: (1) activating mutations of genes in the tyrosine kinase-RAS/BRAF or -FLT3 receptor signal transduction pathway (Ozeki 2004), leading to increased cell proliferation and/or survival of leukemic progenitor cells (class I mutations, e.g. BCR-ABL, TEL-PDGFRB and other translocations); (2) inactivating mutations of genes encoding hematopoietic

transcription factors, resulting in disturbed cell differentiation (class II mutations, e.g. RUNX1-ETO, RUNX1-EVI1, TEL-RUNX1, CBFB-SMMHC, RUNX1 point mutation, PML-RARA) (Speck 2002); and (3) inactivating mutations of the tumor suppressor gene p53.

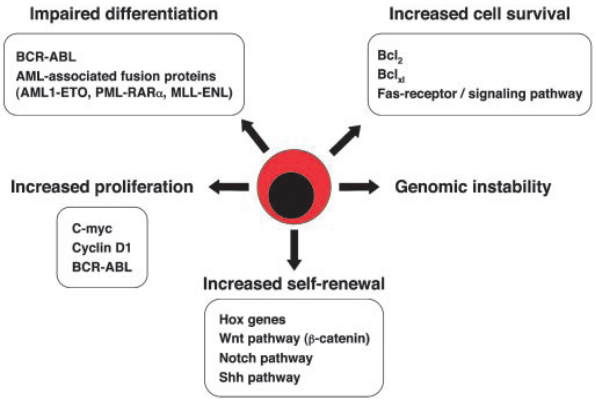

Fig 1.2.3a. Deregulated pathways leading to leukemia (Passegué 2003).

Additionally in the AML with normal karyotype other mutations have been identified in the last few years, which have been shown to correlate differentially with the prognosis, and are therefore often included in the panel of the routine investigations in order to help in taking adequate therapeutic decisions. These mutations include partial tandem duplications (PTD) of the MLL gene, internal tandem duplications (ITD) or tyrosine kinase domain (TKD) mutations of the FLT3 gene, and mutations in the NMP1 (Nucleophosmin1), CEBPA, NRAS and WT1 genes (Fig 1.2.3b). At present many efforts are done in developing molecular therapies which are targeting these aberrantly mutated factors.

Gene	Biological/clinical features	Frequency
NPM1	Protein with pleiotropic functions; associated with FLT3-ITD/TKD mutations	25-35% of AML; 45-62% of CN-AML
FLT3 - ITD - TKD	Class III receptor tyrosine kinase In frame mutation Point mutation	 28-34% of CN-AML 11-14% of CN-AML
CEBPA	Transcription factor mediating lineage specification and differentiation into mature neutrophils	Predominantly in CN-AML
MLL	PTD; rationale for use of DNA methyltransferase/histone deacetylase inhibitors	5-11% of CN-AML
RAS	No prognostic significance	9% of CN-AML
WT1	Wilms tumor gene	10% of CN-AML

Fig 1.2.3b. Gene mutations predominantly occurring in cytogenetically normal AML. CN: cytogenetically normal (American Society of Hematology, 2007).

A number of experiments have shown that the prevention of cell death is one of the crucial events in myeloid leukemogenesis and may even be the first step that

defines a platform for additional mutations (Delia 1992). Mutations leading to the overexpression of the anti-apoptotic proteins like Bcl-2 have been shown to be involved in malignant transformation in follicular lymphoma, lymphoid leukemia as well as in myeloid cells. Many groups are focusing on the research on gain-of-function mutations that promote constitutive self-renewal, such as stabilization of β-catenin. Stabilized β-catenin has been shown to promote the self-renewal of stem cells and other types of progenitor cells (Reya 2001), and activation of β-catenin and deregulation of Wnt signalling pathway is a common phenomenon in cancer (Polakis 2000). Additionally, other factors playing a role in the epigenetic regulation of the DNA have been identified to be relevant in the leukemogenesis. The TET1 protein has been described to catalyse the conversion of cytosine-5 methylation (5mC) to 5hmC, which seems to affect the methylation pattern of DNA. TET1 has been described to be fused to MLL in the t(10;11)(q22;q23), leading to a dysregulated expression of tumor suppressors and oncogenes (Lorsbach 2003). Moreover, TET2 has been reported to be mutated in 12.1% of primary (Abdel-Wahab 2009) and in 34.2% of secondary myeloid malignancies (Delhommeau 2009).

A further classification of AMLs is based on their onset. We can distinguish primary AMLs, which appear to arise *de novo,* and the secondary AMLs, which can develop from myelodysplasia and other hematological diseases, such as myeloproliferative diseases (s-AML) or follow previous treatment with highly mutagenic cytostatic drugs or after irradiation for various types of primary tumors (therapy related, t-AML). Secondary AMLs are more often observed in elderly patients and are associated with a worse prognosis. The myelodysplastic syndromes (MDSs) are very heterogeneous hematopoietic disorders characterized by increasing deficiency of normal bone marrow function, pancytopenias, and tendency to progress to AML. Clonal cytogenetic abnormalities can be identified in approximately 50% of MDS. Also the MDSs can occur *de novo* or as therapy-related. The majority of patients with MDS and AML diagnosed at major centres are *de novo* diseases (80-90%), whereas the therapy-related MDS/AMLs are less frequent (10-20%). The International Prognostic Score System (IPSS) helps to identify MDS patients with higher risk of progression to AML or with bad prognosis, and it is based on the percentage of blasts in the bone marrow, on the grade of cytopenias, and on BM cytogenetic

analysis. The genetic alterations in the *de novo* and the therapy-related cases are often the same in MDS and in AML, although they occur with different frequencies.

1.2.4. Chromosomal translocations in AML

Chromosomal aberrations are a common finding in many cancers and their occurrence correlates with the biology and the progression of the tumor. In the solid cancers the diagnosis is made relatively late in their development, and it is supposed that several chromosomal rearrangements can accumulate after an initial genetic event. In the leukemia the presence of clonal chromosomal aberrations represents at the moment the strongest prognostic factor for prediction of response to therapy and survival, and the cytogenetic analysis of AML samples allows the classification of three risk groups: favourable, intermediate, or adverse. In 80% of AML cases at least one chromosomal rearrangement has been reported (Pandolfi 2001) and over 100 chromosomal translocations have been cloned (Gilliland 2002). Leukemia-associated fusion proteins generally function as aberrantly activated signalling factors or transcriptional regulators that directly perturb the proliferation and differentiation program of hematopoietic cells, as it has been shown from a variety of experimental models. One of the components of each fusion protein is often a transcription factor (AML1, CBFβ, or RARα) whereas the fusion partner has normally a different function, like the control of cell survival and apoptosis as well as structural function in the nucleus like PML. Interestingly, in many AMLs the type of fusion protein often defines the specific stage of maturation arrest in the differentiation cascade (Tenen 2003), and they seems to act through common mechanisms, like the recruitment of aberrant corepressor complexes, alteration of chromatin remodelling, and disruption of specific intracellular compartments (Alcalay 2001). It has been demonstrated that the chimeric fusion protein or the activation of a certain proto-oncogene by a single translocation event can be responsible alone for the transformation (Rabbitts 1991, Rabbitts 1994). The cloning of chimeric genes and the assessment of their oncogenic potential using e.g. mouse bone marrow transplantation models is one of the useful tools to identify new proto-oncogenes and one of the first steps that can be taken to

understand the mechanisms of leukemic transformation. The most common chromosomal abnormalities are reported in Table 1.2.4.

Rearrangement	Frequency	Prognosis
AML1-ETO t(8;21)(q22;q22)	5-12%	Favourable
Inv(16)(p13q22) or t(16;16)(p13;q22) (CBFβ-MYH11)	10-12%	Favourable
PML-RARα t(15;17)(q22;q12) and variants	5-8%	Favourable
Involving MLL 11q23	5-6%	Intermediate
Others, e.g. del(5q), -5, del(7q), -7	5-6%	Unfavourable
Complex karyotype (≥ 3 abnormalities)		Unfavourable

Table 1.2.4. Common chromosomal abnormalities found in AML. AML1 encodes Core-Binding Factor α (CBPα); ETO is Eight-Twenty-One gene; CBFβ: Core-Binding Factor β; MYH11 encodes smooth Muscle mYosin Heavy chain; PML: ProMyelocytic Leukemia gene; RARα: Retinoic Acid Receptor α; APL: acute promyelocytic leukemia; MLL: Mixed Lineage Leukemia gene.

1.3 The homeobox genes

1.3.1. The homeobox genes in hematopoiesis and leukemogenesis

Homeobox genes encode nuclear transcription factors, which regulate the morphogenesis and cellular differentiation during the embryonic development of several animals. In mammals, Hox genes are mainly grouped in the primordial Hox cluster and in the ParaHox cluster, which are supposed to derive from the duplication of a putative ProtoHox cluster of four genes early in evolution (Fig 1.3.1a, Garcia-Fernandez 2005a and 2005b). Moreover, the homeobox genes of vertebrates can be classified in two subgroups: the clustered Hox genes, which are linked on a chromosome, and the non-clustered, or divergent, homeobox genes. The highly conserved homeobox sequence motif (homeobox means binding to the DNA), which encodes the homeodomain, a 60 amino-acid helix-turn-helix DNA-binding domain, is the common element defining these two broad classes of genes. Based on this homology, different Hox genes have been shown to recognize similar regulatory sequences *in vitro*, although the specific sequence they recognize, the affinity of DNA binding, and the transactivating potential depend on the co-factors that are recruited, like Pbx and Meis/Prep. The aminoacidic substitution at position 211 (N→A) has been shown to abolish alone the DNA binding (Beslu 2004). The clustered homeobox genes (class I homeobox genes) are evolutionary highly conserved, and their organization in clusters mirrors the temporal and spatial expression during the development of body structures along the anterior-posterior body axis (Krumlauf 1994). In

mammals, this class of genes comprehends 39 hox genes organized into four genomic clusters (A-D) located on four different chromosomes (*HOXA* on 7p15, *HOXB* on 17q21, *HOXC* on 12q13, *HOXD* on 2q31). Additionally 13 paralogous groups have been identified, which include several Hox genes that belong to different clusters but have similar homeobox sequence (Fig 1.3.1b).

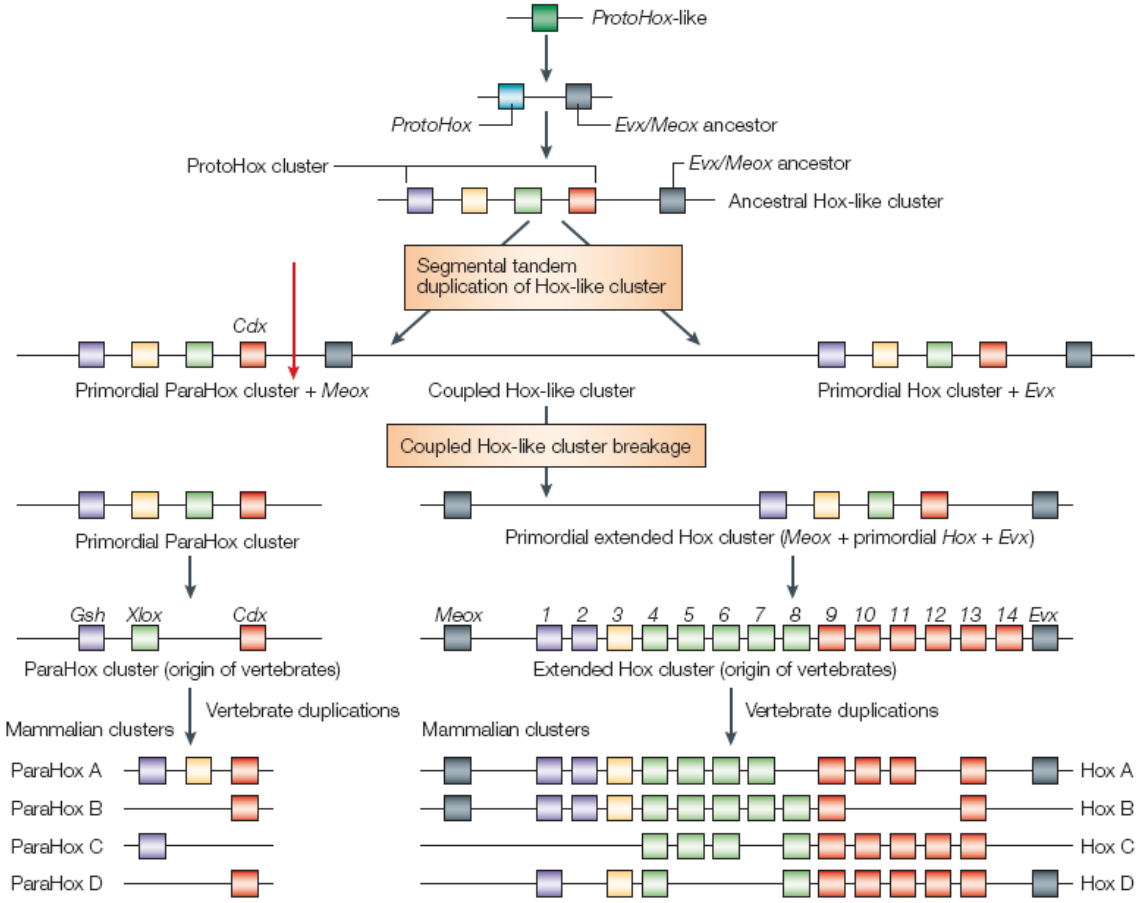

Fig 1.3.1a. Genesis and evolution of Hox and Parahox clusters. It has been postulated that an ancestral *ProtoHox*-like gene underwent a series of *cis*-duplications giving rise to an ancestral Hox-like cluster that consisted of the ProtoHox cluster linked to the ancestor of even-skipped homeotic gene (*Evx*) and mesenchyme homeobox (*Meox*). Segmental tandem duplications generated a set of primordial ParaHox, Meox, Hox and Evx genes, which was subsequently separated into two clusters at the level of the posterior ParaHox gene caudal-type homeobox (*Cdx*) and the *Meox* gene (red arrow). Subsequent *cis*-duplications, expansions and genome duplications led to the current mammalian full set of extended Hox and ParaHox genes, consisting of four clusters of each cluster type (A-D). A further gene cluster, EHGbox (not shown), has been identified, consisting of gastrulation brain homeobox (*Gbx*), motor neuron restricted (*Mnx*) and engrailed (*En*). This cluster derives through a *cis*-duplication of a founder gene that was probably linked to the *ProtoHox* gene. Colour codes for the four paralogous groups are: Anterior, purple; Group 3, yellow; Central, green; Posterior, red. *Gsh*, genomic screened homeobox; *Xlox*, *Xenopus laevis* homeobox 8 (Garcia-Fernàndez 2005b).

Hox genes exhibit a high degree of homology to the clustered homeotic genes (HOM-C) of the fruit fly *Drosophila melanogaster,* which are located in two gene clusters, the *Antennapedia (Ant-C)* and *bithorax* complexes (*BX-C*). The study of

these genes has been initially useful to understand the function of the mammalian hox genes. Non-clustered or non-Hox homeobox genes (class II homeobox genes) are more divergent and numerous (approximately 160 in the humans) (Tupler 2001), and are dispersed throughout the genome. Gene expression analyses of both mouse and human BM samples revealed that the majority of Hox genes of the A, B, and C clusters are expressed in lineage- and stage-specific combinations in HSCs and, for the most part, are preferentially expressed in HSC-enriched subpopulations and in immature progenitor compartments and downregulated during differentiation and maturation (Sauvageau 1994, Pineault 2002). Nowadays, the expression of homeobox genes has been characterized for normal tissues, for cancer cells as well as for other diseases, like metabolic disorders. In the normal development the homeobox genes are controlling proliferation and differentiation, which are major clues in the cancer development. In fact it is known since many years that homeobox genes play an important role in the oncogenesis, and in particular they can be disregulated in AML by several mechanisms, like chromosomal translocations.

For example, in the t(7;11) and t(2;11) the *HOXA9* and *HOXD13* are dysregulated through fusion with the gene encoding the nucleoporin 98 kDa (NUP98) nuclear protein (Nakamura 1996, Raza-Egilmez 1998, Kroon 2001, Pineault 2004). The overexpression of *HOXA9* alone has been reported to strongly correlate as single gene with the poor prognosis in a set of 6817 AMLs (Golub 1999). Another well characterized example is represented by the chromosomal aberrations involving the *MLL* gene (11q23), that leads to the overexpression of the hox genes *HOXA6*, *HOXA7*, *HOXA9*, and the Hox cofactor myeloid ecotropic viral integration site 1 (*MEIS1*) (Schoch 2003). This expression pattern is common in many AML patient samples (Lawrence 1999; Kawagoe 1999, Yeoh 2002). The *MLL* (*mixed lineage leukemia*) gene is the human homolog of the *Drosophila Thritorax* gene and is the archetypal member of the *Trithorax* group of genes that encode chromatin modifiers that are required for the proper maintenance of hox genes expression during development. Rearrangements involving *MLL* gene, generated as a consequence of chromosomal translocations fusing N-terminal sequence of *MLL* to 1 of over 40 functionally diverse groups of C-terminal fusion partners, constitute 5% of all AML

cases and 22% of those with acute lymphoblastic leukemia (De Braekeleer 2005). Interestingly, also in a number of AML cases, bearing rarer translocations, like t(8;16)(p11;p13) where the *MYST3-CREBBP* fusion gene is expressed, the hoxgenes *HOXA9*, *HOXB9*, *HOXA10*, and *MEIS1* are also overexpressed. Interestingly, the upregulation of other genes like *HOXC4* has been reported in the NB4 PML-RARα-positive cell line following all-*trans* retinoic acid–induced (ATRA-induced) differentiation, as well as in BM from acute PML patients during ATRA treatment (Kim 2005). The dysregulated *HOX* expression has been confirmed to be a signature of AML, as well as in lymphoid leukemias where *MLL* expression is disregulated (Imamura 2002).

Considering their transcriptional specificity, hox genes are able to function as both transcriptional repressors and activators. By performing *in vitro* co-precipitation assays, Shen et al have shown that the CBP-p300 histone acetyltransferase (HAT) is binding to representative Hox proteins from each paralog groups (HOX4, 6, 7, 9, 10, 12, 13), but not to the non-Hox homeodomain cofactors Pbx and Meis. Moreover the Pbx-binding motif within the Hox proteins is not required for CBP binding (Shen 2001). The Hox-CBP interaction variably reduces the Hox-DNA binding: the higher paralogs tested (groups 9 through 11) seemed to show somewhat greater sensitivity to CBP-induced blocking of DNA binding than the lower paralog proteins from groups 1 to 8. This could be explained by the ability of the AbdB-like Hox proteins to directly bind to DNA without cofactors, while Hox proteins from 1 to 8 paralog groups can strongly interact with DNA only in the presence of other cofactors, like Pbx and/or PREP1. Moreover, Hox proteins are not acetylated by CBP, whereas they are reported to even inhibit CBP activity *in vitro* and *in vivo* (Shen 2001).

In summary, the Hox proteins are essential for the embryonic development, play a key role in defining the cellular identity and regulate genes involved in the cell division, cell adhesion and migration, morphological differentiation and apoptosis (Ulijaszek 1998) (Fig 1.3.1c). The Hox genes expression is mostly regulated by the Polycomb group proteins (PcG), which were first identified in *Drosophila* and are highly evolutionary conserved. They are known to maintain specific repressive states of hox genes expression patterns within body segments development from flies to humans (Lewis 1978). The PcG proteins are components of multimeric transcriptional repressor complexes, which include

DNA-binding and chromatin remodelling factors, as well as noncoding small RNAs, and RNA interference machinery, and they are essential in maintaining cell fate, sustaining stem cells and lineage specification (Rajasekhar 2007).

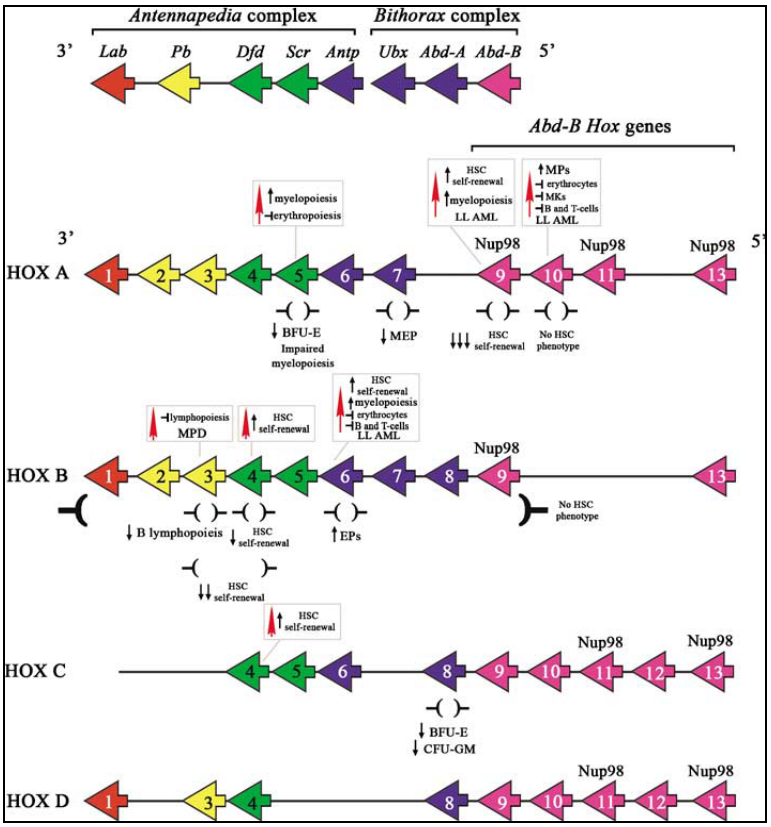

Fig 1.3.1b. Clustered hox genes organization. Each of the four cluster contains 8-11 genes, which are located on four different chromosomes (Chr.7, 17, 12, and 2, respectively). Identical clusters can be aligned into paralogous groups (identical colours) based on the sequence homology within their homeobox regions, and with the homeotic genes of the Drosophila HOM-C cluster. A box above a gene summarizes the important hematopoietic phenotypes exhibited upon engineered overexpression of that hox gene. Brackets under one or more genes, denote mouse knockout models where the role of the indicated gene(s) was assessed in hematopoiesis (Argiropoulos 2007).

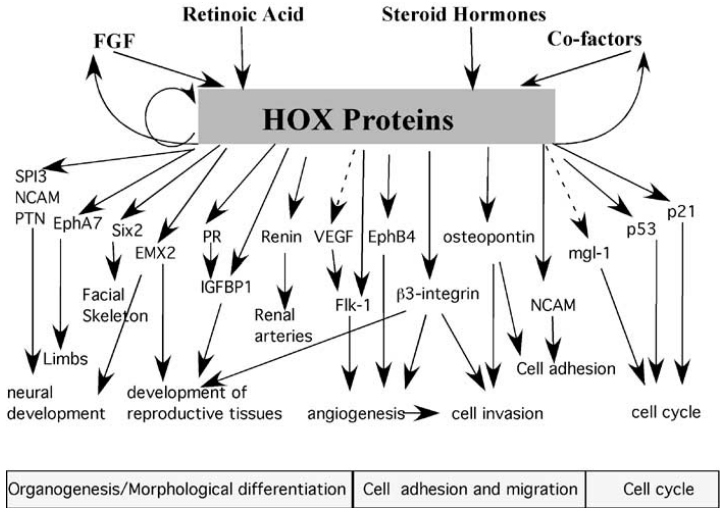

Fig 1.3.1c. Hox downstream targets include a significant number of factors involved in numerous cellular processes like organogenesis, cellular differentiation, cell adhesion and migration, cell cycle and apoptosis (Svingen 2006).

Recently, Hox proteins have been reported to act as general downstream DNA-binding proteins recruited by BMP/Smad pathway, which regulate a broad range of morphogenetic events during embryonic development, and their transcriptional activities are regulated by Smad proteins (Li 2006). Additional studies have revealed that Hox genes transcription is controlled by a modular system of enhancers located within a few kilobases up- or downstream of the gene. Generally, each enhancer can orchestrate tissue- and spatially-specific subsets of expression patterns and can often independently modulate other regulatory factors. Through accurate analysis of these regulatory regions other important regulators of Hox gene expression have been identified, like the retinoic acid and retinoid X receptors, the Cdx family proteins, Krox20, Kreisler, members of the AP-2 family of transcription factors, and Sox/Oct heterodimers. Intriguinly, Hox proteins themselves via interaction with the Pbx and Meis families of cofactors are capable to regulate the Hox genes expression themselves. Some of these factors are involved in the leukemogenesis. For example, the caudal-type homeobox transcription factor 2 (CDX2), which belongs to the ParaHox cluster, affects Hox gene expression during embryogenesis, is aberrantly overexpressed in 90% of patients with AML, whereas it is absent in normal hematopoietic progenitors (Scholl 2007), and its overexpression induces a transplantable AML in murine models (Rawat 2004). Taken together, these observations allow gaining additional alternative explanations for Hox-induced leukemogenesis and contribute to better understand the hierarchy of Hox genes regulation in AML (Rice 2007).

1.3.2 Cofactors of the Hox genes

The Hox genes have been reported to need the interaction with heterologous cofactors to display their functional specificity. The cofactor Pbx1 belongs to subclass of homeodomain proteins, named PBC family, where PBC indicates the conserved motif at the N-terminus of their homeodomain. This PBC subclass together with the MEIS family belongs to the TALE superclass of non-Hox homeodomain proteins, characterized by a Three-Amino-Acid-Loop Extension

within the homeodomain. Pbx1 and Meis1 were both found expressed in subpopulations of BM cells expressing Hox genes, but also had distinct gene-specific differences in their expression pattern throughout hematopoiesis. The primary interaction between Pbx and Hox occurs between the three amino acids loop in the Pbx homedomain, and a tryptophan-containing hexapeptide motif (YPWM) N-terminal to the homeodomain in almost all Hox proteins, with the exception of the paralog groups 11-13 (Chang 1995, Chang 1996). In particular, Hox9 has been shown to directly interact with Pbx and Meis/Prep proteins separately, Hox13 only with Meis/Prep, and Hox10 with both Pbx and Prep. Moreover, the occurrence of functional trimeric interactions between Hox, Pbx and Meis proteins on native Hox enhancers have also been observed (Jacobs 1999). These interactions seem to be Hox protein- and cellular context-dependent in the regulation of hematopoietic cell behaviour. It has been suggested that the Hox genes acquire a more stringent DNA binding selectivity when they cooperatively bind to these cofactors (Mann 2000), but the *in vivo* effects of this binding are not yet completely understood. Depending on the target, Hox-Pbx complexes can act as transcriptional activators or as transcriptional repressors (Fig 1.3.2). Moreover, it has been suggested from several works that the transcriptional effect is not only determined by the presence or absence of cofactors, but also and especially by the recruitment of other factors into the complex depending on the cell signalling involved and/or on the extracellular signals (Saleh 2000).

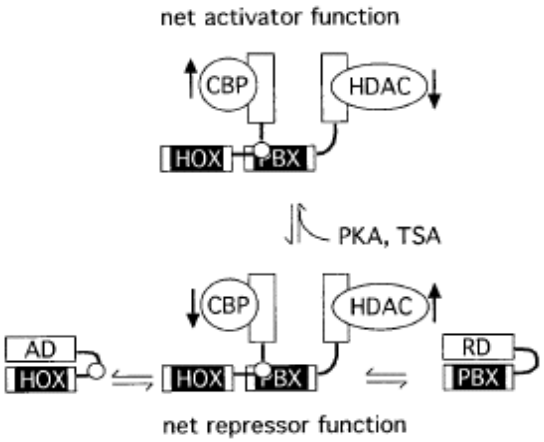

Fig. 1.3.2. A model for the function of Hox-Pbx complexes. The N-terminal activation and repression domains of Hox and Pbx proteins are believed to make intramolecular contact with their respective homeodomains. When Hox and Pbx or other cofactors of the Meis/Prep family interact on cooperative sites on DNA, their domains became exposed to the interaction with coactivators and corepressors such as CBP and HDAC1 and -3. In certain cellular conditions, the

net repressor function dominates. However, in response to enhanced PKA signalling or to treatment with the HDAC inhibitor TSA, net activation function could prevail (top). Other changes could affect this balance, like an increase in the amount of coactivator or an increase of affinity for the Hox N-terminus or for Pbx. However, other possible interactions cannot be excluded. The black vertical arrows indicate increases or decreases in HAT (e.g. CBP) or HDAC activity. AD, HOX activation domain; RD, PBX repression domain; black box, homeodomain; small white circle, HOX YPWM motif (Saleh 2000).

In fact, the abolishment of Pbx-binding with a Hox protein does not only lead to the loss of Hox function, but can even antagonize the Hox downstream effects. Interestingly, the interaction with Pbx has been recently shown to reduce the Hoxb4-dependent self-renewal of hematopoietic stem cells (Beslu 2004). However, this effect was observed under overexpression of Hoxb4, which may not completely reflect *in vivo* functional roles of Hoxb4-Pbx interaction.

1.3.3 Hoxb4

Hoxb4 (initially called Hox-2.6) has been described for the first time in the mouse in 1988 as related to the *Drosophila Deformed gene* (*Dfd*), encoding a protein of 250 amino acids. Interestingly, in several tissues the presence of different transcripts (at least 6 ranging from 2.4 to 10 kb), which are differentially detected with the time during embryonal and post-natal development, has been reported (Graham 1988). Nowadays, Hoxb4 is known to significantly increase self-renewal and proliferation of primitive murine and human hematopoietic progenitor cells *in vitro* and *in vivo* without perturbing the differentiation (Buske 2002). The *Hoxb4* gene is conserved in chimpanzee, dog, cow, mouse, rat, chicken, and zebrafish, and it is expressed in fetal and adult tissues. *In situ* hybridization analysis of mouse embryos showed that the Hoxb4 is expressed in tissues derived from the ectoderm: spinal cord, hindbrain, dorsal root ganglia, and the X^{th} cranial ganglia. In mesodermal derivatives, Hoxb4 is expressed in the kidney, the mesenchyme of stomach and lung, and the longitudinal muscle layer of the gut, whereas it is not detected in structures derived from embryonic endoderm (Graham 1988). At present, several screening methods have been employed to define consensus databases, which are based on all the reports where expression profiling results of known genes have been investigated. In the database of GeneSapiens (www.genesapiens.org) it is possible to obtain information about the transcriptome of human genes. In Fig. 1.3.3a and 1.3.3b the available data regarding the expression of Hoxb4 in normal tissues and in cancers are reported.

Brun et al have shown in Hoxb4-deficient mice that the lack of this gene leads to hypocellularity in hematopoietic organs (spleen and BM) and impaired proliferative capacity, demonstrating that it is not required for the generation of HSCs or the maintenance of normal hematopoiesis. In the murine model established from these authors the animals showed a reduction in red blood cell counts and in hemoglobin values, and a mild reduction in the numbers of primitive progenitors and stem cells in adult BM and fetal liver, whereas lineage distribution was normal. In these Hoxb4-deficient mice the primitive progenitors had normal cell cycle kinetics during endogenous hematopoiesis, whereas the proliferative capacity of BM Lin^- $Sca1^+$ $c\text{-}kit^+$ stem and progenitor cells was reduced *in vitro* and *in vivo* after transplantation of BM and fetal liver derived stem cells.

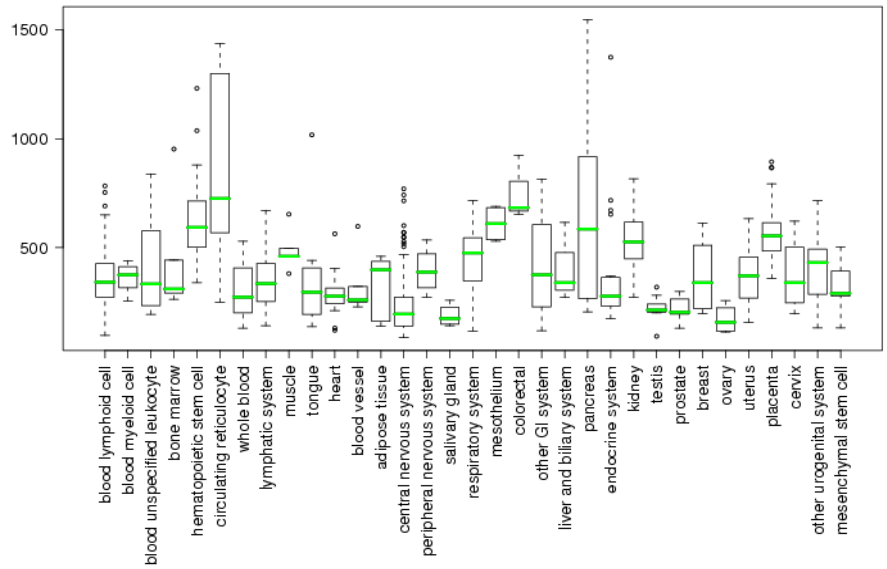

Fig. 1.3.3a. Expression of Hoxb4 in normal tissues. (www.genesapiens.org).

Interestingly, in this mouse model the lack of Hoxb4 led to a change in the expression of several other Hox genes and of genes controlling the cells cycle regulation, as demonstrated by mRNA analysis from fetal liver (Brun 2004).

Several others works have reported Hoxb4 overexpression in different types of cancer, like ovarian carcinoma (Hong 2010), cervical carcinoma (Lopez 2006), osteosarcoma, lung and breast carcinoma (Bodey 2000). However, the significance of these findings has still to be investigated.

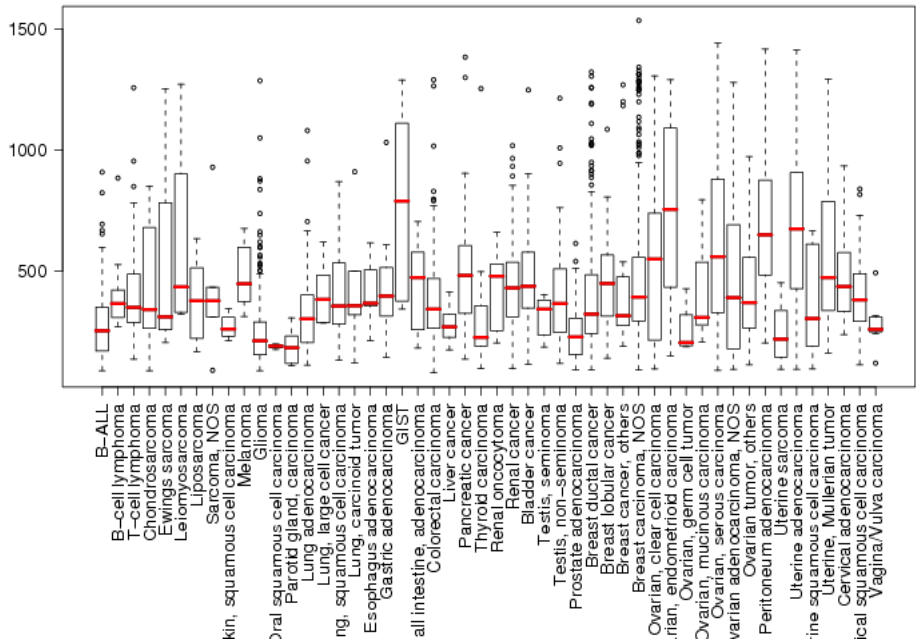

Fig. 1.3.3b. Expression of Hoxb4 in cancers. (www.genesapiens.org).

In the last decades many efforts have been focused to understand the regulation of Hoxb4 expression. The transcription factors NFY and YY1 have been reported to bind the promoter and two intron sequences of Hoxb4 regulating its expression during the embryonic development (Gilthorpe 2002). Additionally, the transcription factors USF-1, USF-2 and MITF have been shown to bind to the E-box binding site within the Hoxb4 promoter. USF-1 and USF-2 induce Hoxb4 expression in presence of signals to self-renew in stem cells downstream of activated MAPK pathway (Giannola 2000). Some promoter sequences seem to be determinant for the maintenance of the expression initiated by the intronic enhancer, whereas other sequences in the 3' untranslated region (UTR) are responsible for the preservation of the specific and correct anterior boundary in the paraxial mesoderm throughout embryonic development. Other control mechanisms have been suggested to occur at transcriptional and post-transcriptional levels. It has been shown that the 3'UTR is required to destabilize *Hoxb4* transcripts, while the 5'UTR to stabilize them, although in different domains of the paraxial mesoderm (Brend 2003). Recently, the homeodomain transcription factor Prep1 has been shown to bind to the 3'UTR of the mRNA of Hoxb4 leading to the inhibition of its translation and the full length of the 3'UTR

has been shown to be necessary for this effect (Villaescusa 2009). Although the promoters and other controlling regions of the majority of Hox genes maybe contribute to the proper spatio-temporal regulation of these genes, their role in the development of cancer disease remain unknown.

1.3.3.1 Hoxb4 in the hematopoiesis

Several hox genes of the Hox A and B clusters, such as *HOXB3* and *HOXB4*, are highly expressed in the most primitive hematopoietic cell types, like the $CD34^+$ cells of the BM (Sauvageau 1994) (Fig. 1.3.3.1a). The engineered overexpression of Hoxb4 in hematopoietic progenitor cells induces a dramatic increase in the proliferation and self-renewal of HSCs without affecting the normal differentiation. Moreover, this gene is the only Hox gene, which is able to convert *in vitro* cultured progenitor cells from the early yolk sac and differentiating embryonic stem cells into HSCs capable to long-term engraft lethally irradiated primary and secondary recipient mice (Kyba 2002). In a recent report a Hoxb4-YFP reporter mouse model has been used to investigate in detail its normal expression in the hematopoietic system, where it has been shown to be expressed in BM $Lin^-Sca1^+c\text{-}kit^+$ cells, in AGM-derived $CD45^+CD144^+$ cells, in HSCs isolated from yolk sac and placenta, whereas its expression in the fetal liver HSCs was significantly lower than in the BM derived HSCs (Hills 2011). Despite these determinant reports on the Hoxb4 activity, the induced expansion of HSCs has not been yet completely clarified.

In Fig. 1.3.3.1b the structures of the *Hoxb4* gene (A) and Hoxb4 protein (B) are reported.

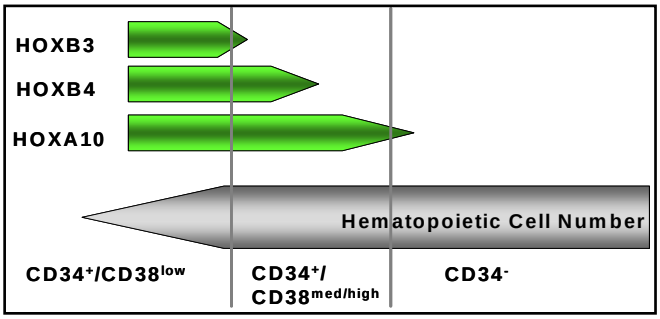

Fig 1.3.3.1a. Expression of hox genes (*HoxB3, B4 and A10*) in human BM cells. Hox genes are expressed in early hematopoietic progenitor cells, and their expression decreases during the differentiation (Sauvageau 1994).

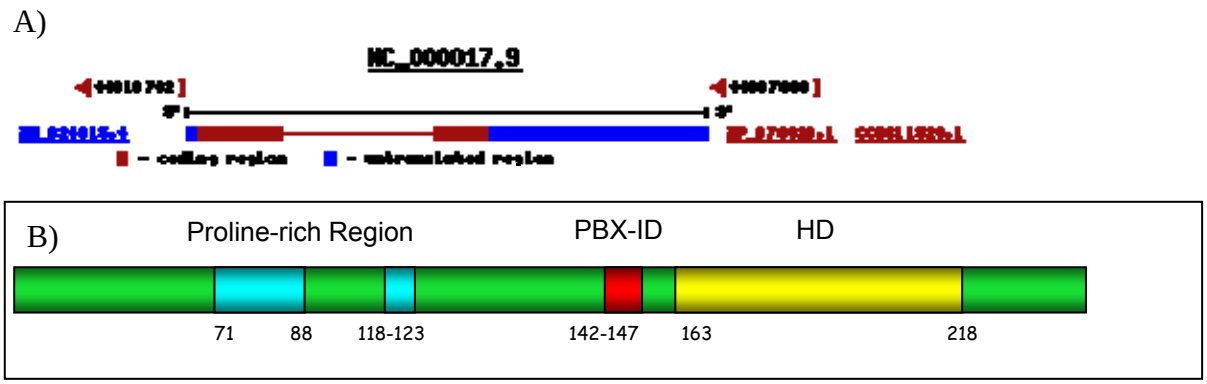

Fig. 1.3.3.1b. A) Structure of the *Hoxb4* gene. B) Structure of Hoxb4 protein. PBX-ID: Pbx interaction domain; HD: homeodomain.

In the protein sequence two known domains are present: the Pbx-interacting domain at position 142-147, and the homeodomain at position 163-218. As other Hox proteins, Hoxb4 dimerizes with the cofactor Pbx1. Mutational studies, where the Pbx-binding motif YPWM was mutated by the substitution W→G, have shown that the direct Hoxb4-Pbx interaction is not required for the HSC-expanding activity of Hoxb4, as mentioned above. Interestingly, the down-regulation of Pbx1 through a vector encoding its antisense sequence led to a further increase of Hoxb4-mediated HSCs expansion. This suggests that these two genes might affect the hematopoietic cells behaviour by different mechanisms (Krosl 2003). The deletion of the homeodomain of Hoxb4 (substitution N→A) leads to the loss of its DNA-binding ability and thereby to the loss of its proliferation activity (Beslu 2004). Between the amino acids 71 and 123 there is a proline rich region where no structural domains have been described so far. The function of this putative domain has been investigated in the present work.

1.3.3.2 Hoxb4 as amplification tool of HSCs

A number of Hox genes have been overexpressed using e.g. retroviral vectors in early murine as well as human hematopoietic progenitor cells, showing significant effects on the proliferation and differentiation programs. As unique Hox gene, *Hoxb4* dramatically enhances the proliferation of primitive murine hematopoietic cells both *in vivo* and *in vitro* without perturbing their differentiation or the production of mature progeny (Thorsteinsdottir 1999, Kondo 2003). By retroviral transduction of primitive lineage-negative human cord blood cells, Hoxb4 has been A) n to increase the number of secondary CFCs both in semisolid and

liquid suspension cultures, to amplify the number of cells with LTC-IC (long-term culture-initiating cells) activity, to promote the development of B cells *in vivo*, and to increase the number of cells able to repopulate NOD/SCID mice (Buske 2002). Moreover, the stable overexpression of *Hoxb4* has been reported to considerably increase the hematopoietic development of human embryonic stem cells *in vitro* (Bowles 2006). Performing serial transplantations in mice Sauvageau et al have demonstrated that the Hoxb4-transduction of BM progenitor cells induces a 50fold increase in the number of transplantable HSCs, compared to control cells (Sauvageau 1995). Additionally, when limiting dilution transplantation assays are performed, the long-term competitive repopulating units (CRUs) are amplified as well by Hoxb4 without leading to any impairment of homeostatic control of the HSCs population size or of the rate of production and maintenance of mature cells (Antonchuk 2001). All these observations have suggested that Hoxb4 could be used as tool to obtain a controlled amplification of genetically modified hematopoietic stem cells. However, the long term effect in the differentiation potential of this amplified HSCs need to be investigated, considering the impairment in lymphoid-myeloid differentiation observed when high-level ectopic Hoxb4 expression in human CB-$CD34^+$ cells was induced (Schiedlmeier 2003). Since its identification, Hoxb4 has not been reported to display any involvement in hematologic malignancy, and its ectopic expression has been applied to amplify HSCs. However, in a recent report the retrovirus-mediated Hoxb4 expression in hematopoietic repopulating cells led to monoclonal leukemia in 2 out of 2 dogs and 1 out of 2 maquaques, approximately 2 years after transplantation (Zhang 2006, Zhang 2008). In these cases retroviral integration events were of clonal nature, affected the expression of oncogenes and were therefore suggested to be determinant for the leukemogenic process in collaboration with the ectopic overexpressed Hoxb4. This result confirms the risk of combining integrating vectors and proliferation-inducing genes for clinical application (Larochelle 2008). These considerations led to the development of a model for Hoxb4 protein delivery without genetic manipulation, ruling out the risk of retroviral integration-associated transformation. Since Hoxb4 protein can passively translocate through cell membrane, other researchers have cultured human LTC-ICs (long term culture-initiating cells) and NOD-SCID-repopulating cells (SRC) on stromal cells genetically modified to secrete Hoxb4, obtaining an

expansion of more than 20- and 2.5fold of these primitive HSCs over their input numbers, respectively (Amsellem 2003). In parallel to these investigations, the clinical established antiepileptic drug valproic acid (VPA) had been reported to enhance the potential of engraftment of human umbilical cord blood hematopoietic stem cells. Seet et al have shown that human VPA-treated $CD45^{+}CD34^{+}$ progenitor cells were able to reconstitute hematopoiesis in NOD/SCID mice with a six-fold higher efficiency than control cells. A probable explanation for this effect was the higher proportion of these cells residing in the S phase and the 2.5fold upregulation of Hoxb4 expression (Seet 2008). More recently, Tang et al have treated human BM cells from normal donors and from aplastic anemia/MDS patients with exogenous recombinant Hoxb4 protein, and reported a significant LTC-ICs expansion *in vitro*, therefore suggesting a promising therapeutic employment of human Hoxb4 in BM failure (Tang 2009).

1.3.3.3 The proline-rich domain

The N-terminal half of human Hoxb4 protein contains a proline rich region between aminoacids 71-123 (50% P). Among these residues there is a stretch of 15 consecutive prolines, and a similar stretch occurs also in the Hoxb4 sequence from chimpanzee, cow, mouse and rat. The long proline stretch is not conserved in dog, chicken and zebrafish (Fig 1.3.3.3). Of note, the canine Hoxb4 protein is much longer than the human one (459 vs. 251 aa). In the panel below partial sequences of Hoxb4 proteins from different species are aligned.

Homo sapiens	**62**	**VQRYAACRDPGPPPPPPPPPPPPPGLSPRAPAPPPAG--ALLPEPGQR**	**109**
Pan troglodytes	**62**	**VQRYAACRDPGPPPPPPPPPPPPPGLSPRAPAPPPAG--ALLPEPGQR**	**109**
Canis lupus	**201**	**VQRYAACRDPGPPPPPSPH----------PLCYTXG--ALLPEPGQR**	**235**
Bos Taurus	**62**	**VQRYAACRDPGPPPPQPPPPPPPPPPGLSPRAPAQPPSG--ALLPEPGQR**	**109**
Mus musculus	**62**	**VQRYAACRDPGPPPP-PPPPPPPPPPGLSPRAPVQPTAG--ALLPEPGQR**	**108**
Rattus norveg.	**62**	**VQRYAACRDPGPPPP-PPPPPPPPPPGLSPRAPVQSTAG--ALLPEPGQR**	**108**
Gallus gallus	**60**	**EQLYPSCQSSGHQAA----------VLSPRGHVHPPAGLQSHLSEPNHP**	**98**
Danio rerio	**60**	**DPPYSSCQGPGQPAA----------VISPRGHVLPTTALSTPLPEPSHH**	**98**

Fig. 1.3.3.3. Comparison between proline regions of Hoxb4 of different species.

Homology between human (h) and murine (m) protein sequence: 89% identity

h- MAMSSFLINSNYVDPKFPPCEEYSQSDYLPSDHSPGYYAGGQRRESS FQPEAGFGRRAAC
m-MAMSSFLINSNYVDPKFPPCEEYSQSDYLPSDHSPGYYAGGQRRESGFQPEAAFGRRAPC

h- TVQRYAACRDPGPPPPPPPPPPPPPGLSPRAPA PPPAGALLPEPGQRCEAVSSSPPPP
m-TVQRYAACRDPGPPPPPPPPPPPPP- GLSPRAPVQPTAGALLPEPGQRSEAVSSSPPPP

h- PCAQNPLHPSPSHSACKEPVVYPWMRKVHVSTVNPNYAGGEPKRSRTAYTRQQVLELEKE
m-PCAQNPLHPSPSHSACKEPVVYPWMRKVHVSTVNPNYAGGEPKRSRTAYTRQQVLELEKE

h- FHYNRYLTRRRRVEIAHALCLSERQIKIWFQNRRMKWKKDHKLPNTKIRSGGAAGSAG
m-FHYNRYLTRRRRVEIAHALCLSERQIKIWFQNRRMKWKKDHKLPNTKIRSGGTAGAAG

h- GPPGRPNGGPRAL
m-GPPGRPNGGPPAL

Interestingly, through all these species Hoxb4 presents several WW(/SH3) domains, which have been described to be responsible for binding to specific protein interaction modules, like RPLPPLP in Src or PPPψPPPPψP in Abl proteins (Kay 2000), and the p300 binding consensus sequences PXXPXXP in Smad4, PXXP in p53, and PXPXP in EKLF (Dornan 2003). Of note, the proline repeat domain of p53 (PXXP/PXPXP, where X denotes any amino acid) has been suggested to bind directly to the transcriptional activator p300, and mediate the DNA-dependent acetylation of p53 (Dornan 2003). This domain seems to play a critical role in the transmission of anti-proliferative signals downstream of the p53 protein (Walker 1996), and it has been suggested to maintain the latent, low affinity DNA binding conformation of p53 (Müller-Tiemann 1998). The proline is a critical amino acid present in many ligands responsible for protein-protein interactions. Different proline-rich sequences that bind to specific protein interaction molecules have been described (Kay 2000) and transcriptional activation domains are often rich in Ser, Thr and Pro residues. A significant example is represented by the proline-rich N-terminal half of Hoxd4, which has been reported to exert a transcriptional activation function in a system where it was fused to the GAL DNA-binding domain (Rambaldi 1994). These observations were supported by other deletion analyses, where conserved regions flanking the homeodomain have been reported to be necessary for the Hoxd4-mediated activation. Interestingly, the transcription factor AP2 contains a proline-rich transcriptional activation domain, and has been shown to inhibit the activity of Hoxd4. AP2 and Hoxd4 contain functionally similar proline-rich transcriptional activation domains, and AP2 is expressed in a similar spatial and temporal pattern as many hox genes during the development. Based on these similarities, Hox proteins and AP2 have been proposed to collaborate during the embryonic development (Rambaldi 1994).

In the protein databases a proline stretch similar to the one present in Hoxb4 can be found in few other unrelated proteins, like in the murine formin 1; in the

essential capsid protein Mv-ORF2 of MNPV baculovirus; in the MGC82812 protein of *X.laevis*, in a putative protein of *Monodelphis domestica*; in a protein similar to JUN in *Gallu gallus* genome; in a putative membrane protein of *Emiliana huxleyi* virus 86; in an unnamed protein in *Tetraodon nigroviridis*. The role of the proline reiterations in all these proteins remains unknown, although for the formin-1 for example it has been reported to induce the production of many circular transcripts.

Interestingly, in the USCS genome databases several human ESTs of Hoxb4 have been reported: in the human adult and fetal lung tissue a sequence starting after the proline-rich region has been described by Bonaldo et al (Bonaldo 1996, BM972326, **EST AW182319,** www.ncbi.nlm.nih.gov/ncicgap.). The importance of this P stretch for the function of all these proteins remains unclear.

1.3.3.4 The downstream targets of Hoxb4

Many efforts have been done to understand the regulation and function of Hox genes, however their downstream targets remains often unknown. Several studies have reported a number of factors affected by Hoxb4 expression, which are involved in similar signalling pathways in differentiating ES cells and in adult HSCs. A recent work based on ChIP-chip analysis showed, that Hoxb4 binds to promoter regions of many genes involved in cell division, cell cycle, and chromosome organization and biogenesis, without direct binding to HSC regulatory genes. However, among these genes *Myb, Erg, Gfi1b, Gata3,* and *Sox17* seem to be indirectly regulated by Hoxb4 (Oshima 2011). Other factors have been previously reported to be activated by Hoxb4, like Bambi, a pseudoreceptor that also inhibits the TGF-β and BMP signalling, and the TALE class homeodomain gene *Irx5*, which seems to direct repress the epidermal development factor BMP4 in *Xenopus* (Schiedlmeier 2007, Theokli 2003). Others, like the small GTPase *Rap1* expressed early in the gastrulation, are negatively regulated by Hoxb4 (El-Kadi 2002). Another interesting finding about the Hoxb4 function in zebrafish suggested a correlation between the clustering of hox genes and post-transcriptional regulation of downstream genes. Woltering et al have shown that the microRNA-10, which is located closely to Hox-4 paralogues, acts to repress *Hoxb1a* and *Hoxb3a* within the spinal cord, and that this repression works cooperatively with Hoxb4 (Woltering 2008).

Taken together, all these results suggest that Hoxb4 is involved in important endogenous cellular pathways modulating the cell cycle, differentiation, and apoptosis processes of progenitor cells, whereas it modulates the reaction of HSCs and EB cells to exogenous stimuli derived by the microenvironment (Fig 1.3.3.4). In the present work we compared the *in vitro* and *in vivo* effect of the mutation of different domains of Hoxb4 in a murine BM transplantation model.

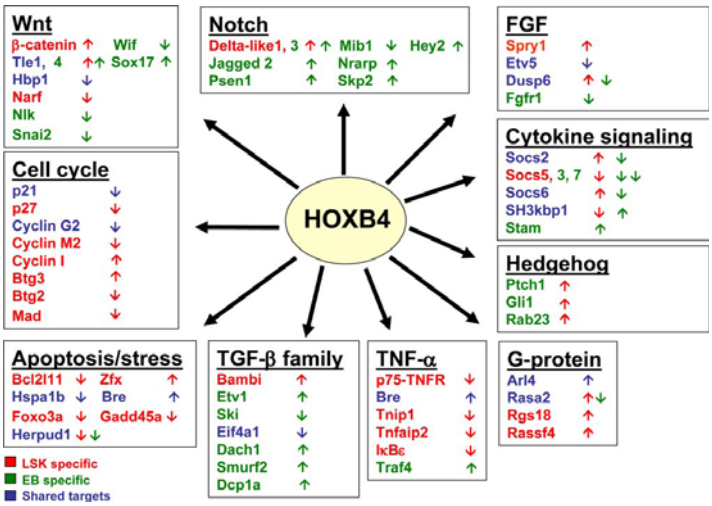

Fig 1.3.3.4. Important regulatory pathways affected by Hoxb4 in adult hematopoietic stem and progenitor cells and EBs. (LSK: lineage$^-$/Sca1$^+$/ckit$^-$; EB: embryoid bodies). These results are based on microarray expression profiling analyses using Affimetrix GeneChips Mouse Genome 430 2.0. Affiliations of the genes with the indicated pathways are based on published reports in various mammalian systems. Arrows indicate up-/down-regulation of gene expression as a consequence of Hoxb4 induction (Schiedlmeier 2007).

1.4 Epigenetic changes in cancer

The cancer development is the result of a stepwise process characterized by the accumulation of heritable changes leading to growth advantage, and eventually to therapy resistance.

The most relevant gene classes involved in this process are the tumor suppressor genes, which become inactivated and cannot inhibit survival and cell growth, and the oncogenes, which become activated and promote survival and proliferation. Often a combined alteration of one or more genes belonging to both classes leads to malignant transformation. These alterations include changes in the number of gene copies and in the protein sequence, or increased gene transcription. Another class of alterations includes covalent modifications of amino acids residues of histone proteins (e.g. acetylation), and methylation of cytosine residues within CpG dinucleotides (called “CpG-islands”) in the DNA (Fig. 1.4). These modifications are called epigenetic changes, they include

mitotically and meiotically heritable variations without alteration of the primary DNA sequence, and a growing body of evidence relates them closely to cancer. In particular, the methylation of clusters of CpGs in the promoter of genes has been associated with heritable gene silencing. However, the epigenetic alterations are reversible, whereas the genetic alterations are not. The mechanisms of gene silencing induction are not yet completely understood, but it is already known that a group of repressive proteins (the methyl-CpG-binding-domain proteins, MBDs) binds to methylated cytosines, and this complex seems to involve histone deacetylases (HDACs). These enzymes remove acetyl groups from lysines of histones, conferring them a positive charge which enhances their affinity for negatively charged DNA. This leads to a dense packaging of the nucleosomes and therefore to a reduced transcription ("closed chromatin structure").

In opposite cellular contexts where the cytosines are not methylated, the histone acetyltransferases (HATs) transfer acetyl groups to histone proteins leading to activation of transcription of target genes in collaboration with transcription factors and other co-factors (Gronbaek 2007). CBP (CREB binding protein) and p300 seem to mediate the transcription control exerted by Hox proteins leading to the expresson of target genes ("open chromatin structure") (Ito 2000).

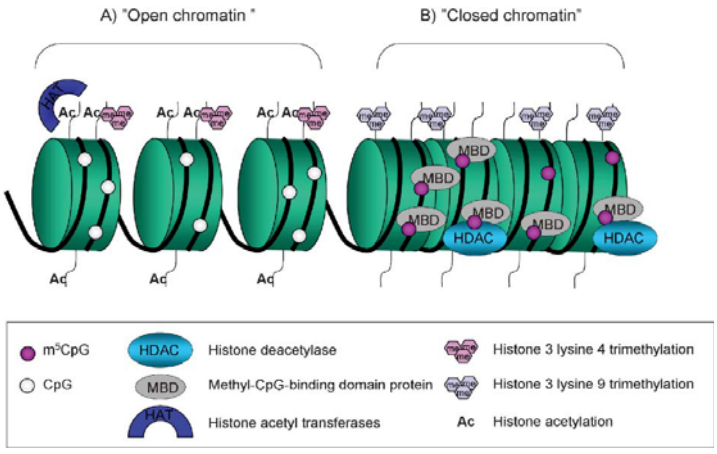

Fig 1.4. Chromatin structure of active and inactive promoters of targeted genes (Gronbaek 2007).

1.4.1. Histone deacetylases (HDACs)

Histone deacetylases (HDACs) catalyze the deacetylation of lysine residues within DNA bound core histone proteins (Lopez 1993). These enzymes work in opposition to histone acetyltransferases (HATs), which catalyze lysine acetylation

(Kuo 1998). The HDACs can deacetylate several proteins in particular cellular contexts (Glozak 2005). In mammals 18 different HDACs have been identified, which are classified into four classes based upon their homology with an archetypal HDAC found in yeast, and have been reported to control different cellular processes (Fig. 1.4.1a).

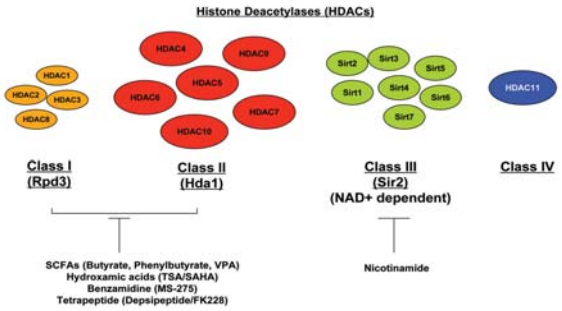

Fig. 1.4.1a . Classes of mammalian HDACs. Different classes can be inhibited by different HDAC inhibitors (Mariadason 2008).

HDACs do not directly bind to DNA, whereas they are part of high molecular weight (1-2MDa) multimeric transcriptional co-repressor complexes that are recruited by sequence-specific transcription factors to promoter regions. Different co-repressor complexes recruit different HDACs. Functionally, two different mechanisms have been suggested to mediate the gene expression control by HDACs: the acetylation of histones and the acetylation of sequence-specific DNA-binding transcription factors (Fig 1.4.1b) (Gu 1997; Ammanamanchi 2003). Acetylation or de-acetylation of transcription factors can either increase or decrease their DNA binding activity, leading to enhanced or repressed transcription. The substrates of HDAC are proteins involved in gene expression, cell proliferation, differentiation and apoptosis, but they can also deacetylate a number of non-histone proteins, that are not involved in transcription processes, like signal transduction mediators, DNA repair enzymes, nuclear import regulators, chaperone proteins, structural proteins, inflammation mediators and viral proteins (Glozak 2005).

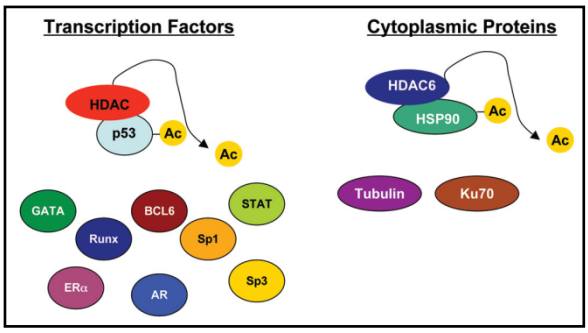

Fig. 1.4.1b. Non-histone substrates for class I and II HDACs (Mariadason 2008).

1.4.2 Histone deacetylase inhibitors (HDACi)

In the last decades, inhibition of HDACs has emerged as additional strategy to reverse aberrant epigenetic changes associated with cancer, and several classes of HDACi have been found to have potent and specific anticancer activities in preclinical studies. Since the 1990s the inhibition of HDACs has been shown to suppress tumor cell growth/survival, to induce growth arrest, differentiation and apoptosis of cancer cells *ex vivo* as well as *in vivo* in tumor-bearing animal models and are included in clinical trials as anti-tumor agents (Richon 1998, Insinga 2005, Kim 2004). Moreover, the HDACi have been shown to display anti-angiogenetic, anti-invasive and immunomodulatory activities *in vitro* and *in vivo*. They have been also shown to induce teratogenesis, and this effect is also mediated by the inhibition of histone deacetylases (Eikel 2006) (Fig 1.4.2).

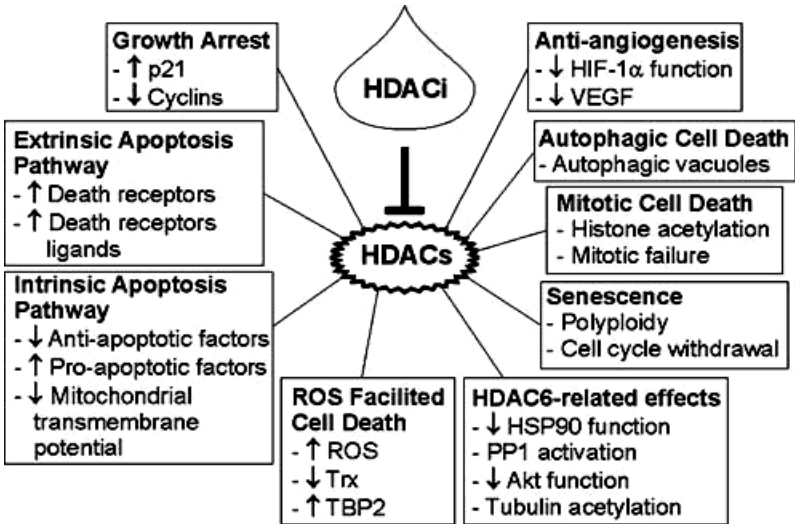

Fig 1.4.2. Multiple HDAC inhibitors-activated antitumor pathways (Xu 2007).

In the present work the HDAC-inhibitor valproic acid (VPA, 2-propylpentanoic acid), which is an established drug in the long-term therapy of epilepsy, has been

used to treat hematopoietic progenitor cells overexpressing Hoxb4 and its mutants. Göttlicher et al had already shown that at the therapeutically employed doses VPA inhibits co-repressor-associated HDACs and strongly induces the differentiation in several types of transformed cells (Göttlicher 2001, Kramer 2003, Liu 2007, Münster 2007). The treatment thereby with VPA could unmask the key role of the HDAC-activity in the transformation process of cancer cells.

1.5 The murine bone marrow transplantation model of leukemia

At present a number of mouse models, like ubiquitous or conditional knock-ins and knock-outs, targeted and random *in vivo* gene perturbation, retrovirally transduced bone marrow transplantation of irradiated recipient mice and transgenic mouse models, have been reported to represent reliable and reproducible systems to investigate the pathogenesis of leukemia at molecular level. The murine bone marrow transplantation model used in the present work is based on *ex vivo* retroviral gene transfer of primary 5-flurouracil (5-FU)-enriched hematopoietic progenitor cells and on their subsequent transplantation into lethally irradiated syngenic mice. The treatment with 5-FU 4 days prior bone marrow collection from donor mice aims to reduce the pool of proliferating progenitor cells inducing the activation of more primitive HSCs to reconstitute it, and thereby making these HSCs more susceptible to the retroviral transduction.

Several studies have demonstrated that ectopic overexpression of proto-oncogenes (Rawat 2004) and of proto-oncogenes combinations (Kelly 2002a, Kelly 2002b) can induce acute leukemia in mice using this model, and most importantly, this disease maintain the characteristics of the corresponding human leukemias. Single genes which are known to be mutated in human leukemias can be singularly investigated for their leukemogenic potential, whereas it is possible at the same time to identify potential cofactors collaborating to the leukemogenesis, which have not been yet identified in the primary leukemic human samples.

For example, the retrovirally induced overexpression of the fusion gene *AML1-ETO* or of the mutant *FLT3-ITD* alone fails to induce leukemic transformation *in vivo*. However, in a mouse model where these two genes were coexpressed the complete leukemic transformation has been observed, in primary, secondary and tertiary murine recipients. This suggests that these two genes could collaborate

even in human leukemia development (Schessl 2005, Palmqvist 2006). With the murine transplantation models it is possible to investigate the subset of cells giving rise to the leukemic bulk, and thereby to identify single events responsible for the leukemic transformation and additional mutations necessary for the full leukemic transformation. One example is done by the leukemia model established in our laboratory, where the overexpression of the *CALM/AF10* fusion gene led to a myeloid leukemia that was propagated by a lymphoid progenitor cell. In these experiments, the hierarchy within the leukemic stem cells have been described (Deshpande 2006).

Moreover, these models are of use for the identification of key regulators of normal hematopoiesis, which are disrupted in the leukemias or other hematologic malignancies.

The hematopathology subcommittee of the Mouse Models of Human Cancers Consortium has proposed a classification of nonlymphoid hematopoietic neoplasms in mice, in order to provide recommendations for classification of mouse diseases as models for the human hematopoietic neoplasms. In this proposal the murine non-lymphoid leukemias have been subclassified in myeloid (without maturation, with maturation, MPD-like, myelomonocytic, monocytic), erythroid, megakaryocytic, and biphenotypic leukemias (Kogan 2002).

We used the retroviral mediated murine bone marrow transplantation model to investigate the leukemogenic potential of the hox gene *HOXB4* and its mutants. Additionally, we investigated by mutagenesis the importance of its single domains in the normal function of this powerful stem cell specific gene.

1.6 Aim of the study

Hoxb4 has been described as one of the most important factors responsible for the proliferative potential and self-renewal of hematopoietic stem cells *in vivo* and *in vitro* models. Nowadays, the regulatory mechanisms and the downstream pathways controlled by Hoxb4 are not completely understood. In many reports Hoxb4 has been employed as exogenous protein or as engineered expressed gene to obtain an ideal amplification of stem cells *ex vivo*, in order to ensure a sufficient pool of transplantable HSCs in BM transplantations. Until now few reports have underlined this gene as a potential factor involved in the leukemogenic process, and these were almost based on integration events using

retroviral transduction systems. However, the contribution of Hoxb4 to the transformation in these cases was probably reduced to the increased proliferation of a subset of cells already mutated by a genomic mutation.

In the present work we attempted to clarify the mechanism responsible of the benign phenotype observed in high proliferating hematopoietic progenitor cells where Hoxb4 is overexpressed and which domain of its structure might avoid the unregulated and aberrant proliferation of the HSCs. In particular we investigated the less known proline rich region at the N-terminal sequence of Hoxb4 and the leukemogenic effect of its deletion in a murine transplantation model. We hypothesized that, like already known for other proteins, the proline domain maybe displays transactivation activity which might mediate the downstream effects of Hoxb4. This work is giving more insights in the complicated machinery of the normal phenotype of the stem cells and contributes to understand the fine regulated biology of the BM progenitor cells, which if deregulated results in the leukemic development. Moreover, the employment of drugs inhibiting putative cofactors of Hoxb4 like the histone deacetylases could help to define new potential targets responsible for the malignant transformation in our model.

2. Materials

2.1 Mice and related reagents and equipment

Mice strains: strains used as bone marrow transplant donors/recipients were either C57Bl6/Ly-Pep3b (Pep3b) or the F1 hybrid of (C57BL/6Ly-Pep3b x C3HeJ) ($[PepC3]_{F1,}$ Ly5.1/CD45.1 positive) or hybrid of (C57Bl/6J x C3H/Hej) ($[B6C3]_{F1,}$ Ly5.1/CD45.1 negative).

Avertin solution: Stock solution was prepared by adding 15.5 ml ter-amyl alcohol to 25 grams Avertin (2-2-2 Tribromoethanol) (both Sigma-Aldrich®, St. Louis, MO) and dissolved overnight. For working solution, 0.5 ml of the stock solution was added to 39.5 ml of cell culture grade phosphate buffered saline (PBS) and dissolved with a magnetic stirrer.

Erythrocytes lysis buffer: 0.8% NH_4Cl with 0.1 mM EDTA (Stem Cell Technologies, Vancouver, Canada).

Formalin: 10% solution of formaldehyde (Sigma-Aldrich®, St. Louis, MO) in water.

5-Fluorouracil: 50 mg/ml stock solution (Medac, Hamburg, Germany). Working solution was 6 ml of the solution above mixed with 4 ml of phosphate buffered saline.

Heparinized capillaries: plastic capillaries (Microvette CB 300) for collection of blood, 15 I.E. Lithium heparin per ml of blood (Sarstedt, Numbrecht, Germany).

Sterile needles: 24 G (0.55 x 25 mm) for bone marrow aspiration from the femur of living mice, 25 G **(**0.5 x 25 mm) for i.v. injection of cells in mice and flushing of bone marrow from prepared bones, and 30 G (0.3 x 13 mm) for i.p. injection of avertin (BD Microlance, Drogheda, Ireland).

Syringes: BD Plastipak 1 ml syringe (BD Biosciences, Palo Alto, CA) for injection of cells in mice and Kendall Monoject 3 ml syringes (Tyco Healthcare, UK) for bone marrow flushing and plating of CFCs. The stubs of 3 ml syringes were used to macerate the spleens and other organs of mice.

Telleyesnickzky´s solution: 450 ml absolute ethanol + 25 ml glacial acetic acid + 25 ml formaldehyde.

2.2 Mammalian cell lines and prokaryotic cells

GP+E86: mouse fibroblast cell line, stable packaging cell line

293T: human embryonic kidney cell line, transient packaging cell lines

Phoenix Eco: 293T mouse cell line, stable packaging cell line

NIH 3T3: mouse fibroblast cell line

32D mouse bone marrow-derived myeloblast cell line, IL-3 dependent

BA/F3 mouse bone marrow-derived pro-B cell line, IL-3 dependent

WEHI-3B mouse myelomonocytic leukemia cell line, producing IL-3

K562 human chronic myelogenous leukemia cell line

Jurkat: acute T cell leukemia cell line

HL-60: acute promyelocytic leukemia cell line

All cell lines were procured from the American Type Culture Collection (ATCC™, Manassas, USA), and from DMSZ GmbH (German collection of microorganisms and cell culture, Braunschweig, Germany).

Escherichia coli epicurian XL1-Blue: subcloning bacterial competent cells (Stratagene® La Jolla, CA).

2.3 Oligonucleotides (Metabion, Martinsried, Germany)

Oligonucleotide	Sequence 5´to 3´
EF1a_fw	CAC GAA CAG CAA AGC GAC C
EF1a_rev	CAC ACG GCT CAC ATT GCA T
Hoxb4_inter_fw	TGA TCA ACT CAA ACT ATG TCG AC
Hoxb4_inter_rev	ACT TGT GGT CTT TTT TCC ACT TCA T
Hoxb4_n_211_s fw	CAAGATCTGGTTCCAG**AGC**CGGCG CAT GAA GTG
Hoxb4_n_211_s rev	CACTTCATGCGCCG**GCT**CTGG AAC CAG ATC TTG
Hoxb4_W_144_A fw	CGTCGT CTA CCC C**GC G**AT GCG CAA AGT TCA C
Hoxb4_W_144_A rev	GTGAACTTT GCG CAT **CGC** GGG GTA GAC GAC G
Hoxb4_C-del_ fw	GTGGAAAAAAGACCAC**TAG**TTGCCCAA CACCAAG
Hoxb4_C-del_ rev	CTTGGTGTTGGGCAA**CTA**GTG GTC TTTTTTCCA C
Hoxb4_full lenght_ fw	GAG TCA GGG GTC GGA ATA AA
Hoxb4_full lenght_ rev	CCA TCC CCT GCA CTC ACT
Hoxb4_alternEST_fw	CACTCCGCGTGCAAAGAG
Hoxb4_Bowles_fw	TCT GTC CCC TCG GGC TCC TGC G
Hoxb4_Bowles_rev	GGC AAC TTG TGG TCT TTT TTC C

LM-PCR primers	Sequence 5´ to 3´
GFP-A	ACT TCA AGA TCC GCC ACA AC
GFP-B	ACA TGG TCC TGC TGG AGT TC
Vectorette primer 224	CGA ATC GTA ACC GTT CGT ACG AGA ATC GCT
Nested linker primer B	TAC GAG AAT CGC TGT CCT CTC CTT
PstI linker top	CTCTCCCTTCTC----------GTCCTCTCC TTC CTG CA
PstI linker bottom	GGAAGGAGAGGACGCTGTCTGTCGAAGGTAAGGA ACGGACGAGAGAAGGGAGAG

2.4 Plasmids, genes and proteins

pMSCV-IRES-GFP (MIG): A modified form of the MSCV vector of 6500 bp; it contains a bicistronic GFP expression cassette with an internal ribosomal entry site (R. Hawley, American Red Cross, Rockville, MD). The selection marker for bacterial growth is ampicillin resistance gene. Upstream of the multiple cloning site there is the packaging signal (ψ_plus_pack sequence).

pMSCV-HOXB4-IRES-GFP: the HOXB4 cDNA region encompassing the complete coding sequence has been subcloned by blunt-end ligation into the *HpaI* site in the multiple cloning site (MCS) of the MIG vector (kindly provided by Dr. K. Humphries, Terry Fox Laboratory, Vancouver, Canada).

HOXB4-wt: the *Hoxb4* gene (2042 bp) is located in the *HOXB* cluster on chromosome 17q21-q22 (44,009,083-44,010,680, NM_024015) and it contains 2 exons and 1 intron sequences.

pMSCV-Flag-HOXB4-ΔPro-IRES-GFP: encodes a mutant of *Hoxb4* containing the 2 exons, a deletion from amino acidic position 78-120, a flag epitope has been cloned in frame at the 5' end and the 5' and 3' UTR sequences are missing (kindly provided by Dr. K. Humphries, Terry Fox Laboratory, Vancouver, Canada).

Protein sequences of generated HOXB4 mutants

(PBX-ID and HD are underlined):

Hoxb4-wt 1 MAMSSFLINSNYVDPKFPPCEEYSQSDYLPSDHSPGYYAGGQRRESSFQPEAGFG 55
Hoxb4ΔPro 1 MAMSSFLINSNYVDPKFPPCEEYSQSDYLPSDHSPGYYAGGQRRESSFQPEAGFG 55
Hoxb4-Pbx 1 MAMSSFLINSNYVDPKFPPCEEYSQSDYLPSDHSPGYYAGGQRRESSFQPEAGFG 55
Hoxb4-cDel 1 MAMSSFLINSNYVDPKFPPCEEYSQSDYLPSDHSPGYYAGGQRRESSFQPEAGFG 55
Hoxb4-HD 1 MAMSSFLINSNYVDPKFPPCEEYSQSDYLPSDHSPGYYAGGQRRESSFQPEAGFG 55

56 RRAACTVQRYAACRDPGPPPPPPPPPPPPPPPGLSPRAPAPPPAGALLPEPGQRCEAVSSSPPPP 120
56 RRAACTVQRYAACRDPGPPPP---------- 76
56 RRAACTVQRYAACRDPGPPPPPPPPPPPPPPPGLSPRAPAPPPAGALLPEPGQRCEAVSSSPPPP120
56 RRAACTVQRYAACRDPGPPPPPPPPPPPPPPPGLSPRAPAPPPAGALLPEPGQRCEAVSSSPPPP120
56 RRAACTVQRYAACRDPGPPPPPPPPPPPPPPPGLSPRAPAPPPAGALLPEPGQRCEAVSSSPPPP120

121 PCAQNPLHPSPSHSACKEPVVYPWMRKVHVSTVNPNYAGGEPKRSRTAYTRQQVLELEKE 180
77 PCAQNPLHPSPSHSACKEPVVYPWMRKVHVSTVNPNYAGGEPKRSRTAYTRQQVLELEKE 136
121 PCAQNPLHPSPSHSACKEPVVYPAMRKVHVSTVNPNYAGGEPKRSRTAYTRQQVLELEKE 180
121 PCAQNPLHPSPSHSACKEPVVYPWMRKVHVSTVNPNYAGGEPKRSRTAYTRQQVLELEKE 180
121 PCAQNPLHPSPSHSACKEPVVYPWMRKVHVSTVNPNYAGGEPKRSRTAYTRQQVLELEKE 180

181 FHYNRYLTRRRRVEIAHALCLSERQIKIWFQNRRMKWKKDHKLPNTKIRSGGAAGSAGGP 240
137 FHYNRYLTRRRRVEIAHALCLSERQIKIWFQNRRMKWKKDHKLPNTKIRSGGAAGSAGGP 196
181 FHYNRYLTRRRRVEIAHALCLSERQIKIWFQNRRMKWKKDHKLPNTKIRSGGAAGSAGGP 240
181 FHYNRYLTRRRRVEIAHALCLSERQIKIWFQNRRMKWKKDH-Stop 221
181 FHYNRYLTRRRRVEIAHALCLSERQIKIWFQSRRMKWKKDHKLPNTKIRSGGAAGSAGGP 240

241 PGRPNGGPRAL 251 (27,6 KDa, 18,6% P)
197 PGRPNGGPRAL 208 (23,4 KDa, 11,6% P)
241 PGRPNGGPRAL 251 (27,6 KDa, 18,6% P)
(24,8 KDa, 18,6% P)
241 PGRPNGGPRAL 251 (27,6 KDa, 18,6% P)

Refence sequences of HOXB4 (protein accession numbers,www.ncbi.nlm.nih.gov**):**

Human (NP_076920.1), chimpanzee (XP_001173043.1), dog (XP_851159.1), cow (NP_001071582.1), mouse (NP_034589.1), rat (XP_573184.1), chicken (NP_990624.1), zebrafish (NP_571193.1).

pEcopac: A packaging vector coding for the gag, pol, and env viral proteins. (Clontech, Palo Alto, CA).

pGEM®-T Easy Vector: A cloning vector to amplify PCR products, encoding beta-lactamase (Promega Corporation, Madison, WI, USA).

2.5 Antibodies

Name	Company	Label	Dilutions
Gr-1	BD Pharmingen, Heidelberg	PE/APC	1:500
CD11b (Mac1)	BD Pharmingen, Heidelberg	PE/APC	1:800
Sca-1	BD Pharmingen, Heidelberg	PE	1:150
Ter119	BD Pharmingen, Heidelberg	PE	1:150
B220	BD Pharmingen, Heidelberg	PE/APC	1:200
CD4	BD Pharmingen, Heidelberg	PE	1:150
CD117 (c-kit)	BD Pharmingen, Heidelberg	APC	1:500
CD8	BD Pharmingen, Heidelberg	APC	1:150

CD3	BD Pharmingen, Heidelberg	PE	1:200
CD45.1 (Ly 5.1)	BD Pharmingen, Heidelberg	Biotin	1:200
CD90.1/Thy1.1	BD Pharmingen, Heidelberg	APC	1:200
CD135/Flk-2	BD Pharmingen, Heidelberg	PE	1:200
HOXB4 (N-18), goat	Santa Cruz Biotech. Inc., CA	-	1:100
GFP	Molecular Probes Inc., OR	-	1:5000
Anti-FLAG M2	Sigma-Ald. Inc., St Louis, MO	-	1:3000
N-term. FLAG-BAP	Sigma-Ald. Inc., St Louis, MO	-	Ctrl.
Anti-actin (I-19)	Santa Cruz Biotech. Inc., CA	HRP	1:200
Goat Anti-Mouse	Invitrogen, Carlsbad, CA	HRP	1:2000
Anti-Goat	Santa Cruz Biotech. Inc., CA	HRP	1:500
Anti-goat	Invitrogen, Carlsbad, CA	Alexa	Fluor®488
Anti-mouse	Invitrogen, Carlsbad, CA	Alexa	Fluor®555

2.6 Reagents, media and apparatus

2.6.1. Molecular biology

Agarose: Molecular biology tested (Sigma-Aldrich, St. Louis, MO).

Acrylamid-Bisacrylamid: 30% solution (29:1), Rotiphorese® (Roth, Karslruhe, Germany)

Ammonium persulfate: 10% solution in water (Fluka, Buchs, Schweiz).

Bradford reagent: Bio-Rad protein assay dye (Bio-Rad, Hercules, CA, USA).

Bromphenol blue: 4X solution for protein loading (Sigma-Aldrich, St. Louis, MO).

BSA: Bovine serum albumin (NEB, Beverly , MA, USA).

1,4-Dithiothreitol: or Clelands reagent, antioxidant reagent (Sigma-Aldrich, St. Louis, MO).

EDTA: (ICN Biomedicals, Aurora, OH, USA).

Enzymes: Ligase, Calf intestine phosphatase, *Xho I, KpnI, NdeI, Xba, PmlI, DpnI, Eco RI, PstI* (New England Biolabs, Beverly, MA).

Ethidium bromide: stock solution 10 mg/ml (Roth, Karlsruhe, Germany).

Ethanol, Methanol, and Isopropanol (Merck, Darmstadt, Germany).

DNeasy mini kit: Genomic DNA extraction kit for small cell numbers (Qiagen GmbH, Hilden, Germany).

Small-scale plasmid preparation: GFX miniprep kit for isolation of plasmid DNA from bacteria (Amersham Biosciences GmbH, Freiburg, Germany)
Gel Elution of DNA and PCR or DNA clean up: GFX gel elution and PCR purification kit for DNA elution from gels and clean up of PCRs (Amersham Biosciences GmbH, Freiburg, Germany).
Propidium Iodide: nucleic acid stain, stock solution 1 mg/ml (Sigma-Aldrich, St. Louis, MO).
Protamine sulfate: (Salamine) from Salmon, cell culture tested, 5 mg/ml stock solution (Sigma-Aldrich, St. Louis, MO).
Protein G-Sepharose: immunoglobulin binding protein (Invitrogen Carlsbad, CA, USA).

Southern blot: Microspin S-300 HR columns and Megaprime DNA labeling system (Amersham Biosciences GmbH, Freiburg, Germany).
Pre-hybridization solution: 0.2 g skimmed milk and 2.0 g dextran sulphate were dissolved in 17 ml water and 6ml 20 X SSC, 2 ml formamide, 1 ml 20% SDS and 80 µl 500 mM EDTA were added to the mixture. (All chemicals were individually obtained from Sigma-Aldrich, St. Louis, MO).
Denaturation solution: A solution of 1.5 M NaCl, 0.5 N NaOH in water.
20X SSC: 175.3 g sodium chloride and 88.2 g sodium citrate were dissolved in 800 ml deionised water and pH adjusted to 7.0 and the final volume to one liter.
DNA Crosslinking: GS Gene linker UV chamber (BIO-RAD Laboratories, Hercules, CA)

Western blot: ECL Western blotting analysis system (Amersham Biosciences GmbH, Freiburg, Germany).
Gel blotting membrane**:** Protran® BA 85 (Schleicher und Schnell, Dassel, Germany).
Gel blotting paper**:** GB003 pore size 0,45 µm (Schleicher und Schnell, Dassel, Germany).
Skim milk powder: **(**Merck KGaA, Darmstadt, Germany).
Tween: (Merck KGaA, Darmstadt, Germany).
Orthovanadate: protein phosphatase inhibitor, stock solution 100 mM (Sigma-Aldrich, St. Louis, MO).

PMSF: phenylmethylsulfonyl fluoride, protein phosphatase inhibitor, stock solution 100 mM (Sigma-Aldrich, St. Louis, MO).
Aprotinin: protease inhibitor, stock solution 10 mg/ml (Sigma-Aldrich, St. Louis, MO).
Acrylamide/bisacrylamide: Rothiphorese® Gel 30% (37.5:1)

Total RNA and genomic DNA isolation: Total RNA isolation reagent (TRIzol®) and Genomic DNA isolation reagent DNAzol® (Invitrogen, Carlsbad, CA). Alternatively, the RNA has been purified using the RNeasy Mini kit (Qiagen GmbH, Hilden, Germany).
Molecular weight markers: Nucleic acid size standards, 1 kb ladder, 1 kb plus ladder and 100 bp ladder (Invitrogen, Carlsbad, CA), Rainbow.
RT and PCR: Platinum® *Taq* DNA polymerase kit, *Pfu* Turbo DNA polymerase, ThermoScript™ kit, RT-PCR kit and *DNaseI* DNA inactivating enzyme kit (all from Invitrogen, Carlsbad, CA); PCR soft tubes (0.2 ml) (Biozym Scientific GmBH, Hessisch Oldendorf, Germany).
Real time PCR kit: LightCycler® FastStart DNA Master SYBR green I kit (Roche Diagnostics, Mannheim, Germany), LightCycler® Carousel and carousel centrifuge (Roche Diagnostics, Mannheim, Germany).
dNTP mix: 10 mM each of dATP, dTTP, dCTP and dGTP (Invitrogen, Carlsbad, CA).
TEMED: Tetramethylethylenediamine (Bio-Rad, Hercules, CA, USA).

2.6.2 Cell and tissue culture

Ammonium chloride: RBC lysis buffer, 0.8% NH_4Cl, 0.1 mM EDTA (Stem Cell Technologies, Vancouver, Canada).
Ampicillin: stock solution 100 mg/ml in water; working solution 100 µg/ml in LB medium (Roth, Kalrsruhe, Germany).
Hepes Buffered Saline: (HBS) (Invitrogen, Carlsbad, CA).
Filtration units: Millex syringe driven filter units 0.22 µm and 0.45 µm filters (Millipore, Billerica, MA).
Methylcellulose media: MethoCult® M3434 for the culture of myeloid CFC assays (Methylcellulose in Iscove's MDM, Fetal Bovine Serum, Bovine Serum Albumin, rh-Insulin, Human Transferrin (Iron saturated), 2-Mercaptoethanol, L-glutamine,

rm-Stem Cell Factor, rm-IL-3, rh-IL-6, rh-Erythropoietin) and MethoCult® M3630 for the pre-B CFC assays (Methylcellulose in Iscove's MDM, Fetal Bovine Serum, 2-Mercaptoethanol, L-glutamine, rh-IL-7) (Stem Cell Technologies, Vancouver, Canada).

Cell strainer: BD Falcon 40 µm Nylon strainer for macerating the spleen and filtering the tissue (BD Biosciences, Palo Alto, CA).

Cell scrapers: 25 cm sterile cell scrapers (Sarstedt, Newton, NC).

Cell culture pipettes: Sterile disposable pipettes (2, 5, 10 and 25 ml)(Corning Inc., Corning, NY).

Cell culture plates and dishes: Sterile 96 well, 24 well, 6 well plates (Sarstedt, Numbrecht, Germany) 100 mm x 20 mm dishes for adherent cells (Corning Inc., Corning, NY), and Petri dishes for suspension cells (Becton Dickinson Labware, Franklin Lakes, NJ) 150 mm x 20 mm dishes for adherent cells (Greiner Bione, Frickenhausen, Germany).

Calcium Chloride: solution for transfection, 2.5 M $CaCl_2$ (Sigma-Aldrich®, St. Louis, MO) solution in water.

DMSO: dymethylsulfoxide (Merck, Darmstadt, Germany).

Hepes Buffered Saline**:** (HBS) (Invitrogen, Carlsbad, CA).

Media: Dulbecco's Modified Eagle's Medium (DMEM) 4,5 g/l glucose, l-glutamine, sodium pyruvate and 3,7 g/l $NaHCO_3$ (PAN biotech GmbH, Aidenbach, Germany).

Fetal Bovine Serum (FBS): 0.2 µm-filtered mycoplasma screened (PAN Biotech GmbH, Aidenbach, Germany).

Dulbecco's phosphate buffered saline (DPBS): without magnesium and calcium, sterile filtered (PAN Biotech GmbH, Aidenbach, Germany).

Trypan Blue: cell viability stain, 0.4% solution (Sigma-Aldrich®, St. Louis, MO).

Trypsin – EDTA: 1 X in HBS without calcium and magnesium with EDTA (Invitrogen, Carlsbad, CA).

Penicillin/Streptomycin: Antibiotic solution with 10,000 U/ml Pen G sodium and 10,000 µg/ml Streptomycin sulfate in 0.85% saline. Used 5 ml per 500 ml medium bottle (Invitrogen, Carlsbad, CA).

Murine cytokines: recombinant m-IL3, m-IL6, m-SCF, m-G-CSF, m-M-CSF and m-GM-CSF (lyophilized) (Tebu-bio, Offenbach, Germany).

Ciprobay®: Ciprofloxacin 400 mg solution, (Bayer AG, Leverkusen, Germany).

LB medium: lysogeny broth/Luria-Bertani medium for bacterial culture, pH 7; Agar for culture plates, 15g/l (GIBCO-BRL, Grand Island).
Valproic acid: stock 155 (Sigma-Aldrich®, St. Louis, MO).

2.6.3 Miscellaneous

X-gal**:** 5-brom-4-chlor-3-indoxyl-β-D-galactosidase, stock solution 100 mg/ml, colorimetric substrate of beta-galactosidase (Roth, Karlsruhe, Germany)
IPTG: isopropyl-β-D-thiogalactopyranosid, stock solution 0.5 M, lactose analogue (Roth, Karlsruhe, Germany)
Giemsa: Giemsa's Azure Eosin Methyleneblue solution modified. (Merck KGaA, Darmstadt, Germany).
May-Gruenwald: May-Gruenwald's Eosin Methyleneblue solution for microscopy (Merck KGaA, Darmstadt, Germany).
Cytospin apparatus: Cytospin 2 Shandon Apparatus (Thermo Electron Corporation, USA).
Cytospin slides: Marienfield pre-cleaned twin frosted slides for fixing single cell suspensions and blood smears (Marienfield, Lauda-Königshofen, Germany).
Cytospin filter cards: ThermoShandon thick white 5991022 filter cards for cytospins (Histocom AG, Zug, Switzerland).
Cytomat medium: mounting medium for confocal microscopy (DAKO, Glostrup, Germany).
Flow cytometry: BD FACS Calibur System (BD Biosciences, Palo Alto, CA).
Fluorescence Activated Cell Sorting: BD FACS Vantage SE System (BD Biosciences, Palo Alto, CA).
Sequencing mix and apparatus: BigDye Terminator v1.1 Cycle Sequencing Kit and the ABI Prism 310 Genetic Analyzer (Applied Biosystems, Foster City, CA).
Microscope: Leitz Diavert Inverted Microscope (Ernst Leitz Wetzlar GmBH, Wetzlar, Germany).
BioPhotometer: Eppendorf®, Hamburg, Germany.
Irradiation source: ^{137}Cs, Gammacell 40, Atomic energy of Canada Limited Commercial Products.

2.6.4 Software

- The software used for Flow cytometry and FACS sorting was the CellQuest Version 3.1(f) (BD Biosciences, Palo Alto, CA).
- Calculations of survival curve were performed using Sigma Plot 2001 Version 7 (SPSS Inc. Chicago, IL).
- Calculations for the frequency of the competitive repopulating units using the L-Calc Limiting dilution analysis software Version 1.1 (StemSoft Inc., Vancouver, Canada).
- The ABI Prism 310 sequencing software (Applied Biosystems, Foster City, CA) was used for sequencing and analysis of sequences.
- The Openlab software 3.0.8 (Improvision Deutschland, Tübingen, Germany) was used for visualizing and photographic documentation of cell morphology.
- Vector NTI Advance® 9 (Invitrogen) was used to design cloning strategies.
- Primers were designed using the Primer3 program, Whitehead Institute, Massachusetts Institute for Technology, MA (http://frodo.wi.mit.edu/cgi-bin/primer3/primer3_www.cgi).

3. Methods

3.1 Mice maintenance

Parental strain mice were bred and maintained under standard conditions at the animal facility of the Helmholtz Zentrum, Munich. After irradiation and bone marrow transplantation the mice were fed with autoclaved chow and supplied with autoclaved drinking water containing ciprofloxacin and acetic acid and housed in individually vented cage systems. The room temperature was 22±2°C in a relative humidity of 50-60% in a 12 hours light-dark cycle.

3.2 Cloning of constructs

A human Hoxb4 complementary DNA (cDNA) containing the complete Hoxb4 open reading frame was cloned as an *EcoRI* fragment and inserted upstream of the internal ribosomal entry site (IRES) into a murine stem cell virus (MSCV) 2.1 vector (from R. Hawley, Rockville, MD) containing the IRES-green fluorescent protein (GFP) cassette originally provided by P. Leboulch (Boston, MA). As a control, the MSCV vector carrying the IRES-GFP cassette alone was used (GFP virus). For proof of protein expression, the Hoxb4 cDNA was subcloned in frame 3' to the FLAG-site of the pSC plasmid (Clontech, Palo Alto, CA) and then subcloned into a MSCV vector. As a control, the MSCV vector carrying the IRES-GFP cassette alone was used (GFP virus).

3.3 Mutagenesis of Hoxb4 constructs

Site directed mutagenesis has been performed using PCR primers containing the modified sequence in the pre-defined domains. As templates for the mutations the Hoxb4-wt and the Hoxb4-ΔProline mutant (kindly provided by K. Humphries, Terry Fox Laboratory, Vancouver, Canada) have been used. A forward primer containing the point mutation of interest has been designed and used together with a reverse primer containing the wild type sequence. The following PCR reaction has been performed using the high fidelity *Pfu*-Polymerase for 12 cycles of amplification. After this step, the reaction has been cooled below 37°C and 1 µl of *DpnI* restriction enzyme was added to the reaction and incubated at 37°C for 1 h. During this step the *DpnI* enzyme, which is specific to methylated and hemi-methylated DNA, digests the parental DNA template but does not digest the

mutant-synthesized DNA. As most E.coli strains produce methylated DNA, they are not resistant to *DpnI* digestion. Undigested DNA has then been used to transform competent bacterial cells to be amplified and sequenced.

3.4 Transient transfection of packaging cell lines for VCM production

$1.5x10^6$ 293T cells were plated in a 15 cm dish and on the following day used for transient transfection. 4 hours before transfection the medium was replaced with fresh medium. 30 µg plasmid DNA harbouring the gene of interest and 30 µg of retroviral packaging construct Ecopac were added to sterile water up to 1 ml. 100 µl of 2.5M $CaCl_2$ sterile solution were added drop wise to the water-DNA mixture. This was added drop wise to a tube containing 1ml of 2X sterile Hepes buffered saline solution (pH 7.2). This mixture was gently mixed, incubated at room temperature for 3-4 minutes, and finally added drop wise to the medium covering the whole plate and without agitating the plates. After 12 hours (the day after) the medium was slowly changed and 24 hours later the supernatant has been collected for 2 days twice daily. This supernatant containing the newly produced viruses was filtered with a 0.45 µm Millipore filter and stored as viral conditioned medium (VCM) at –80°C for later use or used directly to transduce cell lines or primary murine BM cells. The 293T were after this discharged or lysed for western blot anaysis.

3.5 Preparation of high titer stable virus producing cell lines

$5x10^4$ GP+E86 fibroblasts were plated into a 6 well plates one day prior to transduction. The day after, medium was removed from these cells and 500 µl or 1 ml of freshly produced or thawn VCM was layered on top of the cells with the addition of protamine sulfate at final concentration of 10 µg/ml. Fresh medium was added after 4 hours and the transduction was repeated every 12 hours for three-four times. The cells were cultured for two more days to allow GFP expression. Green fluorescent cells were separated twice using the fluorescent activated cell sorter (FACS), propagated and used as stable virus producing cell lines to transduce murine bone marrow cells. Using this protocol, Hoxb4/GFP, Hoxb4-ΔPro/GFP, Hoxb4-Cdel/GFP, Hoxb4-HD/GFP, Hoxb4-Pbx/GFP, Hoxb4-ΔPro-HD/GFP, Hoxb4-ΔPro-Cdel/GFP, Hoxb4-ΔPro-Pbx/GFP, and GFP positive GP+E86 cell lines were established and used for experiments. The supernatant

of these 100% GFP-positive cells was tested for the amount of virus produced (s. below). When the viral titres of bulk cell lines were low, single cells were sorted into 96 well plates and after expansion their viral titres determined on NIH-3T3. Clones producing highest titres were expanded, frozen and used for experiments.

3.6 Titration of the retroviral conditioned medium (VCM)

For the titration of produced virus $2x10^4$ NIH-3T3 cells were plated per well in 6 well plates. The day after the medium was removed and 500 µl of VCM containing 10 µg/ml protamine sulfate were added. Fresh medium was added after 3-4 hours. The transfection of the cells with fresh VCM was performed every 12 hours (thrice totally). Two days after the last transfection, the cells were analysed for GFP expression at the FACS Calibur. The exact calculation of the virus concentration in the supernatant of the packaging cell lines (multeplicity of infection, m.o.i.) has been calculated with the following formula: $\%GFP^+$ cells x NIH 3T3 cells plated d0 x 2 = viral particles/ml.

3.7 Culture conditions of cell lines and murine bone marrow cells

All the cell lines and primary cells used in this work have been cultured under standard conditions (5% CO_2, 37°C, 96% relative humidity) in a SANYO CO_2 incubator. All the adherent cell lines been cultured in DMEM, supplemented with FBS 10% and 1% P/S (Penicillin/Streptomycin). The suspension cell lines have been cultured in RPMI, supplemented with FBS 10% and 1% P/S. The murine bone marrow cells have been cultured in non-adherent dishes with DMEM supplemented with FBS 15% and 1% P/S in presence of rm-IL3 (6 ng/ml), rm-IL6 (10 ng/ml), and rm-SCF (100 ng/ml). The cell counts have been performed by diluting the cells 1:1 with Trypan Blue and using a Neubauer cell count chamber. The cells have been centrifugated in a Rotanta 46 RC centrifuge at 1000 rpm at room temperature or at 4°C. The cells have been frozen in FBS:DMSO (9:1) and stored in liquid nitrogen.

3.8 Retroviral transduction of primary bone marrow cells

Donors of primary BM cells were ≥ 8 weeks old (C57BL/6Ly-Pep3b x C3H/Hej) F_1 (PepC3) mice. 150 mg of 5-Fluorouracil (5-FU) were injected per kg of mouse body weight to eliminate cycling cells and to enrich for hematopoietic progenitors

cells (Fig. 3.8). On the fifth day following 5-FU injection, these mice were sacrificed and bone marrow was obtained by flushing several times femurs and tibias with 2% serum-supplemented medium. The red blood cells were lysed by resuspending them in 0.8% NH_4Cl/0.1 mM EDTA solution followed by an incubation of 20 minutes on ice. The cells were prestimulated by culturing for 2 days in DMEM supplemented with 15% FBS and a cytokine cocktail (10 mg/ml rm-IL6, 6 ng/ml rm-IL3, and 100 ng/ml rm-SCF). On day 3, suspension and adherent cells from primary culture were collected and the transduction was started by layering them on top of adherent packaging GP+E86 cell lines (co-culture). These adherent cell lines were previously irradiated (40 Gy) and plated on adherent 150 mm x 20 mm dishes one day prior to the transduction. 10 µg/ml protamine sulfate was always added to the medium during viral transduction. After 2 days of co-cultivation on the feeder, the BM cells in suspension were removed gently without disturbing the adherent monolayer of GP+E86 cell line.

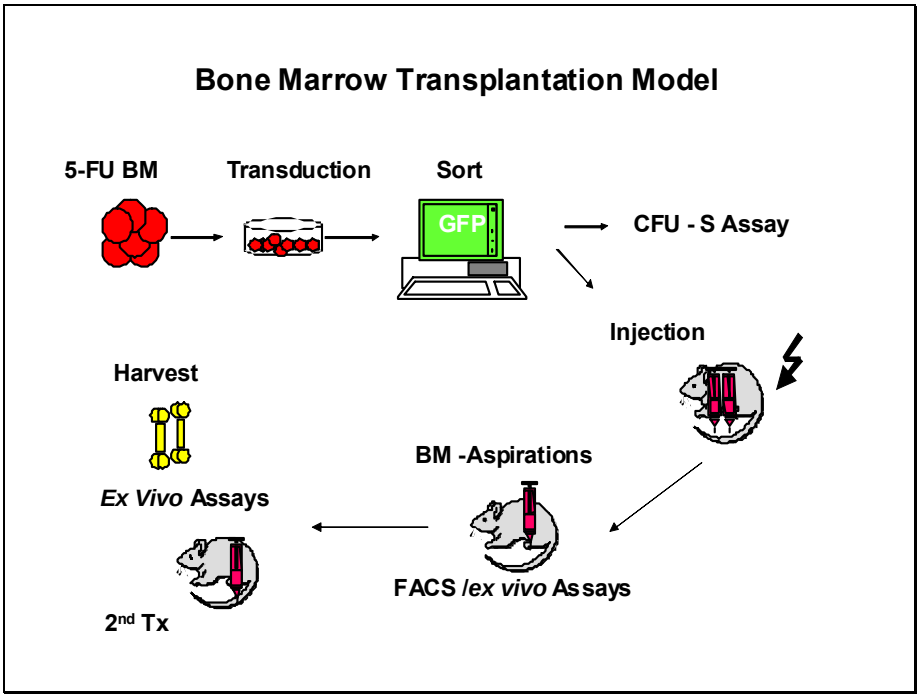

Fig. 3.8. Experimental design of bone marrow transduction and transplantation assay.

The bone marrow cells were cultured in DMEM 15% FBS for two more days to allow GFP expression. On day 7, GFP positive cells were sorted by FACS Vantage and used for bone marrow transplantation or for *in vitro* experiments.

For liquid culture BM cells were maintained in DMEM 15% FBS medium supplemented with 10 mg/ml rm-IL6, 6 ng/ml rm-IL3, and 100 ng/ml rm-SCF.

3.9 Bone marrow transplantation and assessment of mice

As recipients mice ≥ 8 weeks old (C57BL/6J x C3H/Hej) F_1 (B6C3) mice were used. Prior transplantation they were lethally irradiated (0.8 Gy) in a ventilated ^{137}Cs Gammacell 40. Transduced bone marrow or bone marrow from leukemic mice was injected with or without addition of mock non-transduced freshly prepared bone marrow cells intravenously into the tail vein of mice using a sterile 0.5 x 25 mm needle (Table 3.9). Mice were assessed periodically for signs of leukemic symptoms by analysing blood cells obtained from the tail vein using sterile scalpels and heparinized capillaries, by bone marrow aspiration from the femur of anesthetised animals or by the observance of symptoms that included crouching, frizzled body air, paleness in the extremities, heavy breathing and disturbed gait. Mice were considered moribund when one of these symptoms was starkly visible. The RBCs in the peripheral blood were counted by diluting them 1:5000 in PBS, while the white blood cells counts were performed by diluting whole blood 1:25 in ammonium chloride to lyse RBCs and counting living cells after 10 minutes.

Moribund mice were sacrificed by CO_2 asphyxiation and bone marrow was isolated as described before. Spleens were dissected and macerated to produce single cell suspensions and peripheral blood was drawn with a sterile 0.5 x 25 mm needle by puncturing the heart immediately after sacrifice. Red blood cells (RBCs) from peripheral blood, bone marrow and spleen were lysed by incubating the single cell suspensions in ammonium chloride buffer for 10 minutes at room temperature. From BM and spleen cells obtained from primary transplanted mice, secondary recipient mice have been transplanted, and from secondary moribund mice obtained cells, tertiary mice have been finally transplanted.

Experiment no	Gene	Transduced cells	Mock cells
4421	Hoxb4-wt	112500	0
4622 H	Hoxb4-wt	20000	300000
4622 B#4	Hoxb4-wt	2000	300000
3970	Hoxb4-ΔPro	18000000	0
3860	Hoxb4-ΔPro	630000	0
4622 I	Hoxb4-ΔPro	200000	300000
4614 B#2, 2nd	Hoxb4-ΔPro	1200000	0
4614 C#1-4, 2nd	Hoxb4-ΔPro	1000000	0
4614 C#5, 2nd	Hoxb4-ΔPro	500000	0
4577, 2nd	Hoxb4-ΔPro	1000000	1000000
4685, 3rd	Hoxb4-ΔPro	1000000	2000000
4670 C	GFP	10000	300000
4670 B	GFP	50000	300000
4670	GFP	100000	300000
5020	GFP	370000	300000
5029	GFP	1300000	300000
5264	Hoxb4-ΔPro-HD	220000	300000
5331	Hoxb4-ΔPro-HD	300000	300000

Table 3.9. Transplantation conditions of experimental mice.

3.10 FACS analysis of murine primary cells

Purified cells from PB, BM, and spleen of transplanted mice were immunostained with several fluorescence-conjugated antibodies. Staining was performed in PBS containing a 1:200 dilution for each antibody. Samples were incubated for 20 minutes at 4°C in the dark, and subsequently washed with PBS to remove excess of antibody. After centrifugation, cells were resuspended in FACS buffer (2% FBS and 2 µg/ml propidium iodide (PI) in PBS). The antibodies used for FACS staining were recognizing the following surface antigens: Gr-1, CD11b (Mac-1), Sca-1, Ter119, CD4 (all labelled with phycoerythrin, PE, emission 488 nm), and CD11b (Mac-1), CD117 (c-kit), B220, Flk2, Thy1.1, and CD8 (all labelled with allophycocyanin, APC, emission 633 nm). Fluorescence was detected using a FACS Calibur flow cytometer and analysed using the CellQuest software. Dead cells were gated out by high PI staining and forward light scatter.

3.11 *In vitro* and *ex vivo* assays of murine BM cells: proliferation and CFC assays

BM cells were cultured in DMEM supplemented with 15% FBS, 10 mg/ml rm-IL6, 6 ng/ml rm-IL3, and 100 ng/ml rm-SCF, with or without VPA. The cell counts and immunophenotype were assessed after 1 and 2 weeks of proliferation. Myeloid and lymphoid differentiation of clonogenic progenitors was analysed by plating 10^4-10^5 cells in methylcellulose supplemented with cytokines (MethoCult® M3434 for myeloid and MethoCult® M3630 for B-lymphoid differentiation). Re-plating was performed every week in appropriate dilutions.

3.12 Cytospin preparation and May-Grünwald-Giemsa staining

The morphology of cells obtained from liquid culture, CFCs and primary organs of transplanted animals was analysed by performing cytospins. Single cell suspensions in PBS (2-6x10^5 cells per 200 µl) were introduced in the cytospin apparatus and were permanently fixed on glass slides by centrifugation at 500 rpm for 10 min. After air-drying, modified Wright-Giemsa staining was performed by immersing the slides in an undiluted solution of May-Grünwald stain for 5 min. After extensive washing in dH_2O the slides were immersed in 1:50 diluted Giemsa stain for 1 hour. Slides were dipped in water to remove excess stain between the two stainings steps and after the staining procedure and air-dried for observance under the inverted light microscope.

3.13 Histological and immunohistochemical analysis

For histological analysis, the peritoneum of sarificed mice was dissected so as to expose all organs and the blood was drained by aspiration from the heart. The whole mice and single organs were fixed in an aqueous solution of formaldehyde (10% v/v) and sections of selected organs were prepared and haematoxylin-eosin stained using standard protocols. Immunohistochemical analysis has been performed staining the sections with myeloperoxidase antibody (MPO), chloracetate esterase (CAE) and other lineage specific antibodies, such as B220, CD3, CD11b.

3.14 Delta-colony forming unit-spleen (Δ-CFU-S) assay

Primary BM cells were prepared from F_1 donor mice pre-treated with i.v. injected 5-FU (150 mg/kg) 5 days prior to sacrifice, and were transduced as described in 3.8 with the different viruses. Cells were highly purified based on expression of GFP by using FACS-Vantage. 10-4500 transduced cells were incubated for 1 week in DMEM supplemented with cytokines cocktail (rm-IL3, rm-IL6, and rm-SCF) with or without VPA 1 mM. After 1 week the cells were intravenously injected into lethally irradiated F_1 (B6C3) recipient mice. At day 12 post-injection the mice were sacrificed and the spleens were immersed in Telleyesnickzky´s solution. After few minutes the Δ-CFU-S were counted as macroscopic white colonies visible on the spleens.

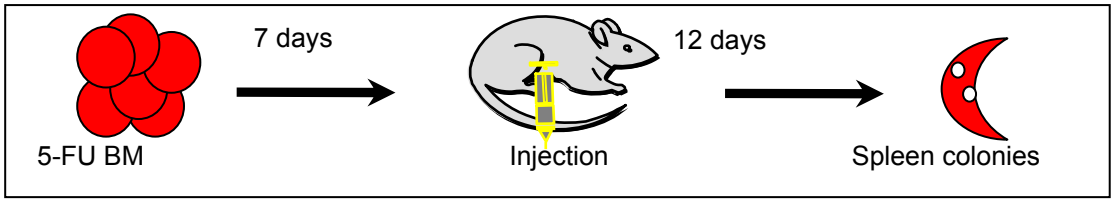

Fig. 3.14. Δ-CFU-S assay.

3.15 Quantification of competitive repopulating units (CRU-assay)

Primary BM cells from F_1 (PepC3) donor mice that had been primed 5 days in advance with i.v. injection of 150 gm/kg 5-fluorouracil were transduced (as described in 3.8) with the different viruses and cells were highly purified based on GFP expression using FACS-Vantage. GFP^+ cells have been injected into lethally irradiated recipient mice in serial dilutions, in order to calculate the frequency of HSCs in the 5-FU BM population that were able to give rise to a normal hematopoietic system in recipient mice. $3x10^5$ native mock bone marrow cells from a syngeneic mouse were additionally injected for radioprotection. 16 weeks post transplantation the mice have been assessed for engraftment (a mouse was considered engrafted when >1% of peripheral blood WBCs were GFP^+ originating from the donor cells). The multilineage engraftment was assessed by measuring the chimerism in the WBCs for each lineage (within each lineage, >1% of the WBCs originated from the GFP positive transplant) (according to K. Humpries et al).The frequency of the hematopoietic repopulating unit was calculated using the L-Calc limiting dilution analysis software.

3.16 Total RNA / genomic DNA isolation and cDNA preparation

For the purification of RNA the Trizol method and RNeasy Mini kit (Quiagen) were used following the instructions of manufacturers. Each RNA sample was treated with *DnaseI* to remove genomic DNA contaminating the sample according to manufacturer´s instructions (Invitrogen). Equal amounts of RNA as quantified by spectrophotometer were added to each reaction (in a set) used for cDNA synthesis for semi-quantitative PCRs. cDNA was prepared from *DnaseI* treated RNA. First strand cDNA synthesis was done with Thermoscript RT-kit (Invitrogen). In 20 µl reaction volume, 1 µg RNA and 50 pmoles of oligo (dT) were mixed to a final volume of 11 µl and incubated 10 min. at 65°C. Four µl of 5X first-strand buffer, 2 µl of DTT 0.1M, 1 µl of 10mM deoxynucleotide triphosphate mix, and 2 µl of Thermoscript reverse Transcriptase were added. The samples were finally incubated for 1 h at 50°C and used for PCR reactions. Genomic DNA was isolated from a minimum of 10^5 - 10^7 cells from various murine organs using DNAzol® reagent (Invitrogen). The DNA was finally resuspended in sterile distilled water and quantified using a Biophotometer (Eppendorf).

3.17 Southern blot

Southern blot analysis was performed in order to assess proviral integration. gDNA was isolated from at least 10^7 cells from bone marrow, spleen and peripheral blood of transplanted mice using DNAzol® reagent. Southern blot was performed using standard protocols. DNA was digested overnight with *PstI*, which cuts the proviral DNA once, to release a fragment specific to the proviral integration site. After digestion DNA was loaded on a 0.8% agarose gel with 0.5 µg/ml ethidium bromide. After 5-6 hours of electrophoresis, the DNA was depurinated by soaking the gel in 0.2 N HCl for 10 min., and subsequently for 1 h in denaturation buffer. After denaturation, DNA was transferred overnight on zeta-Probe GT membrane by capillary action in 10x transfer buffer. Cross-linking of the DNA with the membrane was done by incubating the membrane at 150 mJ in a UV gene linker. The probe used was a 700 bp GFP fragment, which was digested out from the pEGFP-C1 plasmid and labelled with α-^{32}P dCTP using Megaprime DNA labelling system (Amersham). Probe was purified using Microspin S-300 HR columns. Hybridization was done with α-^{32}P GFP labeled overnight at 62°C. After two rounds of washing, the membrane was dried,

covered with a plastic film and placed in a cassette for exposure of the film. The film was placed on the membrane in a dark room and the exposure was done at variable exposing times between 24 hours and one week, depending on the intensity of signal observed.

3.18 Integration analysis: bubble LM-PCR

Integrated LTR and flanking genomic sequences were amplified and isolated using a modification of the bubble LM-PCR strategy (Schessl 2005). 40 pg of the genomic DNA from leukemic and normal mice were digested with *PstI*, and the fragments obtained were ligated overnight at room temperature to a double stranded bubble linker prior to performing a first PCR (PCR-A) on 10 µl (one-tenth) of the ligation product using a linker specific Vectorette primer and an LTR-specific primer. The PCR was performed under the following conditions: one cycle at 94°C for 2 minutes, 20 cycles at 94°C for 30 seconds and 65°C for 1 minute, and one cycle at 72°C for 2 minutes. The bubble linker contains a 30-nucleotide non-homologous sequence in the middle region that prevents binding of the linker primer in the absence of minus strand generated by the LTR-specific primer. 1 µl of the PCR-A reaction was used as template for a second nested PCR (PCR-B) using an internal LTR-specific primer and the same linker-specific Vectorette primer as it was used in PCR-A. 10 µl (one-half) of the final PCR-B product was then separated by electrophoresis using 2% agarose TAE gel. Individual bands were excised, the DNA fragments purified and cloned into pGEMT-easy Vector before sequencing the integration site of the retrovirus in the murine genome. BLAST searches were performed using the genome project website form the University of California, Santa Cruz (UCSC) (http://genome.uscs.edu) to identify the genomic location of the flanking sequences. Identified genomic loci were screened using the retroviral tagged cancer genes databases (RTCGDmm7) custom track on the UCSC Genome browser (August 2005 assembly).

3.19 Western blot

The protein expression was assessed using the stable transfected GP+E86-Hoxb4 and the transient transfected 293T-Hoxb4 cell line. 293T cells from an 80% confluent 15 mm cell culture dish (5-10x10^7 cells) were transiently

transfected with 10 µg of pGFP, pGFP-Hoxb4 and Hoxb4-mutated DNA constructs. The cells were lysed using 150 µl RIPA buffer with fresh added protease inhibitors and detached using a cell culture scraper. This suspension was mixed by inversion and incubated for 30 minutes at 4°C. After sonification, the sample was centrifuged at 1400 rpm for 30 minutes. After centrifugation, the supernatant was transferred to a new Eppendorf tube and either frozen at –80°C, or kept on ice for determination of protein concentration. The Bradford method was used for measuring the protein concentration. The assay is based on the observation that the absorbance maximun for an acidic solution of Comassie Brilliant Blue G-250 shifts from 465 nm to 595 nm when binding to protein occurs. Both hydrophobic and ionic interactions stabilize the anionic form of the dye, causing a measurable color change. The assay is useful since the extintion coefficient of a dye-albumin complex solution is constant over a 10-fold concentration range. Within the linear range of the assay (5-25 µg/ml), there is a linear correlation between the protein present and the Comassie binding. The protein concentration of the sample was determined by comparison to values obtained from the measure of the known range of protein standards (here bovine serum albumin (BSA) was used). Different albumin dilutions (2.5 µg, 5 µg, 10 µg, 15 µg, 20 µg, and 25 µg/ml) were further diluted in distilled water to a final volume of 800 µl. One µl of cell lysate was diluted in distilled water for the measure. 200 µl of protein assay solution was added to the tubes. The tubes were incubated at r.t. for 15 minutes and the content was further transferred to dedicated cuvettes. The determination of the standard curve of the spectrophotometer with distilled water and the protein standards was done using the specific program for estimation of protein concentration in the spectrophotometer used.

Total cell extract proteins were separated on a denaturing gel consisting of 14% SDS-polyacrylamide Tris-glycine separating gel and a 5% SDS-polyacrylamide stacking gel. The concentration of the separating gel was chosen considering the size of wt Hoxb4 protein (37kDa) as indicated in molecular protocols (Sambrook, 1989). The sample was homogenized and diluted 4:1 with 5x loading buffer and incubated in a Thermoblock for 10 minutes. Ca. 80 µg proteins were loaded on each gel lane. The electrophoresis was performed under 100V for 3 hours at r.t. After the electrophoresis, the membrane, the gel and the filter paper were equilibrated in transfer buffer for 10 minutes at 95°C. For the blotting, the semi-

dried system (Trans-blot SD Cell, Bio-Rad) was used. The system was assembled putting 3 layers of 0.8 mm filter paper on the bottom and on top of the membrane- gel sandwich. The transfer has been performed at constant 250 mA at r.t. for 1.5 hours. After the blotting, the membrane has been incubated with blocking solution (TBS 5% milk) for at least 1 hour at r.t. Subsequently, the membrane has been incubated over night at 4°C in TBS 5% milk containing the corresponding first antibody, goat anti-Hoxb4, mouse anti-Flag peptide, or anti-actin (1:200, 1:3000 and 1:2000 diluted, respectively). The day after, the membrane was washed 3 times with TBS 0.05 % Tween to remove the unbounded antibody, and incubated with the HRP-labeled secondary antibody, anti-goat or anti-mouse (1:500 and 1:2000 diluted, respectively) for 1 hour at r.t.. Again the membrane was washed 3 times with TBS 0.1 % Tween and finally incubated with the ECL solution for 5 minutes. The bounded antibodies were then detected by incubating the membrane with an ECL-film in a dark room for 3-5 minutes.

3.20 Immunoprecipitation

Immunoprecipitation (IP) is a method that uses the antigen-antibody reaction principle to identify a protein that reacts specifically with an antibody from mixture of proteins so that its quantity or physical characteristics can be examined. The immunoprecipitation experiments have been performed like previously described (Sambrook 1989). The proteins from the cellular or tissue homogenates were precipitated in RIPA lysis buffer. After centrifugation the supernatants have been incubated with protein A- or G-agarose for at least 3 hours in order to reduce background caused by non-specific adsorption of irrelevant proteins to the agarose. After centrifugation, the supernatant has been pre-incubated for at least 1 hour at 4°C with the specific antibody, e.g. anti-Hoxb4. The protein A- or G-agarose has been then added and the reaction has been incubated at 4°C o.n.. After centrifugation, the immunoprecipited proteins were incubated with loading buffer at 95°C for 10 minutes, centrifugated and further analyzed by SDS-PAGE and immunoblotting to determine their molecular weights and to perform semiquantitative analysis of their expression.

3.21 Polymerase chain reactions

The polymerase chain reactions have been performed following standard procedures: 10x synthesis buffer 2.5 µl, $MgCl_2$ 50mM 0.75 µl, dNTP 10mM 0.5 µl, primer forward 0.5 µl, primer reverse 0.5 µl, *Taq* Polymerase 2.5 U/µl 0.25 µl, H_2O up to 25 µl. PCR conditions: 94°C 2 min., (94°C 30", specific annealing temperature 30", 68°C 30") for 35 cycles, 68°C 5 min. To check the expression of Hoxb4-wt and Hoxb4-ΔPro, we designed internal primers (Hoxb4_inter_fw, Hoxb4_inter_rev), which recognize and amplify 648 bp for Hoxb4-wt and 516 bp for Hoxb4-ΔPro. The PCR reaction has been performed as described above with the addition of 2x Enhancer solution, using the following conditions: 94°C 2 min., (94°C 30", 59°C 30", 68°C 30") for 35 cycles, 68°C 5 min. Alternatively, to check the expression of Hoxb4 mutant missing the first 437 bp and the 5´UTR, we designed an alternative forward primer (Hoxb4-alternEST_fw) binding from nt 438 of the CDS in combination with previously reported reverse primer used to check the full length sequence. The PCR conditions were the same used for the full length. The expected product size was 492 bp. Other primers (Hoxb4_full length_fw, Hoxb4_full length_rev) have been designed to check the expression of the endogenous full length Hoxb4 in cell lines and patients samples. The PCR conditions where: 94°C 2 min., (94°C 30", 58°C 30", 68°C 1-2´) for 35 cycles, 68°C 5 min. Moreover, another set of primers published by Bowles et al have been used under the following conditions: 94°C 5 min., (94°C 30", 55°C 30", 72°C 45") for 35 cycles, 72°C 5 min. The PCR product was 400 bp.

3.22 Immunostaining and confocal laser scanning fluorescence microscopy

For intracellular localization studies, 293T cells were grown on coverslips and transfected with Hoxb4 or FLAG-Hoxb4-ΔProline, FLAG-Hoxb4-Pbx, FLAG-Hoxb4-HD, FLAG-Hoxb4-cDel plasmids, as described above. After 24 hours, cells were fixed with phosphate-buffered saline (PBS) containing 2% paraformaldehyde for 10 min, permealized with PBS 0.1% Triton X for 10 min and blocked with PBS 10% fetal calf serum (FCS) for 1 h. Coverslips were incubated with monoclonal mouse FLAG antibodies (SIGMA) or anti-Hoxb4. Following extensive washing with PBS 0.1% Tween, Alexa 555- and Alexa 488-conjugated secondary -antibodies were added for 1 h. After further washing

steps, cells were stained with DAPI and mounted using Cytomat medium (DAKO, Glostrup, Denmark). Finally, immunostained samples were analyzed in a confocal fluorescence laser scanning system (TCS-SP2 scanning system and DM IRB inverted microscope, Leica, Solms, Germany).

3.23 Statistical analysis

Data were evaluated by using the *t* test for dependent or independent samples (Microsoft EXCEL). Differences of *p* values <0.05 were considered statistically significant. For calculations of frequency of competitive repopulating cells, the L-Calc™ software was used. Cell numbers were entered as doses, the number of mice per cohort as test and the number of engrafted mice as the response for the frequency calculation.

4. Results

4.1 Cloning and expression of Hoxb4 constructs

We sought to determine the effect of constitutive expression of Hoxb4 mutants in hematopoietic stem and progenitor cells upon hematopoietic reconstitution of lethally irradiated mice. For this purpose, a full length Hoxb4 cDNA was subcloned into a MSCV vector with an IRES driven GFP co-expressing cassette to track transduced cells. This vector has been shown to efficiently transduce hematopoietic stem cells and the GFP co-expression enables tracking and purification of transduced cells (Rawat 2004). In each experiment GFP expressing empty vector control transduced cells were used as controls. The Hoxb4-ΔPro mutant was first cloned in frame 3' to the FLAG-site of the pSC plasmid and then cloned into the MSCV vector (Fig 4.1.1, A).

A)

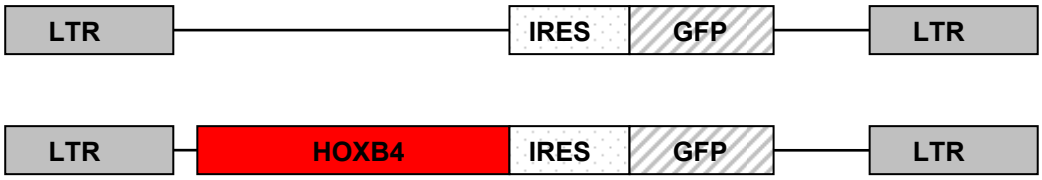

B)

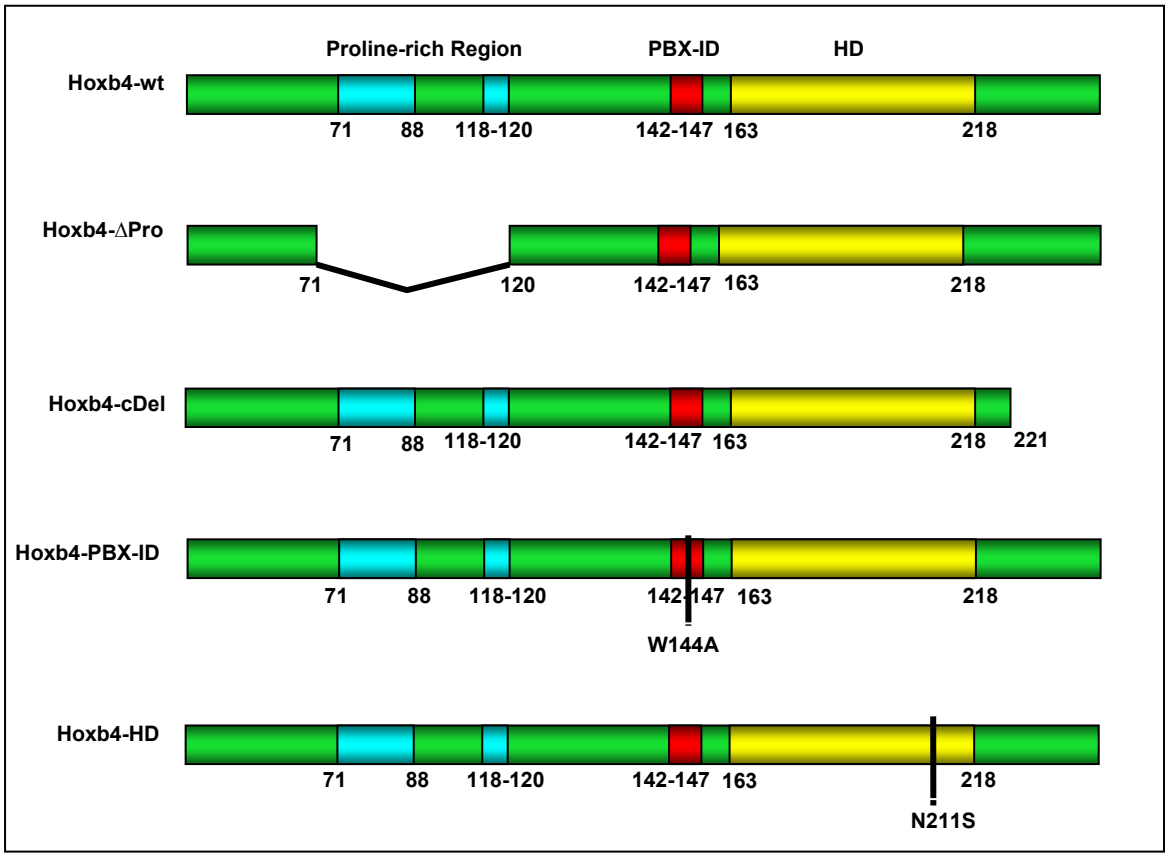

Fig. 4.1.1. A schematic representation of the vectors used for bone marrow transplantation experiments: A) empty vector control and full length Hoxb4 cDNA flanked by long terminal repeat (LTR) sequences. The internal ribosomal entry site (IRES) facilitates co-expression of the GFP. B) The wild type Hoxb4 protein and the obtained mutants used are represented.

The Hoxb4 DNA binding was abolished introducing the point mutation $N^{211}\rightarrow A$ within helix 3 of the homeodomain (Hoxb4-HD mutant), while the direct Hoxb4-PBX interaction was inhibited through the $W^{144}\rightarrow G$ mutation in the conserved tetrapeptide (Hoxb4-PBX mutant), as described before (Beslu 2004). Moreover we generated a mutant where at aminoacidic position 222 a stop codon has been introduced, leading to a truncation of the C terminal sequence of the Hoxb4 protein (Hoxb4-cDel mutant). Additionally, we used a mutant where the aminoacidic sequence between position 78 and 120 is missing (kindly provided by RK Humphries, Vancouver, Canada) (Hoxb4-ΔPro mutant). The Panel B) of Fig. 4.1.1 shows the mutants used in this work. In addition the three last mutations mentioned above have been introduced in the mutant harbouring the proline-deletion. The protein expression of these constructs has been tested on 293T cells lysates (Fig. 4.1.2).

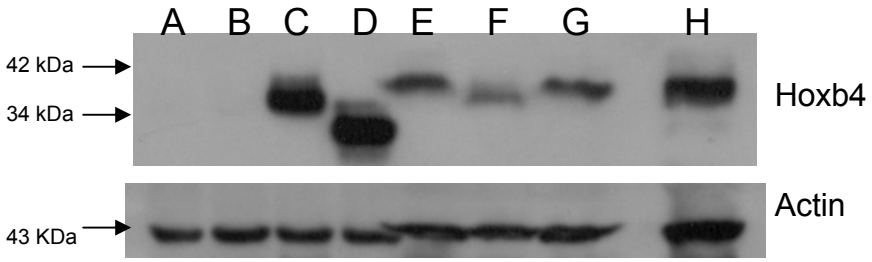

Fig 4.1.2. Protein expression of Hoxb4 constructs in 293T cells. A: 293T cells, B: 293T-GFP cells; C: 293T-Hoxb4-wt, D: 293T-Hoxb4-ΔPro; E: 293T-Hoxb4-PBx; F: 293T-Hoxb4-cDel; G: 293T-Hoxb4-HD; H: K562. The transduction efficiencies in E, F, and G were 50% lower than in A and B.

In order to directly asses the *in vivo* effects of Hoxb4 mutants on transduced hematopoietic cells in syngeneic mice we performed bone marrow transplantation experiments on lethally irradiated murine recipients. Bone marrow cells enriched for stem and progenitor cells by 5-fluorouracil treatment of donor mice were retrovirally transduced with a bicistronic vector encoding the Hoxb4-wt and its mutants or the empty vector and injected into syngeneic recipient mice. Lethally irradiated recipients normally die of bone marrow failure if injected cells fail to engraft the marrow. Following injection of bone marrow cells, it is possible to

assess the effects on stem cell activity as well as the leukemogenic ability of genes retrovirally inserted into these cells.

4.2 Titration of the viral conditioned medium

The transduction of the BM cells has been performed using the supernatant of packaging cell lines. The efficiency of virus production was tested incubating a defined amount of target cells ($5x10^4$ NIH 3T3) with serial dilutions of the supernatant taken from liquid culture of 293T (transient packaging cell lines) or of GP+E86 (stable packaging cell line). After 48 h the percentage of target cells positive for the GFP marker were considered infected and gave a measure of the m.o.i. (multiplicity of infection, viral particles/ml) of the virus-containing supernatant. The efficiency of transfection on NIH3T3 cells was on average 75.5% for GFP control, 60% for Hoxb4-wt, 59% for Hoxb4-Pbx, 50.5% for Hoxb4-ΔPro, 54.2% for Hoxb4-cDel, and 59.5% for Hoxb4-HD.

4.3 Transduction of primary bone marrow progenitor cells

The transduction of bone marrow primary cells has been performed as described in Chapter 3.8. The cells have been obtained by flushing the tibias and femurs of sacrificed 5-FU pre-treated mice. The erythrocytes have been lysed with ammonium chloride and the nucleated cells have been pre-stimulated for 48 hours in the presence of the cytokine cocktail in non-adherent Petri dishes. The cells have been then cultivated for 48-72 hours on a feeder layer of irradiated GP+E86 cell lines producing the different viruses. After the transduction the BM cells have been harvested and cultivated for further 48 hours in non-adherent Petri dishes to allow the expression of GFP protein. Finally, the cells have been then harvested and sorted for GFP expression and used for *in vitro* and *in vivo* assays. The plots below show the transduction efficiencies obtained in representative experiments (Fig. 4.3.1).

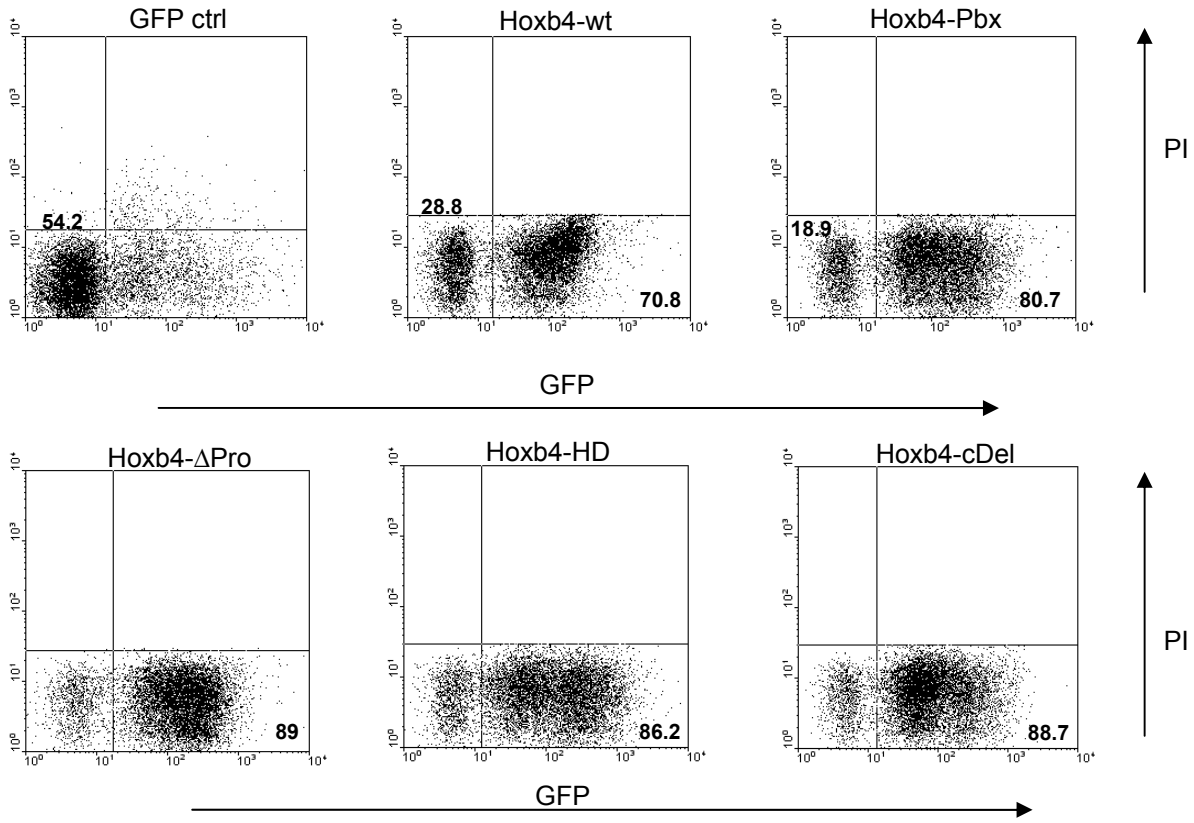

Fig 4.3.1. Transduction efficiencies of 5-FU enriched BM progenitor cells.

4.4 *In vitro* assays

4.4.1 Effect of Hoxb4 and its mutants on liquid expansion of BM progenitor cells

In order to evaluate the effect of the expression of Hoxb4 wild type and its mutants on the proliferation of bone marrow progenitor cells after retroviral transduction and positive selection for GFP marker by FACS, the cells have been grown *in vitro* for 1 week. 10^6 cells have been plated in a 10 cm Petri dish in 10 ml medium (DMEM 15% FBS containing SCF, IL3 and IL6). After 1 week the cells were harvested by collecting the supernatant containing the suspension cells, rinsing the dishes and scraping them in order to collect eventually adherent cells. The cells counts for each mutant are represented in Figure 4.4.1.

The overexpression of the Hoxb4-wt induced an increase in the cells number of 4.2fold and a 1.6fold in comparison to the GFP control ($p<0.012$, $n=7$) and to the Hoxb4-ΔPro mutant ($p=0.352$, $n=5$), respectively. The deletion of the proline rich region led to an increase of 2.6fold of harvested cells in comparison to GFP control ($p<0.17$). The mutation of PBX interacting domain (ID) alone and in

combination with the deletion of the proline rich region led to a decrease in the cell growth (1.69fold, p=0.48 and 2.87fold, p=0.126, respectively) when compared to the Hoxb4-wt. However, we still reported an increase in the number of cells harvested when compared to the GFP control (2.48- and 1.46fold, p=0.330 and p=0.663, respectively). Moreover, the deletion of the homeodomain alone and in combination with the proline region deletion led to a significant decrease of cells output when compared to the Hoxb4-wt (5fold, p=0.094, and 6.2fold, p<0.04, respectively), while it was comparable to the GFP control (0.83- and 0.68fold decrease, respectively, p>0.7). Interestingly, the deletion of the C-terminal region alone or combined with the proline deletion led to a similar significant decrease in cells output in comparison to the Hoxb4-wt (6.4fold, p=0.075, and 4.5fold, p<0.042, respectively), while the cells count was comparable to the GFP control (0.65- and 0.93fold decrease, respectively, p>0.7).

When the cells have been incubated with 1mM VPA for one week, we reported an increase of the harvested cells in GFP ctrl, Hoxb4-wt, Hoxb4-PBX, Hoxb4-cDel and Hoxb4-HD in comparison to the corresponding samples in the absence of VPA ($6x10^7$ vs. $1.57x10^8$, $2.5x10^8$ vs. $3.17x10^8$, $1.5x10^8$ vs. $2.48x10^8$, $3.9x10^7$ vs. $4.18x10^7$, $5x10^7$ vs. $1.03x10^8$ cells, respectively, n.s.). Interestingly, in case of the cells expressing the Hoxb4-ΔPro the incubation with VPA led to a light decrease in the number of harvested cells (Hoxb4-ΔPro $1.58x10^8$ vs. $1.32x10^8$ with VPA, Hoxb4-ΔPro-PBX $8.84x10^7$ vs. $6.66x10^7$, Hoxb4-ΔPro-cDel $5.67x10^7$ vs. $4.9x10^7$, Hoxb4-ΔPro-HD $4.12x10^7$ vs. $2.05x10^7$cells, n.s.). In summary, the proliferative effect induced by VPA was absent when the proline-rich region was deleted.

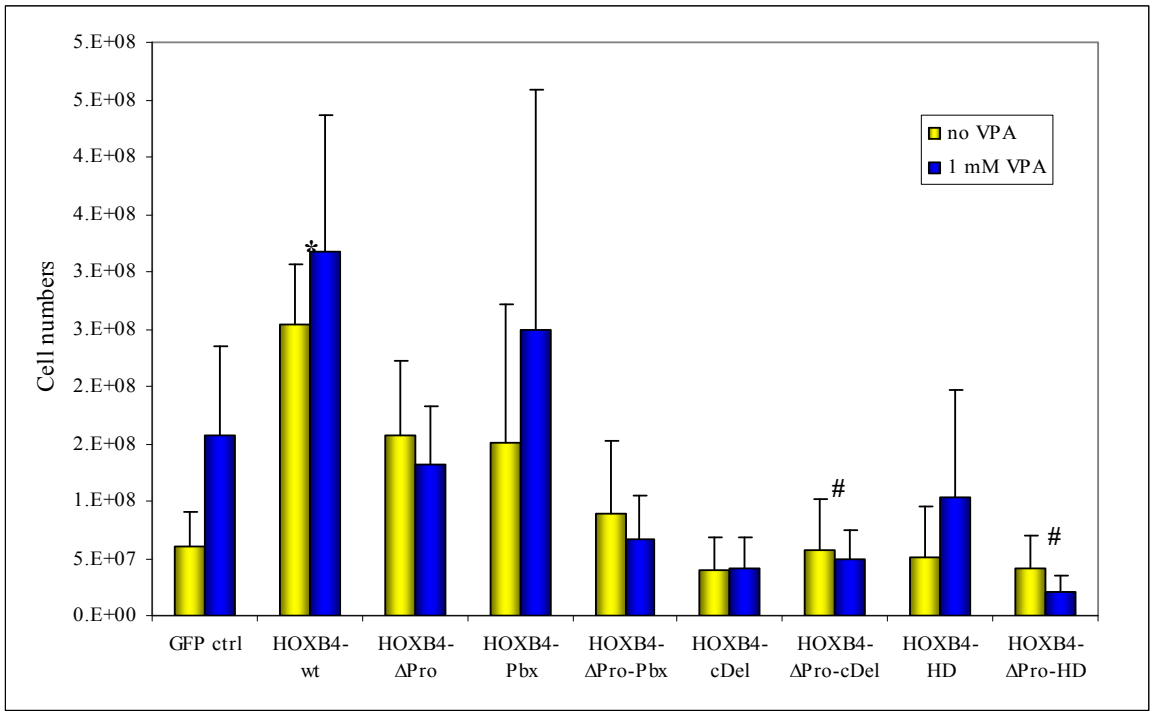

Figure 4.4.1. *In vitro* proliferation assay. Initially plated cells: 10^6. The cells counts after 1 week of liquid culture with and without VPA are reported. * $p<0.05$ vs. GFP ctrl; # $p<0.05$ vs. Hoxb4-wt (n=4).

4.4.2 Immunophenotype of *in vitro* expanded BM progenitor cells

Surface markers Sca-1 and c-kit. After one week of liquid culture in DMEM 15% of FCS, supplemented of IL3, IL6 and SCF, BM cells have been analysed for the expression profile of lineage-specific surface markers.

The percentage of cells positive for the Sca-1 marker was similar in all the samples and in presence of VPA it was overall increased except for the mutants harbouring the homeodomain mutation (Hoxb4-HD and Hoxb4-HD-ΔPro). When considering the absolute number of cells positive for Sca-1, we reported an increase in the number of cells harvested in all the samples in comparison to the GFP control (Hoxb4-wt 6.7fold, Hoxb4-ΔPro 4.8fold), with the exception of Hoxb4-ΔPro-PBX and Hoxb4-HD. The incubation with VPA led to a slight increase of Sca-1^+ cells in almost all the samples, while we reported a decrease of this subpopulation in Hoxb4-wt, Hoxb4-ΔPro-cDel and Hoxb4-ΔPro-HD samples. The deletion of the proline region led in general to a decrease of Sca-1^+ cells in comparison to the corresponding samples still containing the proline region (except for the Hoxb4-HD vs. Hoxb4-ΔPro-HD). Interestingly, the combination of VPA treatment with the deletion of the proline region increased

the number of Sca-1$^+$ harvested cells in all the samples, with the exception of Hoxb4-cDel, in comparison to the corresponding control samples without VPA and without the proline deletion (Table 4.4.2.1a and Fig. 4.4.2.1).

Sample	Sca-1 (%)	Sca-1+VPA (%)	Sca-1 (cells)	Sca-1+VPA (cells)
GFP ctrl	40.92	44.59	$2.8x10^7$	$7.43x10^7$
Hoxb4-wt	40.92	49.1	$1.88x10^8$	$1.85x10^8$ ↓
Hoxb4-ΔPro	39	50.43	$1.37x10^8$	$2.29x10^8$
Hoxb4-PBX	26.96	38.28	$3.85x10^7$	$8.16x10^7$
Hoxb4-ΔPro-PBX	28.97	57.65	$2.72x10^7$	$5.81x10^7$
Hoxb4-cDel	25.65	34.83	$6.15x10^7$	$1.12x10^8$
Hoxb4-ΔPro-cDel	53.83	59.55	$5.32x10^7$	$3.19x10^7$ ↓
Hoxb4-HD	35.07	30.43 ↓	$7.29x10^6$	$3.62x10^7$
Hoxb4-ΔPro-HD	59.5	57.35 ↓	$3.01x10^7$	$1.17x10^7$ ↓

Table 4.4.2.1a. Sca-1 positive cells in liquid culture after 1 week (n=3). Arrows indicate comparison with corresponding samples without VPA, respectively.

The proportion of cells positive for c-kit was in almost all the samples lower than in the GFP control, except for Hoxb4-ΔPro-cDel and Hoxb4-ΔPro-HD. However, the c-kit$^+$ absolute cells numbers were still higher than in the GFP control, except for Hoxb4-PBX, Hoxb4-ΔPro-PBX, Hoxb4-HD and Hoxb4-ΔPro-HD. The VPA led to a decrease of the proportion and of absolute number of the c-kit$^+$ cells in all the samples vs. the corresponding samples without VPA, except for Hoxb4-ΔPro-PBX (4fold increase vs. without VPA) (Table 4.4.2.1b). The deletion of the proline-rich region led to a decrease in the number of c-kit$^+$ cells in Hoxb4-ΔPro vs. Hoxb4-wt (1.4fold) and in Hoxb4-ΔPro-PBX vs. Hoxb4-PBX (5.8fold), while in the other samples it increased this subpopulation of cells.

Sample	c-kit (%)	c-kit+VPA (%)	c-kit (cells)	c-kit+VPA (cells)
GFP ctrl	41	14.12	$3x10^7$	$1.47x10^7$
Hoxb4-wt	11.45	4.09	$6.36x10^7$	$1.79x10^7$
Hoxb4-ΔPro	23.98	16.59	$4.28x10^7$	$2.19x10^7$
HoxbB4-PBX	11.44	2.39	$2.56x10^7$	$5.17x10^6$
Hoxb4-ΔPro-PBX	12.71	15.94 ↑	$4.38x10^6$	$1.75x10^7$ ↑
Hoxb4-cDel	16.53	3.58	$5.74x10^7$	$1.18x10^7$
Hoxb4-ΔPro-cDel	74.46	36.47	$6.1x10^7$	$2.6x10^7$
Hoxb4-HD	31.51	5.62	$9.96x10^6$	$5.98x10^6$
Hoxb4-ΔPro-HD	73.2	22.9	$2.91x10^7$	$4.53x10^6$

Table 4.4.2.1b. C-kit positive cells in liquid culture after 1 week (n=3). Arrows indicate comparison with corresponding samples without VPA, respectively.

When considering the proportion of cells positive for both Sca-1 and c-kit markers, the overexpression of Hoxb4-wt led to a 2.4fold increase of double positive harvested cells in comparison to the GFP control (n.s.). The deletion of the proline region led to a decrease of the double positive cells in comparison to the Hoxb4-wt (1.6fold), while they were still higher than in the GFP control (1.5fold). In the GFP control after one week of liquid expansion most of the cells were mast cells (>70%), while in the Hoxb4-wt and Hoxb4-ΔPro we detected a higher proportion of immature blasts (30-40%). The VPA treatment induced a decrease of double positive cells number in the GFP control, Hoxb4-wt, Hoxb4-ΔPro-HD and Hoxb4-cDel, while in Hoxb4-ΔPro and in all the remaining samples VPA induced a partial increase in comparison to the corresponding samples without VPA (Table 4.4.2.1c and Fig. 4.4.2.1).

Sample	c-kit/Sca-1 (%)	d.p.+VPA (%)	d.p. (cells)	d.p.+VPA (cells)
GFP ctrl	15.48	6.93 ↓	$1.88x10^7$	$1.28x10^7$ ↓
Hoxb4-wt	9.35	4.23 ↓	$4.5x10^7$	$1.46x10^7$ ↓
Hoxb4-ΔPro	6.4	4.5 ↓	$2.9x10^7$	$3.22x10^7$
Hoxb4-PBX	8.91	6.09 ↓	$1.59x10^7$	$2.03x10^7$
Hoxb4-ΔPro-PBX	8.9	10.5	$1.27x10^6$	$8.75x10^6$
Hoxb4-cDel	9.9	3.5 ↓	$2.6x10^7$	$1.49x10^7$ ↓
Hoxb4-ΔPro-cDel	32	22.1 ↓	$2.3x10^6$	$2.5x10^6$
Hoxb4-HD	21.9	5.3 ↓	$5.5x10^6$	$6.6x10^6$
Hoxb4-ΔPro-HD	49	2 ↓	$6.36x10^6$	$6.56x10^5$ ↓

Table 4.4.2.1c. C-kit/Sca-1 double positive cells in liquid culture after 1 week (n=3). Arrows indicate comparison with corresponding samples without VPA, respectively. d.p. = double positive.

In summary, from the analysis of these surface markers, which helps to identify the proportion of more primitive progenitor cells, we noticed that the deletion of the proline region did not dramatically affect the number of $Sca1^+$ cells in comparison to the GFP control and the Hoxb4-wt, while this mutation led to an increase in the number of c-kit^+ cells vs. the Hoxb4-wt. Interestingly, the VPA treatment led in general to an increase of Sca-1^+ and to a decrease in the c-kit^+ cells *in vitro* in comparison to the samples without VPA. However, VPA does not significantly affect the proportion of c-kit^+ cells in the samples where the proline region has been deleted.

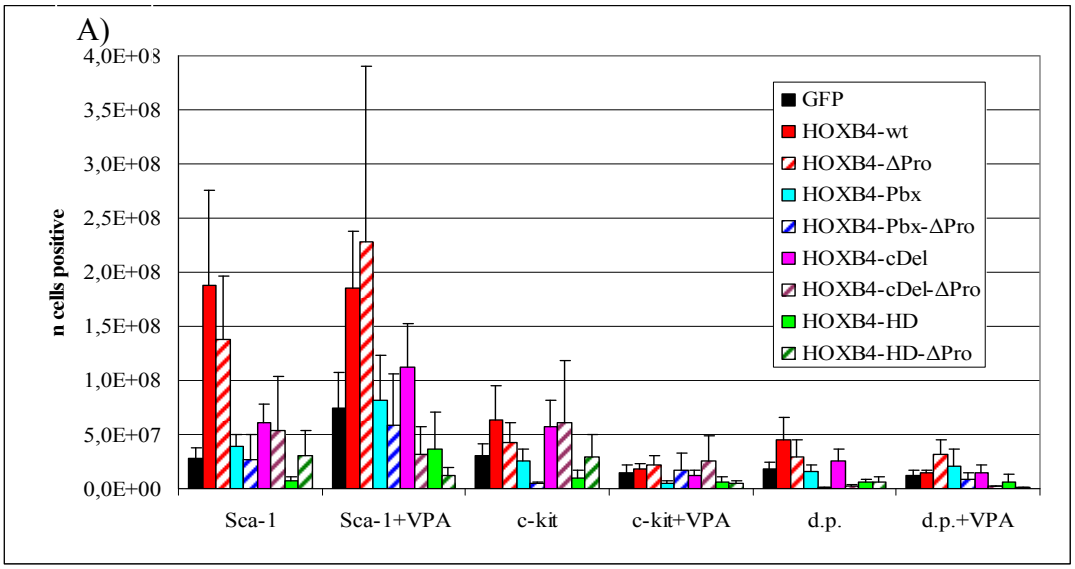

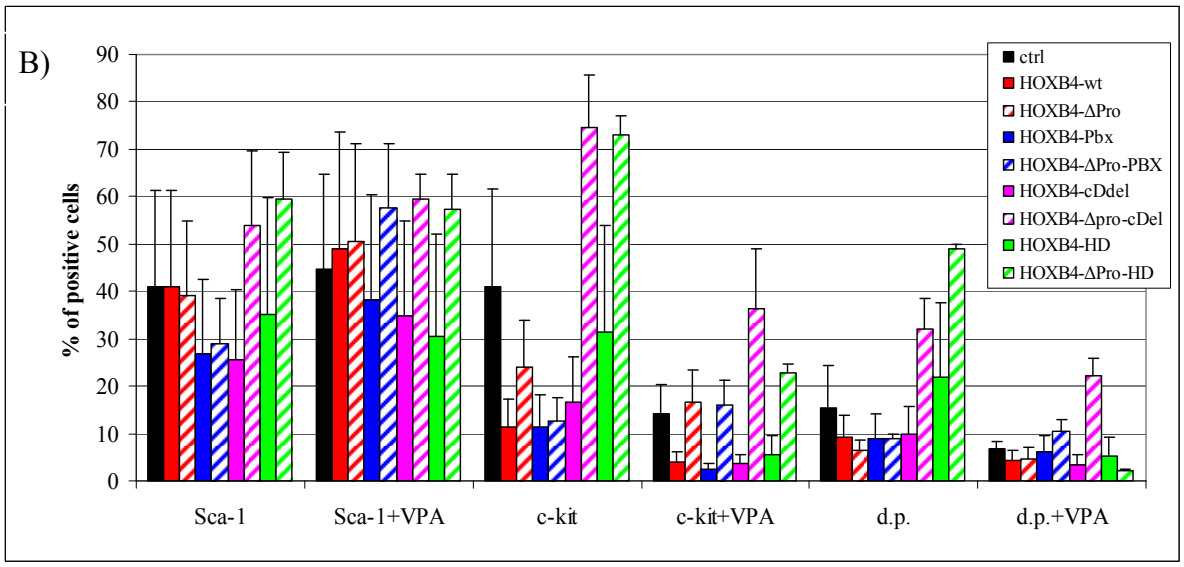

Figure 4.4.2.1. Immunofluorescence staining of BM progenitor cells after 1 week of liquid culture (n=3). A) cell counts; B) cell percentages.

BM myeloid cells surface markers Mac-1 and Gr-1. After 1 week of liquid culture, we analysed the cells for the expression of the myeloid specific surface markers Mac-1 and Gr-1. The deletion of the proline region did not significantly affect the proportion of Mac-1$^+$ cells, however in the samples harbouring this deletion and the double mutations ΔPro-PBX, ΔPro-HD, and ΔPro-cDel we reported a clear decrease in this myeloid subpopulation when compared to the corresponding samples where the proline region was not deleted (Table 4.4.2.1d). In particular, this decrease was significant in the Hoxb4-ΔPro-cDel and in the Hoxb4-ΔPro-HD (6.2- and 6.85fold, $p<0.058$ and $p< 0.012$, respectively) in comparison to the corresponding single mutants Hoxb4-cDel and Hoxb4-HD, as well as in comparison to the Hoxb4-wt (6fold, $p<0.019$, and 4.8fold, $p<0.025$, respectively).

In the presence of VPA the number of Mac-1$^+$ cells was lower in the GFP control, in Hoxb4-wt, in Hoxb4-ΔPro and Hoxb4-ΔPro-PBX in comparison to the corresponding samples without VPA. (Table 4.4.2.1d).

Sample	Mac-1 (%)	Mac-1+VPA (%)	Mac-1 (cells)	Mac-1+VPA (cells)
GFP ctrl	38.81	59.32	$1.9x10^8$	$1.51x10^8$ ↓
Hoxb4-wt	46.97	54.2	$2.95x10^8$	$1.98x10^8$ ↓
Hoxb4-ΔPro	43.15	36.45	$2.79x10^8$	$2.77x10^8$ ↓
Hoxb4-PBX	55.13	49.61	$1.13x10^8$	$1.18x10^8$
Hoxb4-ΔPro-PBX	35.69	32.23	$1.36x10^7$	$7.74x10^6$ ↓
Hoxb4-cDel	47.42	47.99	$2.11x10^8$	$2.14x10^8$
Hoxb4-ΔPro-cDel	7.64	33.36	$6.39x10^5$	$7.35x10^6$
Hoxb4-HD	65.79	37.56	$2.83x10^7$	$3.69x10^7$
Hoxb4-ΔPro-HD	9.74	30.82	$2.09x10^6$	$9.58x10^6$

Table 4.4.2.1d. Mac-1 positive cells in liquid culture after 1 week (n=3). Arrows indicate comparison with corresponding samples without VPA, respectively.

In the GFP control and in all the samples overexpressing a mutated Hoxb4 the number of Gr-1$^+$ cells was lower than in the Hoxb4-wt (Table 4.4.2.1e). In the samples containing the double mutations the number of Gr-1$^+$ cells was lower when compared to the corresponding single mutants and to the GFP control. The treatment with VPA led to a decrease of this myeloid subpopulation, except for the Hoxb4-ΔPro-cDel and Hoxb4-ΔPro-HD, in comparison to the corresponding samples without VPA treatment.

Sample	Gr-1 (%)	Gr-1+VPA (%)	Gr-1 (cells)	Gr-1+VPA (cells)
GFP ctrl	25.81	33.15	$7.14x10^7$	$9.98x10^7$
Hoxb4-wt	25.36	19.35	$2.16x10^8$	$9.22x10^7$ ↓
Hoxb4-ΔPro	28.88	19.13	$2x10^8$	$1.57x10^8$ ↓
Hoxb4-PBX	29.55	16.23	$6.8x10^7$	$3.75x10^7$ ↓
Hoxb4-ΔPro-PBX	28.96	21.89	$9.52x10^6$	$6.81x10^6$ ↓
Hoxb4-cDel	26.54	20.2	$1.37x10^8$	$9.84x10^7$ ↓
Hoxb4-ΔPro-cDel	14.13	30.87	$1.29x10^6$	$8.58x10^6$
Hoxb4-HD	51.97	21.97	$1.69x10^7$	$7.43x10^6$ ↓
Hoxb4-ΔPro-HD	7.1	28.31	$2.63x10^6$	$9.11x10^6$

Table 4.4.2.1e. Gr-1$^+$ cells in liquid culture after 1 week (n=3). Arrows indicate comparison with corresponding samples without VPA, respectively.

In summary, the overexpression of Hoxb4-wt led to a higher number of myeloid cells in comparison to the GFP control (Mac-1$^+$ cells were 2.7fold and Gr-1$^+$ cells

were 3fold higher than in the GFP control), and to all the mutants. The combination of the proline region deletion with all the other mutations, led to a dramatic decrease in the number of myeloid cells (Mac-1$^+$ cells were 21.7fold, 461fold, and 147.5fold less, while Gr-1$^+$ cells were 22.7fold, 167.4fold, and 82fold less in the Hoxb4-ΔPro-PBX, Hoxb4-ΔPro-cDel, and Hoxb4-ΔPro-HD in comparison to the Hoxb4-wt, respectively). On the other hand, the proline region deletion alone, as well as the other single mutations did not significantly affect the number of myeloid cells in comparison to the Hoxb4-wt (Fig. 4.4.2.2).

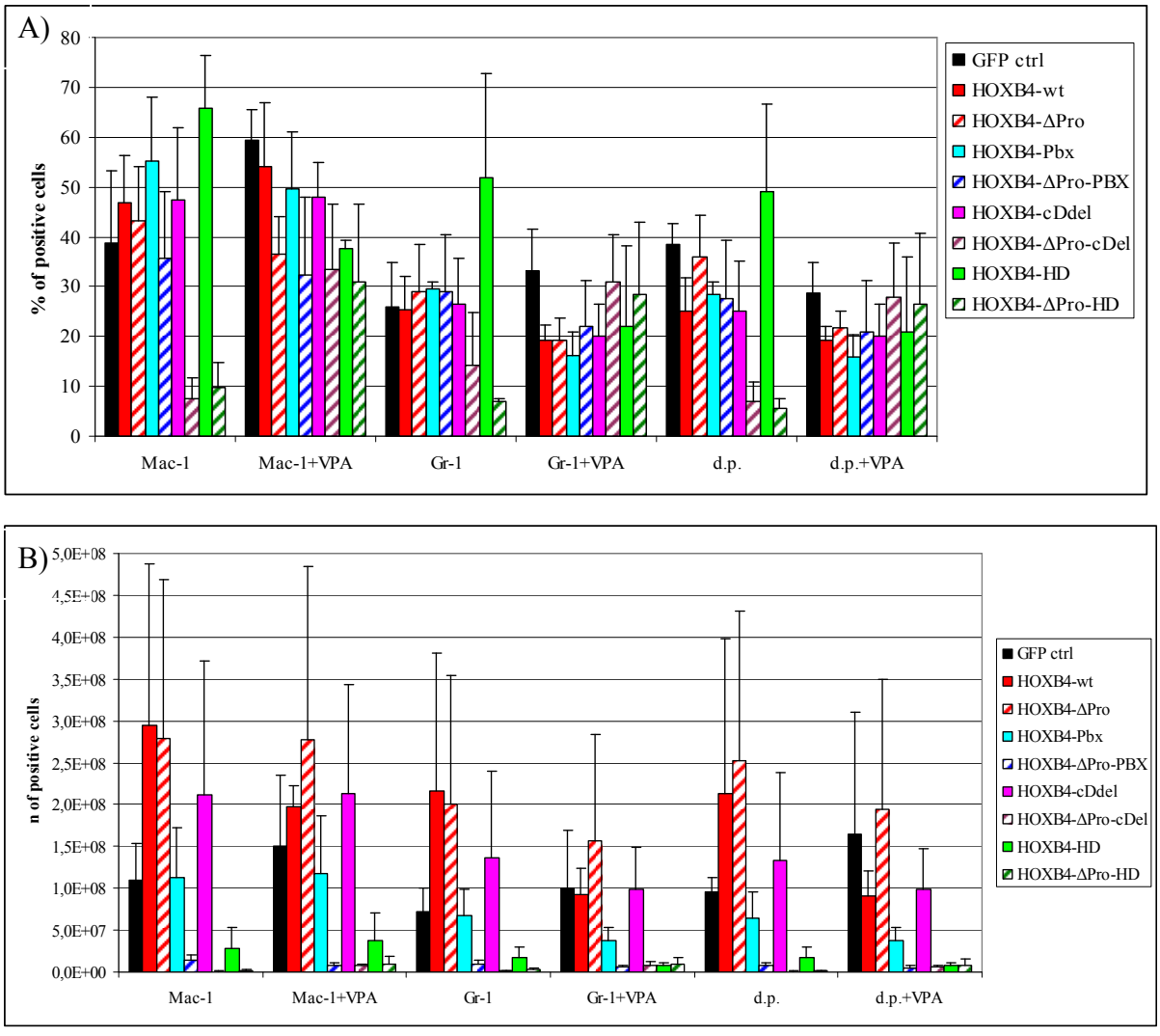

Figure 4.4.2.2 Immunofluorescence staining of BM progenitor cells after 1 week of liquid culture. A) cells percentages. B) cells counts.

BM cells surface markers Ter-119 and B220. After 1 week of liquid culture, we analysed the cells for the expression of the erythroid and lymphoid specific surface markers Ter-119 and B220. In the GFP control, in the samples harbouring the mutations PBX, HD, cDel alone and combined with the proline

deletion we reported a decrease of the Ter119$^+$ cells in comparison to the Hoxb4-wt and to Hoxb4-ΔPro (21-, 7-, 23-, 48-, 57-, 2.7-, and 57fold, respectively). Moreover, in the presence of VPA, we reported a decrease of these cells in the Hoxb4-wt but not in the GFP control, Hoxb4-ΔPro, Hoxb4-ΔPro-cDel, and Hoxb4-ΔPro-HD, in comparison to the corresponding samples without VPA (Table 4.4.2.1f, Fig. 4.4.2.3.).

Sample	Ter119 (%)	Ter119+VPA (%)	Ter119 (cells)	Ter119+VPA (cells)
GFP ctrl	2.54	3.5	$1.85x10^6$	$3.68x10^6$
Hoxb4-wt	3.05	0.43	$3.97x10^7$	$1.26x10^6$ ↓
Hoxb4-ΔPro	4.87	1.79	$4.03x10^6$	$5.06x10^6$
Hoxb4-PBX	5.96	0.26	$5.73x10^6$	$7.05x10^5$ ↓
Hoxb4-ΔPro-PBX	8.15	1.77	$1.7x10^6$	$6.61x10^5$ ↓
Hoxb4-cDel	3.95	0.31	$1.45x10^7$	$1.08x10^6$ ↓
Hoxb4-ΔPro-cDel	5.14	12.41	$7.07x10^5$	$2.46x10^6$
Hoxb4-HD	5.04	0.45	$8.31x10^5$	$3.59x10^5$ ↓
Hoxb4-ΔPro-HD	2.31	2.97	$7.06x10^5$	$1.08x10^6$

Table 4.4.2.1f. Ter-119 positive cells in liquid culture after 1 week (n=3). Arrows indicate comparison with corresponding samples without VPA, respectively.

The number of B220$^+$ cells was similar in the GFP control, Hoxb4-wt, and Hoxb4-ΔPro samples. However in other mutant combinations we saw a significant decrease of these cells when compared to the Hoxb4-wt (Hoxb4-ΔPro-cDel 13.8fold, Hoxb4-HD 57fold, $p<0.05$) and when compared to the Hoxb4-wt+VPA (Hoxb4-PBX+VPA 3.3fold, Hoxb4-ΔPro-PBX+VPA 3.4fold, Hoxb4-ΔPro-cDel+VPA 3.3 fold, Hoxb4-ΔPro-HD+VPA 7fold, $p<0.05$). The B220$^+$ cells in Hoxb4-ΔPro-HD+VPA, Hoxb4-ΔPro-PBX+VPA, and in Hoxb4-ΔPro-cDel+VPA were 24.3fold, 10.2fold, and 9.9fold significantly less than in the Hoxb4-wt sample, respectively ($p<0.05$). The incubation with VPA led to a decrease in the number of B220$^+$ cells in almost all the samples, except for the Hoxb4-ΔPro-cDel, Hoxb4-HD, and Hoxb4-ΔPro-HD samples, in comparison with the corresponding samples without the HDACi (Table 4.4.2.1g, Fig. 4.4.2.3.).

Sample	B220 (%)	B220+VPA (%)	B220 (cells)	B220+VPA (cells)
GFP ctrl	3.7	3.72	$6.61x10^6$	$5.73x10^6$ ↓
Hoxb4-wt	1.73	0.48	$6.78x10^6$	$2.29x10^6$ ↓
Hoxb4-ΔPro	2.43	1.07	$6.07x10^6$	$2.56x10^6$ ↓
Hoxb4-PBX	1.92	0.36	$2.61x10^6$	$6.87x10^5$ ↓

Hoxb4-ΔPro-PBX	5.57	2.05	$1.63x10^6$	$6.64x10^5$ ↓
Hoxb4-cDel	0.8	0.24	$3.05x10^6$	$1.07x10^6$ ↓
Hoxb4-ΔPro-cDel	2.32	2.07	$4.88x10^5$	$6.84x10^5$
Hoxb4-HD	2.17	0.43	$1.18x10^5$	$3.19 x10^5$
Hoxb4-ΔPro-HD	2.97	0.95	$1.06x10^5$	$2.79x10^5$

Table 4.4.2.1g. B220 positive cells in liquid culture after 1 week (n=3). Arrows indicate comparison with corresponding samples without VPA, respectively.

In summary, we observed that the deletion of the proline region led to a decrease in the Ter119$^+$ cells in comparison to the samples where this region was maintained, while the incubation with VPA led to a decrease of Ter-119$^+$ and B220$^+$ cells in almost all the samples in comparison to the corresponding samples without VPA. (Fig. 4.4.2.3).

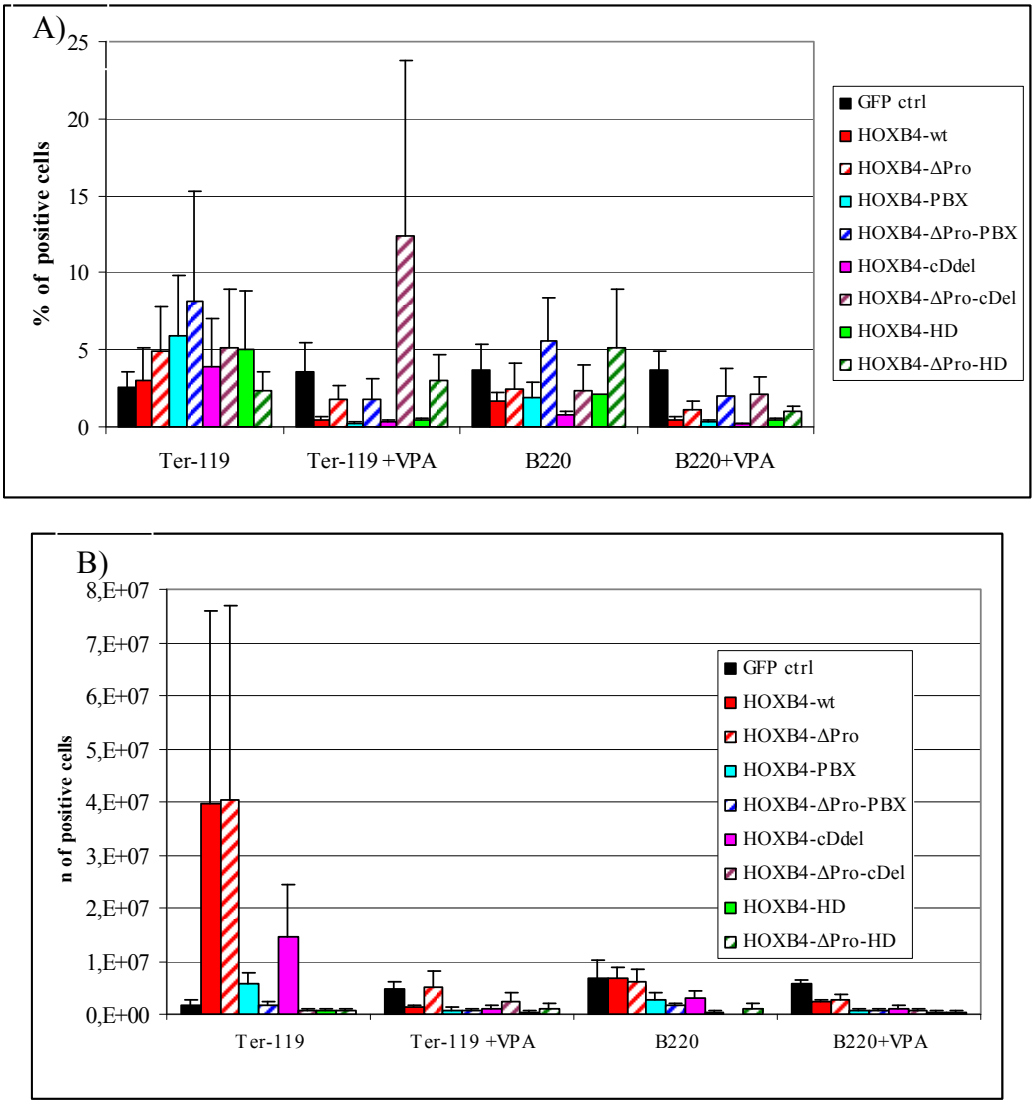

Figure 4.4.2.3. Immunofluorescence staining of BM progenitor cells after 1 week of liquid culture: cells percentages. B) cells counts.

In conclusion, we reported that the deletion of the proline-rich region leads to an increase of the Sca-1/c-kit positive cells proportions in comparison to the GFP control and to all the samples without this mutation, while this subpopulation was still smaller than in the Hoxb4-wt. In contrast, the myeloid cells counts were reduced when the proline-rich region was deleted, and this decrease was even more pronounced in the presence of VPA. The deletion of proline region did not affect the number of Ter-119^{+} and B220^{+}, while the VPA led to a decrease of the expression of these two markers in almost all the samples. Similarly, the single mutations PBX, HD, and cDel did not significantly affect the lineage specificity.

4.4.3 Morphology of *in vitro* expanded BM progenitor cells

The 5-FU enriched progenitor cells from BM of donor mice have been cultivated for up to 3 weeks in the presence of the cytokines cocktail (SCF, IL3, IL6). After 3 weeks the cells overexpressing the Hoxb4-wt were almost mast cells, while the cells overexpressing the Hoxb4-ΔPro maintained an immature phenotype (Fig. 4.4.3).

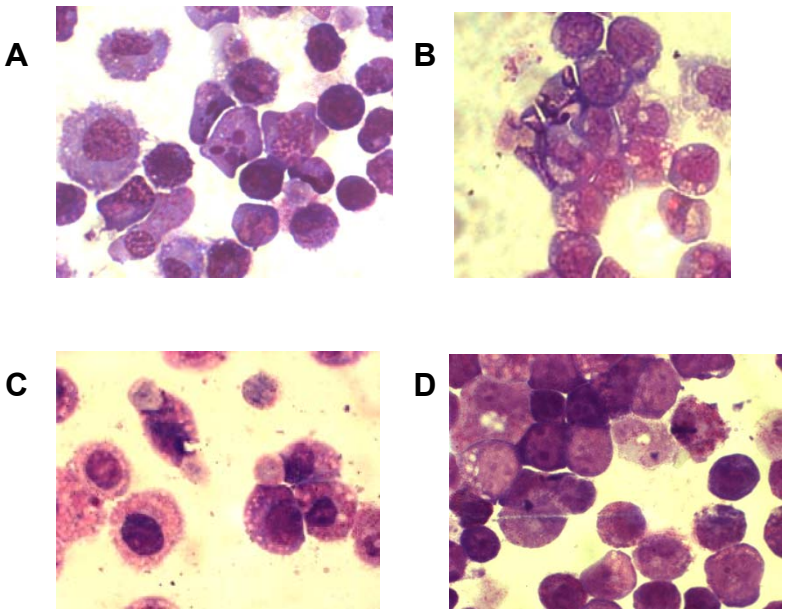

Fig 4.4.3. 5-FU transduced BM cells after liquid culture. Hoxb4-wt after 1 week (A) and 3 weeks (C). Hoxb4-ΔPro after 1 week (B) and 3 weeks (D) (100X).

4.4.4 Colony forming cells (CFC)-assay *in vitro*

5-FU enriched BM progenitor cells have been transduced and sorted for the GFP marker. 500 GFP^+ cells per ml have been plated in semisolid methylcellulose medium containing IL3, IL6 and SCF. After 5-7 days the colonies have been counted.

Sample	GEMM (VPA) [%]	G (VPA) [%]	GM (VPA) [%]	M (VPA) [%]	BFU-E (VPA) [%]	Total (VPA)
GFP ctrl	**1** (1) [0.6]	**15.7** (2) [10]	**52** (21.3) [33,2]	**39.3** (46) [25,1]	**48.5** (82.3) [31]	**156.5** (152.6)
Hoxb4-wt	**3.67** (1) [1.6]	**30** (2) [13.2]	**28** (13.3) [12.4]	**65.8** (60.2) [29.1]	**99.2** (119.7) [44]	**226.7** (196.1)
Hoxb4-ΔPro	**0.2** (0.2) [0.2]	**12.8** (1.1) [11.2]	**12** (2.5) [10.5]	**25** (24.8) [21.8]	**64.5** (99.8) [56]	**114.5** (128.4)
Hoxb4-PBX	**1.2** (0.2) [0.6]	**17** (1.3) [8.1]	**33.3** (22) [15.9]	**42.2** (70.5) [20]	**116.8** (101.7) [56]	**210.3** (195.7)
Hoxb4-cDel	**0** (0.7) [0]	**17.7** (1) [9.6]	**31.7** (31.7) [17.1]	**49.3** (55) [26.7]	**86.3** (104) [46.7]	**185** (192.3)
Hoxb4-HD	**3.7** (1) [1.1]	**78** (2.5) [23.6]	**54** (15.5) [16.3]	**91.3** (118) [27.6]	**104.3** (140) [31.5]	**331.3** (216)

Table 4.4.4.1. 1°CFC *in vitro*. 500 freshly transduced 5-FU enriched BM cells have been plated in methylcellulose containing IL3, IL6 and SCF. After 5-7 days the colonies have been counted (n=3). GEMM: granulocyte/erythrocyte/macrophage/megakaryocyte; G: granulocyte; GM: granulocyte/macrophage; M: macrophage. [ ]: indicate the % of the total colonies without VPA. () indicate no. of CFCs in presence of VPA. [] indicate percentages of the total w/o VPA.

We reported no significant difference in the total number of CFCs in all the samples in comparison to the GFP control (Table 4.4.4.1, Fig. 4.4.4.1a). However, in all the samples where Hoxb4-wt and its mutants (except for Hoxb4-HD) were overexpressed, we reported an increased proportion of BFU-E colonies in comparison to the GFP (44-56% vs. 31%, respectively). Moreover, the proportion of GM-CFCs was in all the samples lower than in the GFP control (10.5-17.1% vs. 52%, respectively). The incubation with VPA led to a decrease in the total number of CFCs in all the samples except for Hoxb4-ΔPro and Hoxb4-cDel, in comparison to the corresponding samples without VPA. However in the presence of VPA we reported higher percentages of BFU-E colonies in all the samples except for Hoxb4-PBX. The Hoxb4-ΔPro led to a decrease in the proportion of mature myeloid CFCs (11.2% vs. 13.2% G-CFC, 10.5% vs. 12.4% GM-CFC, 21.8% vs. 29% M-CFC, 0.2% vs. 1.6% GEMM-CFCs), while the

proportion of BFU-E CFCs was higher (56% vs. 44%) in comparison to the Hoxb4-wt.

In all the samples where the Hoxb4 and its mutants were overexpressed we reported a clear decrease in the ratio between the G/GM/GEMM/M and the BFU-E-CFCs in comparison to the GFP control (Fig. 4.4.4.1b). The VPA led to the inversion of the GM/BFU-E CFCs ratio in almost the samples.

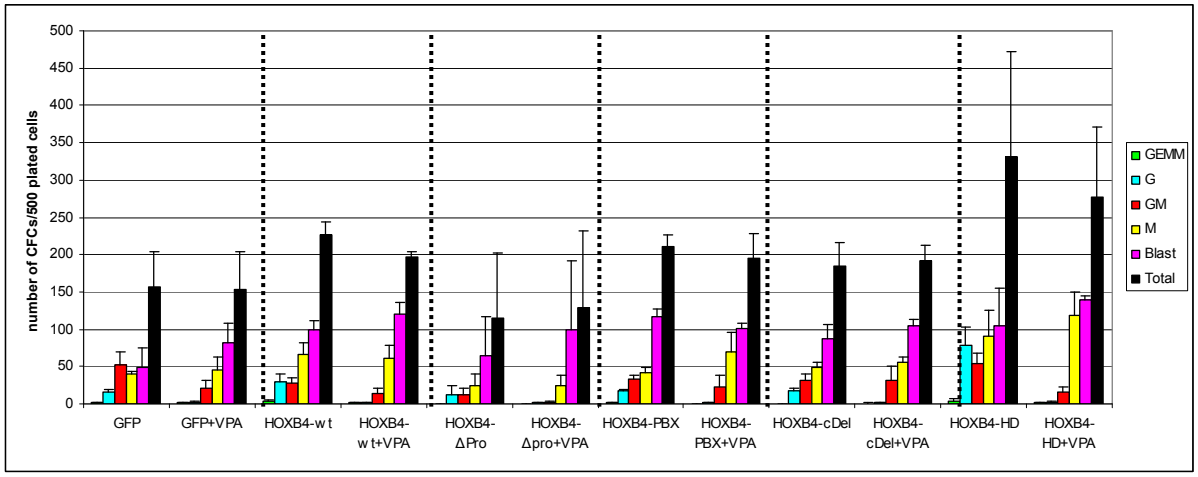

Fig 4.4.4.1a. 1°CFC *in vitro*. 500 freshly transduced 5-FU enriched BM cells have been plated in one ml of methylcellulose containing IL3, IL6 and SCF. After 5-7 days the colonies have been counted (n=3). GEMM: granulocyte/erythrocyte/macrophage/megakaryocyte; G: granulocyte; GM: granulocyte/macrophage; M: macrophage.

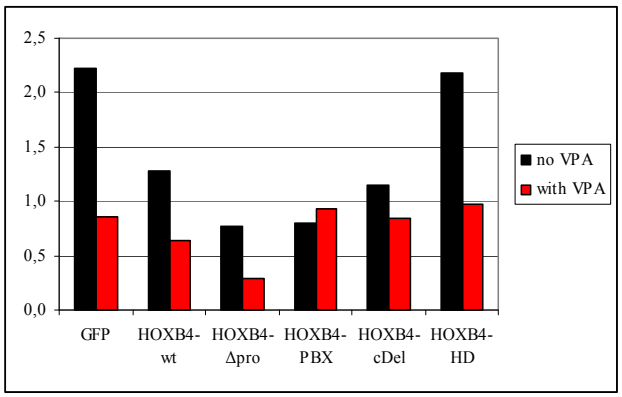

Fig 4.4.4.1b. 1°CFC *in vitro*. Ratio between mature myeloid colonies (CFU-G, CFU-M, CFU-GM, CFU-GEMM) and BFU-E colonies in the presence and in the absence of VPA (n=3).

When the cells harvested from the 1° CFC were replated with a dilution factor of 1:100, we saw a dramatic increase in the frequency of 2°CFCs in the Hoxb4-ΔPro in comparison to all the other samples. The incubation with VPA led to an increase in the number of 2° CFCs and in particular of the BFU-E CFCs in all the samples in comparison to the corresponding samples without VPA (n=2) (Fig. 4.4.4.1c).

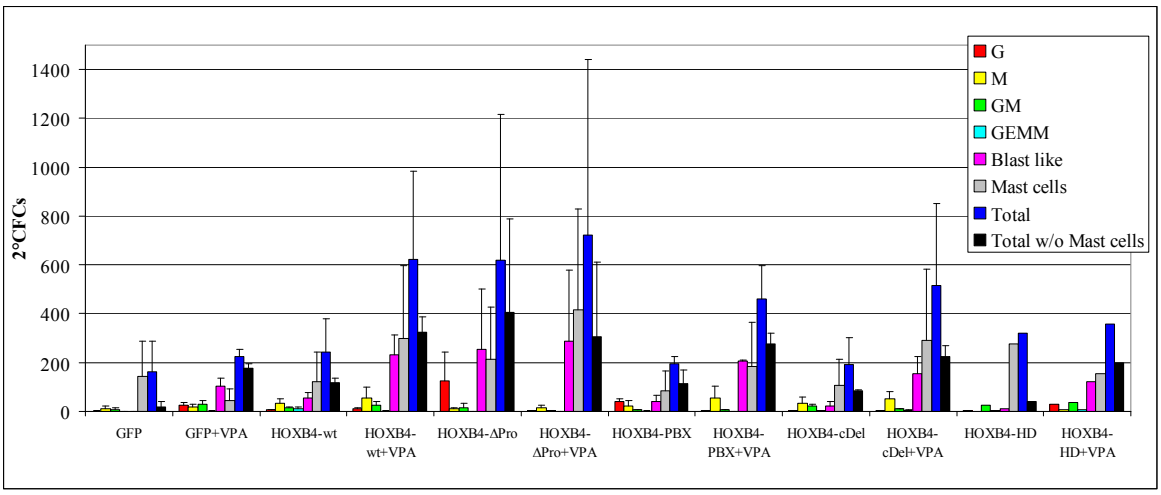

Fig 4.4.4.1c. 2°CFC *in vitro*. The cells collected from the 1°CFC have been replated with a dilution factor of 1:100 in methylcellulose containing IL3, IL6 and SCF. After 1 week the colonies have been counted (n=2).

4.4.5 Intracellular localization

To assess if the deletion of the proline rich region was affecting the subcellular localization of the Hoxb4 protein, we performed an intracellular immunostaining followed by confocal laser scanning fluorescence microscopy. We found that the Hoxb4 missing the proline rich region was still localizing in the nucleus as the wild type (Fig. 4.4.5).

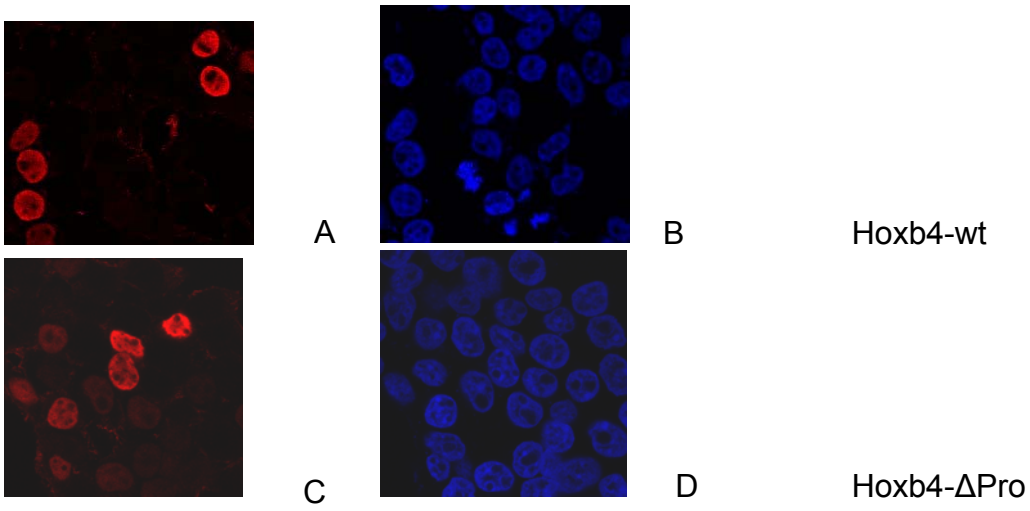

Fig 4.4.5. 293T cells have been transfected with the plasmids of interest. 24 h after transduction the cells have been fixed and stained with the anti-Hoxb4 polyclonal antibody or with the anti-FLAG antibody. A secondary antibody labelled with Alexa Fluor 555 or Alexa Fluor 488 was used, respectively. The comparison with the DAPI-stained cells allowed identifying the localization of Hoxb4. A: 293T-Hoxb4-wt stained with anti-Hoxb4 antibody. B: 293T-Hoxb4-wt stained with DAPI. C: 293T-FLAG-Hoxb4-ΔPro stained with anti-FLAG antibody. D: 293T-FLAG-Hoxb4-ΔPro stained with DAPI.

4.5 *In vivo* assays

4.5.1 ΔColony forming unit in the spleen (ΔCFU-S) assay

The number of short-term hematopoietic stem cells in a cell population can be assayed by the colony forming unit in spleen (CFU-S) assay, which quantifies the frequency of these cells by the formation of visible colonies in the spleen 12 days after injection. To investigate the effect of the different mutations of Hoxb4 after one week of *in vitro* expansion, with and without the pre-incubation with VPA, bone marrow cells transduced with the different vectors were grown for 7 days in liquid medium containing SCF, IL3, IL6 with or without VPA (1mM), injected into lethally irradiated mice, and spleen colony formation was quantified 12 days later in sacrificed animals. Colonies can be macroscopically visualized after immersion of the spleen in Telleyesnickzky´s solution (Fig. 4.5.1a).

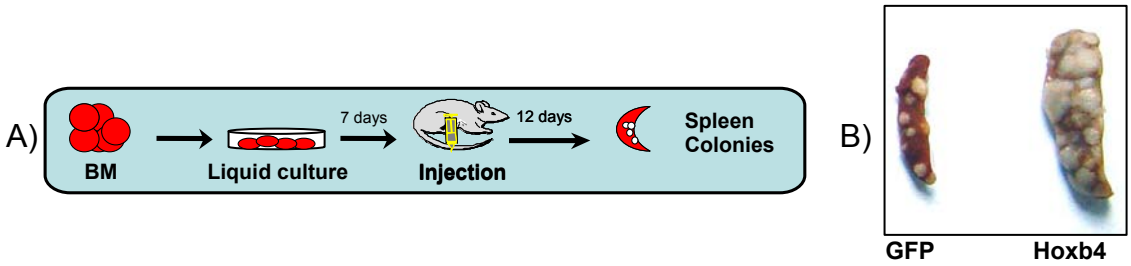

Fig. 4.5.1a. A) Schematic representation of the ΔCFU-S assay. B) Representative example of spleen colonies counted 12 days post injection.

When the Hoxb4-wt was overexpressed we reported a significant increase in the ΔCFU-S frequency in comparison to the GFP control (2627fold, $p<0.05$). When the homeodomain was mutated and the C-terminal region deleted we observed a dramatic decrease in the ΔCFU-S frequency in comparison to the Hoxb4-wt (136fold and 55.7fold, respectively, $p<0.05$). However, these two mutants still induced a significant increase in the ΔCFU-S frequency when compared to the GFP control (19-and 47fold, respectively, $p<0.05$). Similarly, the deletion of the proline-rich region led to a significant increase of 35fold and a decrease of 75fold when compared to the GFP control and to the Hoxb4-wt, respectively ($p<0.001$). In contrast, the mutation of the PBX-interacting domain did not affect ΔCFU-S frequency compared to Hoxb4-wt.

Interestingly, the additional deletion of the proline-rich region in the Hoxb4-HD, Hoxb4-cDel, Hoxb4-PBX mutants led to an additional decrease in the ΔCFU-S frequencies (135fold, $p<0.0001$; 13.2fold, $p<0.052$, and 30fold, $p<0.0004$,

respectively), when compared to the corresponding single mutants. Moreover, in the presence of the double mutants Hoxb4-ΔPro-cDel and Hoxb4-ΔPro-HD, we reported a non-significant increase and even a decrease of the ΔCFU-S frequencies, respectively, in comparison to the GFP control (Fig 4.5.1b, Table 4.5.1). Indeed, the combination of the proline-rich region deletion with the homeodomain mutation, with the PBX-ID mutation, and with the C-terminal deletion seemed to act synergistically in decreasing the short-term progenitor cells frequency in this *in vivo* assay, suggesting that all these regions are important for the normal amplificatory effect of Hoxb4 at the level of short term repopulating stem cells.

In all the samples, the pre-incubation with VPA increased the number of colonies counted when compared to the corresponding samples without VPA, but this increase was significant only in the GFP control (6.4fold), and in Hoxb4-ΔPro (1.87fold), in comparison to the corresponding samples without VPA.

On the other hand, the decrease of ΔCFU-S observed in case of the single mutants in comparison to the Hoxb4-wt, was not anymore significant after the addition of VPA. Only in case of Hoxb4-ΔPro with VPA the ΔCFU-S frequency was still significantly lower than in the Hoxb4-wt (40fold decrease, $p<0.0001$). This suggests that the VPA treatment somehow rescued the short-term progenitor cells proliferation, despite the mutation at the homeodomain, at the PBX-binding domain, and at the C-terminal sequence, respectively. In contrast, in the absence of the proline-rich domain the VPA did not exert the same amplificatory effect otherwise observed on the short term repopulating stem cells.

When the double mutants harbouring the additional deletion of the proline-rich region have been pre-incubated with VPA, the ΔCFU-S frequency was higher when compared to the double mutants without VPA, but this was significantly higher only for the Hoxb4-ΔPro-PBX (2.8fold) and in Hoxb4-ΔPro-cDel (8.5fold) samples. This suggests that the deletion of the DNA interaction domain as well as of the proline-rich region might have opposite effects to the HDAC-inhibition activity exerted from VPA. Moreover, the VPA pre-incubation of the double mutants did not rescue the negative effect of the combined mutations on the ΔCFU-S frequency observed, when compared to the Hoxb4-wt (Hoxb4-ΔPro-HD=6129fold, Hoxb4-ΔPro-PBX=18fold, Hoxb4-ΔPro-cDel=88fold decrease vs. Hoxb4-wt, $p<0.001$), suggesting that the proline-rich domain, which may affect

the histone deacetylase activity control regulated by Hoxb4, plays a crucial role in the proliferation of ΔCFU-S.

Sample	ΔCFU-S/45.000 cells (SEM)	Fold increase vs. GFP ctrl	Fold increase vs. w/o VPA	N of mice
GFP ctrl	7 (1.31)	-	-	11
GFP+VPA	44 (12.5)	6.4	6.4	14
Hoxb4-wt	18387 (4857)	2627	-	5
Hoxb4-wt+VPA	31125 (15399)	4446	1.69 *	4
Hoxb4-ΔPro	245 (47.8)	35	-	14
Hoxb4-ΔPro+VPA	457 (76)	65	1.87	15
Hoxb4-HD	135 (45)	19	-	2
Hoxb4-HD+VPA	585 (225)	84	4.33 *	2
Hoxb4-cDel	330 (286)	47	-	3
Hoxb4-cDel+VPA	22500 (20291)	3214	68.2 *	3
Hoxb4-Pbx	10800 (3836)	1543	-	4
Hoxb4-Pbx+VPA	11700 (6300)	1671	1.08 *	5
Hoxb4-ΔPro-HD	0	0	-	10
Hoxb4-ΔPro-HD+VPA	3 (2.7)	0.43 *	3 *	11
Hoxb4-ΔPro-cDel	25 (9.6)	3.51 *	-	10
Hoxb4-ΔPro-cDel+VPA	209 (62.5)	30	8.5	9
Hoxb4-ΔPro-Pbx	362	52	-	11
Hoxb4-ΔPro-Pbx+VPA	1020	146	2.8	9

Table 4.5.1. 12 days ΔCFU-S. The ΔCFU-S frequencies/45000 initially plated cells at day 0 for each sample are reported. * not significant.

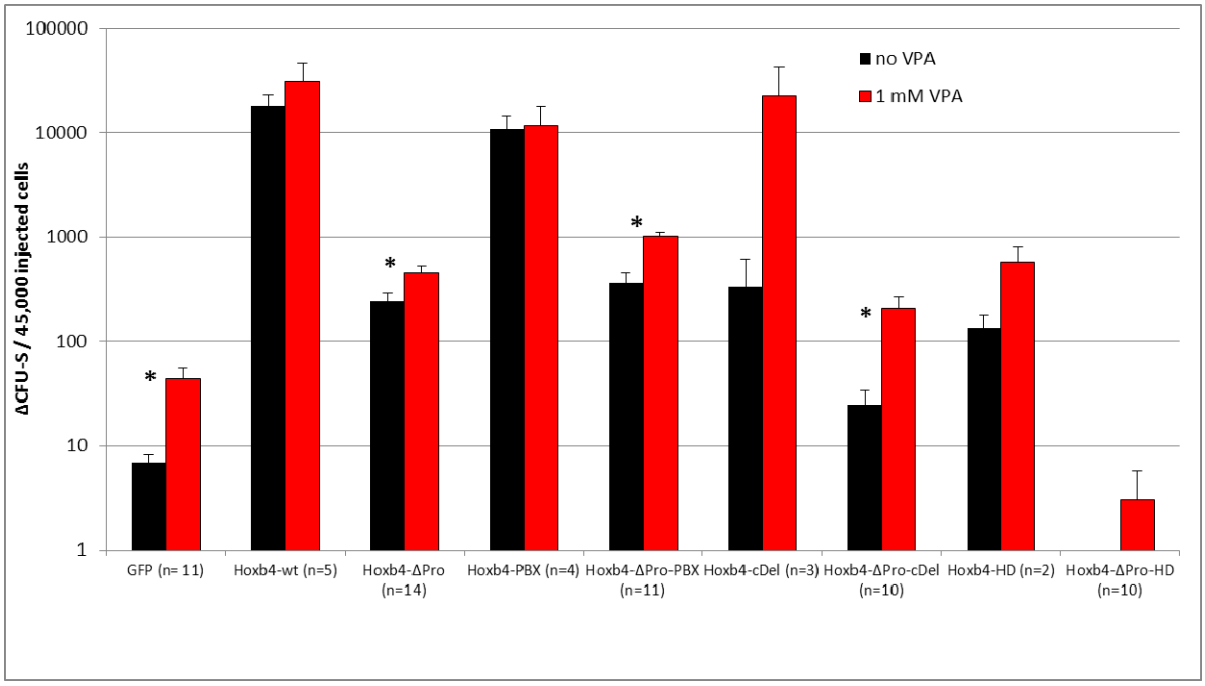

Fig 4.5.1b. 12 days ΔCFU-S. The ΔCFU-S frequencies/45,000 initially plated cells at day 0 for each sample are reported. * indicate $p<0.05$ vs. w/o VPA, respectively.

4.5.2 Hoxb4 BM transplantation experiments in mouse model

4.5.2.1 Peripheral blood analysis at 4th week after transplantation

4 weeks after transplantation peripheral blood from the tail vein has been obtained and the blood cells counts at this time point have been compared, in order to estimate the short term engraftment. As expected, there was no significant difference in the red blood cells counts in all the mice. Considering the GFP^+ white blood cells arising from a single GFP^+ injected cell we reported no difference in the proportion of GFP^+ WBCs in the PB of the different mice (21.22% in Hoxb4-wt, n=2, vs. 32.33% in Hoxb4-ΔPro, n=2, vs. 11.78% in GFP mice, n=3, $p>0.1$).

4.5.2.2 The long term engraftment: analysis of chimerism in peripheral blood

13-16 weeks post transplantation the WBCs isolated from the peripheral blood of healthy mice have been analysed. The number of WBCs GFP^+ generated by 1000 initially injected bone marrow progenitor cells was determined. In case of Hoxb4-wt we obtained 3.68 % of chimerism in the PB (n=19), while in case of the Hoxb4-ΔPro the chimerism was 1.57 % only (n=20) ($p<0.031$). In the GFP control mice the injection of 1000 cells gave rise to 0.11% of GFP^+ WBCs in the peripheral blood (n=3, $p>0.15$) (Fig. 4.5.2.2). Considering these results, we can conclude that the deletion of the proline-rich region of Hoxb4 significantly decreases the *in vivo* proliferation of bone marrow progenitor cells, giving rise to a smaller progeny of mature cells in the peripheral blood in comparison to the Hoxb4-wt. This is according to what has been observed performing the ΔCFU-S, where the proliferation of the short-term repopulating stem cells was less pronounced when the proline region was deleted. However, the Hoxb4-ΔPro still led to a higher engraftment rate per equal number of injected cells than in the GFP control. The chimerism data at this time point originate from serial dilutions transplantation experiments, which have been performed in order to evaluate the frequency of the HSCs able to give rise to the whole hematopoiesis in recipient mice (see paragraph 4.5.2.8).

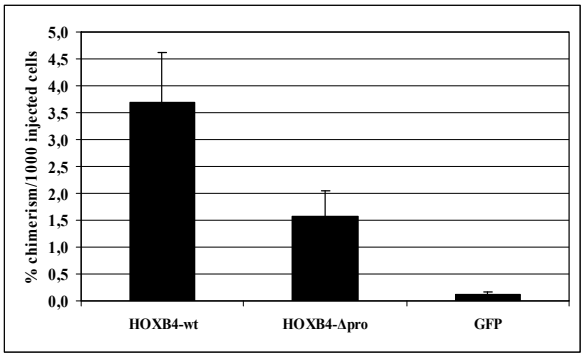

Fig. 4.5.2.2. Chimerism in the peripheral blood 13-16 weeks post transplantation. The percentages of GFP$^+$ WBCs are indicated (Hoxb4-wt n=19; Hoxb4-ΔPro n=20; GFP n=3).

4.5.2.3 The long term engraftment: analysis of differentiation profile in peripheral blood

At 13-16th week post transplantation the phenotype of the WBCs in the peripheral blood has been analysed. The surface antigens analysed were Sca-1, c-kit, Mac-1, Gr-1, Ter-119, B220, CD4 and CD8. The FACS analysis of these markers as well as the morphological analysis did not show significant difference between Hoxb4-wt, Hoxb4-ΔPro and GFP control mice, indicating that the differentiation into mature progeny from the transplanted cells was not perturbed at this time point when the Hoxb4-wt and the Hoxb4-ΔPro were overexpressed (Fig. 4.5.2.3).

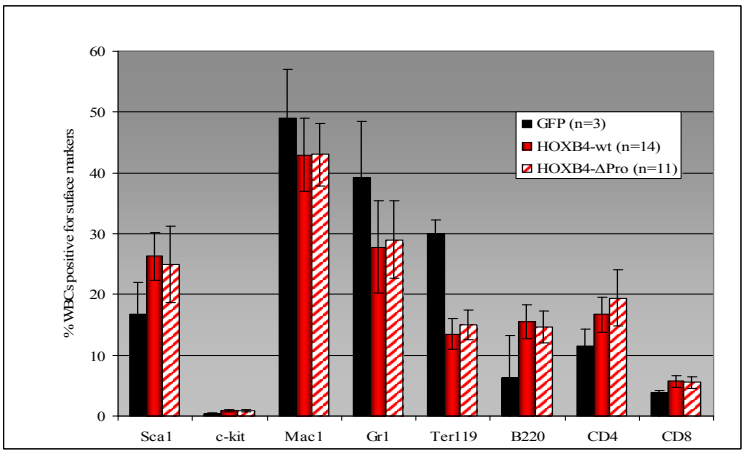

Fig. 4.5.2.3. Surface markers analysis of GFP$^+$ WBCs from peripheral blood of mice 13-16 weeks post transplantation.

4.5.2.4 Overexpression of Hoxb4-ΔPro is associated with acute leukemia in transplanted mice

8-10 weeks old lethally irradiated (850 cGy) recipient mice (C3H-C57Bl/C3H-PeB) were injected with $1.13x10^5$ to $1.8x10^7$ retrovirally transduced 5-FU enriched BM progenitor cells. The recipient mice have been transplanted with

progenitor cells expressing the following genes: *Hoxb4-wt* (n=5), *Hoxb4-ΔPro* (n=9), *Hoxb4-ΔPro* pre-treated for 1 week with VPA (n=3), *Hoxb4-ΔPro-PBX* double mutant (n=3), *Hoxb4-ΔPro-PBX* pre-treated for 1 week with VPA (n=3), *Hoxb4-ΔPro-HD* (n=4) and *GFP* control (n=3) (Table 4.5.2.4). The mice were monitored for symptoms of hematological disorders, which included frizzled body hair, paleness in the extremities and lethargy. The examination of leukemic symptoms at sacrifice includes the measurement and the morphological analysis of leukocytes/erythrocytes in the peripheral blood and in the bone marrow, as well as the analysis of the spleen (weight and size). Various organs of leukemic mice were fixed in formalin for histopathological and immunohistochemical examinations.

All the Hoxb4-wt mice survived more than 404 days (mean 488.3 d) without showing any hematopoietic malignancy. One out of 6 mice died for irradiation-associated illness.

The Hoxb4-ΔPro mice died 90-384 days after transplantation (mean 255 d, $p<0.001$ vs. Hoxb4-wt) by hematological malignancy. From these mice, secondary syngeneic recipient mice (n=6) have been transplanted with 0.5-1x10^6 cells obtained from BM or spleen of diseased primary transplanted animals. The mean survival time of these secondary transplanted mice was 66.5 days post transplantation. The BM and spleen cells of these secondary transplanted mice have been used to transplant tertiary recipient mice (n=4), which died 42.8 days (mean) after transplantation for the same AML. As expected in case of a transplantable disease, we observed a shortening of the latency time of the disease of 3.8fold from primary to secondary and of 1.5fold from secondary to tertiary serial transplantations of recipient animals (Fig. 4.5.2.4c). This suggests that the disease in primary transplanted mice induced by the overexpression of Hoxb4-ΔPro probably reflects a multistep process. Few mice have been also injected with BM progenitor cells expressing Hoxb4-ΔPro pre-incubated with VPA for one week before transplantation. These mice died of leukemia 161 days (mean) after transplantation showing a prevalence of myeloid immature cells in the organs analyzed (84.6% of WBCs were expressing Mac-1), splenomegaly and leukocytosis (3.8x10^7 WBCs/ml). Apparently, the pre-treatment with VPA did not affect the development of the disease.

All the mice transplanted with Hoxb4-ΔPro overexpressing BM progenitor cells died of AML without maturation (Fig. 4.5.2.4a and Fig. 4.5.2.4b). Leukemia progression is often marked by the infiltration of blasts in various organs and therefore we assessed sacrificed moribund mice for these signs by making histopathological sections of fixed organs followed by immunohistochemical staining. In our model the diffuse neoplastic infiltration was involving the spleen, liver, lymph nodes, lung, heart and kidneys. The infiltration of leukemic blasts to the non-hematopoietic organs in general and to the brain in particular was striking, highlighting the aggressive nature of the disease. The type and maturity of the cells involved in leukemia can be identified by performing immunohistochemical stainings. The myeloperoxidase distinguishes between immature cells in acute myeloid leukemia (cell stain positive) and those in acute lymphoid leukemia (cells stain negative) (Fischbach 1996). Lymphoid blasts are characteristically negative for myeloperoxidase and chloracetate esterase. In order to determine the nature of the blasts, we performed various stainings of the organs from primary leukemic mice. Here we found that the neoplastic cells were myeloperoxidase (MPO) positive confirming the diagnosis of acute myeloid leukemia without maturation.

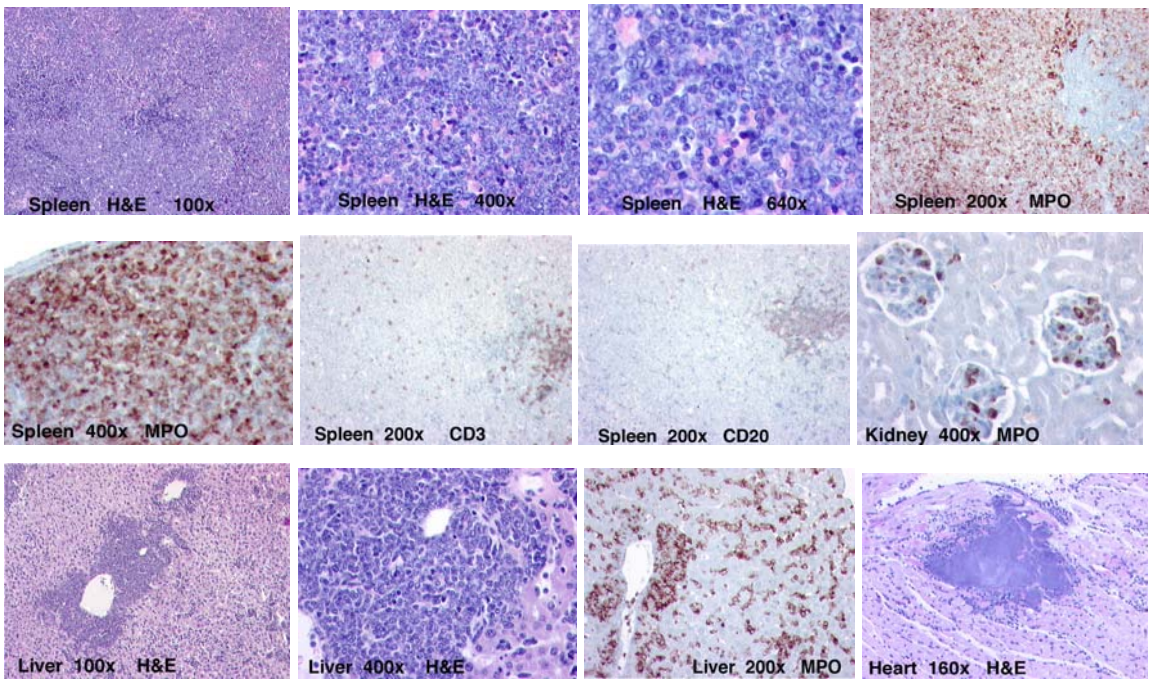

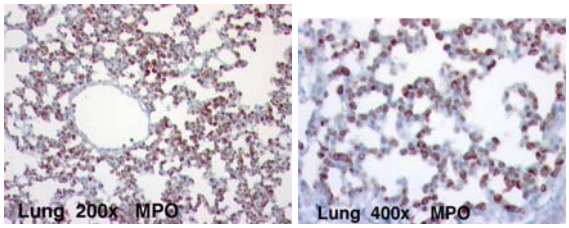

Fig. 4.5.2.4a. Histological analysis of multiple organs obtained from a representative secondary mouse, transplanted with cells obtained from the infiltrated spleen of a diseased primary mouse, originally transplanted with Hoxb4-ΔPro expressing BM progenitor cells (Mouse #33). As well as in Fig. 4.5.2.4b, the cells are large with abundant cytoplasm, blastic chromatin and prominent nucleolus. There is no myeloid differentiation. In the spleen there are some residual small areas of erythropoiesis. In the kidney the neoplastic cells are identified in the capillary lumens in the glomeruli. The type of infiltration in the liver, lung and kidney clearly suggests that the mouse had a leukemic phase. The heart has a recent myocardial infarct with neoplastic cell infiltrating the myocardial wall. The residual white pulp of the spleen reveals cells that are CD3 and B220 positive but the tumor cells are negative for these markers.

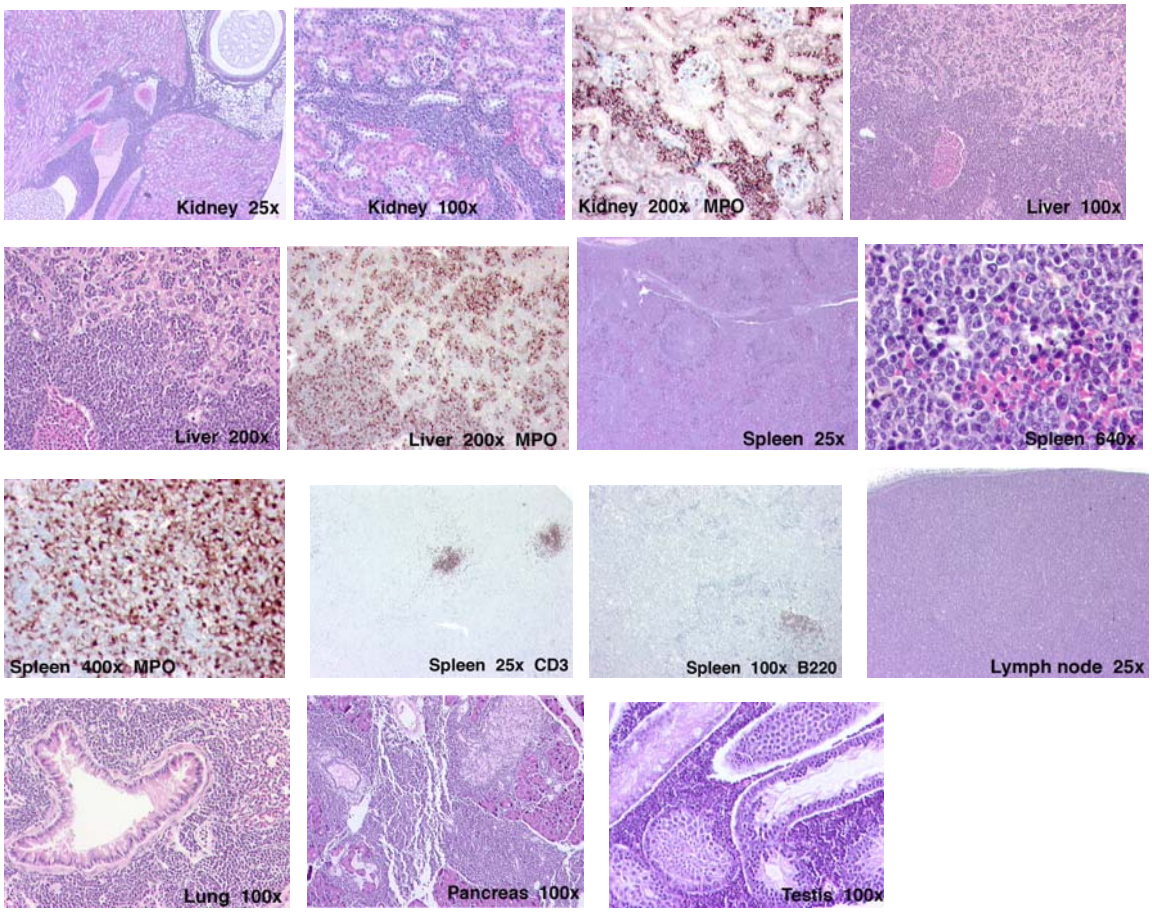

Fig. 4.5.2.4b. Histological analysis of multiple organs obtained from a tertiary mouse, transplanted with cells obtained from the infiltrated BM of a secondary diseased mouse, originally transplanted with Hoxb4-ΔPro expressing BM progenitor cells (Mouse #36). For description, refer to legend Fig. 4.5.2.4a.

Effect of the additional PBX interacting domain (ID) and homeodomain (HD) mutations on the survival of Hoxb4-ΔPro leukemic mice. The combination of the PBX interacting domain mutation with the deletion of the proline-rich region has been investigated by transplanting lethally irradiated recipient mice (n=3) with BM

cells overexpressing the double mutated Hoxb4-ΔPro-PBX. These mice died of leukemia 311 days (mean) after transplantation, showing no significant difference in comparison to the Hoxb4-ΔPro mice. Moreover, BM cells expressing Hoxb4-ΔPro-PBX have been pre-incubated with VPA (1mM) for 1 week, and transplanted into three recipient animals. These mice died 338 days (mean, n=3) after transplantation. This "intermediate" survival rate of these two groups of mice was not significantly different when compared to the survival of the mice transplanted with HOXB4-wt and to the mice transplanted with Hoxb4-ΔPro alone. Moreover, clinical features of these two groups of mice are of note. The Hoxb4-ΔPro-PBX mice showed leukocytosis ($1.2x10^7$/ml), myeloid prevalence in the peripheral blood (81.32% Mac-1^+ WBCs) and moderate splenomegaly (300 mg spleen weight), while the Hoxb4-ΔPro-PBX+VPA mice showed WBCs counts ($6x10^6$/ml), spleen weight (200mg) and myeloid prevalence in the peripheral blood (60.3% of WBCs) comparable to the GFP control mice (Table 4.5.2.4 and Fig. 4.5.2.4c).

Interestingly, in the mice transplanted with BM progenitor cells overexpressing Hoxb4-ΔPro-HD we did not observed a long term engraftment, suggesting that the interaction with the DNA is essential for the stem cell activity as well as for the development of the leukemia observed in this model.

No.	Mouse	Retroviral construct	GFP^+ injected cells	Dead n days after Tx	Average d (p vs wt)	Notes
1	4421 #1	Hoxb4-wt	$1.12x10^5$	404		
2	4421 #2	Hoxb4-wt	$1.12x10^5$	416		
3	4622 H #1	Hoxb4-wt	$2x10^4$	545	488.3	
4	4622 H #2	Hoxb4-wt	$2x10^5$	483		
5	4622 H#3	Hoxb4-wt	$2x10^5$	572		
6	4622 B#4	Hoxb4-wt	$2x10^3$	510		
7	3970 A #2	Hoxb4-ΔPro	$1.8x10^7$	n.a.		
8	3970 A #3	Hoxb4-ΔPro	$1.8x10^7$	279		
9	3970 A #4	Hoxb4-ΔPro	$1.8x10^7$	126		
10	3970 A #5	Hoxb4-ΔPro	$1.8x10^7$	279	255	
11	3860 A#1	Hoxb4-ΔPro	$6.3x10^5$	n.a.	(p<0.001)	
12	3860 A #2	Hoxb4-ΔPro	$6.3x10^5$	337		
13	3860 B #1	Hoxb4-ΔPro	$6.3x10^5$	231		
14	3860 B #2	Hoxb4-ΔPro	$6.3x10^5$	90		
15	3860 B #4	Hoxb4-ΔPro	$6.3x10^5$	244		

16	4622 I #1	Hoxb4-ΔPro	$2x10^5$	325		
17	4622 I #3	Hoxb4-ΔPro	$2x10^5$	384		
18	4622 F #3	Hoxb4-ΔPro	$2x10^4$	384		
19	3970 B #5	Hoxb4-ΔPro-Pbx	$1.7x10^7$	153		
20	3970 C #1	Hoxb4-ΔPro-Pbx	$1.7x10^7$	470	311 (p=0.080)	
21	3970 C #3	Hoxb4-ΔPro-Pbx	$1.7x10^7$	310		
22	3970 B #1	Hoxb4-ΔPro+VPA	$2.5x10^7$	154	161 (p<0.0001)	
23	3970 B #3	Hoxb4-ΔPro+VPA	$2.5x10^7$	156		
24	3970 B #4	Hoxb4-ΔPro+VPA	$2.5x10^7$	174		
25	3970 C #4	Hoxb4-ΔPro-Pbx+VPA	$1.8x10^7$	416	338 (p=0.083)	
26	3970 D #1	Hoxb4-ΔPro-Pbx+VPA	$1.8x10^7$	194		
27	3970 D #2	Hoxb4-ΔPro-Pbx+VPA	$1.8x10^7$	405		
28	4614 B #2	Hoxb4-ΔPro	$1x10^6$	50	66.5 (p<0.0005 vs. 1st Tx)	2nd Tx
29	4614 C #1	Hoxb4-ΔPro	$1x10^6$	54		2nd Tx
30	4614 C #2	Hoxb4-ΔPro	$1x10^6$	54		2nd Tx
31	4614 C #3	Hoxb4-ΔPro	$1x10^6$	54		2nd Tx
32	4614 C #4	Hoxb4-ΔPro	$1x10^6$	82		2nd Tx
33	4614 C #5	Hoxb4-ΔPro	$1x10^6$	105		2nd Tx
34	4685 #1	Hoxb4-ΔPro	$1.2x10^6$	51	43 (p<0.0013 vs. 1st Tx)	3rd Tx
35	4685 #2	Hoxb4-ΔPro	$1.2x10^6$	42		3rd Tx
36	4685 #3	Hoxb4-ΔPro	$1.2x10^6$	43		3rd Tx
37	4685 #4	Hoxb4-ΔPro	$9x10^6$	35		3rd Tx
38	5264 #2	Hoxb4-ΔPro-HD	$2.2x10^5$	321	327	*
39	5331 #1	Hoxb4-ΔPro-HD	$3x10^5$	>331		*
40	5331 #2	Hoxb4-ΔPro-HD	$3x10^5$	>331		*
41	5020	GFP	$3.7x10^5$	>400		
42	5029	GFP	$1.3x10^6$	>400		
43	4951	GFP	$1.5x10^6$	>400		

Table 4.5.2.4. List of transplanted mice. All the #3970 mice have been injected with cells which have been cultivated for 1 week after transduction, with or without VPA. For all the mice a number of 5-FU enriched GFP^- progenitor carrier cells have been injected ($3x10^5$-$2x10^6$). The mice injected with higher dilutions of BM cells for estimation of the CRU frequencies are not reported. * = these animals did not show engraftment.

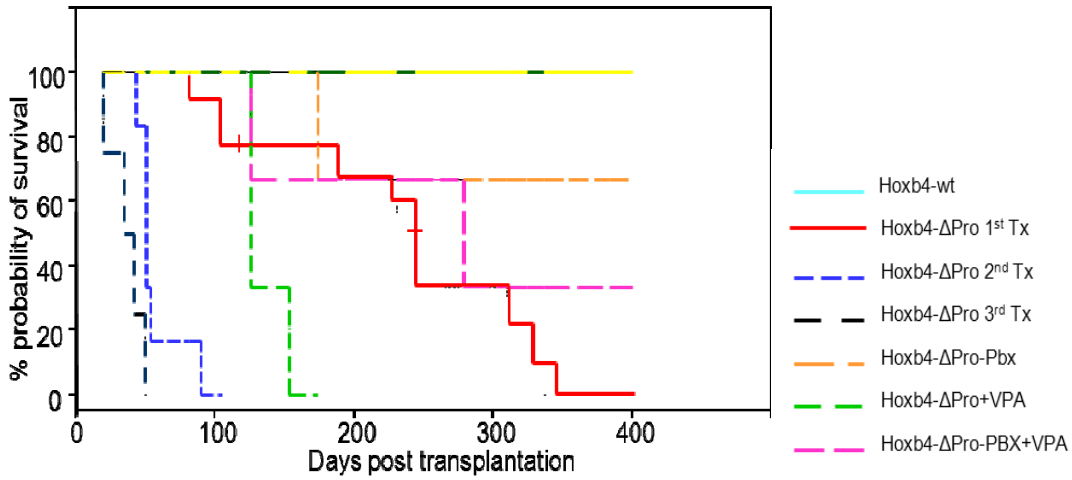

Fig. 4.5.2.4. Kaplan-Meier survival curves of Hoxb4 transplanted mice. The animals which died shortly after transplantation by irradiation related mortality are not included.

4.5.2.5 Clinical features of the Hoxb4-ΔPro associated leukemia

Peripheral blood. At sacrifice there was no significant difference in the RBCs counts in the peripheral blood in almost all the mice. The 1st transplanted Hoxb4-ΔPro mice did not show anemia signs and the RBCs counts were almost in the normal range. Only in the 2nd mice transplanted with Hoxb4-ΔPro cells we reported a significant 2.4fold decrease in the RBCs counts in comparison to the GFP control ($2.2x10^9$/ml vs. $6.2x10^9$/ml, respectively, $p<0.03$) (Fig. 4.5.2.5a). The WBCs counts in almost all the mice were higher than the in the GFP control (range between 1.03fold in the Hoxb4-wt and 68.4fold in the Hoxb4-ΔPro mice vs. GFP control). This increase was statistically significant in comparison to the GFP control ($p<0.018$) only in the 2nd and in the 3rd Hoxb4-ΔPro transplanted mice, as well as in the mice where Hoxb4-ΔPro injected cells have been pre-treated with VPA before transplantation ($3.37x10^7$/ml, $4.33x10^8$/ml and $3.82x10^7$/ml vs. $6.33x10^6$/ml in GFP control, respectively) (Fig. 4.5.2.5b).

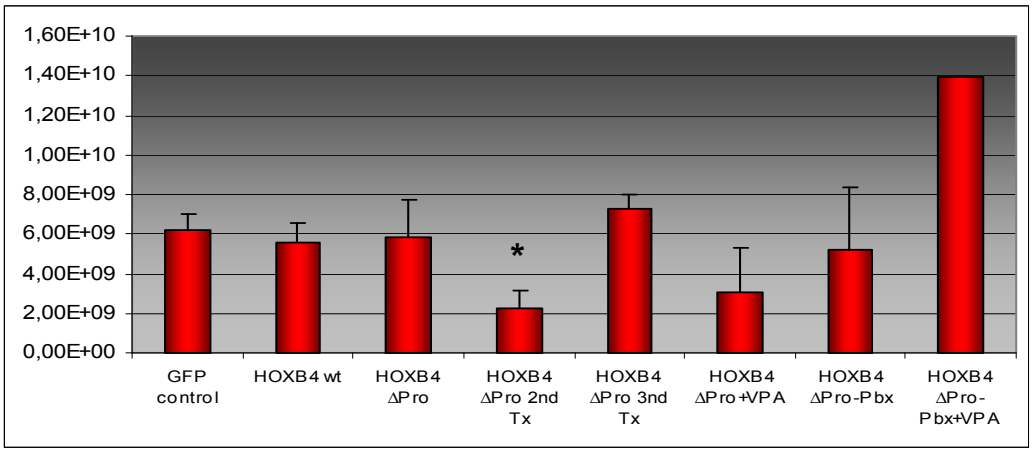

Fig. 4.5.2.5a. RBCs/ml in the PB at sacrifice. * significantly lower than in the GFP control ($p<0.05$).

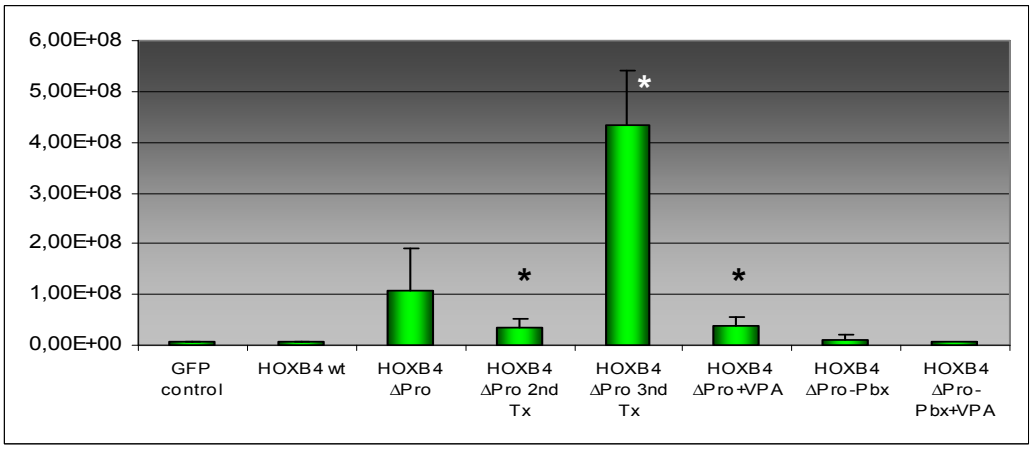

Fig. 4.5.2.5b. WBCs/ml in the PB at sacrifice. * significantly higher than in the GFP control ($p<0.05$).

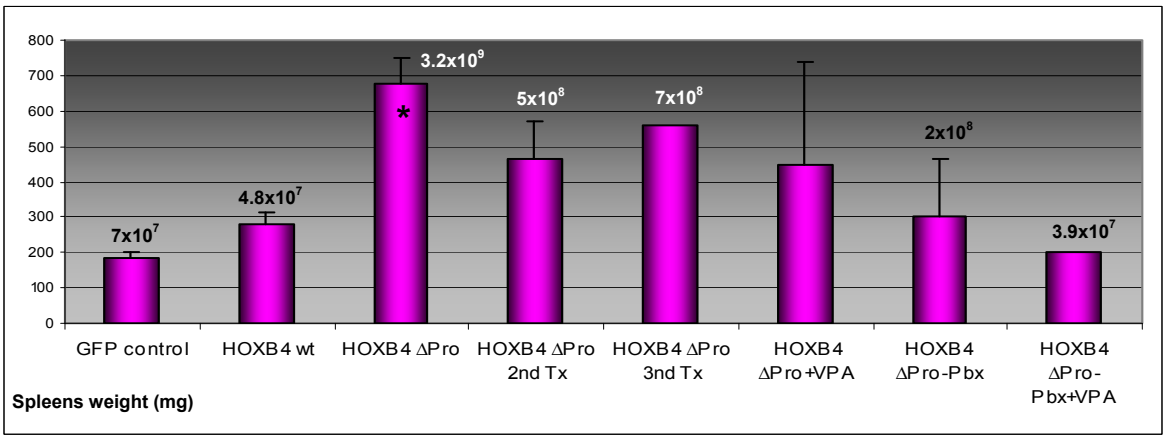

Fig. 4.5.2.5c. Spleen weights from transplanted mice. On top of the bars the average of total cells/spleen is indicated. *significant difference vs. the GFP control ($p<0.05$).

Splenomegaly. Enlargement of the spleen mice was a typical feature observed in Hoxb4-ΔPro leukemic mice. White spots on the surface of the spleen were indicating infiltration with blast colony forming cells, and in some cases

parenchymal infarcts derived from leukocytosis were also visible (Fig. 4.5.2.5c). The number of cells obtained from the spleen parenchyma was 20fold in Hoxb4-ΔPro 1st Tx, up to 92fold in 2nd Tx mice compared to the GFP control mice, while in the Hoxb4-wt mice it was normal.

Immunophenotype of peripheral blood WBCs at sacrifice

At sacrifice the WBCs have been isolated after lysis of the RBCs with ammonium chloride, and they have been stained with fluorochrome-labeled antibodies, specific for the different lineage markers. The percentages of WBCs positive for the single markers are indicated in the tables below. The proportions of Sca-1$^+$ cells in Hoxb4-wt and in Hoxb4-ΔPro was 1.7fold and 1.9fold in comparison to the control, respectively (GFP 16.8% of WBCs, Hoxb4-wt 9.4%, Hoxb4-ΔPro 8.8%, p=n.s.). In the PB of Hoxb4-ΔPro 3rd transplanted mice we reported a significant decrease of Sca-1$^+$ cells in comparison to the GFP and Hoxb4-wt mice ($p<0.04$)(Table 4.5.2.5d). Interestingly, when the double mutant Hoxb4-ΔPro-PBX was overexpressed, we reported a 3fold increase of Sca-1$^+$ cells in comparison to the Hoxb4-wt. In all the mice the proportion of c-kit$^+$ WBCs in the PB was higher than in the GFP control (Hoxb4-wt 5.8fold), and in almost all the Hoxb4-ΔPro mice the proportion of c-kit$^+$ cells was even higher than in the Hoxb4-wt mice (1.5-7.7fold). In almost all the samples where Hoxb4-ΔPro was overexpressed we reported a significant increase of Sca-1 and c-kit double positive WBCs in comparison to the Hoxb4-wt and to the GFP control (1.31% vs. 0.11% and 0.26%, respectively) (Fig. 4.5.2.5d).

Mice (n)	Sca-1 (%)	c-kit (%)	d.p. (%)
GFP control (3)	16.76	0.42	0.26
HOXB4-wt (8)	9.4	2.46	0.11
HOXB4-ΔPro 1st Tx (8)	8.8	6.18	1.31
HOXB4-ΔPro 2nd Tx (3)	3.2	18.89	1.05†
HOXB4-ΔPro 3rd Tx (3)	0.81*†	1.76*	0
HOXB4-ΔPro+VPA (3)	4.16	7.22	1.2†
HOXB4-ΔPro-PBX (3)	28.95†	3.61	0.57†
HOXB4-ΔPro-PBX+VPA (2)	18.45	8.14	0.36

Table 4.5.2.5d. Sca-1 and c-kit immunostaining of WBCs in the PB of mice at sacrifice. The percentages of positive WBCs are indicated. *significant difference vs. the GFP control; †significant difference vs. the Hoxb4-wt ($p<0.05$).

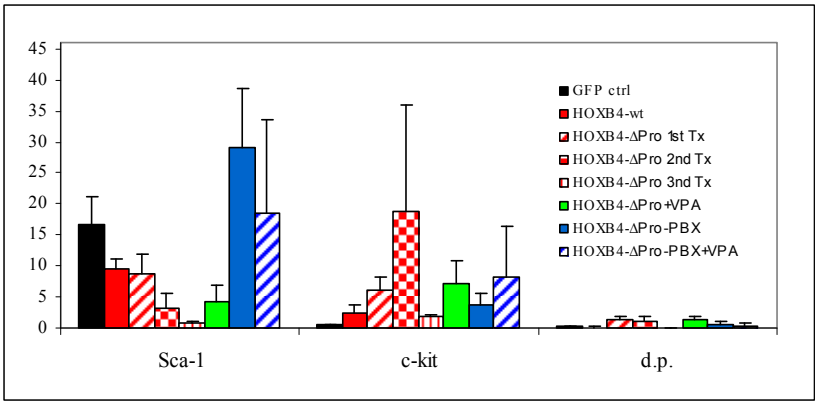

Fig. 4.5.2.5d. Sca-1 and c-kit immunostaining of WBCs in the PB of mice at sacrifice. The percentages of positive WBCs are indicated.

Considering the myeloid compartment, we reported a significant increase of the Mac-1$^+$ and Gr-1$^+$ WBCs in almost all the mice in comparison to the GFP control, while in the Hoxb4-ΔPro-PBX+VPA the myeloid WBCs were even lower than in the GFP control. The Mac-1$^+$ cells in the Hoxb4-ΔPro 1st Tx, in the Hoxb4-ΔPro 3rd Tx, and in the Hoxb4-ΔPro+VPA were significantly higher than in the GFP control (1.8-, 2-, and 1.7fold, respectively, $p<0.05$). In the Hoxb4-ΔPro 1st Tx and 3rd Tx mice the Mac-1$^+$ WBCs were also significantly higher than in the Hoxb4-wt ($p<0.02$). The Gr-1 marker was expressed in a similar proportion of WBCs in the GFP control and in the Hoxb4-wt mice as observed for Mac-1, while it was significantly higher expressed in Hoxb4-ΔPro 2nd and 3rd mice (1.7fold higher vs. Hoxb4-wt, $p<0.04$; 2fold higher vs. GFP control, $p<0.03$). The proportion of WBCs expressing both the Mac-1 and the Gr-1 markers were significantly higher in almost all the Hoxb4-ΔPro mice than in the Hoxb4-wt and the GFP mice (p=n.s.) (Table and Fig. 4.5.2.5e). Interestingly, the proportion of myeloid positive WBCs in the PB of Hoxb4-wt mice decreased significantly over time. Comparing the proportion of myeloid WBCs in the Hoxb4-wt mice at fourth week post transplantation (Mac-1$^+$ 92.17%, Gr-1$^+$ 85.5%, and Mac-1$^+$/Gr-1$^+$ d.p. 85.26%) and at sacrifice (Mac-1$^+$ 63%, Gr-1$^+$ 49%, and Mac-1$^+$/Gr-1$^+$ d.p. 46.93%), we reported a significant over time decrease of 29%, 37%, and 39%, respectively ($p<0.05$). In contrast, in the Hoxb4-ΔPro mice we reported a significant over time increase of 45%, 44%, and 43% in Mac-1$^+$, Gr-1$^+$ and double positive, respectively (at 16 weeks post transplantation, 43.02%, 29.01%, and 29.23%, vs. 88%, 73.08%, and 72.09% at sacrifice, respectively) ($p<0.00001$). We can

conclude that in these two populations of mice there was an opposite development of myeloid WBCs in the PB (Fig. 4.5.2.5e2).

Mice (n)	Mac-1 (%)	Gr-1 (%)	d.p. (%)
GFP control (3)	49.04	39.23	35.68
HOXB4-wt (8)	63.07	49.06	49
HOXB4-ΔPro 1st Tx (8)	88*†	73.08	72.09
HOXB4-ΔPro 2nd Tx (3)	44.3	90.02*†	39.256
HOXB4-ΔPro 3rd Tx (3)	96.81*†	82.76*†	60.12
HOXB4-ΔPro+VPA (3)	84.61*	60.59	60
HOXB4-ΔPro-PBX (3)	81.32	75.7	67.6
HOXB4-ΔPro-PBX+VPA (2)	14.21*†	20.68	14

Table 4.5.2.5e. Mac-1 and Gr-1 immunostaining of WBCs in the PB of mice at sacrifice. The percentages of positive WBCs are indicated. * significant difference vs. the GFP control; † significant difference vs. the Hoxb4-wt.

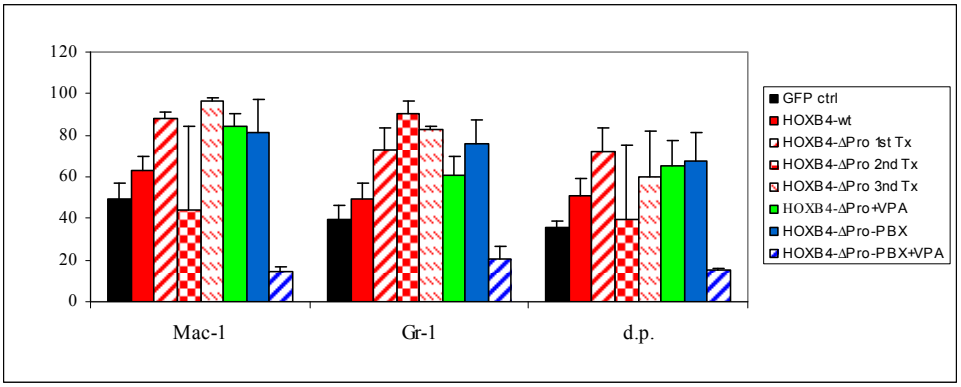

Fig. 4.5.2.5e. Mac-1 and Gr-1 immunostaining of WBCs in the PB of mice at sacrifice. The percentages of positive WBCs are indicated.

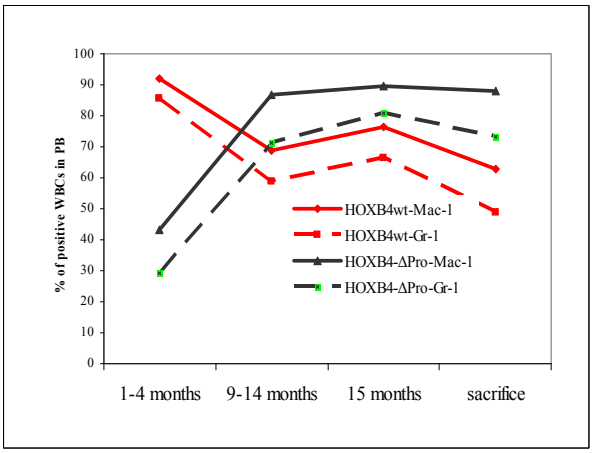

Fig. 4.5.2.5e2. Mac-1 and Gr-1 positive WBCs from peripheral blood of mice transplanted with BM cells overexpressing Hoxb4-wt and Hoxb4-ΔPro. All the differences between the initial value and the final value at sacrifice were significant for each marker ($p<0.05$).

The marker Ter-119 was used to analyse the differentiation into the erythroid lineage. We reported a significant decrease of this subpopulation in almost all the

mice in comparison to the GFP control (p<0.0002). The B-lymphocytes specific antigen B220 was lower expressed in almost all the samples harbouring the ΔPro mutation than in the GFP control and in the Hoxb4-wt (Hoxb4-ΔPro 1st Tx=2.6- and 3fold, 2nd Tx=13- and 15fold, 3rd Tx=9.5- and 10fold lower than in the GFP control and in Hoxb4-wt, respectively) (Table and Figure 4.5.2.5f).

Mice (n)	Ter-119 (%)	B220 (%)
GFP control (3)	83.45†	15.86
HOXB4-wt (8)	19.09*	18.20
HOXB4-ΔPro 1st Tx (8)	20.56*	5.92
HOXB4-ΔPro 2nd Tx (3)	10.05*	1.21
HOXB4-ΔPro 3rd Tx (3)	6.3*	1.66
HOXB4-ΔPro+VPA (3)	9.52*	4.85
HOXB4-ΔPro-PBX (3)	11.96*	5.52
HOXB4-ΔPro-PBX+VPA (2)	30.92	16.11

Table 4.5.2.5f. Ter-119 and B220 immunostaining of WBCs in the peripheral blood of mice at sacrifice. The percentages of positive WBCs are indicated. *significant difference vs. the GFP control; † significant difference vs. the Hoxb4-wt (p<0.05).

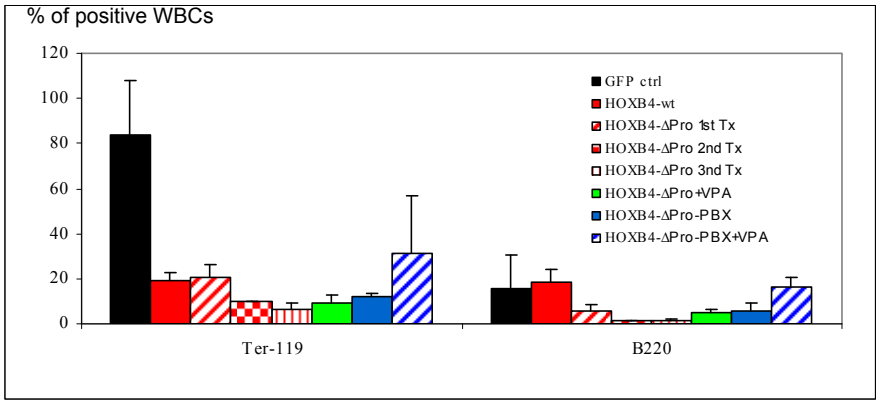

Fig.4.5.2.5f. Ter-119 and B220 immunostaining of WBCs in the PB of mice at sacrifice. The percentages of positive WBCs are indicated.

The T-lymphocytes specific marker CD4 was also significantly lower expressed in almost all the samples in comparison to the GFP control (Hoxb4-wt=3fold, Hoxb4-ΔPro 1st Tx=5fold, 2nd Tx=11fold, 3rd Tx=9.5fold lower than in the GFP control, p<0.04). The percentage of T-lymphocytes expressing both markers in the peripheral blood was significantly lower in all the samples in comparison to the GFP control mice (Table and Figure 4.5.2.5g).

Mice (n)	CD4 (%)	CD8 (%)	d.p. (%)
GFP control (3)	11.4	3.9	0.56
HOXB4-wt (8)	3.74*	1.54	0.11*
HOXB4-ΔPro 1st Tx (8)	2.3*	1.95	0.04*

HOXB4-ΔPro 2nd Tx (3)	1.07	0.48*	0.03
HOXB4-ΔPro 3rd Tx (3)	1.21*†	0.8*	0.8
HOXB4-ΔPro+VPA (3)	n.a.	n.a.	n.a.
HOXB4-ΔPro-PBX (3)	n.a.	n.a.	n.a.
HOXB4-ΔPro-PBX+VPA (2)	1.24	0.62	0

Table 4.5.2.5g. CD4 and CD8 immunostaining of WBCs in the PB of mice at sacrifice. The percentages of positive WBCs are indicated. * significant difference vs. the GFP control; † significant difference vs. the Hoxb4-wt ($p<0.05$).

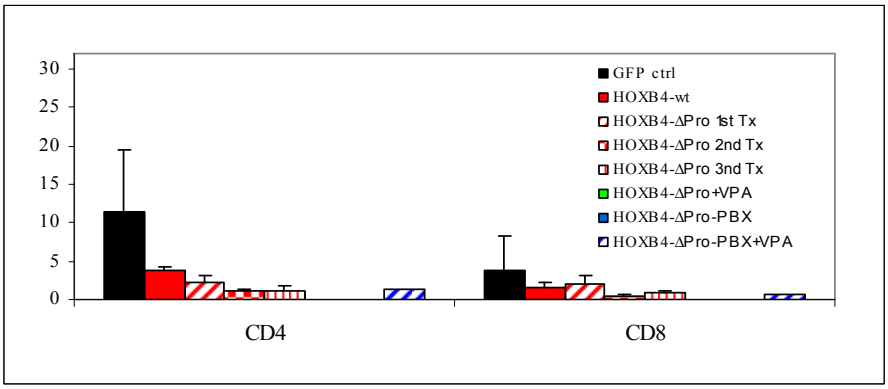

Fig. 4.5.2.5g. CD4 and CD8 immunostaining of WBCs in the PB of mice at sacrifice. The percentages of positive WBCs are indicated.

Lymphoid/myeloid ratio in PB

At sacrifice the WBCs from the peripheral blood of diseased mice have been stained for lymphoid (CD4, CD8, B220) and myeloid (Gr-1, Mac-1, Ter119) surface markers. In the case of Hoxb4-wt overexpression we reported a reduction of the lymphoid proportion when compared to the GFP control (23.5% vs. 67.7 %, respectively), while in the mice where the Hoxb4-ΔPro was overexpressed the majority of the WBCs were myeloid (lymphoid ≤ 10%, myeloid 90-100%) (Fig. 4.5.2.5h). This reflects the amplificatory effect of the Hoxb4-ΔPro on the myeloid compartment.

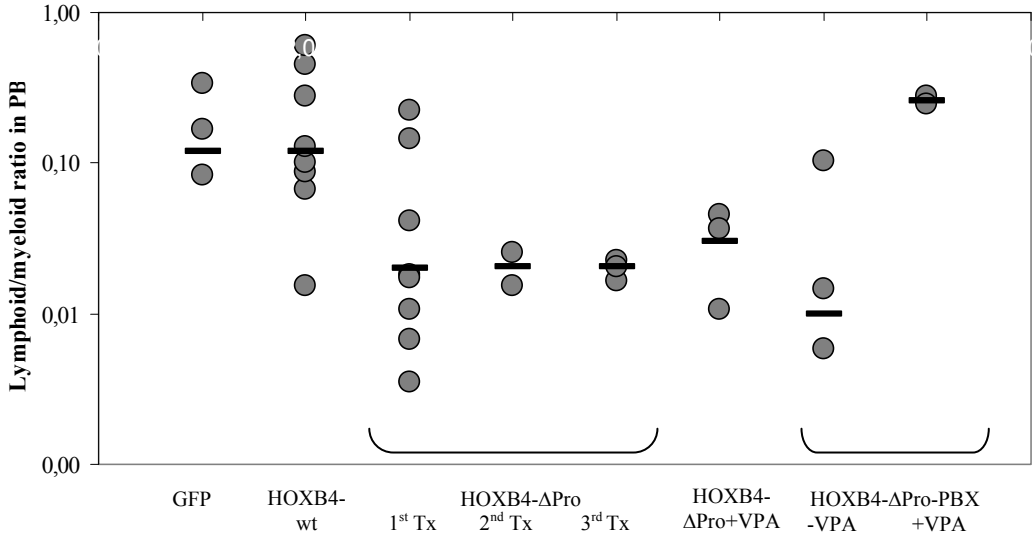

Fig. 4.5.2.5h. Lymphoid/myeloid ratio of WBCs of PB at sacrifice. Horizontal black bars indicate the medians.

Immunophenotype of bone marrow WBCs at sacrifice

At sacrifice the bone marrow has been prepared out of the legs bones and analysed for the expression of lineage specific surface markers. Similarly to the observation in PB, the Sca-1 marker was expressed at lower level in the 2nd and 3rd Hoxb4-ΔPro transplanted mice (32- and 18fold less, p=n.s.) in comparison to the GFP control mice, while in Hoxb4-wt mice it was similar to the control mice. The c-kit marker was higher expressed in the samples overexpressing Hoxb4-wt (1.2fold), Hoxb4-ΔPro 1st and 2nd Tx (1.5- and 3.2fold), Hoxb4-ΔPro-PBX (3.2fold), and in Hoxb4-ΔPro-PBX+VPA (3.6fold, p<0.03) in comparison to the GFP control (Table 4.5.2.5i).

Mice (n)	Sca-1 (%)	c-kit (%)	d.p. (%)
GFP control (3)	5.16	8.72	0.51
HOXB4-wt (3)	2.08	10.89	1.15
HOXB4-ΔPro 1st Tx (7)	10.76	13.86	1.64
HOXB4-ΔPro 2nd Tx (2)	0.16	28.30	0.03
HOXB4-ΔPro 3rd Tx (1)	0.44	2.31	0.01
HOXB4-ΔPro+VPA (3)	2.89	5.58	0.83
HOXB4-ΔPro-PBX (3)	9.6†	28.29	3.34
HOXB4-ΔPro-PBX+VPA (2)	15.94	31.61*†	10.52

Table 4.5.2.5i. Sca-1 and c-kit immunostaining of WBCs in the BM of mice at sacrifice. The percentages of positive WBCs are indicated. * significant difference vs. the GFP control; † significant difference vs. the Hoxb4-wt (p<0.05).

When considering the myeloid compartment, we reported an higher proportion of Mac-1^{+} cells in almost all the Hoxb4-wt and Hoxb4-ΔPro mice when compared to the GFP control mice. In the Hoxb4-wt this increase was 1.4fold, in the Hoxb4-ΔPro (1st, 2nd, 3rd Tx) it was 1.6-, 1.5-, and 1.7fold, respectively, and in Hoxb4-ΔPro+VPA 1.4fold higher than in the GFP control ($p<0.015$). Similarly, the Gr-1 marker was higher expressed in the Hoxb4-wt (1.5fold), and in Hoxb4-ΔPro mice (1st Tx 1.4-, 2nd Tx 1.7-, 3rd Tx 1.6fold) than in the GFP control ($p<0.05$) (Table 4.5.2.5j).

Mice (n)	Mac-1 (%)	Gr-1 (%)	d.p. (%)
GFP control (3)	56.28	53.96	53.96
HOXB4-wt (3)	79.65	79.38	78.16
HOXB4-ΔPro 1st Tx (7)	90.84*	76.75	74.10
HOXB4-ΔPro 2nd Tx (2)	86.86	92.85	81.74
HOXB4-ΔPro 3rd Tx (1)	97.86	86.5	86
HOXB4-ΔPro+VPA (3)	76.52	49.09	49
HOXB4-ΔPro-PBX (3)	60.43	59.3	37.79
HOXB4-ΔPro-PBX+VPA (2)	33.31†	41.66	29.72*†

Table 4.5.2.5j. Mac-1 and Gr-1 immunostaining of WBCs in the BM of mice at sacrifice. The percentages of positive WBCs are indicated. * significant difference vs. the GFP control; † significant difference vs. the Hoxb4-wt ($p<0.05$).

The erythroid lineage was lower represented in the BM pooled cells from all the mice in comparison to the GFP control (Hoxb4-wt 4.4fold, Hoxb4-ΔPro 1st, 2nd and 3rd Tx it was 9-, 44-, and 20fold, respectively, lower than in the GFP). Similarly, the lymphoid marker B220 was lower expressed in the Hoxb4-wt and in the Hoxb4-ΔPro 2nd and 3rd Tx mice than in the GFP control mice (3.6-, 4.4-, 4.4fold, respectively, p=n.s.) (Table 4.5.2.5k).

Mice (n)	Ter-119 (%)	B220 (%)
GFP control (3)	33.77	8.16
HOXB4-wt (3)	7.71	2.26
HOXB4-ΔPro 1st Tx (7)	4.16	7.93
HOXB4-ΔPro 2nd Tx (2)	0.77	1.84
HOXB4-ΔPro 3rd Tx (1)	1.69	1.84
HOXB4-ΔPro+VPA (3)	22.52	15.29
HOXB4-ΔPro-PBX (3)	10.49	21.21
HOXB4-ΔPro-PBX+VPA (2)	12.41	7.05

Table 4.5.2.5k. Ter-119 and B220 immunostaining of WBCs in the BM of mice at sacrifice. The percentages of positive WBCs are indicated.

Considering the T-lymphoid specific markers, in almost all the Hoxb4 mice we reported a decrease in the CD4 positive lymphoid population (Hoxb4-wt 3-, Hoxb4-ΔPro 2nd Tx 1.7- and 3rd Tx 2.3fold) in comparison to the GFP control (Table 4.5.2.5l).

Mice (n)	CD4 (%)	CD8 (%)	d.p. (%)
GFP control (3)	3.47	0.72	0.05
HOXB4-wt (8)	1.18	0.85	0.07
HOXB4-ΔPro 1st Tx (8)	8.58	5.28	0.29
HOXB4-ΔPro 2nd Tx (3)	2	0.47	0.09
HOXB4-ΔPro 3rd Tx (3)	1.51	0.9	0.03
HOXB4-ΔPro-PBX+VPA (2)	2.06	0.37	0.03

Table 4.5.2.5l. CD4 and CD8 immunostaining of WBCs in the BM of mice at sacrifice. The percentages of positive WBCs are indicated.

Interestingly, when the BM WBCs of Hoxb4-wt and of Hoxb4-ΔPro mice were co-stained with the c-kit and the myeloid markers Mac-1/Gr-1 specific antibodies, we observed a dramatic increase in the proportion of double positive cells (7.14% in Hoxb4-wt, 12.3% in the 1st Tx Hoxb4-ΔPro, and 21.4% in the 2nd Tx Hoxb4-ΔPro, respectively) in comparison to the GFP control mice (0.8%). The additional co-staining of the same myeloid markers with Sca-1 antibody did not show significant differences between all the samples analyzed (Fig. 4.5.2.5la).

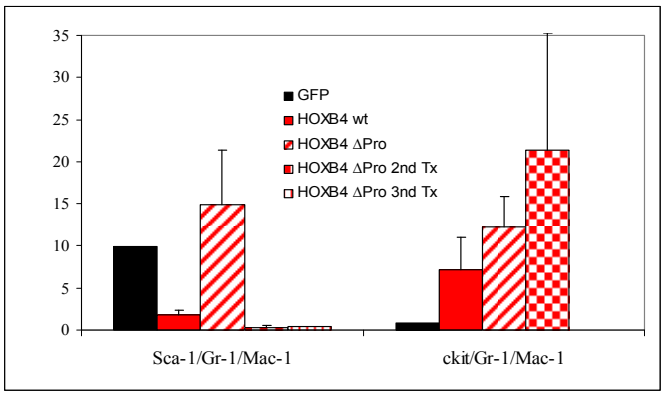

Fig. 4.5.2.5la. Co-staining of WBCs in the BM of mice at sacrifice. The percentages of positive WBCs are indicated.

Immunophenotype of cells obtained from the spleen at sacrifice

The spleen of dead mice has been mashed and the single cells suspension has been stained with the same lineage specific antibodies. The size and the total cells numbers are reported above in this paragraph. We observed the same immunophenotype as reported in case of the WBCs from BM and PB. In the

Hoxb4-wt and the Hoxb4-ΔPro the Sca-1$^+$ cells were 8.8fold and 12fold (in the 2nd Tx 54-, in the 3rd Tx 68fold) lower than in the GFP control, respectively ($p<0.008$). The proportion of c-kit$^+$ cells in the Hoxb4-wt mice was significantly higher than in the GFP control (18% vs. 1.5%, respectively, $p<0.024$), while in the Hoxb4-ΔPro mice it was up to 25fold higher than in the GFP control (Table 4.5.2.5m).

Mice (n)	Sca-1 (%)	c.kit (%)	d.p. (%)
GFP control (3)	55.5	1.5	0.87
HOXB4-wt (8)	6.3*	18.12*	2.71
HOXB4-ΔPro 1st Tx (8)	4.63*	36.54	0.92
HOXB4-ΔPro 2nd Tx (3)	1.03*†	38.4	0.83
HOXB4-ΔPro 3rd Tx (3)	0.81	3.54	0.02
HOXB4-ΔPro+VPA (3)	28.77	12.77*	3.14*
HOXB4-ΔPro-PBX (3)	24.44	21.37*	3.93
HOXB4-ΔPro-PBX+VPA (2)	35.45	48.76*	15.66

Table 4.5.2.5m. Sca-1 and c-kit immunostaining of WBCs in the spleen of mice at sacrifice. The percentages of positive WBCs are indicated. * significant difference vs. the GFP control; † significant difference vs. the Hoxb4-wt ($p<0.05$).

The proportion of Mac-1$^+$ cells was also higher in the Hoxb4-wt (7fold, $p<0.03$), in Hoxb4-ΔPro (11fold in the 1st Tx, 12fold in the 2nd Tx, 13fold in the 3rd Tx, $p<0.0008$), and in Hoxb4-ΔPro-PBX (10fold) in comparison to the GFP control. Similarly, the proportion of Gr-1$^+$ cells was higher in Hoxb4-wt (3.6fold), Hoxb4-ΔPro (4-5.6fold, $p<0.008$), and in the Hoxb4-ΔPro-PBX (5fold) in comparison to the GFP control (Table 4.5.2.5n).

Mice (n)	Mac-1 (%)	Gr-1 (%)	d.p. (%)
GFP control (3)	7.3	13.6	1
HOXB4-wt (8)	50.84*	48.89	47.1*
HOXB4-ΔPro 1st Tx (8)	79.63*	56.24*	48.67*
HOXB4-ΔPro 2nd Tx (3)	84.89*	80.98*	69.52*
HOXB4-ΔPro 3rd Tx (3)	95.64	76.64	76.17
HOXB4-ΔPro+VPA (3)	78.05*	44.07	44*
HOXB4-ΔPro-PBX (3)	76.23	67.46	65.63
HOXB4-ΔPro-PBX+VPA (2)	18.54	12.08	11.69

Table 4.5.2.5n. Mac-1 and Gr-1 immunostaining of WBCs in the spleen of mice at sacrifice. The percentages of positive WBCs are indicated. * significant difference vs. the GFP control; † significant difference vs. the Hoxb4-wt ($p<0.05$).

The proportion of Ter119$^+$ cells was also lower in all the samples, in comparison to the GFP control (Hoxb4-ΔPro 11.5fold lower ($p<0.01$)). The B220$^+$ cells were

similarly less in all the HOXB4 mice in comparison to the GFP control (Hoxb4-wt 8fold, Hoxb4-ΔPro 1st Tx 40-, 2nd Tx 18-, 3rd Tx 13fold lower, $p<0.05$) (Table 4.5.2.5o).

Mice (n)	Ter-119 (%)	B220 (%)
GFP control (3)	19.3	52.3
HOXB4-wt (8)	17.94	6.66*
HOXB4-ΔPro 1st Tx (8)	1.67*	1.28*
HOXB4-ΔPro 2nd Tx (3)	3.02	2.91
HOXB4-ΔPro 3rd Tx (3)	1.94	4.05
HOXB4-ΔPro+VPA (3)	9.6	17.43
HOXB4-ΔPro-PBX (3)	6.41	9.61
HOXB4-ΔPro-PBX+VPA (2)	2.63	9.75

Table 4.5.2.5o. Ter-119 and B220 immunostaining of WBCs from the spleen of mice at sacrifice. The percentages of positive WBCs are indicated. * significant difference vs. the GFP control.

The T-lymphoid cells specific markers $CD4^+$ and $CD8^+$ were less expressed in the Hoxb4-wt as well as in the Hoxb4-ΔPro in comparison to the GFP control, as observed in case of cells from PB and BM (Table 4.5.2.5p).

Mice (n)	CD4 (%)	CD8 (%)	d.p. (%)
GFP control (3)	14.9	8.7	0.1
HOXB4-wt (8)	2.53	2.01	0.13
HOXB4-ΔPro 1st Tx (8)	0.72	0.05	0.03
HOXB4-ΔPro 2nd Tx (3)	3.65	0.93	0.18
HOXB4-ΔPro 3rd Tx (3)	0.84	2.58	0.05
HOXB4-ΔPro+VPA (2)	n.a.	n.a.	n.a.
HOXB4-ΔPro-PBX (3)	n.a.	n.a.	n.a.
HOXB4-ΔPro-PBX+VPA (2)	1.84	0.27	0.05

Table 4.5.2.5p. CD4 and CD8 immunostaining of WBCs in the spleen of mice at sacrifice. The percentages of positive WBCs are indicated.

Interestingly, by performing double stainings for the c-kit/myeloid (Mac-1/Gr-1) markers we reported an increased proportion of these double positive cells also in the spleen of Hoxb4-wt and Hoxb4-ΔPro mice in comparison to the GFP control at sacrifice (Table 4.5.2.5q). In current experiments we are investigating, if the leukemic stem cells in this AML model are residing within this subpopulation.

Mice (n=2)	c-kit$^+$/Mac-1$^+$/Gr-1$^+$ (%)
GFP control	0.82
HOXB4-wt	6.39
HOXB4-ΔPro 1st Tx	11
HOXB4-ΔPro 2nd Tx	31.8

Table 4.5.2.5q. Immunostaining for c-kit, Mac-1 and Gr-1 surface markers of WBCs in the spleen of mice at sacrifice is reported. The percentages of positive WBCs are indicated.

In summary, we observed consistently a significant increase of c-kit$^+$ cells in the peripheral blood, bone marrow and spleen of Hoxb4-ΔPro diseased mice, an increase of myeloid cells (Mac-1 and Gr-1), and a decrease in the proportion of lymphoid cells (B220, CD4, and CD8) in the peripheral blood as well as in the spleen, in comparison to the GFP control and Hoxb4-wt mice. The following panels show the morphology of cells obtained from representative mice (Fig. 4.5.2.5i).

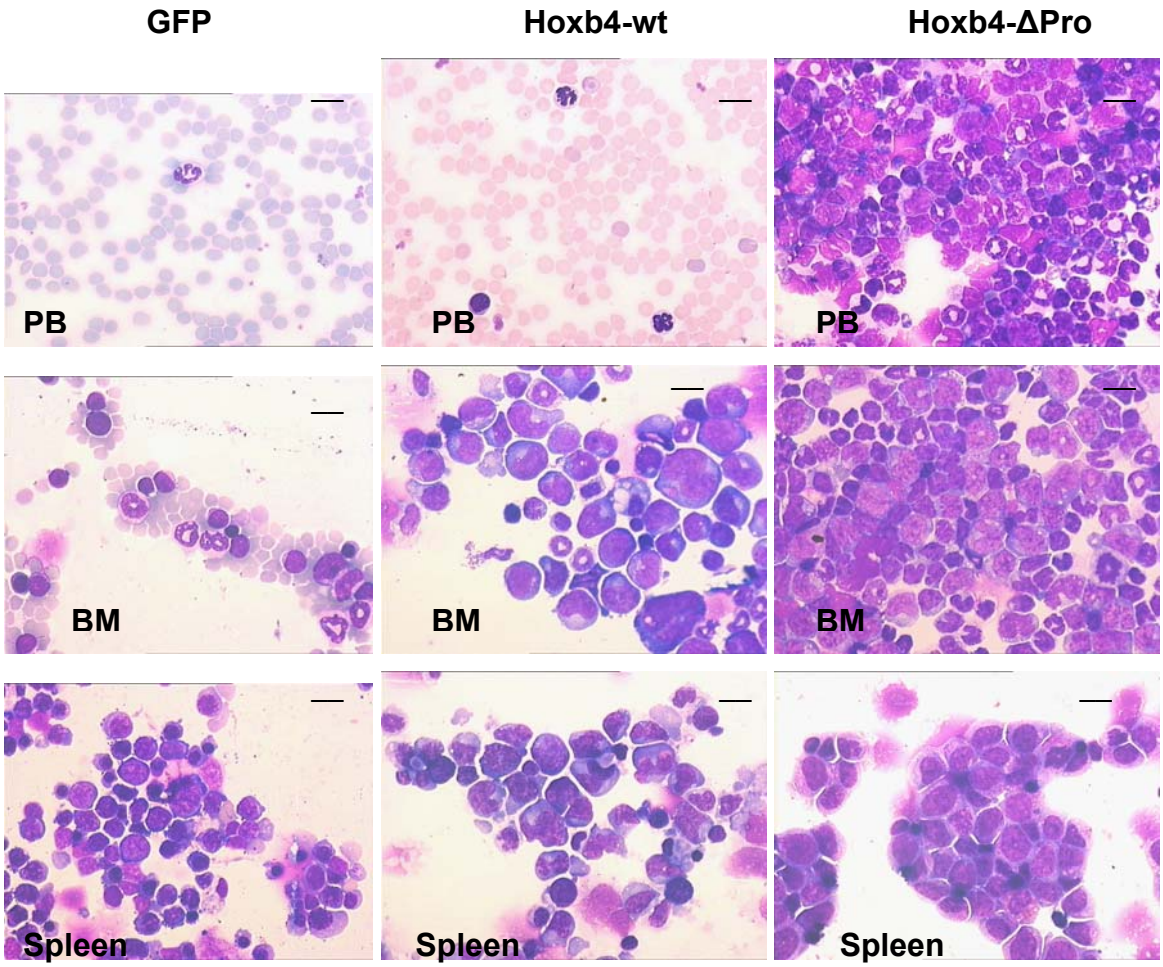

Fig. 4.5.2.5i. May-Gruenwald stainings of blood smears and cytospin preparations from PB, BM, spleen of transplanted mice. Bars: 8 µm, X630.

4.5.2.6 Colony forming cells-assay (CFC) *ex vivo*

Long term. 13 weeks post transplantation BM aspiration has been performed from GFP control (n=1), Hoxb4-wt (n=2) and from Hoxb4-ΔPro (n=1) mice and 20,000 cells/dish have been plated in methylcellulose, to allow the growth of myeloid colonies. At this time point after transplantation we reported 35 CFCs in the GFP control, while in the Hoxb4-wt we counted 256 CFCs, and in the Hoxb4-ΔPro 69 CFCs. In all the samples the presence of VPA (1mM) led to a slight increase in the CFCs frequency (data not shown). Moreover, in the Hoxb4-wt the CFCs were 22,3% G, 26% GM, 22% M, 24% BFU-E, 3% GEMM, and 2.7% Mek, while in the Hoxb4-ΔPro we reported <1% G, 33% GM, 0.3% M, 58.5% BFU-E, and no GEMM/Mek CFCs. In the GFP control we reported 19% G, 31% GM, 37.5% M, and 12.5% BFU-E CFCs. Analyzing the pooled cells from the CFCs of Hoxb4-ΔPro we reported that only 6% and 7.4% of the cells were positive for Mac-1 and Gr-1 respectively, while in the GFP control they were 60.46% and 63.5%, respectively. In the Hoxb4-wt samples 38.2% and 32.9% of the pooled cells from CFCs were positive for Mac-1 and Gr-1, respectively.

In the lymphoid colony forming unit assay (proB) 100,000 primary BM cells have been plated in methylcellulose containing IL7. In the GFP control we reported 39.6 colonies, in the Hoxb4-wt 44.25, and in the Hoxb4-ΔPro 6.5 colonies. We can conclude that 13 weeks after transplantation there is already a reduction of the mature myeloid and lymphoid CFCs in the Hoxb4-ΔPro BM in comparison to the Hoxb4-wt and to the GFP control, while in the Hoxb4-wt the myeloid/lymphoid CFCs counts were similar to the CFCs observed in case of the control. At this time point the Hoxb4-ΔPro mice were healthy and did not show any sign of leukemia, maybe reflecting a pre-leukemic state.

At sacrifice. At sacrifice we performed the CFC assay from bone marrow, peripheral blood and spleen cells by plating 100,000 cells into methylcellulose containing SCF, IL3 and IL6. In the BM from Hoxb4-ΔPro mice we saw a dramatic increase of CFCs (1st Tx=2983 CFCs, n=4, 98.3% blast-like colonies; 2nd Tx=2111 CFCs, n=3, 92.5% blast-like colonies, and 3rd Tx=1296 CFCs, n=2, 90.7% blast-like colonies), in comparison to the Hoxb4-wt (365 CFCs, n=3, 46.3% blast-like colonies) and to the GFP control (204 CFCs, n=3, 21.7% blast-like colonies). In the BM from GFP mice we reported 160 mature myeloid colonies (G=31, GM=98, M=19, GEMM=9, MeK=3) per 100,000 plated cells,

based on the colony morphology, while in the BM of Hoxb4-wt mice we reported 184 myeloid colonies (G=65, GM=65, M=53, GEMM=2, MeK=0) per 100,000 plated cells. In the BM of 1st Tx Hoxb4-ΔPro mice we reported a 3fold decrease in the number of mature myeloid colonies (51 myeloid CFCs: G=20, GM=31, M=0, GEMM=0, Mek=0) when compared to the GFP control (p=0.11), while in the Hoxb4-ΔPro 2nd and 3rd transplanted mice the myeloid colonies were 158 (G=7, GM=36, M=115, GEMM=0, Mek=0) and 120 (G=0, GM=120, M=0, GEMM=0, Mek=0), respectively (Fig.4.5.2.6a).

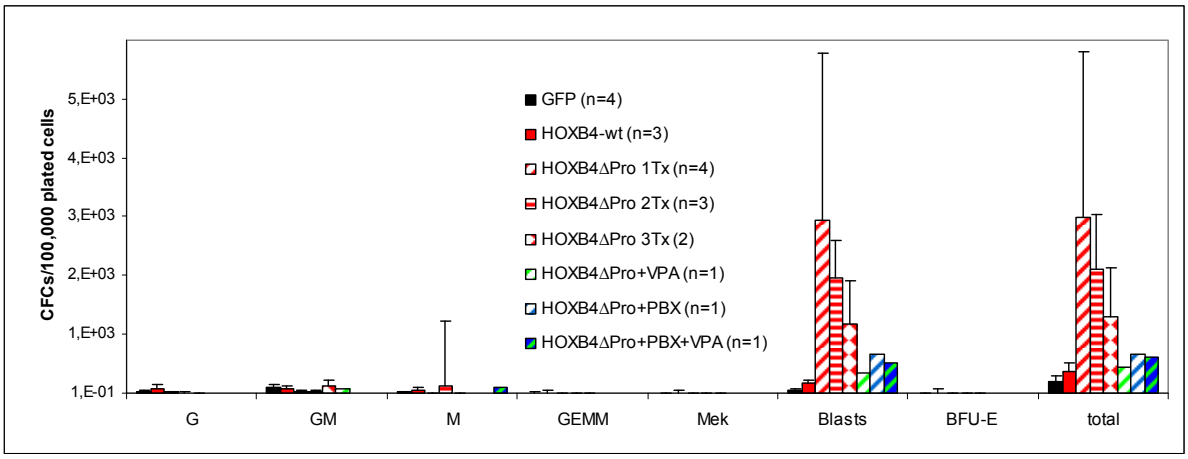

Fig. 4.5.2.6a. 1° CFC from BM of mice at sacrifice. 100,000 BM cells have been plated into methylcellulose containing IL3, IL6 and SCF and after one week the colonies have been counted. The blast CFCs in GFP control and in Hoxb4-wt appeared more similar to mature CFCs like BFU-E.

When plating 100,000 nucleated cells from PB into methylcellulose we reported a significant increase of CFCs in the Hoxb4-ΔPro mice (1st Tx=259 CFCs, n=3, 96.2% blast-like colonies; 2nd Tx=1140 CFCs, n=2, 40.3% blast-like colonies, and 3rd Tx=369 CFCs, n=4, 82.9% blast-like colonies), in comparison to the Hoxb4-wt (3.8 CFCs, n=2, 0% blast-like colonies) and to the GFP control (1 CFCs, n=3, 0% blast-like colonies, p=0.26, p=0.009, p=0.001). In PB from GFP mice we reported 1 myeloid colony (G=0, GM=1, M=0, GEMM=0, MeK=0) per 100,000 plated cells, while in the PB of Hoxb4-wt mice we reported 8.5 myeloid colonies (G=0, GM=8.5, M=0, GEMM=0, MeK=1). In the PB of 1st Tx Hoxb4-ΔPro mice we reported a similar number of mature myeloid colonies (10 myeloid CFCs: G=0, GM=1, M=6, GEMM=1, Mek=2) when compared to the GFP control, while in the corresponding 2nd and 3rd transplanted mice the myeloid colonies were 680 (G=0, GM=0, M=680, GEMM=0, Mek=0) and 63 (G=0, GM=63, M=0, GEMM=0, Mek=0), respectively (Fig. 4.5.2.6b).

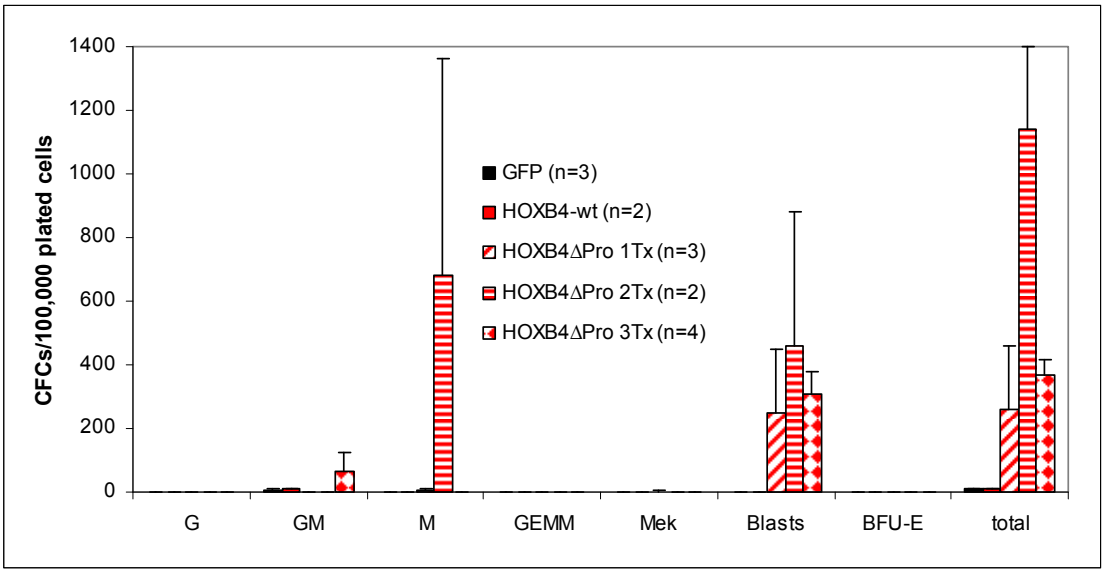

Fig 4.5.2.6b. 1° CFC from PB of mice at sacrifice. 100,000 WBCs have been plated into methylcellulose containing IL3, IL6 and SCF and after one week the colonies have been counted.

Similarly, when plating 100,000 nucleated cells from the spleen into methylcellulose we reported a significant increase of CFCs in the Hoxb4-ΔPro mice (1st Tx=638 CFCs, n=4, 86.8% blast colonies; 2nd Tx=1920 CFCs, n=3, 54% blast colonies, and 3rd Tx=342 CFCs, n=2, 99.4% blast colonies), in comparison to the Hoxb4-wt (35.3 CFCs, n=2, 3% blast colonies, p=0.33, p=0.11, p=0.016, respectively) and to the GFP control (1.3 CFCs, n=4, 0% blast colonies, p=0.198, p<0.045, p<0.002). In the spleen from the GFP mice we reported 1.3 myeloid colonies (G=0, GM=1.3, M=0, GEMM=0, MeK=0) per 100,000 plated cells, while in the spleen of HOXB4-wt mice we reported 25 myeloid colonies (G=7, GM=15, M=2, GEMM=1, MeK=0). In the spleen of 1st Tx Hoxb4-ΔPro mice we reported a higher number of myeloid colonies (84.1 myeloid CFCs: G=0, GM=81.5, M=2.6, GEMM=0, Mek=0) when compared to the GFP control, while in the corresponding 2nd and 3rd transplanted Hoxb4-Δpro mice the myeloid colonies were 883.3 (G=0, GM=0, M=883.3, GEMM=0, Mek=0) and 2 (G=0, GM=2, M=0, GEMM=0, Mek=0), respectively (Fig 4.5.2.6c).

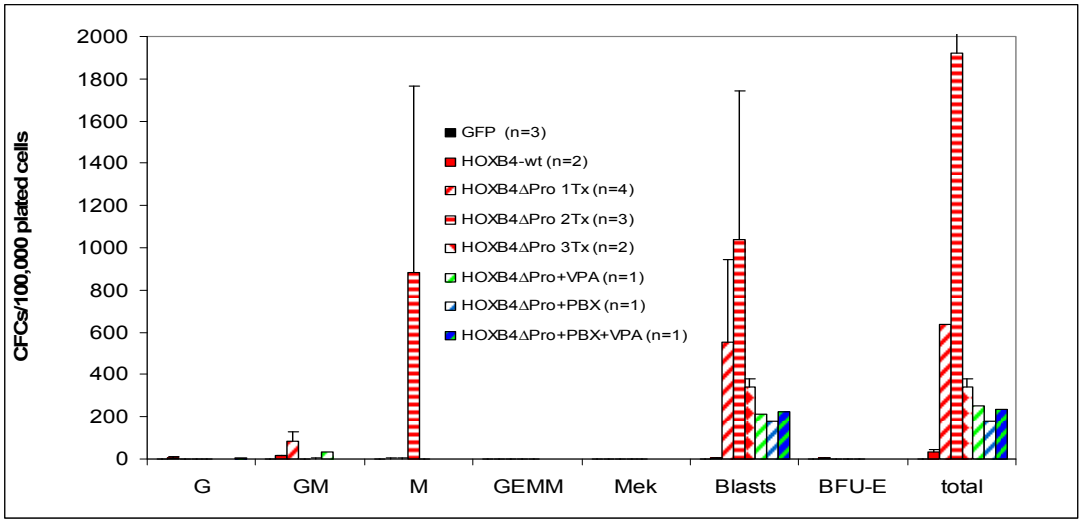

Fig 4.5.2.6c. 1° CFC from spleen of mice at sacrifice. 100,000 WBCs have been plated into methylcellulose containing IL3, IL6 and SCF and after one week the colonies have been counted.

The 1° CFCs have been harvested, pooled and replated into methylcellulose containing IL3, IL6 and SCF. After 1 week the 2°CFCs have been counted. From the BM of GFP control mice we reported 388 2°CFCs per 100,000 replated cells from 1°CFC (30% BFU-E and GM mature myeloid/mast cells CFCs). In the Hoxb4-wt we counted 819 2°CFCs (42% BFU-E, 32% mast cells CFCs), while in the Hoxb4-ΔPro the CFCs counted were 703 (83% blast-like) (n=2) (Fig. 4.5.2.6d).

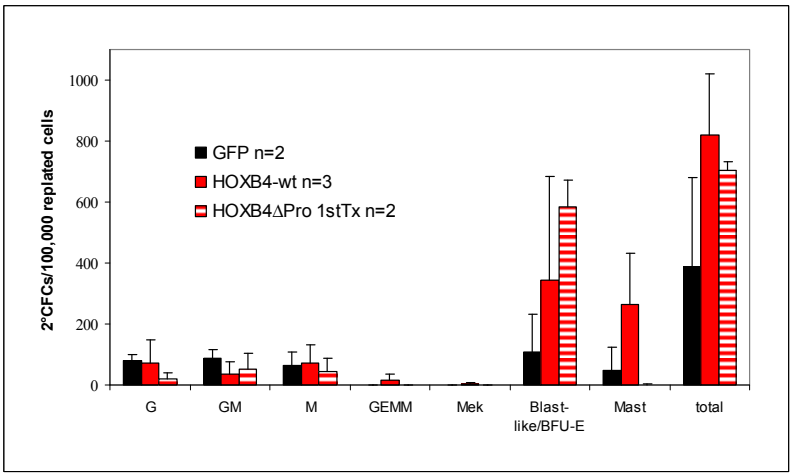

Fig 4.5.2.6d. 2° CFC from BM of mice at sacrifice. 100,000 cells from 1°CFC have been plated into methylcellulose containing IL3, IL6 and SCF and after one week the colonies have been counted.

The 2°CFCs from the spleen of GFP mice were only 0.5/100,000 replated cells, while in the Hoxb4-wt and Hoxb4-ΔPro we reported 876 and 732 2°CFCs/100,000 replated cells, respectively. In case of Hoxb4-wt 29% of 2°CFCs

were mast cells-CFCs and 69% were mature myeloid CFCs, while in case of Hoxb4-ΔPro 68% of the 2°CFCs maintained a blast-like morphology (n=2) (Fig. 4.5.2.6e). These results suggest that in the Hoxb4-ΔPro the hematopoietic progenitor cells transplanted were maintaining a higher replating capacity in comparison to the GFP control, and that this was conserved in the progenitor cells colonizing the spleen.

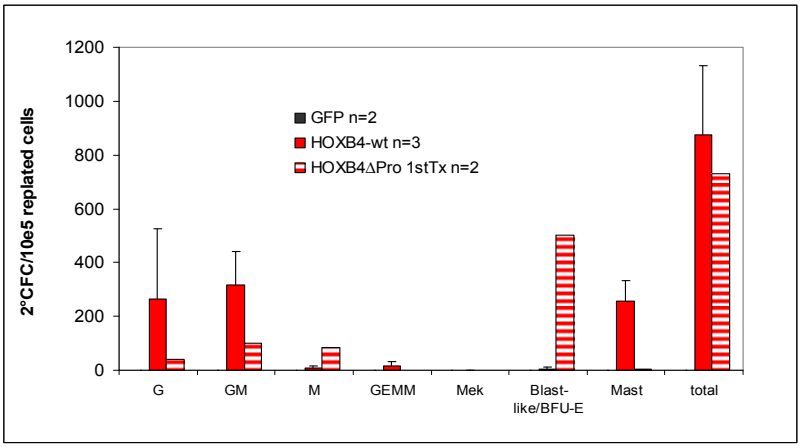

Fig 4.5.2.6e. 2° CFC from spleen of mice at sacrifice. 100,000 cells from 1°CFC have been plated into methylcellulose containing IL3, IL6 and SCF and after one week the colonies have been counted.

Moreover, from the primary samples mentioned above we performed the proB-CFCs assay at sacrifice, by plating 100,000 primary cells in IL7-containing methylcellulose. In the BM of GFP control mice we reported 53 proB-CFCs, while in the BM cells expressing Hoxb4-wt we counted 13.5 proB-CFCs (n=3). Interestingly, when BM cells from Hoxb4-ΔPro mice were plated in the same IL7-containing methylcellulose we counted 755.5 and 1172 CFCs from 1st and 2nd Tx, respectively. Only a small number of these CFCs were effectively proB-CFCs (49.5 from 1st Tx, n=4, and 0 in 2nd Tx, n=2), as confirmed by FACS staining for B220 and myeloid specific markers (data not shown). From the spleen of Hoxb4-wt mice we reported 5 proB-CFCs (n=3), while in the Hoxb4-ΔPro there were 0.17 (1st Tx n=3), and 0 (2nd Tx n=2) proB-CFCs. Moreover, as observed in case of the BM from Hoxb4-ΔPro, we reported also from the spleen of these mice the growth of blast-like colonies (232 and 242 CFCs in the 1st and 2nd Tx mice, respectively). Similarly, from the PB of Hoxb4-ΔPro mice we counted 738 and 159 blast-like CFCs (2nd and 3rd Tx, respectively), which were able to grow only in the presence of IL7, in the absence of normal proB-CFCs (Fig. 4.5.2.6f). In the

immunostaining of the cells harvested from these dishes we reported that >80% of the cells were positive for the myeloid markers Mac-1 and Gr-1 (data not shown). Taken together these results suggest that the 1°CFCs from BM, spleen and PB of Hoxb4-ΔPro leukemic mice were able to grow in the absence of IL3, IL6 and SCF, and were expressing myeloid markers, while the B-lymphoid compartment was displaced.

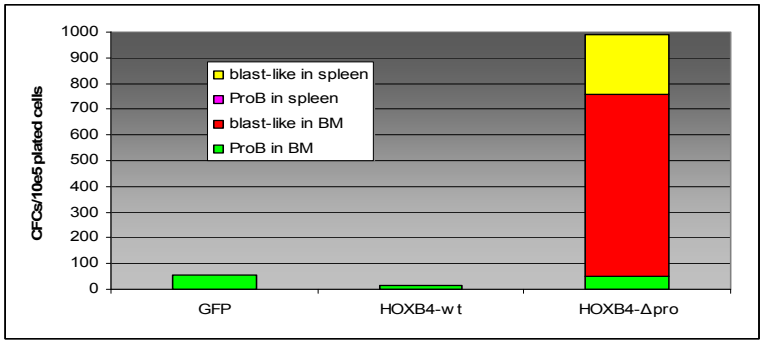

Fig 4.5.2.6f. 1°proB-CFCs from BM and spleen of mice at sacrifice. 100,000 cells have been plated into methylcellulose containing IL7 (proB-CFC assay) and 5 days later the colonies have been counted. Interestingly, in BM and spleen from HOXB4-ΔPro more immature blast-like CFCs were able to grow in the absence of IL3, IL6 and SCF (n=2).

4.5.2.7 Retroviral integration analysis

The analysis of proviral integration sites demonstrated oligoclonal disease in primary, secondary, and tertiary transplanted mice (Fig. 4.5.2.7). The sequencing of retroviral integration sites in diseased mice (n=7) showed in only one case 1 site in or near a region described as common integration site (CIS) in the RTCGD database (http://rtcgd.ncifcrf.gov/) (Akagi, 2004). This site has been found in two different mice transplanted with BM cells originating from the same transduction experiment. We cannot exclude that a clonal event might be responsible for the leukemogenesis in the observed cases. However no proviral recurrent integration sites have been observed (Table 4.5.2.7).

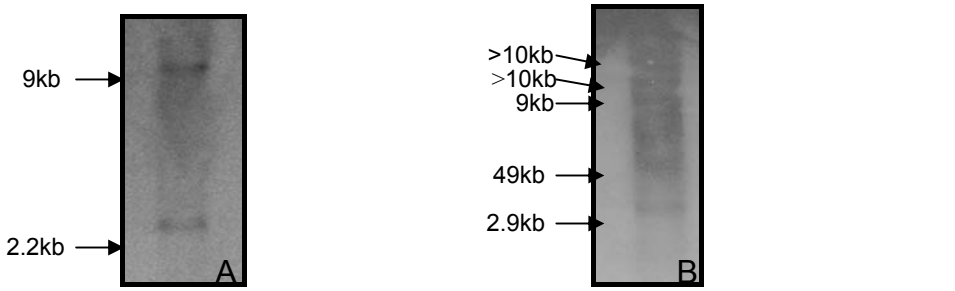

1st Hoxb4-wt mouse no.4 (spleen) 1st Hoxb4-wt mouse no.6 (BM)

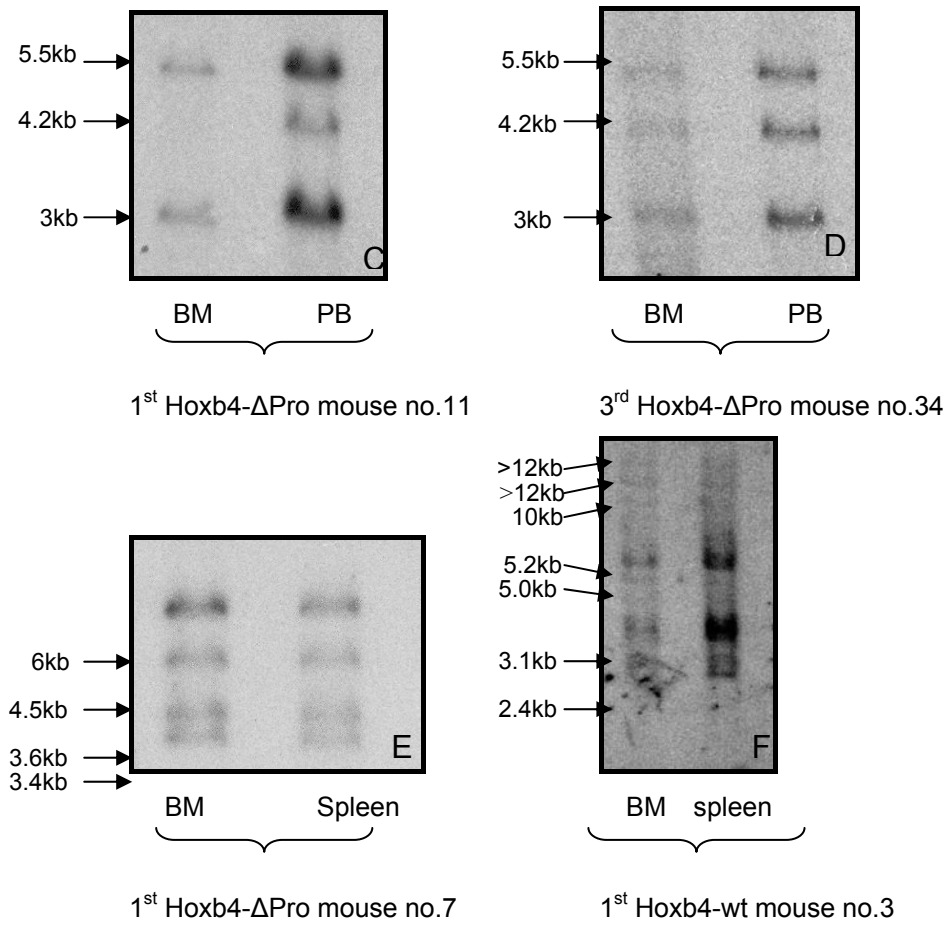

Fig. 4.5.2.7. Retroviral integration sites in diseased mice. A-B-F: Genomic DNA obtained from spleen and BM of Hoxb4-wt primary transplanted mice. C-D-E: Genomic DNA obtained from spleen and BM of Hoxb4-ΔPro primary and tertiary transplanted mice. With the LM-PCR only the integration region corresponding to the lower band has been sequenced. For the numbers of transplanted mice see Table 4.5.2.4a.

Retroviral construct	Gene	Description	Genomic location	Mouse no.
Hoxb4-wt	9 Intron of Palb2	Partner and localizer of BRCA1	7qF3	4
Hoxb4-wt	Intergenic region	-	XqA4	2
Hoxb4-wt	1 Intron AK041797	Murine 3 days neonate thymus cDNA°	5qB3	3
Hoxb4-wt	Intergenic region	-	12qA1.2	3
Hoxb4-wt	2 Intron Bcl9l	B-cell CLL/lymphoma 9-like	9qA5.2	3
Hoxb4-wt	Intergenic region	-	2qC2	6
Hoxb4-wt	5 Intron/6 Exon Cd68	CD68	11qB3	6
Hoxb4-ΔPro	3 Intron of Camk2b*	CaM-kinase II subunit beta	11qA1	11†
Hoxb4-ΔPro	Intergenic region	-	17qA3.3	18
Hoxb4-ΔPro	1 Intron Rreb1	RAS-responsive element-binding protein 1 (RREB-1)	13qA3.3	15†
Hoxb4-ΔPro	3 Intron of Camk2b*	CaM-kinase II subunit beta	11qA1	15†
Hoxb4-ΔPro	Intergenic region	-	13qD1	34

Hoxb4-ΔPro	3´UTR of AK15123	BM macrophage cDNA n.o.c.	13qD1	34
Hoxb4-ΔPro	4 Intron EDAR	EDAR (ectodysplasin-A receptor)-associated death	13qA1	32

Table 4.5.2.7. Identity of retroviral integration sites in diseased mice. N.o.c. = not otherwise characterized. *Identified in or near regions (distance ~50 kb) described as common integration sites (CIS) in the RTCGD database (http://rtcgd.ncifcrf.gov/). ° Hypothetical protein from RIKEN full-length enriched library. † mice transplanted from same transduction experiment.

4.5.2.8 Effect of the proline-rich region deletion on the CRU frequency (CRU assay)

Hoxb4 is a potent enhancer of primitive hematopoietic cell growth, likely by increasing self-renewal probability, without impairing homeostatic control of HSC population size or the rate of production and maintenance of mature end cells. To directly assess the effect of Hoxb4-ΔPro overexpression on earlier stages of hematopoiesis we performed the CRU assay. This assay involves the transplantation of limiting numbers of “test” cells into lethally irradiate syngeneic recipients together with 3 x 10^5 mock carrier cells. Several cohorts of mice have been transplanted with serial dilutions of 5-FU enriched BM progenitor cells transduced with GFP, Hoxb4-wt and Hoxb4-ΔPro constructs. The range of cell numbers useful for this purpose in case of Hoxb4 has been determined based on previous experiments described by other groups (Antonchuck 2001).

A positive engraftment of HSCs was considered when at least 1% of the WBCs in the peripheral blood were originating from the transplanted cells. The proportion of recipients where multilineage hematopoiesis was re-generated has been determined at 16th week post transplantation by analysing the GFP$^+$ chimerism of WBCs in the peripheral blood. Moreover, it is possible to determine the lineage chimerism of the WBCs, by calculating the proportion of cells originating from the transplants within one lineage compartment, in comparison to the proportion of the cells originated from the normal carrier cells injected originally. In this way it is possible to compare if the cells under investigation have a certain advantage versus the normal HSCs, or if they preferentially give rise to lineage-limited progeny. In case of a leukemic phenotype, it is possible to estimate the frequency of the leukemic stem cells (LSCs) in the diseased animals *in vivo*, by injecting serial dilutions of leukemic blasts (bulk or from different subpopulations) (Deshpande 2006) obtained from a diseased mouse. The animals are considered “engrafted” when they develop the disease. Studying Hoxb4, which is known to

be an important gene in the HSCs fate, and that had never been associated with leukemia itself so far in mice and humans, we performed the CRU assay by injecting 5-FU enriched progenitor cells, freshly transduced with GFP, Hoxb4-wt and Hoxb4-ΔPro, and we analysed the mice for engraftment (>1% GFP^+ WBCs in peripheral blood) 16 weeks after the transplantation. Subsequently, the mice injected with Hoxb4-ΔPro expressing BM cells developed leukemia, as described in the previous paragraphs. We transplanted 12 mice with the GFP control, 18 mice with Hoxb4-wt and 18 mice with Hoxb4-ΔPro expressing BM progenitor cells. At 16^{th} week post transplantation, we measured the proportion of GFP^+WBCs in the PB of all the mice. Using the L-Calc limiting dilution analysis software, we reported a frequency of 1 CRU into 834 for Hoxb4-wt, and 1 CRU into 413 for Hoxb4-ΔPro. 12 mice have been injected with up to $6.66x10^5$ GFP control cells, but no one showed engraftment. Accordingly to previous observations, where the GFP CRU frequency was reported to be 1/980,000 at 8 months post transplantation (Antonchuk 2001), we also can postulate that the frequency of CRU in this GFP control was less than 1/666,000. Interestingly, the difference observed between Hoxb4-wt and Hoxb4-ΔPro was not significant. (Table 4.5.2.8a). The similar CRU frequency observed in these two samples may indicate that the proline-rich region deletion might be not sufficient to induce disease after a short latency time, does not perturb the self-renewal of the long term repopulating stem cells (=CRU), but represents an important step leading to malignant transformation, which maybe needs additional hits and is taking place along the differentiation process.

Gene		Injected cells							CRU frequency
		200	2,000	20,000	200,000				
Hoxb4-wt	engrafted (%)	0/5	5/5 (17.7)*	5/5 (62)*	5/5 (72)*				1:834
	Leukemia	0/5	0/5	0/5	0/2				
Hoxb4-ΔPro	engrafted (%)	1/5 (1.8)	5/5 (4.2)*	5/5 (22.3)*	3/3 (38.8)*				1:413
	Leukemia	0/5	1/5	4/5	3/3				
		10,000	50,000	75,000	100,000	370,000	666,000	1,300,000	
GFP	engrafted (%)	0/3	0/3	0/1	0/3	1/1 (63.8)	0/2	1/1 (75.5)	<1:666,000
	Leukemia	0/3	0/3	0/1	0/3	0/1	0/2	0/1	

Table 4.5.2.8a. Serial dilutions of 5-FU enriched BM progenitor cells injected in recipient mice. The engraftment percentages indicate the WBCs-GFP$^+$ in peripheral blood 16 weeks after transplantation. In Hoxb4-ΔPro mice 200 injected cells were sufficient to obtain a long term engraftment (chimerism >1% in PB), while in Hoxb4-wt 2000 cells have to be injected to obtain engraftment at least in 1 mouse per cohort. In the GFP control mice 50,000 cells had to be injected to obtain engraftment. *= averages. Leukemia: the numbers of mice which developed leukemia after 16 weeks are indicated.

Interestingly, we reported a significant decrease in the GFP-chimerism values in the mice injected with Hoxb4-ΔPro in comparison to the Hoxb4-wt, when different numbers of cells have been injected (4.27fold less by 2,000 injected cells, 2.78fold less by 20,000 cells, and 1.86fold less by 200,000 injected cells, in comparison to the Hoxb4-wt, $p<0.032$). This could reflect a decreased proliferative effect at the level of more differentiated progenitor cells induced by Hoxb4 when the proline region was deleted (Fig. 4.5.2.8).

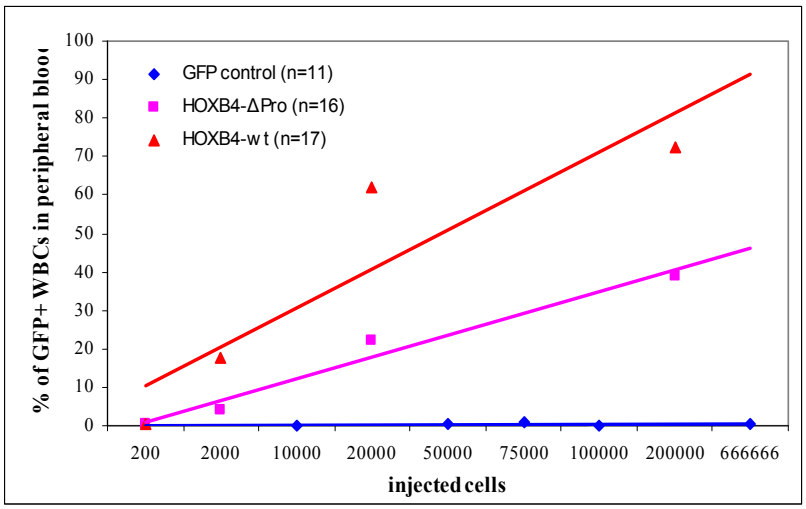

Fig. 4.5.2.8. Engraftment (given as % of WBCs-GFP$^+$ in peripheral blood per numbers of injected cells) 16 weeks after transplantation.

Moreover, all the mice were healthy at this time point (112 days after transplantation) and all showed multi-lineage reconstitution. For each lineage the proportion of GFP$^+$ transplanted cells has been calculated, and these cells can be considered able to reconstitute a lineage, if their proportion within a lineage is higher than 1%. We reported that in the Hoxb4-ΔPro mice the proportion of GFP$^+$ WBCs in the PB within each lineage was significantly lower in comparison to the Hoxb4-wt mice (Table 4.5.2.8b).

Lineage marker (n)	Hoxb4-wt (n=12)	Hoxb4-ΔPro (n=10) (fold decrease vs. wt)
Sca-1	26.84	7.45* (3.6)
c-kit	52.96	35.25 (1.5)
Mac-1	48.45	21.71* (2.2)
Gr-1	48.46	27.79* (1.7)
Ter119	50.47	21.55* (2.3)
B220	34.56	14.22* (2.4)
CD4	32.82	13.45* (2.4)
CD8	22.97	9.15* (2.5)

Table 4.5.2.8b. The chimerism (proportion of GFP^+ cells in %) within each lineage is represented. *significant reduction vs. the Hoxb4-wt ($p<0.05$).

5. Discussion

The Hoxb4 is a well-known gene expressed in the most primitive hematopoietic stem, embryonic and bone marrow progenitor cells. It has been reported to govern central intrinsic cellular pathways implicated in the regulation of cell cycle, differentiation, and apoptosis. Hoxb4 activity exerts influence on negative and positive regulatory signals, leading to HSCs expansion.

In the present work we focused on the possible mechanism responsible for the benign phenotype observed when Hoxb4 is overexpressed, and on its structural regions, which might be vital for the unregulated and aberrant proliferation of the HSCs. Using the murine bone marrow transplantation model, we assessed the oncogenic potential of human Hoxb4 gene by mutagenesis of its domains. As it has been already reported, the single aminoacid mutation in the Pbx-interacting domain did not affect dramatically the activity of Hoxb4, while it was shown that a single aminoacid within the DNA binding homeodomain is essential for its hematopoietic stem and progenitor cells activity (Beslu 2004). In particular we focused on the proline rich region (Hoxb4-ΔPro), which has never been so far described as a functional domain of this protein.

By performing *in vitro* assays we reported that the overexpression of the Hoxb4-ΔPro mutant slightly reduces the amplification of BM progenitor cells and leads to a decrease of the Sca-1/c-kit double positive cells number in comparison to the Hoxb4-wt, while it was still higher than in the GFP-control. Similarly, the deletion of the proline-rich region led to a slight reduction of myeloid cell counts in comparison to the Hoxb4-wt, while we did not observe significant changes in the number of cells expressing erythroid and B-lymphoid markers.

Moreover, Hoxb4-ΔPro did not affect the frequency of 1°CFCs when overexpressed in 5-FU-BM cells, while it induced a significant increase in the replating capacity of these cells in comparison to the Hoxb4-wt and the GFP control. In contrast, its overexpression led to a significant decrease in the 12 days-ΔCFU-S frequency in comparison to the Hoxb4-wt, which may reflect a reduced amplificatory potential at the level of short term repopulating progenitor cells when the proline region is deleted. However, when we analyzed the engraftment rate from the peripheral blood of mice transplanted with BM cells overexpressing Hoxb4-wt and Hoxb4-ΔPro at 4 weeks post transplantation we

did not observe significant differences. Interestingly, at 13-16 weeks post transplantation we could document a significant reduction of circulating GFP^+WBCs in mice transplanted with Hoxb4-ΔPro overexpressing cells in comparison to the mice transplanted with Hoxb4-wt expressing BM cells, despite equal numbers of initially transplanted cells. Taken together, deletion of the proline rich region seems to impair the capacity of HoxB4 to enhance ST-LSC activity. On the other hand it seems to augment serial replating capacity of HoxB4, which often is taken as a surrogate marker for the transforming activity of a gene. In the CRU assay we reported an increase in the frequency of competitive repopulating units when Hoxb4-ΔPro was overexpressed (1 into 413 vs. 1 into 834 transplanted cells in Hoxb4-wt, p=n.s., while in the GFP control the CRU-frequency was < 1 into 666,000). This could reflect that the Hoxb4-ΔPro mutant has a differential effect on short – term versus long – term repopulating stem cells. Of note, the CRU is an assay designed for normal HSCs and might be biased by genes which have leukemogenic potential. Thus, it is difficult to rule out that the - in comparison to the Hoxb4-wt - increased CRU activity of the proline deleted mutant is not due to its leukemogenic effect, which is not present in the Hoxb4-wt.

Since it has been suggested that the Hoxb4-associated regulatory complex might control downstream epigenetic events via binding to CBP / p300 and to histone deacetylases, we investigated the effect of HDAC inhibition by incubating the BM progenitor cells with the well-known HDACi valproic acid (VPA). When the cells were incubated with 1mM VPA for one week, we observed an increase in cell number in GFP ctrl, Hoxb4-wt, Hoxb4-PBX, Hoxb4-cDel and Hoxb4-HD in comparison to the corresponding samples in the absence of VPA. Interestingly, in case of the cells expressing the Hoxb4-ΔPro the incubation with VPA led to a slight decrease in cell number, indicating that the effect of HDAC inhibition is at least partly dependent on the proline rich region. Considering the surface immunophenotype of *in vitro* expanded cells in the presence of VPA, we reported an increase of Sca-1^+ and a decrease of c-kit^+ cells in comparison to the samples without VPA, independently from the deletion of the proline region. This suggests that the HDAC-activity could play a role in the proliferation of the committed progenitors expressing these surface markers, or may induce the differentiation

of progenitor cells *in vitro*, as it has been reported in case of other solid tumors (Göttlicher 2001).

In the presence of VPA the absolute number of Mac-1$^+$ cells was lower in the GFP control and in the Hoxb4-wt in comparison to the corresponding samples without the HDACi, while in the Hoxb4-ΔPro, Hoxb4-PBX, Hoxb4-cDel and Hoxb4-HD the proportion of mature myeloid cells was not affected by the VPA. Moreover, VPA led to a decrease in the total number of CFCs in all the samples except for the Hoxb4-cDel, in comparison to the corresponding samples without VPA, suggesting that the HDAC inhibition was not affecting the differentiation of progenitor cells *in vitro.* In summary, the VPA did not lead to any significant change in the differentiation capacity, while similarly the mutation of the single domains of Hoxb4 did not significantly affect the lineage specificity. According to recent studies, we reported a proliferative effect of VPA on early progenitor cells (Bug 2005, De Felice 2005). Indeed, the pre-incubation with VPA increased the 12 days ΔCFU-S frequency in all the samples *in vivo.* This effect has been suggested from some authors to be mediated by the induction of the endogeneous Hoxb4 expression (Seet 2008), while some others have reported a Hoxb4-indipendent VPA-induced expansion of HSCs (Obier 2010). Interestingly, while performing murine bone marrow transplantation experiments we reported for the first time, that the retroviral induced overexpression of human Hoxb4 harbouring the deletion of the proline rich region leads to a transplantable acute myeloid leukemia *in vivo* 255 days (mean) post transplantation. In the diseased mice the leukemic blasts were infiltrating hematopoietic and non-hematopoietic organs, were MPO$^+$, and showed a higher CFCs frequency in *ex vivo* assays. By analysing the retroviral integration pattern we documented no recurring integration sites, and this suggests that the leukemic phenotype observed was not primarily due to an integration event. We can conclude that the deletion of this region converts Hoxb4 into a pro-leukemogenic gene in the murine transplantation model. However, the relatively long latency time to disease development may reflect the accumulation of further hits collaborating to malignant transformation. In this HoxB4-ΔPro-associated AML model the *in vitro* VPA treatment (1 mM for 1 week) of BM progenitor cells prior to transplantation did not prevent leukemogenesis. This could reflect on one side the resistance of the leukemic stem cells to HDAC inhibition, but on the other side, the treatment

schedule used might be not sufficient to suppress leukemogenesis. In previous reports it has been reported that the VPA induces the differentiation of transformed cells into mature cells (Goettlicher 2001), while it increases the number of more primitive normal stem cells without affecting the differentiation. In the same way, in 5-FU enriched VPA-treated progenitor cells we did not see any significant perturbation of the differentiation of *in vitro* cultured normal hematopoietic progenitor cells.

VPA has been used in clinical trials for the treatment of acute myeloid leukemia and myelodysplastic syndromes. When used as monotherapy or in combination with all-trans-retinoic acid, which synergizes with VPA *in vitro*, VPA led to an hematologic improvement in a subset of patients. The application of other inhibitors of histone deacetylases alone has been sufficient to reach complete or partial remission only rarely (Kuendgen 2007). The effect of the treatment with these drugs strictly depends on the biology of the type of cancer, where genetic as well as epigenetic changes occur. Some of these epigenetic events, which normally are differently regulated during the differentiation, can be absent in transformed cells, and this could explain the reduced sensitivity of immature and tumor cells to HDACi (Taddei 2005).

Moreover, Saleh et al have suggested that HOX-PBX complexes may repress transcription under certain circumstances, and consistent with this, the binding sites of HOX-PBX multimers have been reported to repress reporter gene expression in HEK293 cells. Their work offers a mechanistic explanation of the repressor function by showing that a corepressor complex, containing the histone deacetylases (HDACs) 1 and 3, mSIN3B, and N-CoR/SMRT, interacts with PBX1A. They have mapped a site of interaction with HDAC1 at the PBX1 N-terminus and showed that the PBX partner is required for the normal function of the HOX-PBX complex. Additionally, they have shown that the presence of the HDAC inhibitor trichostatin A not only inhibits the repression function, but also transforms the HOX-PBX complex into a net activator of transcription, and this function was demonstrated to be mediated by the recruitment of the coactivator CREB-binding protein by the HOX partner (Saleh 2000). Interestingly, Shen et al have shown that the HOX proteins inhibit histone acetyltransferase activity of CBP in both *in vitro* and *in vivo* systems, without being acetylated themselves, and this function seems to be independent from the highly conserved PBX-

interacting domain. In summary, HOX proteins may function without CBP HAT to regulate transcription, while they necessitate the interaction with other DNA binding molecules like PBX, MEIS, or with other cofactors. On the other hand the HOX proteins may inhibit the CBP HAT activity and thus function as repressors of gene transcription (Shen 2001).

Considering these reports and the leukemogenic potential of Hoxb4-ΔPro observed *in vivo*, one possibility could be that the proline region functions as HAT/HDAC-interacting domain of Hoxb4. The deletion of this region may then prevent the recruitment of co-repressors/activators. So far this region of Hoxb4 has not been yet well characterized. Further experiments will help to understand which molecular interactions of Hoxb4 are perturbed when this region is deleted, and from another perspective they will help to decipher the key mechanisms which prevent Hoxb4 to act as leukemogenic protein and are responsible for the "benign" maintenance of the normal HSC pool. The mild effect exerted by the VPA treatment could suggest a predominant mediation of Hoxb4 activity via HAT activators. Another explanation could be that VPA induces increased expression of endogenous Hoxb4 in cells, in which the gene is already overexpressed by retroviral gene transfer.

HDAC inhibitors are known to reduce proliferation and induce differentiation in hematological malignacies, like AML and MDS (Bellos 2008). Additionally, in ongoing experiments in our laboratory (data not shown) the VPA treatment of AML/MDS NUP98-HOXD13^{+}/Meis1^{+} cells has been shown to effectively block the growth and differentiation of the leukemic blasts. In contrast, in the present Hoxb4-ΔPro associated leukemia model, we hypothesize that the interaction with the putative partners HDACs/HATs has been perturbed, leading to an inefficient antileukemic effect of VPA treatment.

Moreover, we could argue, that the proline-rich domain of Hoxb4 is modulating a determinant downstream control pathways, which could be responsible of the benign phenotype of normal HSCs, and may play a crucial role in the maintenance of the homeostatic equilibrium of HSCs, which cannot be affected by the HDAC inhibition alone. The malignant phenotype observed in our AML model was absent when the DNA-interacting domain was mutated. This suggests that the DNA-interaction of Hoxb4 is essential for the leukemogenesis.

Interestingly, the additional mutation of the PBX-ID did not prevent the Hoxb4-ΔPro-associated AML, suggesting that the leukemogenesis in this model is independent from the interaction with PBX cofactor.

The significance of a mutation in the proline region of Hoxb4 in human leukemogenesis is not yet known, since the detection of such mutation might be difficult with the screening methods commonly used, because of the high “GC” content in its sequence. Further investigations will allow to determine whether any mutation in this N-terminal regulatory region of Hoxb4 is involved in human leukemias.

The identification of new leukemogenic functions of domains such as the proline region in Hoxb4 opens novel opportunities such as generating peptidomimetics that can antagonize specific protein-protein interaction domains in cultured cells and whole animals (Kay 2000).

Another important aspect that could be elucidated by studying the phenotype regulated by the different regions of Hoxb4, is to get more insights about the HSCs amplificatory activity of this transcription factor. From previous works of Antonchuk et al it has been suggested that a possible way to explain the exponential amplification induced by Hoxb4 is the progenitor cells plasticity. The dramatic increase in the pool of proliferating progenitor cells could theoretically occur via de-differentiation of a committed progenitor into a more primitive, multipotent cell. However, the de-differentiation of cells in adult mammals has not been clearly and equivocally documented, and at present, no evidence directly supports the existence of trans-differentiation or de-differentiation events as prove of putative BM progenitor cells plasticity *in vivo* (Wagers 2004). The investigation of the normal function of Hoxb4 will help to clarify the still incompletely known fascinating control mechanisms of the stem cell biology.

6. Summary

In the present work structural and functional analyses of a member of the Homeobox gene family, Hoxb4, have been performed. These transcription factors are highly conserved, and play a determinant role in the development of the early hematopoiesis. In particular, Hoxb4 represents a determinant factor, because in several experimental reports by using the retroviral gene transfer of Hoxb4 into murine and human haematopoietic stem cells (HSC) this transcription factor has been shown to amplify HSC (Sauvageau 1994, Buske 2002). To date no comprehensive structural / functional analyses of all the potential functional relevant domains of Hoxb4 are available. In this work we report the structural and functional analysis of relevant domains of Hoxb4. For the first time we showed that the deletion of the amino acids 78-120 of Hoxb4 has a leukemogenic effect: mice transplanted with bone marrow retrovirally transduced with this Hoxb4 mutant (Hoxb4-ΔPro) developed acute leukemia after a latency time of 255 days (mean, ±96). These data show, that through the loss of its N-terminal proline-rich region the Hoxb4 transcription factor turns to an oncogene. The overexpression of this mutant led to acute myeloid leukemia with multi-organ infiltration, characterized by the expression of myeloid markers as confirmed by FACS and immunohistochemical analyses.

The primary leukemia was transplantable and generated in secondary and tertiary transplanted mice a similar acute leukemia after a shorter latency time of 66.5 (mean, ±22) and 43 days (mean, ±6), respectively. The analysis of the retroviral integration profile has shown that this leukemia was oligoclonal.

The additional deletion of the PBX-interaction domain together with the deletion of the proline-rich region did not inhibit the development of leukemia. However, the integrity of the DNA-binding was essential for the leukemogenesis induced by Hoxb4-ΔPro. In contrast to the leukemogenic effect observed, the deletion of the proline-rich region did not affect the differentiation and the proliferation rate of short-term repopulating stem cells (CFC assay), as well as the frequency of the competitive repopulating units (long term repopulating stem cells) in comparison to the Hoxb4-wt (CRU assay). However, the Hoxb4-ΔPro mutant led to a significant reduction of the 12 days- ΔCFU-S frequency in comparison to the Hoxb4-wt.

Since in previous works Hoxb4, as well as other Hox factors, have been demonstrated to bind to CBP and the Hox co-factor PBX to bind to histone deacetylases (HDACs), we investigated which effect the HDAC inhibitor valproic acid (VPA) is exerting on the development of early hematopoietic stem cells. Interestingly, VPA has been shown from other authors to amplify human and murine HSCs, and this effect was partially explained through the induction of the expression of endogenous Hoxb4. With use of functional *in vitro* an *in vivo* assays we have been able to show that VPA can increase the HSC-amplificatory effect of Hoxb4. In contrast, the incubation of murine BM cells overexpressing Hoxb4-ΔPro with VPA did not exert any amplificatory effect on stem cells. This suggests a probable involvement of epigenetic events like histone deacetylation for the control of the proliferation of early BM progenitor cells mediated by the proline region.

Our findings allow concluding, that the proline region of Hoxb4 is essential for the benign amplification of normal HSCs. These results point up, that the further analysis of the function of this region could give new insights for the understanding of the biology of normal stem cells as well as of leukemogenesis.

7. Zusammenfassung

In der vorliegenden Arbeit wurden Struktur-Funktionsanalysen eines Mitglieds der Homeoboxgenfamilie – des Hoxb4 durchgeführt. Dabei handelt es sich um eine hochkonservierte Gruppe von Transkriptionsfaktoren, die eine entscheidende Rolle in der frühen hämatopoetischen Entwicklung aufweisen. Hoxb4 spielt in diesem Zusammenhang eine herausragende Rolle, da in zahlreichen Untersuchungen unter Verwendung des retroviralen Gentransfers von Hoxb4 in hämatopoetischen Stammzellen der Maus aber auch des Menschen gezeigt werden konnte, dass es einen Stammzell-amplifikatorischen Effekt aufweist (Sauvageau 1994, Buske 2002). Bislang liegen aber noch keine umfassenden Struktur-Funktionsanalysen zu den potentiell funktionell relevanten Domänen von Hoxb4 vor. In der vorliegenden Arbeit wurden diese Struktur-Funktionsanalysen durchgeführt. Es gelang dabei erstmalig zu zeigen, dass die Deletion der Aminosäuren 78-120 des Hoxb4 Proteins einen leukämogenen Effekt hat: Mäuse, die mit Knochenmark transplantiert wurden, welches retroviral mit dem so mutierten Hoxb4 transduziert wurde, entwickelten nach einer Latenzzeit von 255 Tagen (Mittelwert, ±96) eine akute Leukämie. Damit zeigen die Daten erstmalig, dass durch Verlust der N-terminalen prolinreiche Region der Transkriptionsfaktor Hoxb4 zu einem Onkogen wird. Die Mutante induzierte eine akute myeloische Leukämie mit Multiorganinfiltration durch leukämischen Blasten, charakterisiert durch Expression myeloischer Marker in der FACS Analyse und in der Immunhistochemie.

Die primäre Leukämie war retransplantierbar und generierte in sekundär und tertiär transplantierten Mäusen nach einer kurzen Latenzzeit von 66.5 (Mittelwert, ± 22) bzw. 43 (Mittelwert, ±6) Tagen post transplantationem eine akute Leukämie gleichen Phänotyps. Die Analyse des retroviralen Integrationsprofils zeigte, dass die Leukämie oligoklonaler Natur war.

Die zusätzliche Deletion der PBX-Interaktionsdomäne zusammen mit der Deletion der prolinreichen Region konnte die Entwicklung der Leukämie nicht verhindern, andererseits war die Bindung an die DNS für die Hoxb4-ΔPro induzierte Leukämogenese entscheidend. Im Gegensatz zu dem leukämogenen Effekt bewirkte die Deletion der prolinreichen Region keine Änderung der Differenzierung und der Proliferationsrate von Kurzzeit-repopulierenden

Stammzellen (CFC assay), sowie der Frequenz kompetitiv-repopulierender Einheiten (langzeit-repopulierender Stammzellen) im Vergleich zum Hoxb4-Wildtyp. Nur die 12 Tage-ΔCFU-S Frequenz *in vivo* war durch die Expression von dem Hoxb4-ΔPro Mutant im Vergleich zu Hoxb4-wt signifikant reduziert.

Aufgrund von vorhergehenden Arbeiten, in denen gezeigt wurde, dass Hoxb4 wie andere Hox Faktoren an CBP bzw. den HOX Ko-faktor PBX1 an Histon Deacetylasen (HDACs) bindet, untersuchten wir, ob der HDAC-Inhibitor Valproinsäure (VPA) einen Einfluss auf die durch den Hoxb4-wt bzw. durch die Hoxb4 Mutante induzierten Effekte auf die frühe hämatopoetische Stammzellentwicklung hat. VPA wurde von anderen Autoren gezeigt, eine Amplifizierung von humanen und murinen HSZ zu bewirken, wobei dieser Effekt teilweise durch die Induktion der endogene Hoxb4-Expression erklärt werden konnte (Seet 2008). Unter Verwendung funktioneller *in vitro* und *in vivo* Analysen gelang es uns zu zeigen, dass VPA den bekannten Stammzell-amplifikatorischen Effekt des Hoxb4-wt sogar noch verstärken konnte. Im Gegensatz hierzu, führte die Inkubation von Mausknochenmarkzellen, die Hoxb4-ΔPro überexprimierten, mit VPA nicht zu einer Verstärkung des Stammzell-amplifikatorischen Effektes. Dies könnte auf eine Bedeutung von epigenetischen Faktoren im Rahmen der Zellproliferation früher hämatopoetischer Vorläuferzellen hinweisen.

Unsere Ergebnisse zeigen, dass die Prolinregion des Hoxb4 für die normale stammzellamplifikatorische Wirkung von Hoxb4 essentiell ist. Die Daten unterstreichen, dass die weitere Analyse der Wirkungsweise der Prolinregion von Hoxb4 sowohl für ein besseres Verständnis der normalen Stammzellbiologie als auch der möglichen leukämischen Transformation von großer Bedeutung ist.

8. References

Abdel-Wahab O, Mullally A, Hedvat C et al 2009. Genetic characterization of TET1, TET2, and TET3 alterations in myeloid malignancies. Blood 114:144-147.

Akagi K, Suzuki T, Stephens RM et al (2004). RTCGD: retroviral tagged cancer gene database. Nucleic Acids Res. 1:32(Database issue):D532-7.

Alcalay M, Orleth A et al (2001). Common themes in the pathogenesis of acute myeloid leukemia. Oncogene 20(40):5680-94.

Ammanamanchi S, Freeman JW, Brattain MG (2003). Acetalyted sp3 is a transcriptional activator. J Biol Chem 278:35775-80.

Amsellem S, Pflumio F et al (2003). Ex vivo expansion of human hematopoietic stem cells by directly delivery of the HOXB4 homeoprotein. Nat Med 9(11):1423-27.

Antonchuk J, Sauvageau G et al (2001). HOXB4 overexpression mediates very rapid stem cell regeneration and competitive hematopoietic repopulation. Exp Hematol 29:1125-1134.

Argiropoulos B, Humphries RK (2007). Hox genes in hematopoiesis and in leukemogenesis. Oncogene 26:6766-6776.

Bellos F, Mahlknecht U (2008). Valproic acid and all-trans retinoic acid: meta-analysis of a palliative treatment regime in AML and MDS patients. Onkologie 2008;31:629–633

Bennet JH (1845). Two cases of disease and enlargement of the spleen in which death took place from the presence of purulent matter in the blood. (Edinb Med Surg J 64:413-431.

Beslu N, Krosl J et al (2004). Molecular interactions involved in HOXB4-induced activation of HSC self-renewal. Blood 104(8):2307-2314.

Bhardwaj G, Murdoch B, et al (2001). Sonic hedgehog induces the proliferation of primitive human hematopoietic cells via BMP regulation. Nat Immunol 2(2):172-80.

Bodey B, Bodey B Jr, Siegel et al (2000). Homeobox B3, B4, and C6 gene product expression in osteosarcomas as detected by immunocytochemistry. Anticancer Res. 20(4):2717-21.

Bonnet D, Dick JE (1997). Human acute myeloid leukemia is organized as a hierarchy that originates from a primitive hematopoietic cell. Nat Med 3(7):730-7.

Bonnet D. (2002). Hematopoietic stem cells. J Pathol 197:430-440.

Bonnet D. (2003). Hematopoietic stem cells. Birth Defects Research C Embryo Today 69:219-229.

Bowles KM, Vallier L et al (2006). HOXB4 overexpression promotes hematopoietic development by human embryonic stem cells. Stem Cells 24(5):1359-1369.

Brend T, Githorpe J, Summerbell D, Rigby PWJ (2003). Multiple levels of transcriptional and post-transcriptional regulation are required to define the domain of Hoxb4 expression. Development 130:2717-2728.

Bryder D, Rossi DJ, and Weissman IL (2006). Hematopoietic stem cells. Am J Pathol. 169(2):338-346.

Brun AC, Bjornsson JM et al (2004). Hoxb4-deficient mice undergo normal hematopoietic development but exhibit a mild proliferation defect in hematopoietic stem cells. Blood 103(11):4126-33.

Brunning R (1999). Proposed World Health Organization (WHO) classification of acute leukemia and myelodysplastic syndromes. Mod Pathol 12:101-106.

Bug G, Gul H et al (2005). Valproic acid stimulates proliferation and self-renewal of hematopoietic stem cells. Cancer Res 65:2537-2541.

Buske C, Feuring-Buske M et al (2002). Deregulated expression of HOXB4 enhances the primitive growth activity of human hematopoietic cells. Blood 100(3):862-868.

Chang CP, Shen WF, et al (1995). Pbx proteins display hexapeptide-dependent cooperative DNA binding with a subset of Hox proteins. Genes Dev 9(6):663-74.

Chang CP, Brocchieri L et al (1996). Pbx modulation of Hox homeodomain amino-terminall arms establishes different DNA-binding specificities across the Hox locus. Mol Cell Biol 16:1734-45.

Cheng TN, Rodrigues N et al (2000). Hematopoietic stem cell quiescence maintained by p21cip1/waf1. Science 287(5459):1804-8.

Chesier SH, Morrison SJ, et al (1999). In vivo proliferation and cell cycle kinetics of long-term self-renewing hematopoietic stem cells. Proc Natl Acad Sci USA. 96(6):3120-5.

De Braekeleer M, Morel F et al (2005). The MLL gene and translocations involving chromosomal band 11q23 in acute leukemia. Anticancer Res 25(3B):1931-44**.**

De Felice L, Tatarelli C et al (2005). Histone deacetylase inhibitor valproic acid enhances the cytokine-induced expansion of human hematopoietic stem cells. Cancer res 65:1505-1513.

Delhommeau f, Dupont S et al. (2009). Mutation in TET2 in myeloid cancers. N Engl J Med. 360:2289-2301.

Delia D, Aiello A et al (1992). Bcl-2 proto-oncogene expression in normal and neoplastic human myeloid cells. Blood 79(5):1291-8.

Deshpande AJ, Cusan M, et al (2006). Acute myeloid leukemia is propagated by a leukemic stem cell with lymphoid characteristics in a mouse model of CALM/AF10-positive leukemia. Cancer Cell 10(5):363-74.

Dick JE (2003). Stem cells: self-renewal writ in blood. Nature 423(6937):231-3.

Dixon R, Rosendaal M (1981). Contrast between the response of the mouse hematopoietic system to 5-fluorouracil and irradiation. 7(3):575-87.

Domen J (2000). The role of apoptosis in regulating hematopoiesis and hematopoietic stem cells. Immunol Res 22(2-3):83-94.

Dornan D, Shimizu H et al (2003). The proline repeat domain of p53 binds directly to the transcriptional coactivator p300 and allosterically controls DNA-dependent acetylation of p53. Mol Cell Biol 23(23):8846-61**.**

Dzierzak E. (2003). Ontogenic emergence of definitive hematopoietic stem cells. Curr Opin Hematol 10:229-234.

Dzierzak E., Speck NA (2008). Of lineage and legacy: the development of mammalian hematopoietic stem cells. Nat Immunol 9(2):129-36.

Ebstein W (1889). Ueber die acute leukamie und pseudoleukamie. Dtsch Arch Klin Med 44:343-358.

Eikel D, Lampen A Nau H (2006). Teratogenic effects mediated by inhinition of histone deacetylases: evidence from quantitative atructure activity relationships of 20 valproic acid derivatives. Chem Res Toxicol 19(2):272-8.

El-Kadi ASM, Reiden P et al (2002). The small GTPase Rap1 is an immediate douwnstream atrget for Hoxb4 transcriptional regulation. Mech Develop 113:131-139.

Feuring-Buske M, Frankel AE et al (2002). A diphteria toxin-interleukin 3 fusion protein therapy is cytotoxic to primitive acute myeloid leukemia progenitors but spares normal progenitors. Cancer Res 62:1730-1736.

Fischbach F (1996). Manual of Laboratory and Diagnostic Tests. Philadelphia: Lippincott.

Friedrich N (1857). Ein neuer Fall von Leukämie. Arch Pathol Anat 12:37-58.

Fröhling S, Scholl C, Gilliland DG, et al (2005). Genetics of myeloid malignancies-pathogenetic and clinical implications. J Clin Oncol. 23:6285-6295.

Garcia-Fernandez J (2005a). Hox, ParaHox, ProtoHox: facts and guesses. Heredity 94:145-152.

Garcia-Fernandez J (2005b). The genesis and evolution of homeobox gene clusters. Nature 6:881-892.

Giannola DM, Shlomchik WD, Jegathesan M, Liebowitz D, et al (2000). Hematopoietic expression of HOXB4 is regulated in normal and leukemic stem cells through transcriptional activation of the HOXB4 promoter by upstream stimulating factor (USF)-1 and USF-2. J Exp Med. 2000 Nov 20;192(10):1479-90.

Gilliland DG, Tallman MS (2002). Focus on acute leukemias. Cancer cell 1(5):4127-20.

Gilthorpe J, Vandromme M, Brend T, Gutman A, et al (2002). Spatially specific expression of Hoxb4 is dependent on the ubiquitous transcription factor NFY. Development 129:3887-3899.

Glozak MA, Sengupta N et al (2005). Acetylation and deacetylation of non-histone proteins. Gene 363:15-23.

Goardon N, Marchi E, Atzberger A, Quek L, Schuh A, et al (2011). Coexistence of LMPP-like and GMP-like Leukemia Stem Cells in Acute Myeloid Leukemia. Cancer Cell 19, 138–152.

Goodell MA (2003). Stem cell „plasticity“: befuddled by the muddle. Curr Opin Hematol 10:208-213.

Golub TR, Slonim DK et al (1999). Molecular classification of cancer: class discovery and class prediction by gene expression monitoring. Science 286:531-537.

Göttlicher M, Minucci S, et al (2001). Valproic acid defines a novel class of HDAC inhibitors inducing differentiation of transformed cells. EMBO 20(24):6969-6978.

Graham A, Papalopulu N et al (1988). Characterization of a murine homeo box gene, Hox-2.6, related to the Drosophila deformed gene. Genes Dev 2(11):1424-38.

Gronbaek K, Hother C, Jones PA (2007). Epigenetic changes in cancer. APMIS 115:1039-1059.
Gu W, Roeder RG. (1997). Activation of p53 sequence-specific DNA binding by acetylation of the p53 C-terminal domain. Cell 90:595-606.

Hanahan D, Weinberg RA (2000). The hallmarks of cancer. Cell 100(1):57-70.

Hills D, Gribi R, Ure J, Buza-Vidas N, Luc S, Jacobsen SEW, Medvinsky A (2011). Hoxb4-YFP reporter mouse model: a novel tool for tracking HSC development and studying the role of Hoxb4 in hematopoiesis. Blood 117, 13:3521-3528.

Hirsch E, Iglesias et al (1996). Impaired migration but not differentiation of hematopoietic stem cells in the absence of beta 1 integrins. Nature 380(6570):171-5.

Holyoake T, Jiang X et al (1999). Isolation of a highly quiescent subpopulation of primitive leukemic stem cells in chronic myeloid leukemia. Blood 94(6):2056-64.

Hong JH, Lee JK, Park JJ et al (2010). Expression pattern of the class I homeobox genes in ovarian carcinoma. 21(1):29-37.

Jacobs Y, Schnabel CA, Cleary ML (1999). Trimeric association of Hox and TALE homeodomain proteins mediates Hoxb2 hindbrain enhancer activity. Mol Cell Biol 19:5134-42.

Jordan CT, Upchurch D et al (2000). The interleukin-3 receptor alfa chain is a unique marker for human acute myelogenous leukemia stem cells. Leukemia 14:1777-1784.

Imamura T, Morimoto A et al (2002). Frequent co-expression of HoxA9 and Meis1 genes in infant acute lymphoblastic leukemia with MLL rearrangement. Br J Heamatol 119(1):119-21.

Insinga A, Monestroli S, PG Pelicci (2005). Inhibitors of histone deacetylases indice tumor-selective apoptosis through activation of the death receptor pathway. Nat Med 11(1):71-6.

Ito T, Ikehara T et al (2000). P300-mediated acetylation facilitates the transfer of histone H2A-H2B dimers from the nucleosomes to a histone chaperone. Genes & Devel 14:1899-07.

Karanu FN, Murdoch B, et al (2000). The Notch ligand Jagged-1 represents a novel growth factor of human hematopoietic stem cells. J Exp Med 192(9):1365-72.

Kay BK, Williamson MP, Sudol M (2000). The importance of being proline: the interaction of proline-rich motifs in signalling proteins with their cognate domains. FASEB J 14:231-241.

Kawagoe H, Humphries RK et al (1999). Expression of HOX genes, HOX cofactors, and MLL in phenotypically and functionally defined subpopulations of leukemic and normal human hematopoietic cells. Leukemia 13:687-698.

Kelly LM, Kutok JL, Williams IR et al. (2002a). PML/RARalpha and FLT3-ITD induce an APL-like disease in a mouse model. Proc Natl Acad Sci USA 99:8283-8288

Kelly LM, Gilliland DG (2002b). Genetics of myeloid leukemia. Annu Rev Genomics Hum Genet. 3:179-198.

Kim YH, Park JW, Lee JY, Kwon TK (2004). Sodium butyrate sensitizes TRAIL-mediated apoptosis by induction of transcription from the DR5 gene promoter through Sp1 sites in colon cancer cells. Carcinogenesis 25(10):1813-1820.

Kim DY, Choi SJ, Kim SH, et al (2005). Upregulated hoxC4 induces CD14 expression during the differentiation of acute promyelocytic leukemia cells. Leuk. Lymphoma 46:1061-1066.

Kogan SC, Ward JM, Anver MR, et al (2002). Bethesda proposals for classification of nonlymphoid hematopoietic neoplasms in mice. Blood 100(1):238-245.

Kondo M, Wagers AJ, et al (2003). Biology of hematopoieic stem cells and progenitors for clinical application. Annu Rev Immunol 21:759-806.

Kramer OH, Zhu P et al (2003). The histone deacetylase inhibitor VPA selectively induces proteasomal degradation of HDAC2. 22(13):3411-3420.

Kroon E, Thorsteindottir U et al (2001). NUP98-HOXA9 expression in hematopoietic stem cells induces chronic and acute myeloid leukemias in mice. EMBO J 20:350-361

Krosl J, Beslu N, Laurin M, Mayotte N, Humphries RK, Sauvageau G (2003). The competitive nature of HOXB4 transduced HSC is limited by PBX1: the generation of ultra-competitive stem cells retaining full differentiation potential Immunity 18:561-571.

Krumlauf R (1994). Hox genes in vertebrate development. Cell 78(2):191-121.

Kucia M, Ratajczak J, Ratajczak MZ (2005). Bone marrow as a source of circulating CXCR4+ tissue-committed stem cells. Biol. Cell 97,133-146.

Kuendgen A, Gattermann N (2007). Valproic acid for the treatment of myeloid malignancies. Cancer 110(5):943-954.

Kuo MH, Allis CD (1998). Roles of histone deacetylases in gene regulation. Bioessays. 20:615-26.

Kyba M, Perlingeiro RCR, Daley GQ (2002). Hoxb4 confers definitive ly,phoid-myeloid engraftment potential on embryonic stem cell and yolk sac hematopoietic progenitors. Cell 109, 29-37.

Lagasse E, Connors H et al (2000). Purified hematopoietic stem cells can differentiate into hepatocytes in vivo. Nat Med 6(11):1229-34.

Larochelle A, Dunbar CE (2008). HOXB4 and retroviral vectors: adding fuel to the fire. J Clin Invest 118(4):1350-3.

Lawrence HJ, Rozenfeld S et al (1999). Frequent co-expression of the HOXA9 and MEIS1 homeobox genes in human myeloid leukemias. Leukemia 13:1993-1999.

Lemischka IR (1997). Microenvironmental regulation of hematopoietic stem cells. Stem cells 15 Suppl 1:63-8.

Lessard J, Sauvageau G (2003). Polycomb group genes as epigenetic regulators of normal and leukemic hematopoiesis. Exp Hematol 31:567-585.

Lewis EB (1978). A gene complex controlling segmentation in Drosophila. Nature 276(5688):565-70.

Li X, Nie S et al (2006). Smads oppose Hox transcriptional activities. Exp Cell Res 312:854-64.

Liu S, Klisovic RB et al (2007). Targeting AML1/ETO-Histone deacetylase repressor complex: a novel mechanism for valproic acid-mediated gene expression and cellular differentiation in AML1/ETO-positive acute myeloid leukemia cells. JPET 321:953-960.

Lopez RG, Brosch G, Georgieva EI, Sendra R, Franco L, Loidl P (1993). Histone deacetylase. A key enzyme for the binding of regulatory proteins to chromatin. FEBS Lett 317:175-80.

Lopez R, Garrido E, Pina P et al (2006). HOXB homeobox gene expression in cervical carcinoma. Int J Gynecol Cancer 16, 329-335.

Lorsbach RB, Moore J, Mathew S, Raimondi SC, Mukatira ST, Downing JR (2003). TET1, a member of a novel protein family, is fused to MLL in acute myeloid leukemia containing the t(10;11)(q22;q23). Leukemia 17:637-641.

Mann RS, Morata G (2000). The developmental and molecular biology of genes that subdivide the body of *Drosophila* embryos and larvae. Annu Rev Cell Dev Biol 16:283-271.

Mariadason JM (2008). HDACs and HDAC inhibitors in colon cancer. Epigenetics 3(1):20-37.

Miller CL, Eaves CJ (1997). Expansion in vitro of adult murine hematopoietic stem cells with transplantable lympho-myeloid reconstituting ability. Proc Natl Acad Sci USA 94(25):13648-53.

Morrison SJ, Weissman IL (1994). The long-term repopulating subset of hematopoietic stem cells is deterministic and isolable by phenotype. Immunity 1,661-673

Morrison SJ, Hemmati HD et al (1995a). The purification and characterization of fetal liver hematopoietic cells. Proc Natl Acad Sci USA. 92(22):10302-6.

Morrison SJ, Uchida N, Weissman IL (1995b). The biology of hematopoietic stem cells. Annu Rev Cell Dev Biol 11,35-71.

Müller-Tiemann BF, Halazonetis TD et al (1998). Identification of an additional negative regulatory region of p53 sequence-specific DNA binding. Proc Natl Acad Sci USA 95:6079-84.

Münster P, Marchion D et al (2007). Phase I trial of histone deacetylase inhibitor by valprioic acid followed by the topoisomerase II inhibitor epirubucun in advanced solid tumors: a clinical and translational study. J Clin Oncology 25(15):1979-1985.

Nakamura T, Largaespada DA, Lee MP et al (1996). Fusion of the nucleoporin gene NUP98 to HOXA9 by the chromosome translocation t(7;11)(p15;p15) in huiman myeloid leukemia. Nat. Genet. 12:154-158.

Nakamura T. (2005). NUP98 fusion in human leukemia: dysregulation of the nuclear pore and homeodomain proteins. Int J Hematol. 82(1):21-7.

Obier N, Uhlemann CF, mMüller AM (2010). Inhibition of histone deacetylases by Trichostatin A leads to a HOXB4-indipendent increase of hematopoietic progenitor/stem cell frequencies as a result of selective survival. Cytotherapy.

Orkin SH, Zon LI (2002). Hematopoiesis and stem cells: plasticity versus developmental heteroneity.

Orlic D, Bodine DM (1994). What defines a pluripotent hematopoietic stem cell (PHSC): will the real PHSC please stand up! Blood 84(12):3991-4.

Orlic D, Kajstura et al (2001). Bone marrow cells regenerate infarcted myocardium. Nature 410:701-705.

Osawa M, Hanada K et al (1996). Long-term lymphohematopoietic reconstitution by a single CD34-low/negative hematopoietic srem cell. Science 273(5272):242-245.

Oshima M, Endoh M, Endo TA, Toyoda T, et al (2011). Genome-wide analysis of target genes regulated by Hoxb4 in hematopoietic stem and progenitor cells developing from embryonic stem cells. Blood 14;117(15):e142-50.

Ozeki K, Kiyoi H et al (2004). Biologic and clinical significance of the FLT3 transcript level in acute myeloid leukemia. Blood 103(5): 1901-1908.

Palmqvist L, Argiropoulos B et al (2006). The Flt3 receptor tyrosine kinase collaborates with NUP98-HOX fusions in acute myeloid leukemia. Blood 108(3):1030-1036.

Pandolfi PP (2001). Transcription therapy of cancer. Oncogene 20(24):3116-27.

Passegué E, Janieson CH et al (2003). Normal and leukemic hematopoiesis: are leukemias a stem cell disorder or a reacquisition of stem cell characteristics? Proc Natl Acad Sci USA 100(suppl.1):11842-9.

Passegué E, Weissman IL (2005). Leukemic stem cells: where do they come from?

Pineault N, Helgason CD et al (2002). Differential expression of Hox, Meis1, and Pbx1 genes in primitive cells throughout murine hematopoietic ontogeny. Exp Hematol 30:49-57.

Pineault N, Buske C et al (2003). Induction of acute myeloid leukemia in mice by the human leukemia-specific fusion gene NUP98-HOXD13 in concert with Meis1. Blood 101(11):4529-38.

Pineault N, Abramovich C et al (2004). Differential and common leukemogenic potentials of multiple NUO98-Hox fusion proteins alone or with Meis1. Mol Cell Biol 24(5):1907-1917.

Polakis P (2000). Wnt signaling and cancer. Genes Dev 14(15):1837-51.

Rabbitts TH, Boehm T (1991). Structural and functional chimerism results from chromosomal translocation in lymphoid tumors. Adv Immunol 50:119-146.

Rabbitts TH (1994). Chromosomal translocation in human cancer. Nature 372(6502):143-9.

Raff M (2003). Adult stem cells plasticity: fact or arctifact? Annu Rev Cell Dev Biol 19:1-22.

Rajasekhar VK, Begemann M (2007). Concise review: roles of polycomb group proteins in development and disease: a stem cell perspective. Stem cells 25:2498-2510.

Rambaldi I, Kovacs EN et al (1994). A proline-rich transcriptional activation domain in murine HOXD4 (HOX-4.2). Nuc Acid Res 22(3):376-382.

Raza-Egilmez S, Jani-Sait SN et al (1998). NUP98-HOXD13 gene fusion in therapy-related acute myelogenous leukemia. Cancer Res 58:4269:4273.

Rawat VP, Cusan M et al (2004). Ectopic expression of the homeobox Cdx2 is the transforming event in a mouse model of t(12;13)(p13;q12) acute myeloid leukemia. Prot Natl Acad Sci USA 101:817-822.

Reya T, Morrison SJ et al (2001). Stem cells, cancer, and cancer stem cells. Nature 414(6859):105-11.

Reya T (2003). Regulation of Hematopoietic stem cell self-renewal. Recent Prog Horm Res. 58:283-95.

Rice KL, Licht JD (2007). Hox deregulation in acute myeloid leukemia. J Clin Invest 117(4):865-868.

Richon VM, Sandhoff TW et al (2000). Histone deacetylase inhibitor selectively indices p21WAF1 expression and gene-associated histone acetylation. Prot Natl Acad Sci USA 97(18): 10014-9.

Richon VM, Emiliani S, Verdin E, Webb Y, Breslow R, Rifkin RA, Marks P (1998). A class of hybrid polar inducers of transformed cell differentiation inhibitis histone deacetylases. Proc Natl Acad Sci USA 95:3003-3007.

Saleh M, Rambaldi I, Yang XJ, Featherstone MS (2000). Cell signaling switches HOX-PBX complexes from repressors to activators of transcription mediated by histone deacetylases and histone acetyltranferases. Mol Cell Biol 20(22):8623-8633.

Sambrook J, Fritsch EF, Maniatis (1989). Molecular cloning: a laboratory manual. Cold Spring Harbor Laboratory Press; 2nd edition .

.

Sauvageau G, Lansdorp PM et al (1994). Differential expression of homeobox genes in functionally distinct CD34+ subpopulations of human bone marrow cells. Proc Natl Acad Sci USA 91:12223-12227.

Sauvageau G, Thorsteinsdottir U (1995). Overexpression of HOXB4 in hematopoietic cells causes the selective expansion of more primitive populations in vitro and in vivo. Genes Devel 9:1753-1765.

Schessl T, Rawat VP, Cusan M et al (2005). The AML1-ETO fusion gene and the FLT3 lenght mutation collaborate in inducing acute leukemia in mice. J Clin Invest 115(8):2159-2168.

Schiedlmeier B, Santos AC et al (2007). HOXB4´s road map to stem cell expansion. Proc Natl Acad Sci USA 104(43):16952-16957.

Schiedlmeier B, Klimp H et al (2003). High-level ectopic HOXB4 expression confers a profound in vivo competitive grwth advantage on human cord blood CD34+ cells, but impairs lymphomyeloid differentiation. Blood 101(5):1759-1768.

Schoch C, Schnittger S, et al (2003). AML with 11q23/MLL abnormalities as defined by the WHO classification: incidence, partner chromosomes, FAB subtype, age distribution, and prognostic impact in an unselected series of 1897 cytogenetically analyzed AML cases. Blood 102(7):2396-402.

Seet LF, Teng E, Lai YS, Laning J et la (2008). Valproic acid enhances the engraftability of human umbilical cord blood hematopoietic stem cells expanded under serum-free conditions. Eur J Haematol. 82(124-132).

Shen WF, Krishnan K et al (2001). The HOX homeodomain protein blocks CBP histone acetyltransferase activity. Mol Cell Biol 21:7509-7522.

Sholl C, Bansal D et al (2007). The homeobox gene CDX2 is aberrantly expressed in most cases of acute myeloid leukemia and promotes leukemogenesis. J Clin Invest 117:1037-48.

Siminovitch L., McCulloch EA. et al. (1963). The distribution of colony-forming cells among spleen colonies. J Cell Physiol 62:327-336.

Speck N, Gilliland G (2002). Core-binding factors in hematopoiesis and leukemia. Nature 2:502-513.

Svingen T, Tonissen KF (2006). Hox transcription factors and their elusive mammalian gene targets. Heredity 97:88-96.

Szilvassy SJ, Humphries RK et al. (1990). Quantitative assay for totipotent reconstituting hematopoietic stem cells by a competitive repopulation strategy. Proc Natl Acad Sci USA 87(22):8736-40.

Taddei A, Roche D et al (2005). The effects of histone deacetylase inhibitors on heterochromatin: implications for anticancer therapy? EMBO 6(6):520-524.

Taussig DC, Pearce DJ, Simpson C, Rohatiner AZ, Lister TA, Kelly G, et al (2005). Hematopoietic stem cells express multiple myeloid markers: implications for the origin and targeted therapy of acute myeloid leukemia. Blood 106(13):4086-92

Tang Y, Chen J, Young NS (2009). Expansion of hematopoietic stem cells from normal donors and bone marrow failure patients by recombinant Hoxb4. Br J Haematol. 144(4):603-612.

Tenen DG (2003). Disruption of differentiation in human cell cancer: AML shows the way. Nat Rev Cancer 3(2):89-101.

Teokli C, El-Kadi M, Morgan R (2003). TALE class homeodomain gene Irx5 is an immediate douwnstream target for Hoxb4 transcriptional regulation. Dev Dynam 227:48-55.

Thorsteinsdottir U, Sauvageau G, et al (1999). Enhanced in vivo regenerative potential of HOXB4-transduced hematopoietic stem cells with regulation of their pool size. Blood 94(8):2605-2612.

Till JE, McCulloch EA (1961). A direct measurement of the radiation sensitivity of normal mouse bone marrow cells. Radiat Res 14,1419-1430.

Tupler R, Perini G, Green MR (2001). Expressing the human genome. Nature 409:832-833.

Ulijaszek SJ, Johnston FE, Preece MA (1998). The Cambridge Encyclopedia of human growth an development. Cambridge University Pree: Cambridge.

Vardiman JW, Thiele J, Arber DA, Brunning RD, Borowitz MJ, Porwit A, Harris NL, Le Beau MM, Hellström-Lindberg E, Tefferi A, Bloomfield CD (2009). The 2008 revision of the World Health Organization (WHO) classification of myeloid neoplasm and acute leukemia: rationale and important changes. Blood 1114; 5, 937-951.

Vardiman JW (2010). The World Health Organization (WHO) classification of tumors of the hematopoietic and lymphoid tissues: an overview with emphasis on the myeloid neoplasms. Chemico-Biological Interactions 184(2010)16-20.

Villaescusa JC, Buratti C, Penkov D, Mathiasen L, Planagumà J, Ferretti E, Blasi F (2009). Cytoplasmatic Prep1 interacts with 4EHP inhibiting Hoxb4 translation. Plos One 4:4:e5213: 1-12.

Virchow R (1846). Weisses Blut und Milztumoren. Med Ztg 15:151-163.

Wagers AJ, Weissman IL (2004). Plasticity of adult stem cells. Cell 116:639-648.

Walker K, Levine AJ (1996). Identification of a novel p53 functional domain that is necessary for efficient growth suppression. Proc Natl Acad Sci USA 93:15340-15340.

Warner JK, Wang JC et al (2004). Concepts of human leukemic development. Oncogene 23:7164-7177.

Weissman I.L. (2000). Stem cells: units of development, units of regeneration, and units in evolution. Cell 100(1): 157-168.

Weissman IL (2000b). Translating stem and progenitor cell biology to the clinic: barriers and opportunities. Science 287:1442-1446.

Woltering JM, Durston AJ (2008). MiR-10 represses Hoxb1a and Hoxb3a in zebrafish. Plos One 1:e1396:1-13.

Xu Ws, Parmigiani RB, Marks PA (2007). Histone deacetylase inhibitors. Molecular mechanisms of action. Oncogene 26:5541-5552.

Yeoh EJ, Ross ME et al (2002). Classification, subtype discovery, and prediction of outcome in pediatric acute lymphoblastic leukemia by gene expression profiling. Cancer cell 1:133-143.

Zhang XB, Beard BC, et al (2006). Differential effects of HOXB4 on nonhuman primate short- and long-term repopulating cells. PLoS Med 3(5):e173.

Zhang XB, Beard BC et al (2008). High incidence of leukemia in large animals after stem cells gene therapy with a HOXB4-expressing retroviral vector. J Clin Invest 118(4):1502-10.

At this point it is difficult to find the appropriate words to express my gratitude towards the people who have supported me through these years of pleasant and fascinating work done at the KKG-Leukemia research laboratory of the Department of Medicine III.

Above all, I want to express my special thanks to Prof. Hiddemann, who made my research possible in the unique fecund facility of his Clinic.
I would like to thank my supervisor, Prof. Christian Buske, and his wife, Dr. Michaela Feuring-Buske, who introduced me to the enchanting research of hematopoietic stem cells and have been exemplar in combining the clinical practice with sophisticated research based on animal models. I will never forget the enthusiasm of Christian, when we got our first leukemic mouse in his young laboratory in Munich!
The next most important person I want to show my gratitude is Dr. Aniruddha Deshpande. He was “always” there, open to discussion, to give suggestions, to make jokes and especially he has been an unforgettable lab companion, with whom it was possible to share successes and frustrations anytime.
Dr. Vijay Rawat, Dr. Natalia Arseni, Dr. Naidu Vegi, Bianka Ksienzyk have also been unique friends and supporters while repeating and repeating countless experiments.
Prof. Stefan Bohlander has been really available all the time for any small or complicated question, giving his optimism and precious suggestions for free.
I guess I have scarce vocabulary to thank everybody in a special way, but each person I met during my doctoral research made it unforgettable. I don´t want to omit these other very important colleagues and friends, like Dr. Florian Kuchenbauer, Dr. Farid Ahmed, Dr. Susan King, Dr. Christine Maier, Dr. Luca Perabo.
Finally I want to dedicate this work to my family, Graziella, Franco and Barbara, which although so far away have always been close to me and ready to participate in all my small improvements!

Ectopic expression of the homeobox gene *Cdx2* is the transforming event in a mouse model of t(12;13)(p13;q12) acute myeloid leukemia

Vijay P. S. Rawat*†, Monica Cusan*†, Aniruddha Deshpande*†, Wolfgang Hiddemann*†, Leticia Quintanilla-Martinez‡, R. Keith Humphries§¶, Stefan K. Bohlander*†, Michaela Feuring-Buske*†, and Christian Buske*†‖

*GSF–Clinical Cooperative Group Leukemia and †Department of Medicine III, Grosshadern, Ludwig Maximilians University, 81377 Munich, Germany; ‡GSF–Department of Pathology, 85764 Neuherberg, Germany; and §Terry Fox Laboratory, BC Cancer Agency and ¶Department of Medicine, University of British Columbia, Vancouver, BC, Canada V5Z 4E6

Edited by Janet D. Rowley, University of Chicago Medical Center, Chicago, IL, and approved November 21, 2003 (received for review August 29, 2003)

Creation of fusion genes by balanced chromosomal translocations is one of the hallmarks of acute myeloid leukemia (AML) and is considered one of the key leukemogenic events in this disease. In t(12;13)(p13;q12) AML, ectopic expression of the homeobox gene *CDX2* was detected in addition to expression of the *ETV6-CDX2* fusion gene, generated by the chromosomal translocation. Here we show in a murine model of t(12;13)(p13;q12) AML that myeloid leukemogenesis is induced by the ectopic expression of *CDX2* and not by the *ETV6-CDX2* chimeric gene. Mice transplanted with bone marrow cells retrovirally engineered to express *Cdx2* rapidly succumbed to fatal and transplantable AML. The transforming capacity of *Cdx2* depended on an intact homeodomain and the N-terminal transactivation domain. Transplantation of bone marrow cells expressing *ETV6-CDX2* failed to induce leukemia. Furthermore, coexpression of *ETV6-CDX2* and *Cdx2* in bone marrow cells did not accelerate the course of disease in transplanted mice compared to *Cdx2* alone. These data demonstrate that activation of a protooncogene by a balanced chromosomal translocation can be the pivotal leukemogenic event in AML, characterized by the expression of a leukemia-specific fusion gene. Furthermore, these findings link protooncogene activation to myeloid leukemogenesis, an oncogenic mechanism so far associated mainly with lymphoid leukemias and lymphomas.

The molecular dissection of balanced chromosomal translocations in patients with acute leukemia has greatly advanced our knowledge of the pathogenesis of this disease, demonstrating that chromosomal translocations often affect genes that regulate hematopoiesis. Chromosomal translocations involve mainly two mechanisms that lead to malignant transformation: deregulation of the expression of a protooncogene by juxtaposition of a potent enhancer or promoter elements or creation of a fusion gene (1–3). Although both mechanisms are found in lymphoid leukemia or lymphoma, formation of a fusion gene predominates in acute myeloid leukemia (AML). In fact, to date, there are no experimentally confirmed instances in which the transcriptional deregulation of a protooncogene is the key leukemogenic event in a fusion gene-positive AML.

The oncogenic potential of fusion genes has been well documented experimentally. However, emerging data, mostly from murine *in vivo* models, have demonstrated that many of these fusion genes are not able to induce leukemia on their own. This observation suggests an important role for other genetic alterations that cooperate with fusion genes in patients with AML (4–6). The intriguing differences in the oncogenic potential of fusion genes are well documented for the large family of chimeric genes involving the *ets* transcription factor *ETV6*, located at 12p13. *ETV6* is one of the genes most frequently involved in chromosomal translocations. Chromosomal translocations affecting the *ETV6* locus have been reported with >40 different partners (7). Fusion partners of *ETV6* can be phosphotyrosine kinases (PTK) or transcription factors and genes of unknown function, dividing *ETV6* fusion genes into two distinct groups. Fusions of *ETV6* with PTKs such as *PDGFRB*, *JAK2*, *ABL1*, *ABL2*, or *NTRK3* create highly leukemogenic proteins in murine experimental models (8–12). In the group of *ETV6*-transcription factor fusions, the N-terminal portion of *ETV6* is fused to the partner gene in most cases, retaining (e.g., *ETV6-AML1*) or losing the *pointed* domain (e.g., *ETV6-CDX2*, *ETV6-MDS1/EVII*) (13–15). Although data about the leukemogenic potential of this group of fusion genes are still limited, extensive analyses of the most frequent *ETV6* chimeric transcription factor, *ETV6-AML1*, failed to show any major transforming activity in a transgenic or bone marrow (BM) transplantation mouse model (16, 17). Based on these data, expression of an *ETV6*-transcription factor fusion might not be sufficient to induce disease. Indeed, recent evidence corroborates that *ETV6* acts as a tumor suppressor gene and that, in almost all cases of *ETV6/AML1*-positive acute lymphoblastic leukemias, there is a deletion or loss of expression of the nonrearranged *ETV6* allele (18, 19). Furthermore, several chromosomal translocations involving the *ETV6* locus associated with myeloid malignancies such as t(4;12), t(5;12), or t(12;17) do not form any functional fusion gene at all, pointing to a key variant oncogenic mechanism in these cases (20, 21). In this regard, the t(12;13)(p13;q12) associated with the *ETV6-CDX2* fusion gene in human AML is of notable interest. The translocation breakpoint leaves the *CDX2* gene intact, and expression of both the fusion gene and full-length *CDX2*, normally restricted to intestinal epithelial cells, was observed in leukemic cells, thus raising the possibility that ectopic expression of *CDX2* is the key pathogenic event (14).

To clarify this particular issue and to gain insight into alternative mechanisms of transformation in patients with AML and *ETV6* rearrangements, we established a mouse model for t(12;13)(p13;q12) human AML. We demonstrate that ectopic expression of *Cdx2* is the key transforming event that induces fatal AML in transplanted mice. In contrast, expression of the ETV6-CDX2 fusion protein is unable to induce leukemia. Furthermore, we show that the transforming potential of *Cdx2* depends on the integrity of its DNA-binding domain and the N-terminal domain of Cdx2. Our data point to a previously uncharacterized mechanism of leukemogenesis in patients with AML, in which a balanced chromosomal translocation contributes to malignant transformation by activating the expression of a protooncogene, a mechanism so far associated mainly with lymphoid leukemias or lymphomas (3).

Materials and Methods

cDNA Constructs and Retroviral Vectors. cDNAs of *ETV6-CDX2* and *Cdx2* (93% overall and 98% identity in the homeodomain between

This paper was submitted directly (Track II) to the PNAS office.

Abbreviations: AML, acute myeloid leukemia; BM, bone marrow; YFP, yellow fluorescent protein; CFU-S, colony-forming unit–spleen; PB, peripheral blood.

‖To whom correspondence should be addressed. E-mail: buske@gsf.de.

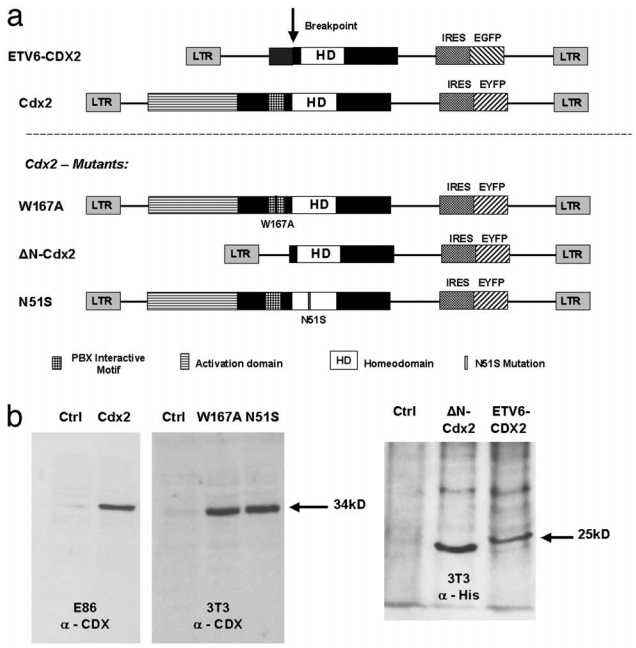

Fig. 1. (*a*) Retroviral vectors used to express *ETV6-CDX2*, *Cdx2*, and the different *Cdx2* mutants in murine BM. IRES, internal ribosomal entry site. (*b*) Western blot analysis of cellular extracts from NIH 3T3 or E86 cells transfected with the different constructs. The molecular mass is indicated.

the human and murine proteins) were kindly provided by D. G. Gilliland (Division of Hematology/Oncology, Harvard Medical School, Boston) and N. Cross (Department of Haematology, Hammersmith Hospital, London). A histidine-tagged version of *ETV6-CDX2* was constructed by ligating a PCR product of the fusion gene in frame to the 3′ end of the histidine epitope of the pCDNA6/V5-His A plasmid (Invitrogen), *Cdx2* mutants were created that were previously shown to inactivate a putative PBX1 interacting motif (W167A-Cdx2) (22) or to inactivate the DNA-binding homeodomain (N51S-Cdx2) (23) by using the QuikChange XL Site-Directed Mutagenesis Kit (Stratagene). The *Cdx2* mutant lacking the first 179 N-terminal amino acids, which are deleted in the *ETV6-CDX2* fusion, was generated and histidine tagged by PCR following standard procedures (ΔN-Cdx2) (4). For retroviral gene transfer into primary BM cells, the different constructs were subcloned into the multiple cloning site of the modified murine stem cell virus (MSCV) 2.1 vector (4) upstream of the internal ribosomal entry site (IRES) and the enhanced GFP or yellow fluorescent protein (YFP) gene. As a control, the MSCV vector carrying only the IRES-enhanced GFP cassette was used.

Production of high-titer helper-free retrovirus was carried out following standard procedures by using the ecotropic packaging cell line GP^+E86 (4). The number of provirus integrants was determined by *Eco*RI digestion and full length integration by *Nhe*I digestion, followed by Southern blot analysis using standard techniques (24). Protein expression of the *ETV6-CDX2*, *Cdx2*, and *Cdx2* mutant plasmids was documented by Western blotting using standard procedures. Membranes were probed with an antihistidine monoclonal antibody (Sigma) for ETV6-CDX2 and the ΔN-Cdx2 mutant or with an anti-CDX2 monoclonal antibody (kindly provided by DCS Innovative, Hamburg, Germany) for expression of the Cdx2, W167A-Cdx2, and N51S-Cdx2 mutants (25) (Fig. 1).

***In Vitro* Assays.** Cell proliferation was assessed in DMEM supplemented with 15% FBS/10 ng/ml mIL-6/6 ng/ml mIL-3/100 ng/ml murine stem cell factor (standard medium) (Tebu-bio, Offenbach, Germany). Differentiation of clonogenic progenitors was analyzed by plating cells in methylcellulose supplemented with cytokines (Methocult M3434, StemCell Technologies, Vancouver). IL-3-dependent cell populations expressing Cdx2 or coexpressing ETV6-CDX2 and Cdx2 were established *in vitro* directly after sorting in DMEM/15% FBS with IL-3 alone (6 ng/ml). The differentiation capacity of cultured cells was tested in DMEM/15% FBS supplemented with granulocyte colony-stimulating factor 100 ng/ml or macrophage colony-stimulating factor 10 ng/ml (R & D Systems) and *all-trans* retinoic acid at 1 μM final concentration. After 5 days, the morphology was determined by Wright–Giemsa-stained cytospin preparations (4, 25).

Mice and Retroviral Infection of Primary BMC. Parental strain mice were bred and maintained at the GSF animal facility. Donors of primary BM cells were >12-wk-old (C57BL/6Ly-Pep3b × C3H/HeJ) F_1 (PepC3) mice, and recipients were >8- to 12-wk-old (C57BL/6J × C3H/HeJ) F_1(B6C3) mice. Primary mouse BM cells were transduced as described (4). For transduction, cells were cocultured with irradiated (40 Gy) ETV6-CDX2/GFP or Cdx2/YFP GP^+E86 producers or with a mixture of 40–50% Cdx2/YFP and 50–60% ETV6-CDX2/GFP producers in cotransduction experiments.

Colony-Forming Unit–Spleen (CFU-S) Assay. Primary BM cells from F_1(PepC3) donor mice treated 4 days previously with 5-fluorouracil were transfected with the different viruses, and retrovirally transduced cells were highly purified based on expression of GFP or YFP by using a FACSVantage (Becton Dickinson). Transduced cells were cultured 7 days in standard medium. The day 0 equivalent of $2.5–3 \times 10^4$ cells was injected into lethally irradiated F_1(B6C3) recipient mice. The recovery of CFU-S cells was quantified by determining the number of macroscopic colonies on the spleen at day 12 postinjection after fixation in Telleyesnickzky's solution.

BM Transplantation and Assessment of Mice. Recipient F_1(B6C3) mice (8–10 wk old) were irradiated with 850 cGy from a ^{137}Cs γ-radiation source. FACS-purified transduced BM cells, or a defined ratio of transduced and untransduced cells was injected into the tail vein of irradiated recipient mice. Peripheral blood (PB) or BM cell progeny of transduced cells were tracked by using the GFP or YFP fluorescence (26). The lineage distribution was determined by FACS analysis as described (4): phycoerythrin-labeled Gr-1, ScaI, Ter-119, CD4, and allophycocyanin-labeled Mac1, cKit, B220, or CD8 antibodies were used for analysis (all PharMingen). For histological analyses, sections of selected organs were prepared and hematoxylin/eosin-stained by using standard protocols.

RT-PCR. Expression of *Hoxa9* and *Meis1* was assayed by RT-PCR in $Sca\text{-}1^-Lin^+$ cells sorted from a mouse repopulated with Cdx2 expressing BM cells or a control animal. Total RNA was isolated by using Trizol reagent (GIBCO/BRL) and treated with DNase I (amp grade) to remove contaminating genomic DNA. First-strand cDNA was synthesized from 1 μg of total RNA by using the thermoScript RT-PCR system (all reagents from Invitrogen). Equal amounts of cDNA originating from 50 ng of starting RNA were loaded to assess transcription levels. Intron-spanning primer pairs were selected to avoid amplification of contaminating genomic DNA. The annealing temperatures were 58°C and 60°C for *Meis1* and *Hoxa9*, respectively. The number of PCR cycles for each gene was chosen to stop the reaction in the linear phase of amplification (25 cycles for mβ-2 microglobulin, 35 cycles for *Meis1* and *Hoxa9*).

Statistical Analysis. Data were evaluated by using the *t* test for dependent or independent samples (Microsoft EXCEL). Differences with P values < 0.05 were considered statistically significant.

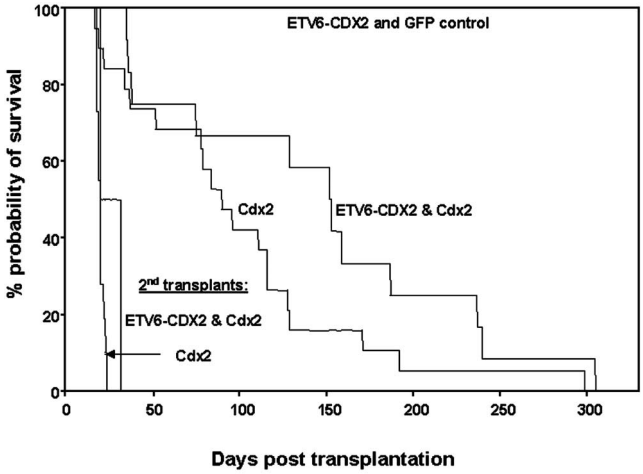

Fig. 2. Survival curve of mice transplanted with BM cells expressing *Cdx2* ($n = 18$), *ETV6-CDX2* ($n = 9$), or coexpressing *Cdx2* and the fusion gene ($n = 13$). The control group was injected with BM infected with the GFP empty retrovirus ($n = 7$). The survival time of secondary recipient mice, transplanted with BM from diseased primary *Cdx2* or *ETV6-CDX2* and *Cdx2* recipients, is indicated.

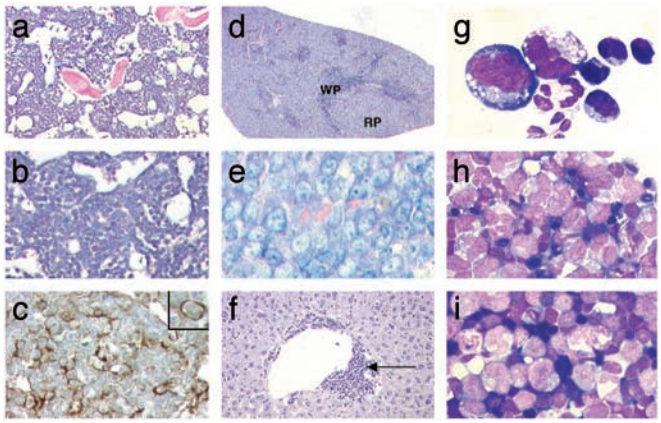

Fig. 3. Histological analysis of diseased *Cdx2* mice. (*a*) BM [hematoxylin/eosin (H&E)]. Immunohistochemistry of the BM (×200) for *N*-acetyl-chloroacetate esterase (×400) (*b*) and CD34 expression (×640) (*c*). Histology of the spleen H&E (×25) (*d*) and Giemsa staining (×640) (*e*) and liver with perivascular infiltration (×200) (*f*). Cytospin preparations from PB (*g*), BM (*h*), and spleen (*i*) (all ×1,000).

Results

Ectopic Expression of *Cdx2* Causes AML in Transplanted Mice. To analyze whether expression of the t(12;13)-associated *ETV6-CDX2* fusion gene and/or the ectopic expression of the homeobox gene *Cdx2* is able to transform early murine hematopoietic progenitors *in vivo*, we generated MSCV-based retroviral constructs and documented full-length protein expression by Western blotting (Fig. 1). Murine hematopoietic progenitors constitutively expressing *ETV6-CDX2* or *Cdx2* were highly purified by FACS based on GFP^+ or YFP^+ expression, respectively, and injected into lethally irradiated recipient mice directly after sorting (3–3.5 × 10^5 and 2–3.6 × 10^5 cells per mouse for *Cdx2* and *ETV6-CDX2*, respectively).

Mice transplanted with BM cells expressing *Cdx2* became moribund after a median of 90 days posttransplantation ($n = 18$) (Fig. 2). Diseased mice were characterized by cachexia, shortness of breath, and lethargy when they were killed for further analysis. In striking contrast, mice transplanted with *ETV6-CDX2*-expressing cells did not succumb to terminal disease ($n = 9$) (Fig. 2). Diseased *Cdx2* mice were characterized by elevated peripheral white blood count (WBC) (3.8-fold) with up to 48 × 10^6 circulating WBC per milliliter. Furthermore, moribund mice were anemic, with a 5-fold decrease in peripheral erythrocyte count ($P < 0.001$) (Table 1). All *Cdx2* mice analyzed ($n = 7$) suffered from splenomegaly, with an average spleen weight of 0.6 g (range 0.4–0.9; $P < 0.01$ compared to control animals) (Table 1). More detailed hematological analyses demonstrated that animals suffered from AML with a high percentage of blasts in the BM (42% ± 6), PB (14% ± 3), and spleen (35% ± 5) ($n = 8$; $P < 0.01$ compared to the control animal) (Table 1). Furthermore, leukemic mice showed multiple organ infiltration with blast cells. Thirty percent of the blasts expressed CD34 but were negative for *N*-acetyl-chloroacetate esterase, periodic acid/Schiff reagent, and terminal deoxynucleotidyltransferase, as shown by immunohistochemistry, consistent with an undifferentiated myeloblastic phenotype of the disease (Fig. 3). Immunophenotypic

Table 1. Hematological parameters of experimental mice

Mouse no.	Retroviral construct	Day of death	RBC per ml ×10^9	WBC per ml ×10^6	Spleen weight, mg	BM % blasts	Spleen % blasts	PB % blasts	Lymphoid/myeloid ratio in PB
1	GFP	90	6	4.5	150	0	0	0	5:1
2	GFP	90	4.8	3.2	200	0	0	0	2:1
3	GFP	90	5.0	3.6	200	0	0	0	2:1
1*	Cdx2	128	1.0	3.2	400	28	21	8	0.5:1
2*	Cdx2	79	2.0	37	650	40	35	12	0.4:1
3*	Cdx2	52	0.7	9	600	38	30	15	0.2:1
4*	Cdx2	116	0.4	48	nd	ND	60	14	0.4:1
5*	Cdx2	37	0.6	5	400	25	22	5	0.3:1
6*	Cdx2	171	0.8	24	900	71	48	18	0.3:1
7*	Cdx2	192	1.1	10	800	60	41	30	0.5:1
8*	Cdx2	84	0.4	28	400	32	24	8	0.8:1
1*	++	168	1.0	3.2	400	25	18	3	0.6:1
2*	++	230	1.1	8	500	45	30	10	0.1:1
3*	++	151	0.2	8	600	58	37	16	0.4:1
4*	++	237	1.5	24	300	25	18	5	0.6:1
5*	++	187	0.5	25	900	50	43	8	0.3:1
1	ETV6-CDX2	375	6.5	2.4	160	10	8	0	0.3:1
2	ETV6-CDX2	375	5	3.2	200	25	15	0	0.4:1
3	ETV6-CDX2	375	5.2	6	180	15	9	0	2:1

*, diseased; ++, ETV6-CDX2 and Cdx2; RBC, red blood cell count; WBC, white blood cell count; ND, not determined.

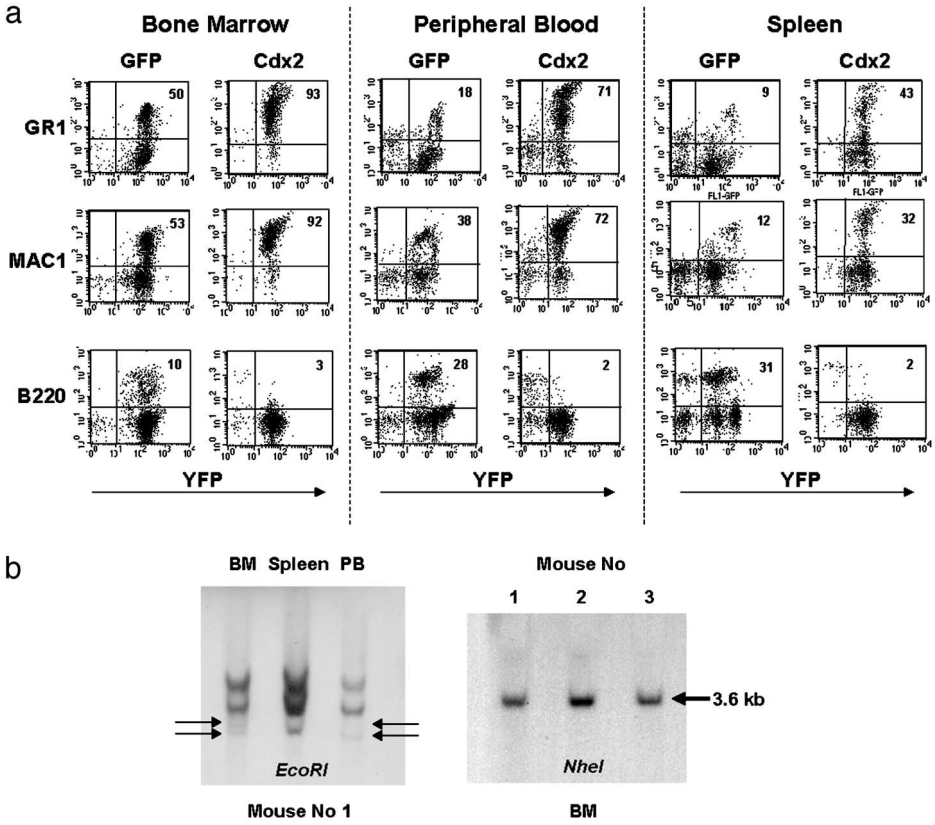

Fig. 4. (*a*) Flow cytometry from a representative leukemic *Cdx2* mouse from PB, BM, and spleen in comparison to a GFP control animal. Cells were stained for the myeloid markers Gr1 and Mac1 and the lymphoid marker B220. The proportion of positive cells within the GFP^+ compartment is indicated. (*b*) Southern blot analyses of genomic DNA from BM, PB, and spleens of representative leukemic *Cdx2* mice. Genomic DNA was digested with *Eco*RI, which cuts once in the provirus, to determine the number of provirus integrants. Signals with different intensity, indicating the presence of different leukemic clones, are indicated. Full-length provirus integration was documented by digestion with *Nhe*I, which cuts only in the LTRs of the provirus.

characterization of PB, BM, and spleen in diseased mice confirmed the predominance of myeloid $Mac1^+$ and $Gr\text{-}1^+$ cells (84% ± 10 and 73% ± 15 in the PB, 65% ± 14 and 53% ± 14 in the spleen, respectively; $n = 4$) compared to the GFP control mice ($Mac1^+$ and $Gr\text{-}1^+$ cells 47% ± 5 and 25% ± 3 in the PB, 14% ± 9 and 10% ± 1 in the spleen, respectively; $n = 4$). Furthermore, diseased mice were characterized by a greatly reduced normal $B220^+$ lymphoid population in the spleen and PB compared to controls (1.8% ± 1 vs. 35% ± 8 and 1.3% ± 0.5 vs. 46% ± 21 in the PB and in the spleen, respectively; $n = 4$) (Fig. 4*a*). Mice transplanted with *Cdx2*-expressing BM cells were characterized by a 19-fold increased frequency of clonogenic cells in the PB and a >100-fold increase in the spleen compared to the control as quantified by *ex vivo* CFC assays (248 vs. 13 clonogenic cells per 1×10^6 cells/ml in the PB and 1,400 clonogenic cells vs. 13 per 1×10^6 cells/ml in the spleen, respectively) ($n = 3$). Twenty-eight percent (±3) of these clonogenic progenitors were not able to terminally differentiate and formed blast colonies in methylcellulose with high serial replating capacity (data not shown).

The *Cdx2*-induced AML was transplantable and all lethally irradiated mice ($n = 11$) injected with BM cells of diseased *Cdx2* animals died within 24 days posttransplantation (Fig. 2). Analysis of the clonality of the disease by Southern blot analysis demonstrated different intensities and patterns of proviral signals in the different hematopoietic organs consistent with an oligoclonal nature of the disease (Fig. 4*b*).

To analyze whether the *ETV6-CDX2* fusion caused subtle perturbations in hematopoietic development, healthy animals ($n = 3$) were killed 44 wk after transplantation with *ETV6-CDX2*-expressing BM cells. Interestingly, two of three animals showed an expansion of the mature neutrophil compartment in the PB with an inversion of the lymphoid/myeloid ratio (Table 1) and 87% and 68% $Mac1^+/Gr1^+$ cells in the GFP-positive compartment. Furthermore, spleens from all mice were infiltrated with terminally differentiated myeloid cells (86% ± 0.9 $Gr1^+/Mac1^+$ cells). However, none of the animals suffered from anemia, splenomegaly, or the emergence of a blast population in the PB (Table 1). Thus, *ETV6-CDX2* was able to induce a myeloproliferation without causing disease but failed to induce leukemic transformation.

In addition, 13 mice were transplanted with a mixture of *ETV6-CDX2*, *Cdx2*, and *Cdx2* and *ETV6-CDX2* coexpressing cells, containing between $1.9–4.5 \times 10^4$ *Cdx2* and *ETV6-CDX2* cells and <4,000 *Cdx2* cells per mouse. The addition of *Cdx2* and *ETV6-CDX2* coexpressing cells did not accelerate the course or change the phenotype of the disease compared to only *Cdx2*-expressing cells. All animals succumbed to AML, and the leukemic population consisted of *Cdx2*- and *ETV6-CDX2*-coexpressing or *Cdx2*-expressing cells in all mice analyzed ($n = 4$) (Fig. 2). These data indicate that aberrant expression of the wild-type *Cdx2* gene is crucial for malignant transformation in this model.

The Transforming Potential of *Cdx2* Depends on the N-Terminal Transactivation Domain and the Intact Homeodomain. In an effort to characterize the contribution of different motifs of *Cdx2* to the transforming capacity of the gene, three different mutants were designed: a mutant inactivating the homeodomain (N51S-Cdx2), a Cdx2 mutant with an inactivating mutation in the putative PBX1-interacting motif (W167A-Cdx2), and a mutant lacking the N-terminal portion of Cdx2, which is not present in the *ETV6-CDX2* fusion (ΔN-Cdx2). Protein expression of the mutants was confirmed by Western blot analysis (Fig. 1*b*). Expression of wild-type Cdx2 and W167A-Cdx2 in primary bone marrow cells rapidly induced the outgrowth of IL-3-dependent cell populations in liquid cultures. The cells showed blast morphology, were $Gr^+/Mac1^+$-positive, and had lost their differentiation capacity when incubated with macrophage colony-stimulating factor, granulocyte colony-stimulating factor, or *all-trans* retinoic acid (data not shown). Furthermore, mice transplanted with 1×10^6 of these cells developed leukemia 8 wk posttransplant in contrast to mice injected with nontransduced or GFP-expressing control cells. Cells expressing

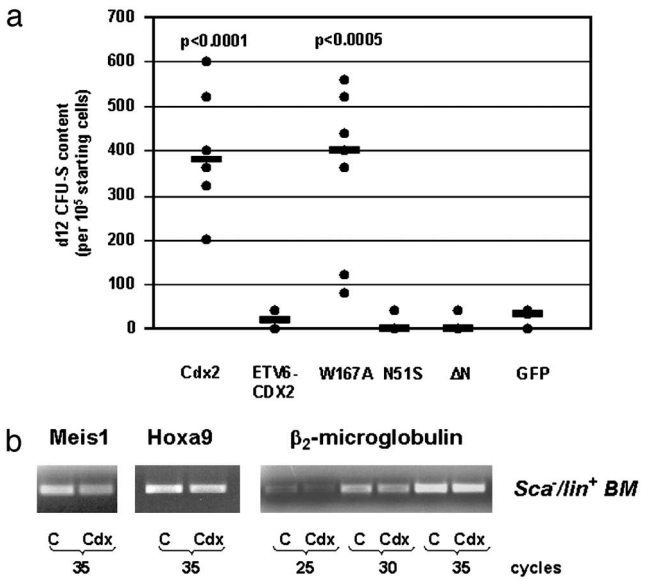

Fig. 5. (*a*) Total number of d12 CFU-S colonies derived per culture initiated with 1×10^5 cells transduced with the different viruses after 1 wk in liquid culture. The median is indicated. (*b*) Expression of *Meis1* and *Hoxa9* analyzed by RT-PCR in Sca^-lin^+ BM cells isolated from a *Cdx2* mouse or a control mouse. The number of PCR cycles for each gene was chosen to stop the reaction in the linear phase of the amplification (25 cycles for mβ-2 microglobulin, 35 cycles for *Meis1* and *Hoxa9*). C, control; Cdx, Cdx2.

ETV6-CDX2, the ΔN-Cdx2, or the N51S mutant as well as the control cells were not able to form blast cell populations *in vitro*. When colony formation was tested, Cdx2-positive cells generated a higher number of primary CFC in methylcellulose compared to GFP (76 ± 22 vs. 41 ± 20 per 500 initially plated cells, respectively; $n = 5$; $P < 0.02$). Furthermore, Cdx2-positive colonies contained ≈10 times more cells per colony than the controls (33×10^3 vs. 3.9×10^3 per colony, respectively; $n = 5$; $P < 0.004$). The expression of the other constructs did not change the size or number of colonies compared to the control. To investigate the effect of the different mutants on primitive hematopoietic cells, cells infected with the different viruses were injected into lethally irradiated mice after 7 days of *in vitro* culture, and spleen colony formation was quantified 12 days after injection in killed mice (CFU-S assay). Cdx2 expression as well as expression of the W167A-Cdx2 mutant induced a significant >10-fold increase in the yield of day 12 CFU-S compared to the GFP control ($n = 8$; $P < 0.0001$). In contrast, deletion of the N-terminal portion of Cdx2 ($n = 5$) or inactivation of the homeodomain ($n = 5$) resulted in complete loss of the Cdx2 activity in these assays. ETV6-CDX2 ($n = 6$) did not show any increase in CFU-S compared to the GFP control (Fig. 5*a*).

The Expression of *Hoxa9* and *Meis1* Is Not Increased by Ectopic Expression of *Cdx2*. Given the role of *Cdx2* as an upstream regulator of *Hox* gene expression, we asked whether *Cdx2* would perturb expression of leukemogenic homeobox genes such as *Hoxa9* or *Meis1*. First, expression of *Hoxa9* and *Meis1* was determined by RT–PCR in the 32D cell line transduced with the Cdx2, the ETV6-CDX2, or the GFP virus. Compared to the control, *Cdx2* did not increase expression of Hoxa9 or Meis1 (data not shown). In addition, Sca^-lin^+-differentiated cells were recovered and highly purified from a mouse transplanted with *Cdx2*-expressing BM cells and a control animal, a cell population with normally no detectable expression of *Hoxa9* and *Meis1* (27): specific amplification products were not detectable by RT-PCR after 25 cycles in both experimental arms. Amplification products could be detected after 35 cycle but without considerable differences in the intensity between *Cdx2*-transduced and control cells (Fig. 5*b*). Thus, ectopic expression of *Cdx2* was not associated with up-regulation of *Meis1* or *Hoxa9* in this model system.

Discussion

The formation of fusion genes with oncogenic properties by balanced chromosomal rearrangements is considered one of the crucial steps for leukemic transformation in patients with AML. By using the murine BM transplantation model, we now provide direct evidence that the ectopic expression of the protooncogene *Cdx2* and not the expression of the fusion gene *ETV6-CDX2* is the key transforming event in t(12;13)(p13;q12)-positive AML. Activation of protooncogenes by balanced chromosomal translocations is a well-known oncogenic mechanism in lymphoid leukemias or lymphomas but has, to our knowledge, not been functionally demonstrated for AML and translocations involving *ETV6* (3). In addition, these data present evidence that the homeobox gene and *Hox* gene upstream regulator *Cdx2*, which so far has been linked to intestinal metaplasia and colon cancer (28), is highly leukemogenic when aberrantly expressed in hematopoietic progenitor cells.

Cdx2 belongs to the large group of homeobox genes, which were originally described as master regulators of embryonic body development. The *Cdx* genes and their homologues *caudal* in *Drosophila* and *Xcad* in *Xenopus* belong to the ParaHox cluster, which is considered an ancient paralog of the *Hox* gene cluster (29). Although the *Cdx* genes show similarities to the 5′-located Abdominal-B like genes of the *Hox* gene cluster, they possess a Pbx recognition motif, a characteristic of 3′-located *Hox* genes (30). *Cdx* genes play a key role in the homeobox regulatory network, acting as upstream regulators of several *Hox* genes (30, 31). Thus, perturbation of *Cdx2* might be linked to critical alterations in downstream *Hox* genes that are central regulators of normal early hematopoietic development in the adult with a distinct expression profile in human and murine early progenitor cells (27, 32, 33). Gene expression profiling of acute leukemias using DNA microarray technology linked aberrant expression of *Hox* genes such as *HOXA9*, *HOXA10*, and of the nonclustered homeobox gene *MEIS1* to leukemogenesis (34–37). Retrovirally enforced expression of these genes induced severe perturbations of normal hematopoietic development in human and murine experimental models (24, 38). Altered expression of several *Hox* genes might be one of the reasons for the strong oncogenic potential of *Cdx2* (30, 39–42). However, RT–PCR analyses in the 32D cell line model and in Sca^-/lin^+ BM population of a *Cdx2* repopulated mouse did not indicate gross up-regulation of *Meis1* and *Hoxa9* by *Cdx2*. However, this does not exclude that perturbation of other *Hox* genes might play a role in the transformation process initiated by ectopic *Cdx2* expression.

Of note, perturbed expression of *Hox* genes such as *HOXA9* or *HOXA10* in hematopoietic progenitor cells is not able to induce frank AML in transplanted mice after a short latency time but requires collaboration with the *Hox* co-factor *MEIS1*. In striking contrast, constitutive expression of *Cdx2* rapidly caused leukemia in recipient mice. The underlying cause for the difference in the leukemogenic activity between *Cdx2* and *HOXA9* or *HOXA10* is not known. But, in contrast to *HOXA9* and *HOXA10*, which are normally expressed at high levels in progenitor cells, *CDX2* is not expressed in hematopoietic cells (14). Thus, ectopic expression of *CDX2* in leukemia patients might result in the activation of *de novo* downstream pathways, which are normally silent in early blood development.

Despite the differences in the oncogenic potential, many of the *in vitro* and *in vivo* hematopoietic effects induced by *Cdx2* are highly reminiscent of the effects of retrovirally overexpressed hematopoietic *HOX* genes as well as leukemia-specific fusion genes such as *NUP98-HOXD13* with regard to the impact on short-term repopulating CFU-S or clonogenic progenitors (4, 38, 43). The striking similarities of the phenotypes induced by the over-expression of

homeobox genes of the *Hox* cluster and of *Cdx2* as a member of the ParaHox complex (29) point to a high level of functional redundancy among homeobox proteins in hematopoiesis.

The hematopoietic activity of *Cdx2* strictly depended on its intact homeodomain, implicating that DNA binding of *Cdx2* is essential for its transforming activity. Furthermore, deletion of the Cdx2 N-terminal portion resulted in a complete loss of activity in our assays. Of note, it was demonstrated that the N-terminal part of Cdx2 is necessary for transcriptional activation of *Hox* genes, supporting the concept that activation of downstream *Hox* genes is a potential key mechanism of *Cdx2*-induced transformation (44). Furthermore, it was demonstrated that the transcriptional activity of CDX proteins depends on the interaction of the p38 mitogen-activated protein kinase and the N-terminal transactivation domain of Cdx2 (45). As a consequence, N-terminal deletion would diminish the transactivation capacity of CDX2. Importantly, the *ETV6-CDX2* fusion gene lacks the N-terminal portion of *CDX2*, presumably hampering its capability to transactivate target genes. This would explain the obvious discrepancy in the oncogenic potential between *Cdx2* and the *ETV6-CDX2* fusion gene; this is supported by our data, which demonstrate a complete loss of activity when this N-terminal portion of *Cdx2*, which is not present in the *ETV6-CDX2* fusion gene, is deleted in the ΔN-Cdx2 mutant. Notably, mice transplanted with BM cells expressing the chimeric gene developed myeloproliferation after a long latency time but without any clinical symptoms. These data indicate that, despite the loss of the N-terminal portion, the fusion gene is able to perturb hematopoietic development, although to a significantly lesser extent than full-length *Cdx2*. However, it cannot be excluded from our experiments that the first 54 amino acids of ETV6, which are fused to CDX2, are responsible for or at least contribute to the observed disturbances of hematopoiesis. Taken together, our data propose a model in which the chromosomal translocation t(12;13)(p13;q12) causes AML by inducing the ectopic expression of CDX2. The mechanism of transcriptional induction is not precisely known, but it was demonstrated that the chromosome 13 breakpoint lies upstream of the *CDX2* gene. Therefore, one possible explanation for the ectopic expression of CDX2 could be that the translocated protooncogene might now be under the control of one of the two alternative ETV6 enhancer/promoters, located between exons 2 and 3 of ETV6 (14). Intriguingly, it was recently shown that the homeobox gene GSH2 and IL-3 are ectopically expressed in patients with AML and the translocations t(4;12)(q11–12;p13) and t(5;12)(q31;p13), respectively. Both translocations involve *ETV6* but do not create any functional fusion genes (20). This observation suggests that activation of protooncogenes is a more common phenomenon in ETV6-associated leukemias than previously thought. Taking into consideration that several AML-associated fusion genes are not leukemogenic on their own, it is tempting to speculate that activation of protooncogenes by chromosomal rearrangements might be quite a widespread mechanism in myeloid leukemogenesis. This hypothesis is supported by observations in AML cases not affecting ETV6, in which expression of the putative protooncogene EVI1 is activated by juxtaposition to the enhancer sequences of the ribophorin-I gene in patients with AML and 3q21 alterations (46). Our data provide compelling evidence that myeloid leukemogenesis can be initiated by this mechanism and emphasize the relevance of protooncogene activation for the development of AML.

We acknowledge D. G. Gilliland for generously providing the ETV6-CDX2 and Cdx2 cDNA, T. Haferlach and B. Ksienzyk for excellent technical assistance, and the members of the GSF animal facility for maintenance of the animals. This work was supported by Deutsche Forschungsgesellschaft Grant Bu 1177/2-1 (to C.B.)

1. Rowley, J. D. (1999) *Semin. Hematol.* **36,** 59–72.
2. Bohlander, S. K. (2000) *Cytogenet. Cell Genet.* **91,** 52–56.
3. Look, A. T. (1997) *Science* **278,** 1059–1064.
4. Pineault, N., Buske, C., Feuring-Buske, M., Abramovich, C., Rosten, P., Hogge, D. E., Aplan, P. D. & Humphries, R. K. (2003) *Blood* **101,** 4529–4538.
5. Kroon, E., Krosl, J., Thorsteinsdottir, U., Baban, S., Buchberg, A. M. & Sauvageau, G. (1998) *EMBO J.* **17,** 3714–3725.
6. Castilla, L. H., Garrett, L., Adya, N., Orlic, D., Dutra, A., Anderson, S., Owens, J., Eckhaus, M., Bodine, D. & Liu, P. P. (1999) *Nat. Genet.* **23,** 144–146.
7. Odero, M. D., Carlson, K., Calasanz, M. J., Lahortiga, I., Chinwalla, V. & Rowley, J. D. (2001) *Genes Chromosomes Cancer* **31,** 134–142.
8. Million, R. P., Aster, J., Gilliland, D. G. & Van Etten, R. A. (2002) *Blood* **99,** 4568–4577.
9. Schwaller, J., Frantsve, J., Aster, J., Williams, I. R., Tomasson, M. H., Ross, T. S., Peeters, P., Van Rompaey, L., Van Etten, R. A., Ilaria, R., Jr., *et al.* (1998) *EMBO J.* **17,** 5321–5333.
10. Tomasson, M. H., Sternberg, D. W., Williams, I. R., Carroll, M., Cain, D., Aster, J. C., Ilaria, R. L., Jr., Van Etten, R. A. & Gilliland, D. G. (2000) *J. Clin. Invest.* **105,** 423–432.
11. Iijima, Y., Okuda, K., Tojo, A., Tri, N. K., Setoyama, M., Sakaki, Y., Asano, S., Tokunaga, K., Kruh, G. D. & Sato, Y. (2002) *Oncogene* **21,** 4374–4383.
12. Wai, D. H., Knezevich, S. R., Lucas, T., Jansen, B., Kay, R. J. & Sorensen, P. H. (2000) *Oncogene* **19,** 906–915.
13. Golub, T. R., Barker, G. F., Bohlander, S. K., Hiebert, S. W., Ward, D. C., Bray-Ward, P., Morgan, E., Raimondi, S. C., Rowley, J. D. & Gilliland, D. G. (1995) *Proc. Natl. Acad. Sci. USA* **92,** 4917–4921.
14. Chase, A., Reiter, A., Burci, L., Cazzaniga, G., Biondi, A., Pickard, J., Roberts, I. A., Goldman, J. M. & Cross, N. C. (1999) *Blood* **93,** 1025–1031.
15. Peeters, P., Wlodarska, I., Baens, M., Criel, A., Selleslag, D., Hagemeijer, A., Van den Berghe, H. & Marynen, P. (1997) *Cancer Res.* **57,** 564–569.
16. Andreasson, P., Schwaller, J., Anastasiadou, E., Aster, J. & Gilliland, D. G. (2001) *Cancer Genet. Cytogenet.* **130,** 93–104.
17. Bernardin, F., Yang, Y., Cleaves, R., Zahurak, M., Cheng, L., Civin, C. I. & Friedman, A. D. (2002) *Cancer Res.* **62,** 3904–3908.
18. Wlodarska, I., Baens, M., Peeters, P., Aerssens, J., Mecucci, C., Brock, P., Marynen, P. & Van den Berghe, H. (1996) *Cancer Res.* **56,** 2655–2661.
19. Patel, N., Goff, L. K., Clark, T., Ford, A. M., Foot, N., Lillington, D., Hing, S., Pritchard-Jones, K., Jones, L. K. & Saha, V. (2003) *Br. J. Haematol.* **122,** 94–98.
20. Cools, J., Mentens, N., Odero, M. D., Peeters, P., Wlodarska, I., Delforge, M., Hagemeijer, A. & Marynen, P. (2002) *Blood* **99,** 1776–1784.
21. Penas, E. M., Cools, J., Algenstaedt, P., Hinz, K., Seeger, D., Schafhausen, P., Schilling, G., Marynen, P., Hossfeld, D. K. & Dierlamm, J. (2003) *Genes Chromosomes Cancer* **37,** 79–83.
22. Knoepfler, P. S. & Kamps, M. P. (1995) *Mol. Cell. Biol.* **15,** 5811–5819.
23. Shanmugam, K., Green, N. C., Rambaldi, I., Saragovi, H. U. & Featherstone, M. S. (1999) *Mol. Cell. Biol.* **19,** 7577–7588.
24. Buske, C., Feuring-Buske, M., Antonchuk, J., Rosten, P., Hogge, D. E., Eaves, C. J. & Humphries, R. K. (2001) *Blood* **97,** 2286–2292.
25. Buske, C., Feuring-Buske, M., Abramovich, C., Spiekermann, K., Eaves, C. J., Coulombel, L., Sauvageau, G., Hogge, D. E. & Humphries, R. K. (2002) *Blood* **100,** 862–868.
26. Feuring-Buske, M., Frankel, A. E., Alexander, R. L., Gerhard, B. & Hogge, D. E. (2002) *Cancer Res.* **62,** 1730–1736.
27. Pineault, N., Helgason, C. D., Lawrence, H. J. & Humphries, R. K. (2002) *Exp. Hematol.* **30,** 49–57.
28. Silberg, D. G., Sullivan, J., Kang, E., Swain, G. P., Moffett, J., Sund, N. J., Sackett, S. D. & Kaestner, K. H. (2002) *Gastroenterology* **122,** 689–696.
29. Brooke, N. M., Garcia-Fernandez, J. & Holland, P. W. (1998) *Nature* **392,** 920–922.
30. van den Akker, E., Forlani, S., Chawengsaksophak, K., de Graaff, W., Beck, F., Meyer, B. I. & Deschamps, J. (2002) *Development (Cambridge, U.K.)* **129,** 2181–2193.
31. Isaacs, H. V., Pownall, M. E. & Slack, J. M. (1998) *EMBO J.* **17,** 3413–3427.
32. Buske, C. & Humphries, R. K. (2000) *Int. J. Hematol.* **71,** 301–308.
33. Sauvageau, G., Lansdorp, P. M., Eaves, C. J., Hogge, D. E., Dragowska, W. H., Reid, D. S., Largman, C., Lawrence, H. J. & Humphries, R. K. (1994) *Proc. Natl. Acad. Sci. USA* **91,** 12223–12227.
34. Golub, T. R., Slonim, D. K., Tamayo, P., Huard, C., Gaasenbeek, M., Mesirov, J. P., Coller, H., Loh, M. L., Downing, J. R., Caligiuri, M. A., *et al.* (1999) *Science* **286,** 531–537.
35. Debernardi, S., Lillington, D. M., Chaplin, T., Tomlinson, S., Amess, J., Rohatiner, A., Lister, T. A. & Young, B. D. (2003) *Genes Chromosomes Cancer* **37,** 149–158.
36. Ferrando, A. A., Armstrong, S. A., Neuberg, D. S., Sallan, S. E., Silverman, L. B., Korsmeyer, S. J. & Look, A. T. (2003) *Blood* **102,** 262–268.
37. Yeoh, E. J., Ross, M. E., Shurtleff, S. A., Williams, W. K., Patel, D., Mahfouz, R., Behm, F. G., Raimondi, S. C., Relling, M. V., Patel, A., *et al.* (2002) *Cancer Cell* **1,** 133–143.
38. Thorsteinsdottir, U., Kroon, E., Jerome, L., Blasi, F. & Sauvageau, G. (2001) *Mol. Cell. Biol.* **21,** 224–234.
39. Lorentz, O., Duluc, I., Arcangelis, A. D., Simon-Assmann, P., Kedinger, M. & Freund, J. N. (1997) *J. Cell Biol.* **139,** 1553–1565.
40. Charite, J., de Graaff, W., Consten, D., Reijnen, M. J., Korving, J. & Deschamps, J. (1998) *Development (Cambridge, U.K.)* **125,** 4349–4358.
41. Subramanian, V., Meyer, B. I. & Gruss, P. (1995) *Cell* **83,** 641–653.
42. Margalit, Y., Yarus, S., Shapira, E., Gruenbaum, Y. & Fainsod, A. (1993) *Nucleic Acids Res.* **21,** 4915–4922.
43. Sauvageau, G., Thorsteinsdottir, U., Hough, M. R., Hugo, P., Lawrence, H. J., Largman, C. & Humphries, R. K. (1997) *Immunity* **6,** 13–22.
44. Taylor, J. K., Levy, T., Suh, E. R. & Traber, P. G. (1997) *Nucleic Acids Res.* **25,** 2293–2300.
45. Houde, M., Laprise, P., Jean, D., Blais, M., Asselin, C. & Rivard, N. (2001) *J. Biol. Chem.* **276,** 21885–21894.
46. Nucifora, G. (1997) *Leukemia* **11,** 2022–2031.

The *AML1-ETO* fusion gene and the *FLT3* length mutation collaborate in inducing acute leukemia in mice

Christina Schessl,[1,2] Vijay P.S. Rawat,[1,2] Monica Cusan,[1,2] Aniruddha Deshpande,[1,2] Tobias M. Kohl,[1,2] Patricia M. Rosten,[3] Karsten Spiekermann,[1,2] R. Keith Humphries,[3,4] Susanne Schnittger,[2] Wolfgang Kern,[2] Wolfgang Hiddemann,[1,2] Leticia Quintanilla-Martinez,[5] Stefan K. Bohlander,[1,2] Michaela Feuring-Buske,[1,2] and Christian Buske[1,2]

[1]Clinical Cooperative Group "Leukemia," National Research Center for Environment and Health (GSF), Munich, Germany. [2]Department of Medicine III, Grosshadern, Ludwig Maximilians University, Munich, Germany. [3]Terry Fox Laboratory, British Columbia Cancer Agency, Vancouver, British Columbia, Canada. [4]Department of Medicine, University of British Columbia, Vancouver, British Columbia, Canada. [5]Department of Pathology, GSF, Munich, Germany.

The molecular characterization of leukemia has demonstrated that genetic alterations in the leukemic clone frequently fall into 2 classes, those affecting transcription factors (e.g., *AML1-ETO*) and mutations affecting genes involved in signal transduction (e.g., activating mutations of *FLT3* and *KIT*). This finding has favored a model of leukemogenesis in which the collaboration of these 2 classes of genetic alterations is necessary for the malignant transformation of hematopoietic progenitor cells. The model is supported by experimental data indicating that *AML1-ETO* and *FLT3* length mutation (*FLT3-LM*), 2 of the most frequent genetic alterations in AML, are both insufficient on their own to cause leukemia in animal models. Here we report that *AML1-ETO* collaborates with *FLT3-LM* in inducing acute leukemia in a murine BM transplantation model. Moreover, in a series of 135 patients with AML1-ETO–positive AML, the most frequently identified class of additional mutations affected genes involved in signal transduction pathways including *FLT3-LM* or mutations of *KIT* and *NRAS*. These data support the concept of oncogenic cooperation between *AML1-ETO* and a class of activating mutations, recurrently found in patients with t(8;21), and provide a rationale for therapies targeting signal transduction pathways in AML1-ETO–positive leukemias.

Introduction

The cloning of recurring chromosomal translocations and, increasingly, the molecular characterization of point mutations in patients with acute leukemia have substantially contributed to the understanding of the pathogenesis of this disease. In acute myeloid leukemia (AML), chromosomal translocations most frequently target transcription factors involved in the regulation of normal hematopoietic differentiation, whereas point mutations often affect genes involved in signal transduction pathways associated with cell proliferation (1–3). The systematic analyses of genetic alterations in patients with AML have demonstrated that genetic lesions of more than 1 transcriptional regulator, such as *AML1-ETO* (*RUNX1-MTG8*), *HOX* fusion genes, or *PML-RARA*, rarely occur in the leukemic clone. Similarly, patients with concurrent mutations of *FLT3*, *KIT*, or *NRAS* are rare. However, there are numerous examples in which fusion genes are identified together with activating mutations of receptor tyrosine kinases, exemplified by *PML-RARA* and the *FLT3* length mutation (*FLT3-LM*), which occur together in up to 35% of all patients with t(15;17)–positive AML (4).

These observations have favored a model of pathogenesis of acute leukemia in which the 2 groups of genetic alterations, 1 affecting transcriptional regulation and hematopoietic differentiation, the other altering signal transduction cascades associated with cell proliferation, collaborate in inducing acute leukemia (5). This concept is supported by experimental data demonstrating that *AML1-ETO*, one of the most frequent fusion genes in AML, is not able, on its own, to induce leukemia in experimental in vivo models but requires additional mutations in yet unknown genes for induction of hematological disease. In a conditional AML1-ETO murine model, for example, only mice treated additionally with *N*-ethylnitrosourea (ENU) developed AML as well as T cell lymphoblastic lymphoma, whereas untreated AML1-ETO mice showed only minimal hematopoietic abnormalities (6). Similar observations were reported from an hMRP8–AML1-ETO transgenic mouse model, which developed AML as well as T–acute lymphoblastic leukemia/lymphoma (T-ALL/lymphoma) only after ENU mutagenesis (7), and from a murine BM transplantation model inducing constitutive expression of AML1-ETO in hematopoietic progenitor cells by retroviral gene transfer (8). In a recent report, mice targeted to express AML1-ETO in the HSC compartment developed a nonlethal long-latency myeloproliferative syndrome but failed to develop acute leukemia (9).

To test the hypothesis of oncogenic cooperation between different classes of mutations, we analyzed a series of 135 patients with AML1-ETO–positive AML for the occurrence of activating mutations involving signal transduction pathways (*FLT3-LM*, *FLT3D835*, *KITD816*, *NRAS* codon 12/13/61). Because almost one-third of all AML1-ETO–positive patients had such activating mutations, we asked whether AML1-ETO would be able to collaborate with 1 of

Nonstandard abbreviations used: ALL, acute lymphoblastic leukemia; AML, acute myeloid leukemia; B6C3, C57BL/6J × C3H/HeJ (mice); CBF, core-binding factor; CFU-S, colony-forming spleen unit(s); cy, cytoplasmic; ENU, *N*-ethylnitrosourea; FLT3-LM, FLT3 length mutation; GSF, National Research Center for Environment and Health; IRES, internal ribosomal entry site; KD, kinase dead; LTR, long-terminal repeat; MSCV, murine stem cell virus; PepC3, C57BL/6Ly-Pep3b × C3H/HeJ (mice); VCM, virus-containing medium; YFP, yellow fluorescent protein.

Conflict of interest: The authors have declared that no conflict of interest exists.

Citation for this article: *J. Clin. Invest.* **115**:2159–2168 (2005). doi:10.1172/JCI24225.

Table 1
Genetic alterations in patients with *AML1-ETO* rearrangement

	No. of patients analyzed	No. of patients with mutation detected
FLT3-LM	135	11 (8.1%)
FLT3D835	135	3 (2.2%)
KITD816	135	11 (8.1%)
NRAS codon 12/13/61	135	13 (9.6%)
FLT3, *KIT*, or *NRAS* mutation	135	38 (28.1%)
MLL-PTD	87	0

these alterations to induce leukemia. Here we demonstrated that retrovirally engineered coexpression of *AML1-ETO* and *FLT3-LM* potently synergizes to trigger the development of aggressive leukemia in a murine transplantation model.

This model will allow valuable insights into the pathogenesis of core-binding factor (CBF) leukemias and demonstrates, for the first time to our knowledge, the functional collaboration of AML1-ETO with a class of activating mutations frequently found in patients with t(8;21)–positive leukemia.

Results

AML1-ETO occurs frequently together with activating mutations involving signal transduction pathways in patients with AML. In order to characterize genetic alterations that occur together with the *AML1-ETO* fusion gene in AML, 135 patients with *AML1-ETO* (93 male, 42 female; median age 50.9, range 15.8–89.1) were screened for activating mutations in the receptor tyrosine kinases *FLT3* and *KIT* as well as in *NRAS* (*KITD816*, *NRAS* codon 12/13/61). Patients included 118 with newly diagnosed AML, 4 in first relapse, and 13 classified as having therapy-related AML. Activating mutations were detected in 38 patients (28.1%) and included mutations in the receptor tyrosine kinase *FLT3* or *KIT* (25 patients in total) or in *NRAS* (13 patients). In contrast, no *MLL-PTD* (partial tandem duplication) mutations were detected in 87 samples subjected to this analysis (Table 1). These data demonstrate that genetic alterations occurring with the *AML1-ETO* fusion gene frequently affect signal transduction pathways.

AML1-ETO cooperates with FLT3-LM in inducing acute leukemia in transplanted mice. To test the functional significance of the association of AML1-ETO with mutations involving critical signal transduction cascades, we used the murine BM transplantation model. Murine stem cell virus–based (MSCV-based) retroviral constructs carrying the AML1-ETO cDNA upstream of an internal ribosomal entry site–green fluorescent protein (IRES-GFP) cassette or the FLT3-LM cDNA upstream of an IRES–yellow fluorescent protein (IRES-YFP) cassette were generated to transduce and track hematopoietic cells expressing AML1-ETO (GFP^+), FLT3-LM (YFP^+), or both AML1-ETO and FLT3-LM (GFP^+/YFP^+) in vitro and in vivo (Figure 1). In order to investigate the impact of expression of AML1-ETO or FLT3-LM individually on primary primitive hematopoietic progenitor cells, we performed the colony-forming spleen assay (CFU-S). BM cells transduced with the *AML1-ETO*/GFP or *FLT3-LM*/YFP vector or both vectors were highly purified 96 hours after the start of infection by FACS. Their ability to form spleen colonies (day 0 equivalent) was measured by transplantation of transduced cells after purification into lethally irradiated recipient mice and quantification of spleen colony formation 12 days after injection. Constitutive expression of FLT3-LM did not increase the CFU-S content compared with the GFP control. In contrast, AML1-ETO increased the CFU-S content 3.1-fold compared with the control ($P < 0.002$). Strikingly, coexpression of FLT3-LM together with AML1-ETO increased CFU-S numbers a further 2.1-fold for a net increase of 6.5-fold CFU-S compared with the control ($P < 0.013$), thus demonstrating functional collaboration of these 2 genetic alterations in enhancing the CFU-S frequency (Figure 2A). In an effort to characterize the domains responsible for the collaboration of the 2 aberrations, an FLT3-LM and an AML1-ETO mutant were generated: the FLT3-LM mutant with loss of its kinase activity (kinase dead [KD]) (FLT3-LM-KD) and the AML1-ETO mutant with an L148D point mutation in the Runx1 domain of AML1-ETO (AML1-ETO-L148D), previously reported to lack DNA-binding activity. Expression of the constructs was tested by Western blot and FACS analysis, and FLT3-LM-KD was also tested for autophosphorylation as a surrogate marker for kinase activity and for its capacity to induce IL-3–independent growth in Ba/F3 cells (Figure 1, B, D, F, and G). Of note, AML1-ETO-L148D was not able to collaborate with FLT3-LM. Furthermore, the collaboration between AML1-ETO and FLT3-LM was dependent on the kinase activity of FLT3, as FLT3-LM-KD did not collaborate with the fusion gene (Figure 2A). Inhibition of the kinase activity of FLT3-LM by the protein tyrosine kinase (PTK) inhibitor PKC412 was tested in a ΔCFU-S assay after 48 hours of incubation with the inhibitor. The compound induced a 62% reduction of the day 0 equivalent of the CFU-S frequency (42 versus 16 per 1×10^5 initiating BM cells) of cells cotransfected with *FLT3-LM* and *AML1-ETO* compared with the untreated control, whereas the CFU-S frequency of cells infected with the GFP control vector was unchanged by the inhibitor (Figure 2B).

To further assess the potential collaboration of AML1-ETO with FLT3-LM, we carried out long-term BM transplantation studies using BM transduced with *AML1-ETO* or *FLT3*-LM alone or with both together. Over an observation period extending to 20.6 months, no disease developed in recipients of BM singly transduced with *AML1-ETO* (3×10^5 to 4×10^5 highly purified GFP^+ cells; $n = 9$) or *FLT3-LM* (7×10^4 to 2×10^5 highly purified YFP^+ cells together with 3×10^5 to 1×10^6 nontransduced helper cells; $n = 9$). To obtain mice engrafted with AML1-ETO/FLT3-LM–coexpressing BM cells, mice were injected with a mixture of GFP^+/YFP^+ cells (range 1×10^3 to 5.5×10^4 cells) and nontransduced normal BM cells (range 2.3×10^5 to 1.9×10^6). All recipients of doubly transduced BM ($n = 11$ from 5 independent experiments) succumbed to an aggressive acute leukemia after a median latency time of 233 days post-transplantation (Figure 3). These mice were engrafted with GFP/YFP–coexpressing cells that were positive for AML1-ETO and FLT3-LM transcripts in the RT-PCR analysis (Figure 1C). At diagnosis the mice were moribund, cachectic, and short of breath and suffered from splenomegaly (median spleen weight 441 mg) (Table 2). Peripheral blood and BM contained a high proportion of blasts, and peripheral blood wbc counts were highly elevated in 5 of 11 animals (range 2×10^6 to 430×10^6 cells/ml) compared with the GFP control (range 3.5×10^6 to 9×10^6) (Table 2), consistent with a diagnosis of acute leukemia. Additionally, mice were anemic, with a 45% reduction in erythrocyte counts compared with the mean count in the control.

Coexpression of AML1-ETO and FLT3-LM causes both acute myeloblastic and lymphoblastic leukemia. In 7 animals the morphology of the blasts was myeloblastic (Figure 4A), whereas 4 animals were characterized by a lymphoblastic cell population (Figure 4, B and C, and Table 2). In 2 of the 7 animals with AML (mice nos. 16 and 24) the blast population was accompanied by a dominant mast cell

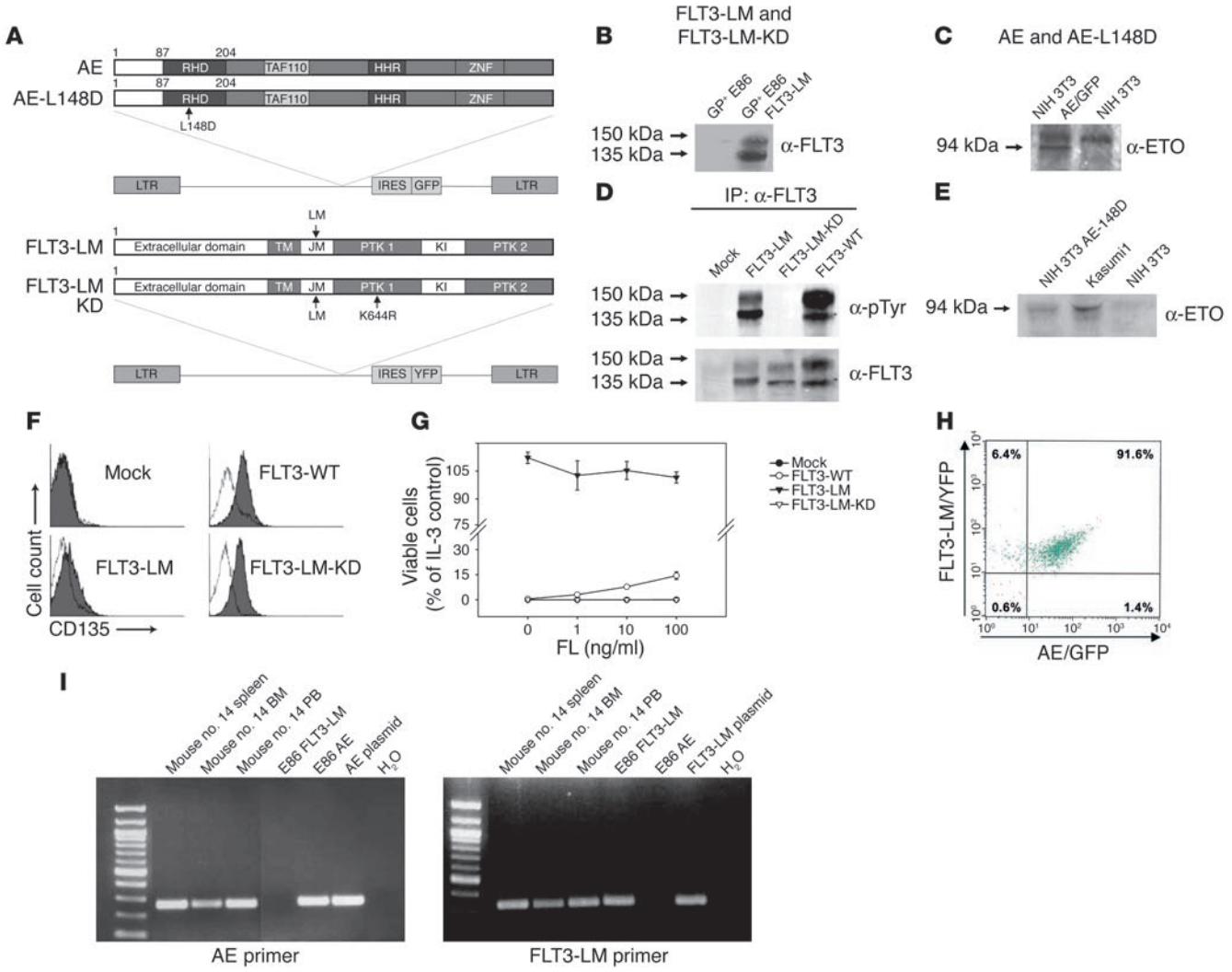

Figure 1

Schematic diagram and analysis of expression of different constructs. (**A**) Retroviral constructs for expression of AML1-ETO and of the AML1-ETO-L148D (31, 47), FLT3-LM, and FLT3-LM-KD mutant proteins. The GFP vector served as a control. AE, AML1-ETO; LTR, long-terminal repeat; RHD, runt homology domain; TAF110, TATA-binding protein–associated factor 110; HHR, hydrophobic heptad repeat; ZNF, zinkfinger; TM, transmembrane; JM, juxtamembrane; PTK, protein tyrosine kinase; KI, kinase insert. (**B**, **C**, and **E**) Western blot analysis of cellular extracts from GP+ E86 and NIH 3T3 cells transfected with the different constructs (the molecular mass is indicated). Kasumi cells served as a positive control. (**D**) α-pTyr plot demonstrating phosphorylation of FLT3-LM and FLT3-WT but not of FLT3-LM-KD. (**F**) FACS analysis of Ba/F3 cells transduced with the FLT3 constructs. (**G**) Growth of IL-3–dependent Ba/F3 cells infected with the different constructs. (**H** and **I**) Flow cytometry and RT-PCR analysis of cells coexpressing FLT3-LM/YFP and AML1-ETO/GFP, isolated from a representative leukemic mouse. FL, FLT3 ligand; PB, peripheral blood.

population with fine metachromatic granulation in the panoptic staining (Figure 4A). The BM and spleen were infiltrated with up to 80% and 80% blasts, respectively, in the mice with AML and up to 85% and 95%, respectively, in the mice suffering from ALL (Table 2 and Figures 4 and 5).

In order to determine more precisely the immunophenotype of the leukemic population, flow cytometric analyses from BM cells were performed. Seven animals suffered from AML with a Gr-1/Mac-1–positive cell population in the transduced compartment, which coexpressed Sca-1 (45.2%, range 19–73%). Of note, in 4 of the 7 animals with AML, coexpression of CD4 was detected in 21%, 27%, 31%, and 32% of BM cells (animals nos. 15, 16, 22, and 23, respectively; Table 2). Three mice suffered from B-lymphoblastic leukemia, with 90.4% of the transduced cells expressing B220 (range 85–97%) and lacking expression of myeloid antigens (Gr-1–positive 1.5%, range 0.4–2.3%; Mac-1–positive 1.7%, range 1.4–1.9%). One animal developed T cell leukemia, with coexpression of CD4 and CD8 (99% $CD8^+$, 86% $CD4^+$ in the transduced compartment) and expression of Sca-1 in 76% of all cells (Figure 4C). Histological tissue sections and immunohistochemistry were performed in 2 diseased mice with AML, including 1 of the animals with an increase in mast cells in the peripheral blood (mouse no. 16). Both animals showed multiple-organ infiltration into hematopoietic and nonhematopoietic organs with effacement of the normal follicular architecture of the spleen (Figure 5, D and E [right side]) and an infiltration with leukemic blasts in the liver and spleen (Figure 5, A–D and F). Immunohistochemistry

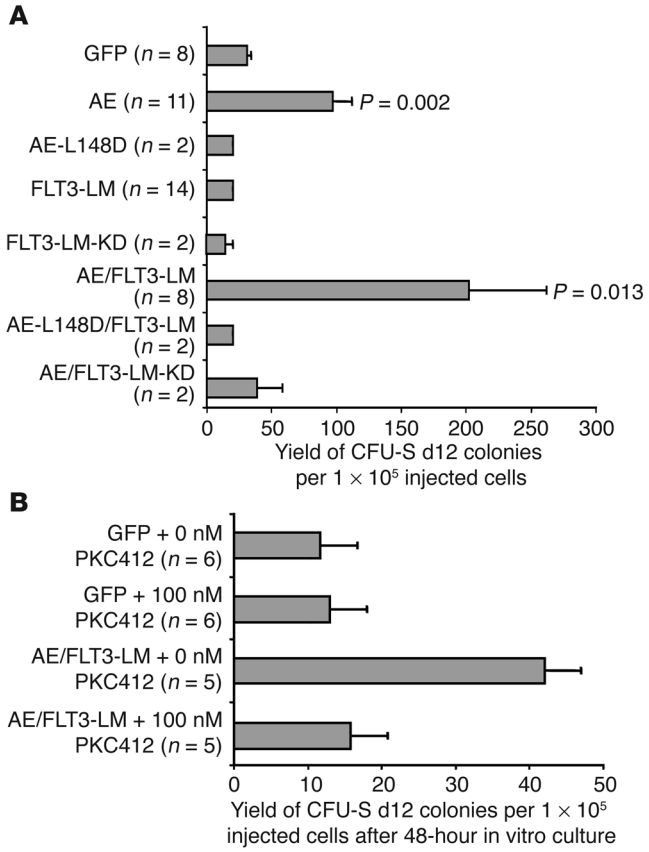

Figure 2
Analyses of CFU-S frequencies. (**A**) Primary BM cells retrovirally transduced with GFP, AML1-ETO, AML1-ETO-L148D, FLT3-LM, or FLT3-LM-KD vectors or with combinations of the different vectors were isolated by FACS 48 hours after infection and injected into lethally irradiated mice to assess initial (day 0) CFU-S numbers. CFU-S frequency per 1×10^5 initiating BM cells was determined in 3 independent experiments. The number of analyzed mice and the *P* value compared with the GFP control are indicated. (**B**) CFU-S frequency of primary BM cells infected with GFP or with both AML1-ETO and FLT3-LM and treated with the inhibitor PKC412 for 48 hours compared with untreated controls.

confirmed the diagnosis of AML: blasts were positive for myeloperoxidase but showed differentiation into more mature myeloid cells with positivity for chloracetatesterase (mouse no. 14; Table 2 and Figure 5, B, C, and F). In the second mouse with AML, infiltration of organs with cells expressing mast cell–specific tryptase and CD117 could be confirmed in the primarily and secondarily transplanted mouse, indicating the presence of a malignant infiltrating mast cell population in this animal (mouse no. 16).

The leukemias were readily transplantable and had the same histomorphology within 106 days after transplantation (median survival 68 days, range 57–106 days; $n = 5$) (Figure 3 and Figure 5, G–O). Southern blot analyses of BM from leukemic mice revealed modest numbers of proviral integrations, consistent with double infection and monoclonal or, at most, oligoclonal disease (Figure 6A). Monoclonal or oligoclonal disease is consistent with the relatively small transplant doses used but could also reflect a possible contribution of retroviral insertional mutagenesis to the transformation process. To further explore this latter possibility, 10 retroviral integration sites were subcloned and sequenced from 4 leukemic mice; all 10 sites were unique, and thus there was no indication of a common integration site associated with the leukemic transformation. Moreover, 5 sites were intergenic or not linked to known genes. The remaining sites were in introns in a 5′ to 3′ orientation most likely to lead to gene knock down rather than activation (Figure 6B and Table 3).

Since we observed coexpression of CD4 in leukemic cells of the majority of mice who developed AML in our model, we analyzed expression of CD4 and cytoplasmic (cy) CD3 in patients with AML1-ETO–positive AML; 17 of 52 patients analyzed (32.7%) and 39 of 50 patients analyzed (78%) were positive for CD4 or cyCD3, respectively. Furthermore, 31 of 52 patients (59.6%) expressed the B cell antigen CD19, 27 of 52 patients cyCD22 (51.9%), and 38 of 39 patients cyCD79a (97.4%) (Figure 7). There was no difference in the extent of coexpression of lymphoid antigens in AML1-ETO–positive AML with additional activating mutations of *FLT3*, *KIT*, and *NRAS* ($n = 14$) versus cases without this class of mutations ($n = 38$) (data not shown). This indicates that coexpression of lymphoid and myeloid antigens in myeloblastic leukemia, which is detected in the murine model, is a common characteristic in patients with AML1-ETO–positive AML.

Discussion

The translocation t(8;21)(q22;q22), which generates the AML1-ETO fusion gene, is one of the most frequent chromosomal translocations, detected in 12% of all AML patients and in up to 40% of FAB-M2 AML patients (10, 11). The translocation targets *AML1* (*RUNX1*), a member of the RUNX family characterized by a DNA-binding *Runt* domain at the amino terminus that is retained in the fusion gene (12). This domain is necessary for DNA binding and heterodimerization of AML1 with CBFB, the non–DNA-binding subunit of the complex. As predicted by the discovery that the *AML1* gene is rearranged in human hematopoietic disease, the AML1/CBFB complex was shown to be a key regulator of definitive hematopoiesis, and loss of either of these genes resulted in embryonic lethality with complete lack of definitive HSCs (13). In addition, it was recently reported that $AML1^{+/-}$ adult mice suffer from a 50% reduction of long-term repopulating stem cells (14). Although it is yet not fully understood how the

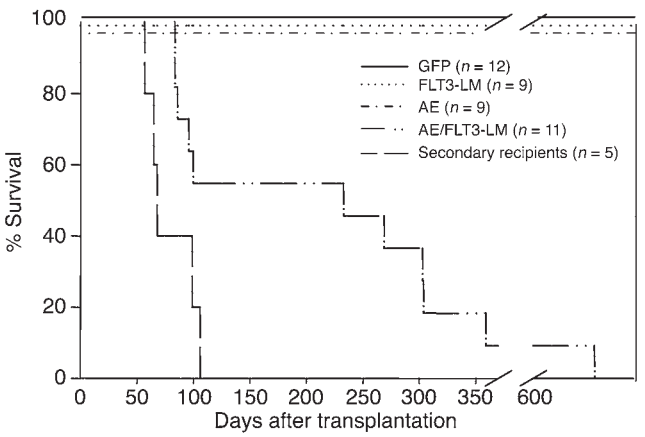

Figure 3
Survival of transplanted mice. Survival curve of mice transplanted with BM cells expressing AML1-ETO ($n = 9$), FLT3-LM ($n = 9$), or GFP ($n = 12$), of mice transplanted with marrow cells coexpressing AML1-ETO and FLT3-LM ($n = 11$), and of secondarily transplanted mice ($n = 5$).

Table 2
Hematological parameters of analyzed experimental mice

Mouse no.	Retroviral construct	Day of sacrifice	rbc/ml $\times 10^9$	wbc/ml $\times 10^6$	Spleen size (mm)	Spleen weight (mg)	BM % blasts	Spleen % blasts	PB % blasts
1	GFP	ND	4.8	7.6	ND	ND	1	0	0
2	GFP	ND	6.4	8.1	ND	ND	0	0	0
3	GFP	90	7	5	14 × 4	51	2	0	0
4	GFP	ND	5.4	9	ND	ND	0	0	0
5	GFP	689	5.6	4.5	15 × 4	78	0	0	0
6	GFP	721	7.25	3.5	ND	ND	3	0	0
7	AE	444	6	13	13 × 3.5	63	8	0	0
8	AE	479	3.1	15	14 × 4	60	11	0	0
9	AE	493	5.7	6.9	14 × 4	82	2	0	0
10	AE	615	5	7.6	16 × 5	117	14	0	0
11	FLT3-LM	88	4.5	10	15 × 4	95	4	ND	0
12	FLT3-LM	ND	4.5	13	ND	ND	2	ND	0
13	FLT3-LM	ND	5.6	8.3	ND	ND	1	ND	0
14[A]	AE/FLT3-LM	233	ND	23	27 × 7	600	80	52	20
15[A]	AE/FLT3-LM	100	0.85	26.5	19 × 6	166	48	80	75
16[A]	AE/FLT3-LM	612	1.7	12.5	14 × 4	118	20	50	25
17[B]	AE/FLT3-LM	84	ND	430	24 × 9	572	80	22	60
18[B]	AE/FLT3-LM	84	4.4	3.3	21 × 7	270	85	43	62
19[B]	AE/FLT3-LM	94	7.7	7.2	12 × 4	ND	85	20	95
20[B]	AE/FLT3-LM	96	3.8	60	21 × 6	310	40	95	60
21[A]	AE/FLT3-LM	269	4	2	28 × 9	650	38	62	30
22[A]	AE/FLT3-LM	303	2.6	10	15 × 3	200	24	76	38
23[A]	AE/FLT3-LM	304	2.6	2.5	29 × 10	1,400	27	55	78
24[A]	AE/FLT3-LM	359	2.5	35	28 × 9	760	39	77	64

[A]AML; [B]ALL. PB, peripheral blood; ND, not determined; AE, AML1-ETO.

AML1-ETO fusion gene contributes to leukemogenesis, it is thought that 1 key mechanism is the suppression of AML1- and C/EBPα-dependent activation of genes responsible for myeloid development (15, 16). Perturbation of hematopoiesis by expression of *AML1-ETO* results in an increase in the replating capacity of murine clonogenic progenitors and in the growth of primitive human progenitor cells in vitro (6, 17). Furthermore, in vivo and ex vivo analyses demonstrated alterations in the differentiation pattern and proliferative capacity of murine hematopoietic cells expressing the fusion gene (8, 9, 18, 19). However, numerous murine in vivo models documented that *AML1-ETO* on its own is not able to induce leukemia (6, 7, 9, 18, 19). The observation that *AML1-ETO* as a single factor is nonleukemogenic is further supported by findings that nonleukemic *AML1-ETO*–expressing progenitor cells can be isolated from healthy individuals as well as AML patients in remission, which suggests that additional mutations in these AML1-ETO–positive progenitors are necessary for the transformation into leukemia-initiating cells (20–22). The importance of collaborating genetic events in the pathogenesis of AML1-ETO–positive leukemias has indeed been shown in different murine models, such as a conditional *AML1-ETO* murine model as well as an hMRP8–*AML1-ETO* transgenic mouse model. Only mice treated additionally with ENU developed AML or T cell lymphoma (6, 7). Furthermore, retrovirally expressed *AML1-ETO* induced myeloblastic transformation in vivo only in a background deficient in the IFN-regulatory factor IFN consensus sequence-binding protein (18). These data strongly suggest that genetic alterations cooperating with *AML1-ETO* play a role in inducing leukemia.

In order to characterize genetic alterations that potentially collaborate with *AML1-ETO*, we screened 135 patients with AML for activating mutations of signal transduction pathways or mutations affecting the *MLL* gene. Whereas *MLL-PTD* mutations, which exemplify genetic alterations involved in transcriptional regulation, were not found at all, 28% of the patients were positive for activating mutations such as *FLT3-LM*, *FLT3D835*, *KITD816*, or *NRAS*. The frequent coexistence of such mutations with *AML1-ETO* fits well in the model of leukemogenesis in which the collaboration of 2 classes of genetic alterations, 1 affecting transcription factors associated with hematopoietic differentiation, the other affecting signal transduction pathways associated with cell proliferation, is necessary for the malignant transformation of hematopoietic progenitor cells (3). Using the murine BM transplantation model, we obtained direct evidence for a functional collaboration of *AML1-ETO* with *FLT3-LM* in inducing leukemia, supporting the aforementioned model of leukemogenesis. Furthermore, these data demonstrate the collaboration of the 2 most frequent genetic alterations in AML, providing an important model for the understanding of both the AML1-ETO–positive and the FLT3-LM–positive leukemias.

Of note, 4 of 7 AML mice reported here expressed the T cell antigen CD4. Although the mechanisms underlying the coexpression of myeloid and lymphoid antigens in AML1-ETO–positive myeloid leukemia are not clear, one possibility is that in this AML subtype an early progenitor cell with a lineage-overlapping mixed phenotype is the target of leukemogenic transformation, as recently proposed for hematological malignancies (23). Of note, it was recently demonstrated that, in AML1-ETO–positive leukemia, evidence of lineage overlap is not restricted to the expression of cytoplasmic or surface antigens but extends to the transcriptional apparatus, since *PAX5* is selectively expressed in one-third of patients with t(8;21) AML in

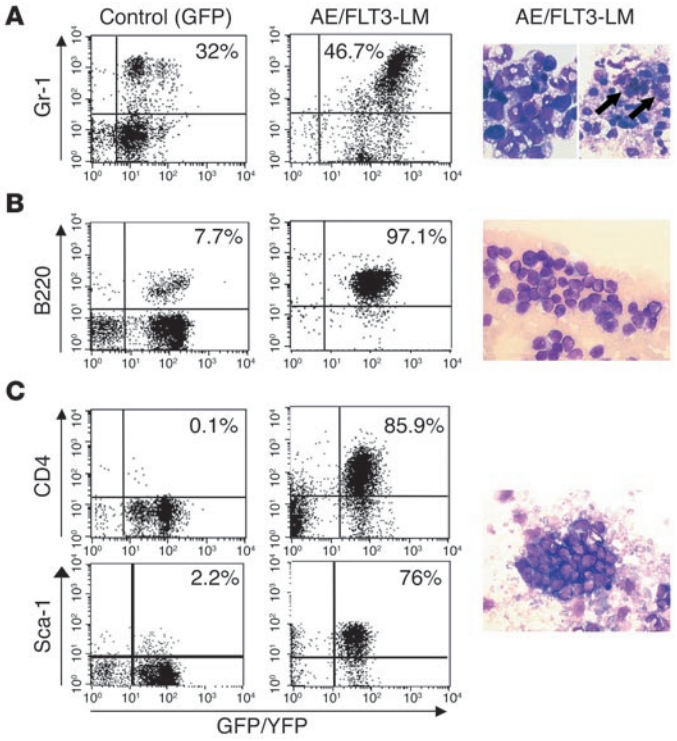

Figure 4
Immunophenotype and morphology of hematopoietic cells recovered from leukemic mice. The plots show representative FACS profiles from BM cells in comparison with cells from GFP control animals, with indication of the proportion of positive cells within the GFP^+/YFP^+ compartment. The photographs show cytospin preparations (H&E; magnification, ×630) from peripheral blood (**A**, right image; **B** and **C**) and from BM (**A**, left image). (**A**) AML with a dominant mast cell population (marked by arrows) (mouse no. 16). (**B**) B-ALL (mouse no. 17). (**C**) T-ALL (mouse no. 20).

contrast to all other cytogenetically defined AML subtypes (24). Furthermore, both myeloblastic and lymphoblastic leukemias of B and T cell type developed in this model of *AML1-ETO* and *FLT3-LM* cooperation. This observation was also reported in other murine models: in a conditional *AML1-ETO* murine model, mice treated additionally with ENU developed AML as well as T cell lymphoblastic lymphoma, although most of the T cell neoplasms did not express the fusion gene (6). Similar observations were reported from an hMRP8–*AML1-ETO* transgenic mouse model, which developed AML as well as T-ALL/lymphoma after ENU treatment (7). In addition, expression of *AML1-ETO* might contribute to the lymphoid phenotype of the leukemias in our model, as it was reported that *FLT3-LM* is able to induce a long-latency T cell lymphoma–like disease in the C57BL/C3H background (25). However, the association of *FLT3-LM* with a lymphoid disease seems to depend on the genetic background of the mouse strain, as *FLT3-LM* induced a myeloproliferative syndrome in BALB/c mice (26). In our model, also using the C57BL/C3H background, constitutive expression of *FLT3-LM* alone did not induce any perturbation of the hematopoietic development in vivo; this result was also recently reported in a mouse model of collaboration of *FLT3-LM* with *MLL-SEPT6* using the C57BL/6 strain (27).

Of note, overexpression of FLT3 and activating FLT3 mutations are associated with ALL in humans, in particular in cases of ALL with hyperdiploidy or *MLL* rearrangement, characterized by a primitive B cell or a mixed lymphoid-myeloid phenotype (28–30). The observations that ETV6-PDGFBR, which already by itself causes a lethal myeloproliferative syndrome in transplanted mice, induces exclusively a myeloblastic leukemia when coexpressed with *AML1-ETO* might point to the importance of the collaborating partner for the phenotype of the induced leukemia (31). Another possible explanation for the development of lymphoid malignancies in our model is that, in individual mice, lymphoid-committed stages of differentiation were hit by the retrovirus, resulting in lymphoblastic leukemia in these animals. This would potentially be a key difference from the human situation, in which both *AML1-ETO* and *FLT3-LM* are already present in the HSC pool (21, 32). An important question is whether the results were influenced by retroviral insertional mutagenesis. Most of the leukemic animals were transplanted with a low transplant dose and then suffered from monoclonal or oligoclonal disease. Although the number of retroviral integration events was low in the mice, insertional mutagenesis might have contributed to the leukemogenesis. However, analyses of the retroviral integration sites in the diseased animals showed integration into intergenic regions or introns of genes, more likely resulting in their knock down than in their activation. These data suggest that retroviral insertional mutagenesis might not play the key part in disease development, an issue that might be more accurately addressed in mouse models expressing *AML1-ETO* from an endogenous promoter. The long latency of the leukemias, even of secondary disease, however, strongly argues that additional secondary in vivo genetic events in the animals contributed to disease development.

To our knowledge, this is the first functional evidence of a leukemogenic collaboration of *AML1-ETO* with a complementary class of mutation, recurrently found in patients with t(8;21). It facilitates our understanding of acute leukemias associated with 2 of the most frequent genetic alterations in this disease. Furthermore, our experimental data support recent reports that show the functional relevance of activating mutations in patients with CBF leukemias [*AML1-ETO* or *CBFB-MYH11*] by demonstrating a significantly shortened overall and event-free survival for AML1-ETO–positive leukemias harboring activating mutations of *FLT3* or *KIT* compared with those without these mutations. In contrast, *RAS* mutations did not affect the treatment outcome (S. Schnittger, unpublished observations) (33, 34). In line with these findings, it was recently shown that in patients with AML1-ETO–positive leukemia, most leukemic cells at diagnosis additionally harbored mutations in *KIT*, whereas in 3 patients analyzed in complete remission, only the fusion gene, but not the *KIT* mutation, could be detected by PCR; this strongly supports the concept of a stepwise development of disease involving 2 collaborating genetic aberrations (35). These observations encourage the systematic screening of activating mutations in patients with CBF leukemias in prospective clinical trials to evaluate more precisely their prognostic impact, and they form a rationale to consider treatment strategies targeting the signal transduction apparatus in this AML subtype.

Methods

Patient samples. BM samples from 135 adult patients with newly diagnosed AML — de novo AML (n = 118), secondary AML after treatment of a previous malignancy (n = 13), and AML at relapse (n = 4) — were analyzed. The diagnosis of AML was performed according to the French-American-British criteria and the WHO classification (36, 37). Cytomorphology, cytochemistry, cytogenetics, and molecular genetics were applied in all cases

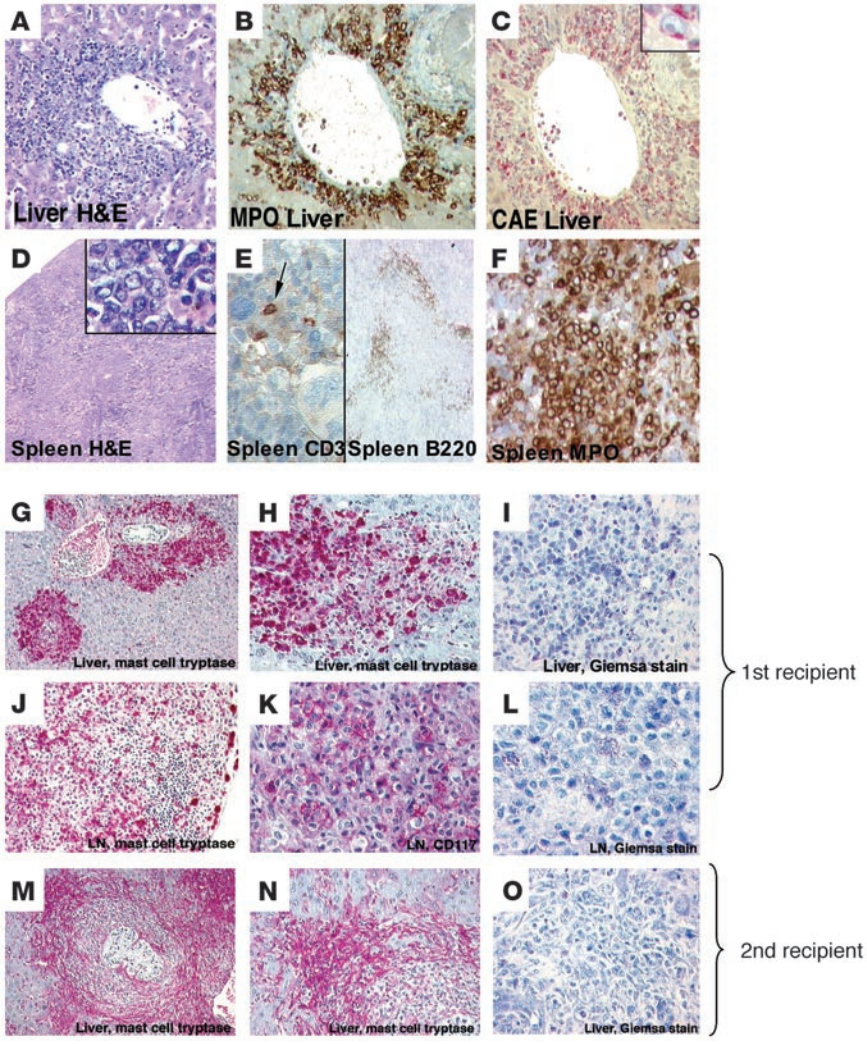

Figure 5
Histological analyses of leukemic mice. (**A**–**F**) Histological analyses of AML (mouse no. 14). Original magnifications: **A**–**C**, ×200; inset in **C**, ×1,000; **D** and right side of **E**, ×250; inset in **D**, ×650; left side of **E**, ×400; **F**, ×400. (**G**–**O**) Histological analyses of AML with a dominant mast cell population (mouse no. 16). (**G**–**L**) Primary recipient. (**M**–**O**) Secondary recipient. Original magnifications: **G** and **M**, ×100; **H**, **J**, and **N**, ×200; **I**, **K**, and **O**, ×400; **L**, ×600. Mast cells with metachromatic granulation in the Giemsa stain are indicated by an arrow. MPO, myeloperoxidase; CAE, *N*-acetyl-chloroacetate esterase.

as described below. Both animal and human studies were approved by the Ethics Committee of Ludwig Maximilians University and abided by the tenets of the revised World Medical Association Declaration of Helsinki (http://www.wma.net/e/policy/b3.htm).

Cytogenetic and FISH analysis. Cytogenetic analyses were performed using standard techniques. For FISH, a commercially available AML1-ETO probe was used according to the manufacturer's instructions (Vysis Inc.) (38).

PCR. Molecular genetic analysis for *AML1-ETO* (38), *MLL-PTD* (39), *FLT3-LM* (4), *NRAS* mutations, *FLT3D835*, and *KITD816* (40) in patient samples was performed as has been described previously (41). In leukemic mice, expression of AML1-ETO and FLT3-LM was assessed by RT-PCR in animals transplanted with BM cells coexpressing AML1-ETO/GFP and FLT3-LM/YFP. Preparation of cDNA was performed as previously described (41). For AML1-ETO the primer forward 5′-ATGACCTCAGGTTTGTCGGTCG-3′ and the primer reverse 5′-TGAACTGGTTCTTGGAGCCTCCT-3′ (corresponding to positions nucleotide 395 and nucleotide 633 of GenBank accession number D13979, respectively) were used; for *FLT3-LM* the primer forward 5′-GCAATTTAGGTATGAAAGCCAGC-3′ and the primer reverse 5′-CTTTCAGCATTTT-GACGGCAACC-3′ (corresponding to positions nucleotide 1,704 and nucleotide 1,920 of GenBank accession number NM_004119, respectively) were used. The annealing temperature was 57°C. The number of PCR cycles for each gene was chosen to stop the reaction in the linear phase of amplification (35 cycles for AML-ETO and FLT3-LM). The integrity of the RNA in all samples was confirmed by mβ-2 microglobulin RT-PCR.

For the linker-mediated PCR (LM-PCR), integrated long-terminal repeats (LTRs) and flanking genomic sequences were amplified and then isolated using a modification of the bubble LM-PCR strategy (42, 43). Aliquots of the cell lysates from leukemic mice were digested with *Pst*I or *Ase* (New England Biolabs Inc.), and the fragments were ligated overnight at room temperature to a double-stranded bubble linker (5′-CTCTCCCTTCTCGAATCGTAACCGTTCG-TACGAGAATCGCTGTCCTCTCCTTG-3′ and 5′-ANTCAAGGAGAGGACGCTGTCTGTCGAAGG-TAAGGAACGGACGAGAGAAGGGAGAG-3′). Next, a first PCR (PCR-A) was performed on 10 μl (one-tenth) of the ligation product using a linker-specific Vectorette primer (5′-CGAATCGTAACC-GTTCGTACGAGAATCGCT-3′) (Invitrogen Corp.) and an LTR-specific primer (LTR-A: 5′-CAACACA-CACATTGAAGCACTCAAGGCAAG-3′) under the following conditions: 1 cycle of 94°C for 2 minutes, 20 cycles of 94°C for 30 seconds and 65°C for 1 minute, and 1 cycle of 72°C for 2 minutes. The bubble linker contains a 30-nucleotide nonhomologous sequence in the middle region that prevents binding of the linker primer in the absence of the minus strand generated by the LTR-specific primer. A 1-μl aliquot of the PCR-A reaction (one-fifteenth) was then used as a template for a second nested PCR (PCR-B) using an internal LTR-specific primer (LTR-B: 5′-GAGAGCTCCCAGGCTCA-GATCTGGTCTAAC-3′) and the same linker-specific Vectorette primer as was used in PCR-A, with the following conditions: 1 cycle of 94°C for 2 minutes, 30 cycles of 94°C for 60 seconds and 72°C for 1 minute, and 1 cycle of 72°C for 2 minutes. Ten microliters (one-half) of the final PCR-B product was electrophoresed using 2% agarose tris-acetate-EDTA gel. Individual bands were excised and purified using the QIAEX II Gel Extraction Kit (QIAGEN) and then cloned into PCR2.1 (Invitrogen Corp.) before sequencing of the integration site of the retrovirus.

Multiparameter flow cytometry. Immunophenotypic analyses were performed as previously described (44). The following combinations of antibodies were used: CD34/CD2/CD33, CD7/CD33/CD34, CD34/CD56/CD33, CD11b/CD117/CD34, CD64/CD4/CD45, CD34/CD13/CD19, CD65/CD87/CD34, CD15/CD34/CD33, HLA-DR/CD33/CD34, CD4/CD13/CD14, CD34/CD135/CD117, CD34/CD116/CD33, CD90/CD117/CD34, CD34/NG2(7.1)/CD33, CD38/CD133/CD34, CD61/CD14/CD45,

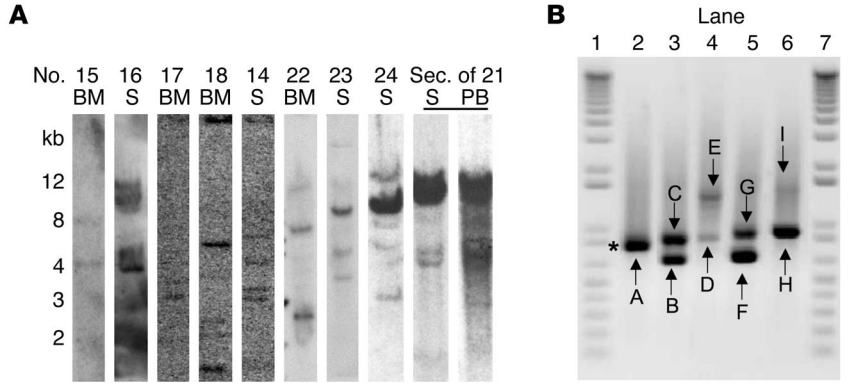

Figure 6
Analysis of proviral integrations. (**A**) Southern blot analysis of genomic DNA from different primary mice and a secondary recipient to detect clonal proviral integrations. DNA was digested with *Eco*RI, which cuts once in the proviral sequence, and blots were hybridized to a GFP/YFP probe. The mouse numbers are indicated (corresponding to those in Table 2). S, spleen; PB, peripheral blood; sec. of 21, second mouse of 1° mouse no. 21. (**B**) Bubble PCR analyses of retroviral integration sites in diseased mice. The bands (A–I) were isolated, subcloned, and sequenced. A description of the PCR products is given in Table 3. Asterisk indicates resolution as 2 unique bands after subcloning and sequencing of integration sites.

CD36/CD235a/CD45, CD15/CD13/CD33, CD9/CD34/CD33, CD38/CD34/CD90, CD34/CD79a/CD19, TdT/cyCD33/cyCD45, myeloperoxidase/lactoferrin/cyCD15, TdT/cyCD79a/cyCD3, and TdT/cyCD22/cyCD3. All antibodies were purchased from Beckman Coulter Inc., except for CD64 and CD15 (Medarex Inc.), CD133 (Miltenyi Biotec), and myeloperoxidase and lactoferrin (CALTAG Laboratories). For the analysis of cytoplasmic antigens, cells were fixed and permeabilized before staining with FIX & PERM (CALTAG Laboratories). Multiparameter flow cytometry analysis was performed with a FACSCalibur flow cytometer (BD).

The purity of all samples was 80–100%. Furthermore, immunophenotyping was performed with triple staining in all cases as indicated above, testing simultaneous expression of myeloid and lymphoid antigens to exclude contaminating normal lymphoid cells.

In mice, immunophenotypic analysis of single-cell suspensions from BM, spleen, and peripheral blood was performed by flow cytometry (FACSCalibur cytometer; BD) using PE-labeled Sca-1, Gr-1, Ter-119, and CD4 antibodies and allophycocyanin-labeled Mac-1, Kit, B220, and CD8 antibodies (all from BD Biosciences — Pharmingen), as previously described (45). The surface expression of the FLT3-LM construct and the FLT3-LM-KD mutant of Ba/F3 cells was confirmed by FACS analysis (Figure 2B) using anti–human CD135–PE mAb (BD) and an isotype-matched IgG1-PE control (Beckman Coulter Inc.).

cDNA constructs and retroviral vectors. For retroviral gene transfer into primary BM cells, AML1-ETO cDNA was subcloned into the multiple cloning site of the modified murine stem cell virus (MSCV) 2.1 vector (41) upstream of the enhanced GFP (EGFP) gene and the internal ribosomal entry site (IRES). The FLT3-LM cDNA was subcloned into the identical MSCV vector construct carrying the enhanced YFP (Figure 1A). The MSCV vector carrying only the IRES-EGFP cassette was used as a control. The cDNA of FLT3-LM was kindly provided by D.G. Gilliland (Harvard Medical School, Boston, Massachusetts, USA) and contained a 28–amino acid duplicated sequence (CSSDNEYFYVDFREYEYDLKWEFPRENL) inserted between amino acids 610 and 611. The AML1-ETO cDNA was provided by S.W. Hiebert (Vanderbilt University School of Medicine, Nashville, Tennessee, USA).

The FLT3-LM-KD mutation K672R (a point mutation of Lys644 to Arg that disrupts an ion pair with Glu661 that is critical for nucleotide binding in FLT3-WT; ref. 46), and the L148D AML1-ETO point mutation (31, 47) to prevent AML1-ETO DNA binding, were generated from the full-length human FLT3-LM cDNA and the AML1-ETO cDNA, respectively, using the QuikChange Site-Directed Mutagenesis Kit (Stratagene) according to the manufacturer's instructions. The correct sequences of the constructs were confirmed by complete nucleotide sequencing, and expression was proved by Western blot and FACS analysis (Figure 1).

Cell culture. Gag-pol and envelope (GP^+ E86) packaging cells, NIH 3T3 cells, and 293T cells were grown in DMEM with 10% FBS and 1% penicillin/streptomycin in a humidified incubator at 37°C and 5% CO_2. Primary murine BM cells were plated in transplant medium consisting of DMEM supplemented with 15% FBS, 1% penicillin/streptomycin, 6 ng/ml IL-3, 10 ng/ml IL-6, and 100 ng/ml SCF (tebu-bio GmbH). IL-3–dependent Ba/F3 cells stably expressing the empty vector alone, FLT3-WT, FLT3-LM, and FLT3-LM-KD were seeded at a concentration of 0.05×10^6 per milliliter in the presence or absence of IL-3 and FLT3 ligand, as described previously (48). At 72 hours, viable cells were counted in a standard hemacytometer after staining with trypan blue.

Retrovirus production. High-titer helper-free retrovirus was produced with the constructs above by individual cotransfection of each construct with Ecopac (Cell Genesys Inc.) into 293T cells using calcium chloride precipitation. The retrovirus was subsequently collected in the conditioned medium.

Table 3
Identity of retroviral integration sites in diseased mice

Lane[A]	PCR product[A]	Gene	Protein family	Chromosome	Mouse no.
2	A 1	Intergenic		17qE3	15
	A 2	Intron 1 of Rnf8 alias AIP37 and 5 kbp 3′ of Pim1	Ring finger protein 8	17qA3	
3	B	Intergenic		15qE2	16
	C	Intron 1 of Ptp4a3	Protein tyrosine phosphatase 4a3	15qD3	
4	D	Hypothetical gene		10qC2	12
	E	Intron 3 of GATA	Transcription factor	6qD1	
5	F	Intergenic		18qD3	
	G	Intron 4 of SF3b	Splicing factor subunit b3	8qE1	
6	H	Intergenic in intron of hypothetical gene		3qF1	18
	I	Intergenic in intron of hypothetical gene		16qA1	

[A]Lanes and PCR products according to Figure 6B.

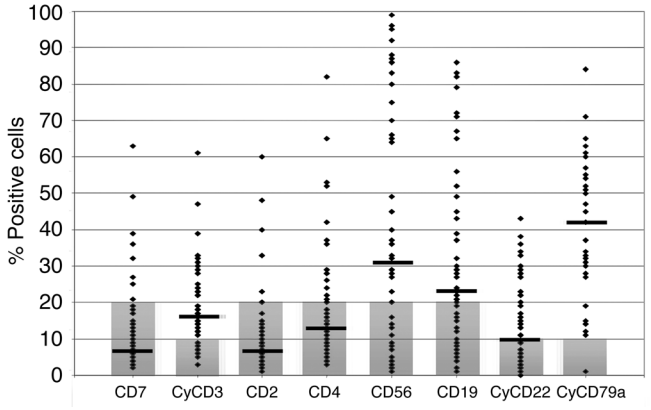

Figure 7
Expression of lymphoid antigens on 52 samples of patients with AML1-ETO–positive AML, determined by immunophenotyping. Samples were defined as negative for expression of cytoplasmic antigens when less than 10% of the cells stained with the antibody, and as negative for expression of surface antigens when less than 20% of the cells stained with the antibody (shaded areas).

To optimize transduction efficiency, the virus-containing medium (VCM) of different constructs was used to transfect GP$^+$ E86 cells to establish stable packaging cell lines, or to directly infect 5-FU–mobilized BM cells in the case of FLT3-LM. Ba/F3 cells were transfected with the different constructs as previously described (48, 49).

Mice and retroviral infection of primary BM cells. Parental-strain mice were bred and maintained at the GSF animal facility. Donors of primary BM cells [(C57BL/6Ly-Pep3b × C3H/HeJ) F_1 (PepC3) mice] and recipient mice [(C57BL/6J × C3H/HeJ) F_1 (B6C3)] were more than 8 weeks old. Primary mouse BM cells were transduced as previously described (41). For transduction of AML1-ETO, cells were cocultured in transplant medium with AML1-ETO/GFP producer cells irradiated with 40 Gy of ^{137}Cs γ-radiation. For infection with the FLT3-LM virus, BM cells were cultured in FLT3-LM/VCM, supplemented with cytokines (IL-3, IL-6, and SCF), to achieve optimal transduction efficacy. For coinfection with the FLT3-LM and AML1-ETO retroviruses, BM cells were cultured on a mixture of 30–50% AML1-ETO/GFP and 50–70% FLT3-LM/YFP producer cells in transplant medium or FLT3-LM/VCM supplemented with IL-3, IL-6, and SCF. Retroviral transfection of primary BM cells with the AML1-ETO mutant L148D and the FLT3-LM-KD mutant was performed as described for FLT3-LM, by cultivation of the BM in VCM supplemented with IL-3, IL-6, and SCF. All transductions were performed with the addition of 5 μg/ml protamine sulfate. Infected cells were highly purified (FACSVantage; BD) based on expression of GFP (for AML1-ETO alone), expression of YFP (for FLT3-LM alone), or coexpression of GFP and YFP (for AML1-ETO/FLT3-LM cotransduction) before transplantation.

BM transplantation and assessment of mice. FACS-purified transduced BM cells or ratios of transduced and nontransduced cells (if less than 3×10^5 transduced cells per recipient were available) were injected into the tail vein of 8- to 10-week-old irradiated recipient F_1 (B6C3) mice (800 cGy from a ^{137}Cs γ-radiation source). Peripheral blood or BM cell progeny of transduced cells were tracked using the GFP and/or YFP fluorescence in vivo (41). For transplantation of secondary mice, 1×10^6 to 2×10^6 cells of diseased primary animals were injected into the recipients after 800 cGy irradiation.

CFU-S and ΔCFU-S assay. 5-FU–mobilized primary BM cells from F_1 (PepC3) donor mice were retrovirally transduced with AML1-ETO; AML1-ETO-L148D; FLT3-LM; FLT3-LM-KD; both AML1-ETO and FLT3-LM; both AML1-ETO and FLT3-LM-KD; or both AML1-ETO-L148D and FLT3-LM. Cells transfected with the empty GFP vector served as control. Successfully transduced cells were isolated 48 hours after termination of infection by FACS (FACSVantage; BD). To assess initial (day 0) CFU-S numbers, purified cell populations were injected into lethally irradiated F_1 (B6C3) recipient mice 96 hours after the start of infection (45). To study the effect of the selective protein tyrosine kinase inhibitor PKC412 on double-positive cells, freshly sorted cells were cultured in transplant medium with 0 and 100 nM PKC412. After 48 hours, the cells were injected into lethally irradiated mice as described above, and the day 0 equivalent of the CFU-S frequency was calculated for both experimental groups. In this ΔCFU-S assay the base-line frequency of CFU-S is lower than in the CFU-S assay. The recovery of CFU-S cells was quantified by determination of the number of macroscopic colonies on the spleen at day 12 postinjection after fixation in Telleyesniczky's solution.

Southern blot. Genomic DNA was isolated from BM, spleen, and peripheral blood of diseased mice with DNAzol as recommended by the manufacturer (Invitrogen Corp.). Southern blot analysis was performed as previously described (45). DNA was digested with *Eco*RI and probed with a ^{32}P-labeled GFP/YFP DNA. Hybridizing bands were visualized by autoradiography.

Western blot. Protein expression of AML1-ETO, AML1-ETO-L148D, FLT3-LM, and FLT3-LM-KD was demonstrated by Western blotting using standard procedures (41). Membranes were probed with an anti-ETO polyclonal goat antibody and an anti-FLT3 polyclonal rabbit antibody (Santa Cruz Biotechnology Inc.). Protein expression of FLT3-LM showed 2 bands, as previously reported: in detail, the FLT3 receptor occurs in 2 different forms due to glycosylation that can be resolved in SDS-PAGE gradient gels — a 158- to 160-kDa membrane-bound protein that is glycosylated at N-linked glycosylation sites in the extracellular domain and an unglycosylated 130- to 143-kDa protein that is not membrane bound (50–52). Phosphorylation of FLT3 was tested by Western blot using 293T cells that were starved for 12 hours at 37°C, 5% CO_2. After cell harvesting and lysis, 300 μg of the lysates was immunoprecipitated with polyclonal rabbit anti-FLT3 antibody (s-18; Santa Cruz Biotechnology Inc.). Immunoprecipitates were analyzed by SDS-PAGE with mouse monoclonal anti-phosphotyrosine antibody (PY-99; Santa Cruz Biotechnology Inc.) and reprobed with anti-FLT3 antibody.

Histology. For histological analyses, sections of selected organs were prepared and stained at the Academic Pathology Laboratory, GSF (Munich, Germany), using standard protocols, as previously described (41). The mast cell–specific tryptase and the CD117 antibody were purchased from Dako-Cytomation. All the tumors were histopathologically classified according to the Bethesda proposals for classification on nonlymphoid and lymphoid hematopoietic neoplasms in mice (53, 54).

Statistical analysis. Data were evaluated using the 2-tailed Student's *t* test for dependent or independent samples (Microsoft Excel 2002, Microsoft Corp.). Differences with *P* values less than 0.05 were considered statistically significant.

Acknowledgments

We thank D.G. Gilliland and S.W. Hiebert for generously providing the AML1-ETO and FLT3-LM cDNA. We are grateful to T. Haferlach and C. Schoch for cytogenetic and FISH data from AML samples, to E. Wolf for careful reading of the manuscript, to B. Ksienzyk for excellent technical assistance, to T. Meyer and Novartis for PKC412, and to the members of the GSF animal facility for maintenance of the animals. This work was supported by the Deutsche Forschungsgemeinschaft (SP 556/3-1 to C. Buske and K. Spiekermann), the Deutsche Krebshilfe (70-2968-Fe I to C. Schessl and M. Feuring-Buske), and the Nationales Genomforschungsnetz-2 (WP3-SP12 to C. Buske and M. Feuring-Buske).

Received for publication December 16, 2004, and accepted in revised form May 17, 2005.

Address correspondence to: Christian Buske, Department of Medicine III, Grosshadern, Ludwig Maximilians University, Marchioninstrasse 15, 81377 Munich, Germany. Phone: 49-89-7099-425; Fax: 49-89-7099-400; E-mail: buske@gsf.de.

Christian Buske and Michaela Feuring-Buske contributed equally to this work.

1. Look, A.T. 1997. Oncogenic transcription factors in the human acute leukemias. *Science.* **278**:1059–1064.
2. Rowley, J.D. 1999. The role of chromosome translocations in leukemogenesis. *Semin. Hematol.* **36**:59–72.
3. Gilliland, D.G., and Tallman, M.S. 2002. Focus on acute leukemias. *Cancer Cell.* **1**:417–420.
4. Schnittger, S., et al. 2002. Analysis of FLT3 length mutations in 1003 patients with acute myeloid leukemia: correlation to cytogenetics, FAB subtype, and prognosis in the AMLCG study and usefulness as a marker for the detection of minimal residual disease. *Blood.* **100**:59–66.
5. Gilliland, D.G. 2002. Molecular genetics of human leukemias: new insights into therapy [review]. *Semin. Hematol.* **39**:6–11.
6. Higuchi, M., et al. 2002. Expression of a conditional AML1-ETO oncogene bypasses embryonic lethality and establishes a murine model of human t(8;21) acute myeloid leukemia. *Cancer Cell.* **1**:63–74.
7. Yuan, Y., et al. 2001. AML1-ETO expression is directly involved in the development of acute myeloid leukemia in the presence of additional mutations. *Proc. Natl. Acad. Sci. U. S. A.* **98**:10398–10403.
8. de Guzman, C.G., et al. 2002. Hematopoietic stem cell expansion and distinct myeloid developmental abnormalities in a murine model of the AML1-ETO translocation. *Mol. Cell. Biol.* **22**:5506–5517.
9. Fenske, T.S., et al. 2004. Stem cell expression of the AML1/ETO fusion protein induces a myeloproliferative disorder in mice. *Proc. Natl. Acad. Sci. U. S. A.* **101**:15184–15189.
10. Nucifora, G., et al. 1993. Detection of DNA rearrangements in the AML1 and ETO loci and of an AML1/ETO fusion mRNA in patients with t(8;21) acute myeloid leukemia. *Blood.* **81**:883–888.
11. Downing, J.R. 1999. The AML1-ETO chimaeric transcription factor in acute myeloid leukaemia: biology and clinical significance. *Br. J. Haematol.* **106**:296–308.
12. Peterson, L.F., and Zhang, D.E. 2004. The 8;21 translocation in leukemogenesis. *Oncogene.* **23**:4255–4262.
13. Wang, Q., et al. 1996. Disruption of the Cbfa2 gene causes necrosis and hemorrhaging in the central nervous system and blocks definitive hematopoiesis. *Proc. Natl. Acad. Sci. U. S. A.* **93**:3444–3449.
14. Sun, W., and Downing, J.R. 2004. Haploinsufficiency of AML1 results in a decrease in the number of LTR-HSCs, while simultaneously inducing an increase in more mature progenitors. *Blood.* **104**:3565–3572.
15. Licht, J.D. 2001. AML1 and the AML1-ETO fusion protein in the pathogenesis of t(8;21) AML. *Oncogene.* **20**:5660–5679.
16. Pabst, T., et al. 2001. AML1-ETO downregulates the granulocytic differentiation factor C/EBPalpha in t(8;21) myeloid leukemia. *Nat. Med.* **7**:444–451.
17. Mulloy, J.C., et al. 2002. The AML1-ETO fusion protein promotes the expansion of human hematopoietic stem cells. *Blood.* **99**:15–23.
18. Schwieger, M., et al. 2002. AML1-ETO inhibits maturation of multiple lymphohematopoietic lineages and induces myeloblast transformation in synergy with ICSBP deficiency. *J. Exp. Med.* **196**:1227–1240.
19. Rhoades, K.L., et al. 2000. Analysis of the role of AML1-ETO in leukemogenesis, using an inducible transgenic mouse model. *Blood.* **96**:2108–2115.
20. Nucifora, G., Larson, R.A., and Rowley, J.D. 1993. Persistence of the 8;21 translocation in patients with acute myeloid leukemia type M2 in long-term remission. *Blood.* **82**:712–715.
21. Miyamoto, T., Weissman, I.L., and Akashi, K. 2000. AML1/ETO-expressing nonleukemic stem cells in acute myelogenous leukemia with 8;21 chromosomal translocation. *Proc. Natl. Acad. Sci. U. S. A.* **97**:7521–7526.
22. Reya, T., Morrison, S.J., Clarke, M.F., and Weissman, I.L. 2001. Stem cells, cancer, and cancer stem cells. *Nature.* **414**:105–111.
23. Miyamoto, T., et al. 2002. Myeloid or lymphoid promiscuity as a critical step in hematopoietic lineage commitment. *Dev. Cell.* **3**:137–147.
24. Tiacci, E., et al. 2004. PAX5 expression in acute leukemias: higher B-lineage specificity than CD79a and selective association with t(8;21)-acute myelogenous leukemia. *Cancer Res.* **64**:7399–7404.
25. Kelly, L.M., et al. 2002. PML/RARalpha and FLT3-ITD induce an APL-like disease in a mouse model. *Proc. Natl. Acad. Sci. U. S. A.* **99**:8283–8288.
26. Kelly, L.M., et al. 2002. FLT3 internal tandem duplication mutations associated with human acute myeloid leukemias induce myeloproliferative disease in a murine bone marrow transplant model. *Blood.* **99**:310–318.
27. Ono, R., et al. 2005. Dimerization of MLL fusion proteins and FLT3 activation synergize to induce multiple-lineage leukemogenesis. *J. Clin. Invest.* **115**:919–929. doi:10.1172/JCI200522725.
28. Armstrong, S.A., et al. 2002. MLL translocations specify a distinct gene expression profile that distinguishes a unique leukemia. *Nat. Genet.* **30**:41–47.
29. Armstrong, S.A., et al. 2004. FLT3 mutations in childhood acute lymphoblastic leukemia. *Blood.* **103**:3544–3546.
30. Taketani, T., et al. 2004. FLT3 mutations in the activation loop of tyrosine kinase domain are frequently found in infant ALL with MLL rearrangements and pediatric ALL with hyperdiploidy. *Blood.* **103**:1085–1088.
31. Grisolano, J.L., O'Neal, J., Cain, J., and Tomasson, M.H. 2003. An activated receptor tyrosine kinase, TEL/PDGFbetaR, cooperates with AML1/ETO to induce acute myeloid leukemia in mice. *Proc. Natl. Acad. Sci. U. S. A.* **100**:9506–9511.
32. Levis, M., et al. 2005. Internal tandem duplications of the FLT3 gene are present in leukemia stem cells. *Blood.* doi:10.1182/blood-2004-05-1902.
33. Boissel, N., et al. 2004. Incidence and prognosis of RTKs and RAS mutations in CBF AML. A retrospective study of French adult ALFA and pediatric LAME trials [abstract]. *Blood.* **103**:2022.
34. Cairoli, R., et al. 2004. Prognostic impact of C-Kit mutations in core binding factor-leukemia [abstract]. *Blood.* **103**:2013.
35. Wang, Y.Y., et al. 2005. AML1-ETO and C-KIT mutation/overexpression in t(8;21) leukemia: implication in stepwise leukemogenesis and response to Gleevec. *Proc. Natl. Acad. Sci. U. S. A.* **102**:1104–1109.
36. Bennett, J.M., et al. 1976. Proposals for the classification of the acute leukaemias. French-American-British (FAB) co-operative group. *Br. J. Haematol.* **33**:451–458.
37. Harris, N.L., et al. 1999. World Health Organization classification of neoplastic diseases of the hematopoietic and lymphoid tissues: report of the Clinical Advisory Committee meeting. Airlie House, Virginia, November 1997. *J. Clin. Oncol.* **17**:3835–3849.
38. Schnittger, S., et al. 2003. New score predicting for prognosis in PML-RARA+, AML1-ETO+, or CBFBMYH11+ acute myeloid leukemia based on quantification of fusion transcripts. *Blood.* **102**:2746–2755.
39. Schnittger, S., Wormann, B., Hiddemann, W., and Griesinger, F. 1998. Partial tandem duplications of the MLL gene are detectable in peripheral blood and bone marrow of nearly all healthy donors. *Blood.* **92**:1728–1734.
40. Spiekermann, K., et al. 2002. A new and recurrent activating length mutation in exon 20 of the FLT3 gene in acute myeloid leukemia. *Blood.* **100**:3423–3425.
41. Rawat, V.P., et al. 2004. Ectopic expression of the homeobox gene Cdx2 is the transforming event in a mouse model of t(12;13)(p13;q12) acute myeloid leukemia. *Proc. Natl. Acad. Sci. U. S. A.* **101**:817–822.
42. Riley, J., et al. 1990. A novel, rapid method for the isolation of terminal sequences from yeast artificial chromosome (YAC) clones. *Nucleic Acids Res.* **18**:2887–2890.
43. Imren, S., et al. 2004. High-level β-globin expression and preferred intragenic integration after lentiviral transduction of human cord blood stem cells. *J. Clin. Invest.* **114**:953–962. doi:10.1172/JCI200421838.
44. Kern, W., et al. 2004. Determination of relapse risk based on assessment of minimal residual disease during complete remission by multiparameter flow cytometry in unselected patients with acute myeloid leukemia. *Blood.* **104**:3078–3085.
45. Pineault, N., et al. 2003. Induction of acute myeloid leukemia in mice by the human leukemia-specific fusion gene NUP98-HOXD13 in concert with Meis1. *Blood.* **101**:4529–4538.
46. Griffith, J., et al. 2004. The structural basis for autoinhibition of FLT3 by the juxtamembrane domain. *Mol. Cell.* **13**:169–178.
47. Lenny, N., Meyers, S., and Hiebert, S.W. 1995. Functional domains of the t(8;21) fusion protein, AML-1/ETO. *Oncogene.* **11**:1761–1769.
48. Spiekermann, K., et al. 2003. The protein tyrosine kinase inhibitor SU5614 inhibits FLT3 and induces growth arrest and apoptosis in AML-derived cell lines expressing a constitutively activated FLT3. *Blood.* **101**:1494–1504.
49. Spiekermann, K., Faber, F., Voswinckel, R., and Hiddemann, W. 2002. The protein tyrosine kinase inhibitor SU5614 inhibits VEGF-induced endothelial cell sprouting and induces growth arrest and apoptosis by inhibition of c-kit in AML cells. *Exp. Hematol.* **30**:767–773.
50. Stirewalt, D.L., and Radich, J.P. 2003. The role of FLT3 in haematopoietic malignancies. *Nat. Rev. Cancer.* **3**:650–665.
51. Lyman, S.D., et al. 1993. Molecular cloning of a ligand for the flt3/flk-2 tyrosine kinase receptor: a proliferative factor for primitive hematopoietic cells. *Cell.* **75**:1157–1167.
52. Carow, C.E., et al. 1996. Expression of the hematopoietic growth factor receptor FLT3 (STK-1/Flk2) in human leukemias. *Blood.* **87**:1089–1096.
53. Kogan, S.C., et al. 2002. Bethesda proposals for classification of nonlymphoid hematopoietic neoplasms in mice. *Blood.* **100**:238–245.
54. Morse, H.C., 3rd, et al. 2002. Bethesda proposals for classification of lymphoid neoplasms in mice. *Blood.* **100**:246–258.

Acute myeloid leukemia is propagated by a leukemic stem cell with lymphoid characteristics in a mouse model of *CALM/AF10*-positive leukemia

Aniruddha J. Deshpande,[1,2] Monica Cusan,[1,2] Vijay P.S. Rawat,[1,2] Hendrik Reuter,[2,3] Alexandre Krause,[1,2] Christiane Pott,[4] Leticia Quintanilla-Martinez,[5] Purvi Kakadia,[1,2] Florian Kuchenbauer,[1,2] Farid Ahmed,[1,2] Eric Delabesse,[6] Meinhard Hahn,[3] Peter Lichter,[3] Michael Kneba,[5] Wolfgang Hiddemann,[1,2] Elizabeth Macintyre,[6] Cristina Mecucci,[7] Wolf-Dieter Ludwig,[8] R. Keith Humphries,[9] Stefan K. Bohlander,[1,2] Michaela Feuring-Buske,[1,2] and Christian Buske[1,2,*]

[1] Department of Medicine III, Klinikum Grosshadern, D-81377 Munich, Germany
[2] Clinical Cooperative Group Leukemia, GSF-National Research Center for Environment and Health, D-81377 Munich, Germany
[3] German Cancer Research Center, Division of Molecular Genetics, D-69120 Heidelberg, Germany
[4] Second Medical Department, University Hospital Schleswig-Holstein, Campus Kiel, D-24116 Kiel, Germany
[5] Institute of Pathology, GSF, D-85758 Neuherberg, Germany
[6] Laboratoire d'Hématologie, Tour Pasteur, Hôpital Necker, 75743 Paris, France
[7] Hematology and Bone Marrow Transplantation Unit, University of Perugia, 06122 Perugia, Italy
[8] Department of Hematology, Oncology, and Tumor Immunology, Robert-Rossle-Klinik, D-13125 Berlin, Germany
[9] The Terry Fox Laboratory, BC Cancer Agency and the Department of Medicine, University of British Columbia, Vancouver, British Columbia V5Z 1L3, Canada
*Correspondence: buske@gsf.de

Summary

A challenge for the development of therapies selectively targeting leukemic stem cells in acute myeloid leukemia (AML) is their similarity to normal hematopoietic stem cells (HSCs). Here we demonstrate that the leukemia-propagating cell in murine *CALM/AF10*-positive AML differs from normal HSCs by B220 surface expression and immunoglobulin heavy chain rearrangement. Furthermore, depletion of $B220^+$ cells in leukemic transplants impaired development of leukemia in recipients. As in the murine model, human *CALM/AF10*-positive AML was characterized by CD45RA (B220)-positive, *IG* DH-JH rearranged leukemic cells. These data demonstrate in a murine leukemia model that AML can be propagated by a transformed progenitor with lymphoid characteristics, which can be targeted by antibodies that do not crossreact with normal HSCs.

Introduction

For most cancers, the cell that propagates tumor growth and is thought to play a key role in recurrence of disease is unknown. The study of normal and malignant hematopoiesis has formed a roadmap for the detailed analysis of the concept of the tumor-initiating cell and has demonstrated that, in leukemia, the malignant clone is organized in a hierarchy in which only a small subpopulation of cells—the leukemic stem cells (LSCs)—are able to initiate and propagate the disease (Hope et al., 2004). In AML most studies indicate that malignant transformation targets cells within the hematopoietic stem cell compartment. However, more recent data demonstrated that multipotential progenitors or more committed myeloid progenitors can also acquire leukemic stem cell properties when transformed by appropriate oncogenes (Cozzio et al., 2003; So et al., 2003). These reports clearly demonstrated that cells other than hematopoietic stem cells can be the target of fully transforming oncogenes, which are characterized by their ability to transfer self-renewal potential to committed stages of differentiation (Huntly et al., 2004; Jamieson et al., 2004). The identification of leukemic stem cell properties is a key step for an improved understanding of the biology of acute leukemias and might also have clinical implications: because of its essential role for the initiation and maintenance of the leukemic clone, a curative therapeutic strategy should be able to eradicate the LSC in the diseased patients.

SIGNIFICANCE

The identification of tumor stem cells is one of the major goals of cancer research. We report on a murine model demonstrating that myeloid malignancies such as acute myeloid leukemia can be propagated by a transformed progenitor with lymphoid characteristics. These data extend our previous knowledge about leukemia stem cell candidates in acute leukemia and indicate that leukemia-propagating cells in AML might differ from the myeloid blast population as well as from the normal hematopoietic stem cell in their surface antigen profile. These findings suggest that such leukemic stem cell candidates can be targeted with antibodies that spare the normal stem cell pool. This may pave the way for innovative antibody-based therapeutic strategies in this disease.

At the same time, such a strategy should spare normal hematopoietic stem cells (HSCs) to avoid intolerable therapy-associated stem cell toxicity. However, the major challenge for the development of such therapeutic approaches is the often striking similarity between leukemic and normal HSC, e.g., with regard to their cell surface markers (Reya et al., 2001; Warner et al., 2004). The limitations of the therapeutic tools available today are well known: although standard chemotherapy is highly effective in inducing remissions in patients with AML, the majority of patients finally relapse and succumb to this disease (Hiddemann et al., 2005). One of the reasons for treatment failure is that even dose-intensive conventional chemotherapy is not able to efficiently target the LSC, demonstrated, for example, by the observation that patients in morphological complete remission harbor $CD34^+/CD38^-$ progenitor cells with the leukemia-specific genetic alteration in their bone marrow (Feuring-Buske et al., 1999). A major step toward the development of stem cell-targeted AML therapies would be the identification of key differences between normal HSCs and the LSC. It has been reported that the LSC differs from its normal counterpart by the expression of CD90 or the interleukin-3α receptor, and in a preclinical NOD/SCID mouse model a diphtheria toxin (DT) human interleukin 3 fusion protein (DT388IL3) was able to selectively kill LSCs in patients with different subtypes of AML (Blair et al., 1997; Feuring-Buske et al., 2002; Jordan et al., 2000).

The recent reports demonstrating that acute leukemias can also arise from transformed committed progenitor cells might improve the chances to define biological differences between the LSC and the HSC (Huntly et al., 2004; So et al., 2003). However, leukemic stem cell candidates such as multipotent progenitor cells (MPPs) might be difficult to distinguish from normal HSCs, although first strategies were established in mice to discriminate MPPs from long-term repopulating stem cells by immunophenotype (Forsberg et al., 2005; Morrison et al., 1997). In this report we present experimental evidence that acute myeloid leukemia can be propagated by a transformed progenitor, which differs from normal hematopoietic stem cells by surface expression of B220 and immunoglobulin heavy chain (*IG* DH-JH) rearrangement. We established a murine model of *CALM/AF10* (C/A)-positive acute myeloid leukemia using the bone marrow transplantation model and retroviral gene transfer to constitutively express the fusion gene in hematopoietic progenitor cells. The established model well predicted our findings in patients with *C/A*-positive AML, who showed a cell population expressing CD45RA, the human homolog of B220. This human $CD45RA^+$ cell population displayed *IG* DH-JH rearrangements, was positive for the fusion gene as detected by fluorescence in situ hybridization (FISH), and was able to form CFU-blast colonies in vitro. In these patients the fusion gene is formed by the translocation t(10;11) (p13;q14), which involves the *CALM* gene (associated with clathrin-mediated endocytosis) and *AF10* (a putative transcription factor). This fusion gene is found in a variety of leukemias, which are all characterized by a very poor prognosis (Dreyling et al., 1998). Of note, the malignant phenotypes associated with C/A span AML, undifferentiated leukemia, acute lymphoblastic leukemia, and T cell lymphoma, thus making it appealing to determine the nature of the leukemic stem cell candidate(s) in *C/A*-positive disease. The results of this study demonstrate in a murine leukemia model that a transformed progenitor cell population with lymphoid characteristics can play a key role in propagating *C/A*-positive AML.

Results

CALM/AF10 induces acute myeloid leukemia in mice

To test the impact of constitutive expression of *C/A* on murine hematopoietic development, we employed the murine bone marrow (BM) transplantation model. The fusion gene was expressed in a murine stem cell virus (MSCV)-based retroviral construct carrying the *C/A* cDNA upstream of an internal ribosomal entry site (IRES)-green fluorescence protein (GFP) cassette that has been shown to efficiently transduce hematopoietic stem and progenitor cells (Figures S1A–S1C in the Supplemental Data available with this article online).

All mice (n = 13) transplanted with highly purified GFP^+ *C/A* transduced cells (median retroviral transduction efficiency of 5.7, range 1.2%–16.4%) with or without nontransduced helper cells developed a disease after a median of 110 days posttransplantation (range 46–366) (Figure 1A) and suffered from cachexia, lethargy, and shortness of breath. Detailed analyses of the hematopoietic compartments showed a more than 10-fold elevated white blood cell count in the peripheral blood (PB) of all animals with a median of 4.9×10^7 cells/ml (range 3.2–8.5×10^7) compared to the GFP control (median 0.48, range 0.32–0.8×10^7) ($p < 0.002$). Furthermore, mice were anemic, with a 7.3-fold reduced median red blood cell count of 0.75×10^9 cells (range 0.6–1.25×10^9) versus 5.5×10^9 (range 4.8–7×10^9) in the control mice ($p < 0.0001$), and suffered from splenomegaly (Table 1). Panoptic staining of PB smears and cytospin preparations of BM and spleen cells revealed an accumulation of blasts accounting for medians of 32%, 40%, and 39%, respectively, of all cells (Table 1; Figure 1B). The spleen showed a massive infiltration with myeloid cells (median of 86.9% $Mac1^+$ cells [range 72.8%–91.1%] versus 12% in the control [range 7%–26.5%] and 62.5% $Gr1^+$ cells [range 40%–76.2%] compared to 9.5% in the control [range 7.5%–11.3%]) (Figure 1B). Histological sections demonstrated infiltration of blasts in multiple nonhematopoietic organs, including the brain (Figure 1C). Immunohistochemistry showed positivity of the blasts for myeloperoxidase (*MPO*) and chloracetate esterase and negativity for B220 and CD3, indicating the myeloid nature of the population (Figure 1D). Taken together, the mice suffered from acute myeloid leukemia according to the Bethesda proposal for classification of nonlymyphoid and lymphoid hematopoietic neoplasms in mice (Kogan et al., 2002; Morse et al., 2002).

Transplantation of BM cells of leukemic mice into secondary recipients (n = 22) rapidly induced leukemia with the same characteristics after a median of 15 days (range 14–21 days) posttransplantation (Figure 1A). Bone marrow aspirations of anesthetized primary recipients 8 weeks posttransplantation did not show any myeloproliferative or lymphoproliferative syndrome before the onset of leukemia (n = 5). Analysis of proviral integration sites demonstrated oligoclonal disease in primary and secondary mice (Figure S2). Sequencing of the retroviral integration sites (n = 18) in the diseased mice showed 10 out of 18 sites in or near regions described as common integration sites (CIS) in the RTCGD database (http://rtcgd.ncifcrf.gov/) (Akagi et al., 2004). No recurrent integration sites or any association of the leukemic phenotype with individual proviral integrations were observed (Table S1). In summary, these data demonstrated that constitutive expression of *CALM/AF10* induced short-latency AML in transplanted animals.

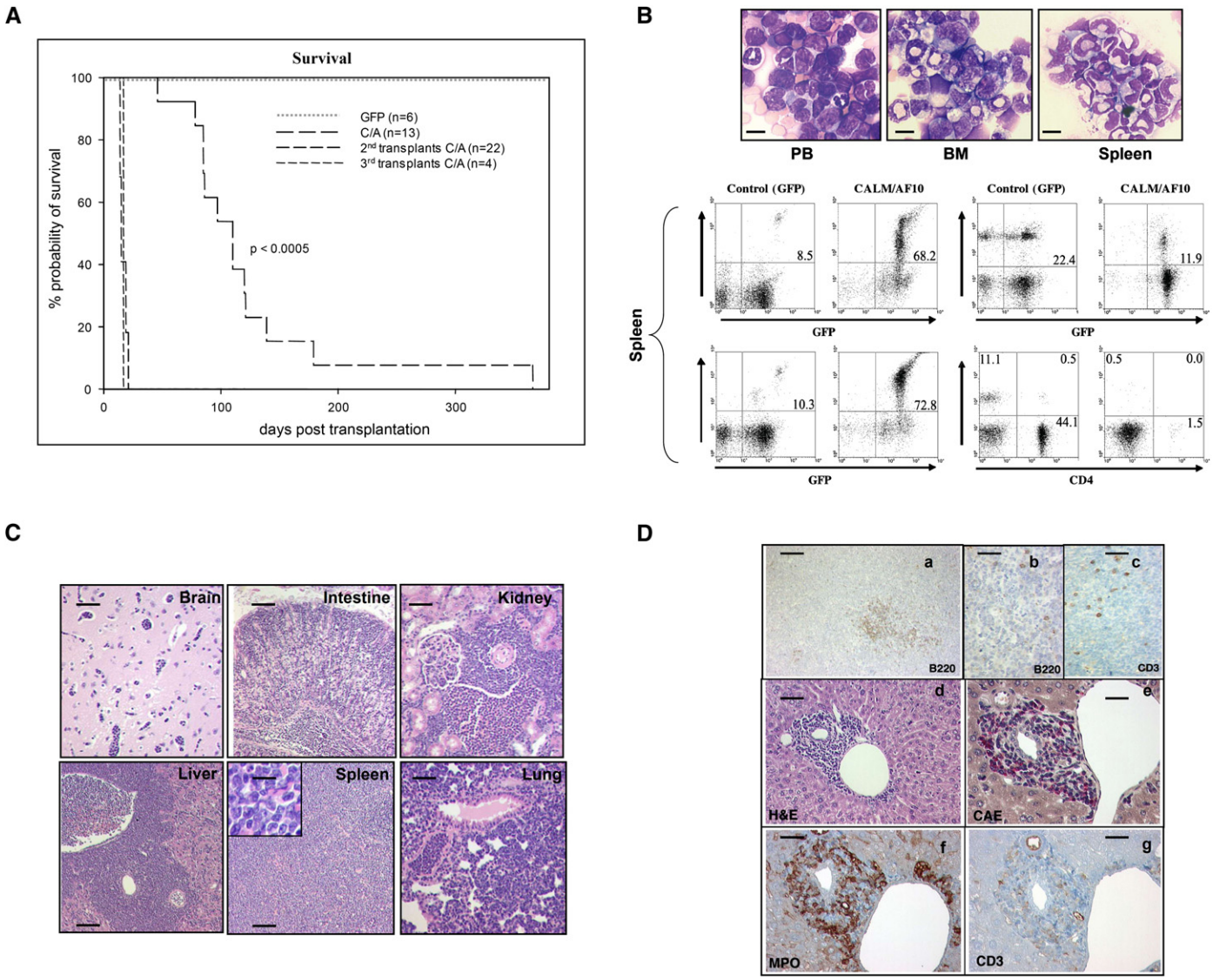

Figure 1. CALM/AF10 induces transplantable AML

A: Survival curve of mice transplanted with BM cells expressing *CALM/AF10* (n = 13, originating from five independent sets of transduction experiments). The control group was transplanted with BM infected with the GFP empty retrovirus (n = 6). The survival time of secondary recipient mice, transplanted with BM from diseased primary *CALM/AF10* mice or tertiary recipient mice injected with BM from leukemic secondary mice, is indicated. C/A, CALM/AF10.

B: Cytospin preparations from PB, BM, and spleen and immunophenotype of the spleen of a representative leukemic *CALM/AF10* mouse in comparison to a GFP control animal. Cells were stained for the myeloid markers Gr1 and Mac1 and the lymphoid markers B220, CD4, and CD8. The proportion of positive cells within the GFP^+ compartment is indicated; the CD4/CD8 costaining was gated for GFP^+ cells. BM, bone marrow; PB, peripheral blood. Scale bar, 10 μm.

C: Histological analysis of diseased *CALM/AF10* mice. Blast infiltration in the different organs is shown (brain, intestine, glomerular and tubular areas of the kidney, sinusoidal and portal areas of the liver, spleen, and lungs) Scale bar, 100 μm; scale bar in inset picture of spleen, 25 μm.

D: Histochemical and immunohistological analysis of the spleen and liver of a diseased *CALM/AF10* mouse. Anti-B220 (**Da** and **Db**) and anti-CD3 staining (**Dc**) of spleen sections and hematoxylin-eosin (**Dd**), CAE (**De**), MPO (**Df**), and anti-CD3 staining (**Dg**) of liver sections. MPO, myeloperoxidase; CAE, N-acetyl-chloroacetate esterase. Scale bars, 100 μm in **Db**–**Dg**, 25 μm in **Da**, 50 μm in **Dd**.

CALM/AF10-induced leukemia is propagated by a transformed $B220^+$, immunoglobulin DH-JH rearranged progenitor cell

More detailed analyses of the leukemic BM population (GFP^+ cells) revealed that, in addition to a majority of cells expressing myeloid markers (MM) ($Mac1^+$ cells, 82.9% [±8.6]; $Gr1^+$ cells, 86.4% [±3.7]), there was a small $B220^+/MM^-$ cell population in all animals obtained from five independent sets of experiments, which accounted on average for 6.7% (±2.1%) of the cells, comparable to the proportion of these cells in control mice (on average 9.4% ± 3%). An average of 26.0% (±8.6) and 32.5% (±13.2) of the BM cells coexpressed B220 with Mac1 or B220 with Gr1, respectively (n = 4) ($B220^+/MM^+$). Highly purified cells of the $B220^+/MM^-$ population had an immature, blast-like appearance, whereas the $B220^-/MM^+$ population included blasts as well as terminally differentiated myeloid cells (Figure 2A). Interestingly, all three subpopulations, including the cells expressing solely the MMs Mac1 or Gr1, showed DJ

Table 1. Hematological parameters in representative experimental mice

Mouse no.	Retroviral construct	Day of sacrifice	RBCs/ml × 10^9	WBCs/ml × 10^7	Spleen weight (mg)	Percent BM blasts	Percent spleen blasts	Percent PB blasts	IgH DJ rearrangement
1	C/A	10	0.75	3.5	700	30	32	27	ND
2	C/A	78	0.75	5.0	400	40	30	33	+
3	C/A	85	0.6	8.5	250	65	60	61	+
4	C/A	121	0.82	5.2	300	38	38	31	+
5	C/A	85	0.6	4.8	200	78	40	ND	+
6	C/A	86	1.25	3.2	400	ND	42	32	+
7[a]	C/A	67	4	2.5	240	32	29	33	+
8[a]	C/A	98	2.65	ND	350	36	ND	28	–
9	GFP	90	6	0.45	150	0	0	0	ND
10	GFP	157	4.8	0.32	200	0	0	0	ND
11	GFP	85	5	0.36	200	0	0	0	ND
12[b]	GFP	ND	4.8	0.76	ND	1	0	0	ND
13[b]	GFP	ND	6.4	0.8	ND	0	0	0	ND
14	GFP	90	7	0.5	51	2	0	0	ND

C/A, CALM/AF10; ND, not determined; RBC, red blood cell; WBC, white blood cell; BM, bone marrow; PB, peripheral blood.
[a]Mice were injected with highly purified B220-negative progenitor cells with IgH in germline configuration.
[b]Determined by bone marrow aspiration and bleeding of the mouse.

rearrangements of the heavy chain of the IgH locus, indicating that the myeloid population originated from DJ rearranged cells (Figure 2A). The bulk leukemic population isolated from diseased mice showed unlimited IL3-dependent growth in vitro and retained its characteristic phenotype with appearance of the $B220^+/MM^-$ as well as the $B220^+/MM^+$ and the $B220^-/MM^+$ population (n = 3).

To determine whether the growth potential differed between the three subpopulations, single cells of the $B220^+/MM^-$, $B220^+/MM^+$, and the $B220^-/MM^+$ population were sorted and tested for their proliferative capacity: strikingly, only the $B220^+/MM^-$ population displayed high clonal proliferative potential at the single-cell level, with a mean seeding efficiency of 29.3% compared to 1% in the other two populations (Figure 2B). When competitive transcriptional profiling of highly purified $B220^+/Mac1^-$ and $B220^-/Mac1^+$ cells was performed by cDNA microarray analysis, 944 genes out of a total of 3643 present genes were differentially expressed between the two populations. The gene categories, which were significantly overrepresented in the $B220^+/Mac1^-$ cells, comprised genes linked to mitosis and S phase, to response to DNA damage, to translation, and to DNA repair and replication. In contrast, the $B220^-/Mac1^+$ cells showed overrepresentation of genes belonging to the categories cell death, cell communication, and actin cytoskeleton organization, reflecting the profound differences in the transcriptome and the proliferative status between the two populations (http://www.ncbi.nlm.nih.gov/geo/; GEO accession number GSE5030) (Figure 2C). Importantly, a single $B220^+/MM^-$ cell isolated from leukemic mice could give rise to the $B220^+/MM^+$ and the $B220^-/MM^+$ populations in vitro, further indicating the hierarchical organization of the leukemic population (Figure 2D). These $B220^-/MM^+$ cells were functionally intact myeloid cells and were able to actively phagocytose yeast cells (Figure 2D). Furthermore, all the $B220^+/MM^+$ and the $B220^-/MM^+$ cells derived from a single $B220^+/Mac1^-$ cell in vitro displayed identical genomic DJ rearrangements like the original progenitor (Figure 2E). In conclusion, these data demonstrated that the $B220^+/MM^-$ cells isolated from leukemic mice are able to give rise to DJ rearranged myeloid cells and have the highest proliferative potential at the single-cell level compared to the MM^+ subpopulations.

Next it was determined whether highly purified $B220^+/MM^-$ cells generated from a single cell in vitro would be able to cause acute myeloid leukemia in vivo: all animals (n = 3) succumbed to acute myeloid leukemia after a short latency time of 35 days posttransplantation when 1×10^6 cells per mouse were injected. Thus, the data demonstrated that single $B220^+/MM^-$ cells isolated from a leukemic mouse can initiate the leukemia of the same phenotype as bone marrow cells freshly transduced with CALM/AF10 retrovirus. In order to test the hypothesis that the leukemia-propagating cell resides in the $B220^+/MM^-$ compartment, we purified the three distinct populations from leukemic primary recipients and performed limiting dilution transplantation assays that allowed us to determine the frequency of the leukemia-propagating cell in the three different subpopulations as previously described (Kroon et al., 1998). Importantly, the frequency of the leukemia-propagating cell was 1 in 36 cells in the $B220^+/MM^-$ population as opposed to 1 in 437 cells in the $B220^+/MM^+$ and 1 in 19,717 cells in the $B220^-/MM^+$ compartment. Thus, the frequency of the leukemia-propagating cell was over 548-fold higher in the $B220^+/MM^-$ population compared to the $B220^-/MM^+$ population (Figure 3A; Table S2). Strikingly, in our model removal of the $B220^+$ cells from the leukemic transplant prevented the development of leukemia in mice, in contrast to the animals, which were transplanted with leukemic $B220^+/MM^-$ cells and died after a median of 34 days posttransplantation (Figure 3B).

To test the possibility that the leukemic stem cells would also reside in the cell compartment lacking expression of B220 and the MMs Gr1 and Mac1 ($B220^-/Gr1^-/Mac1^-$), bone marrow cells of leukemic mice were costained with B220-APC, Gr1-PE, and Mac1-PE: the proportion of this cell population in the bone marrow was very small, with a median of 0.03% (range 0.01%–0.05%) in four mice tested. Furthermore, only very few cells expressed the stem cell-associated markers Sca1 and c-Kit (Figure S3A). To test this population functionally, we highly purified this subpopulation from leukemic mice and compared the clonogenic potential of these cells with the $B220^+/MM^-$ subpopulation: while the $B220^-/Gr1^-/Mac1^-$ population was not able to form any colonies in vitro, an equal number of $B220^+/MM^-$ cells generated replatable colonies with a frequency of 85 ± 13 blast colonies per 1000 cells (data from three mice

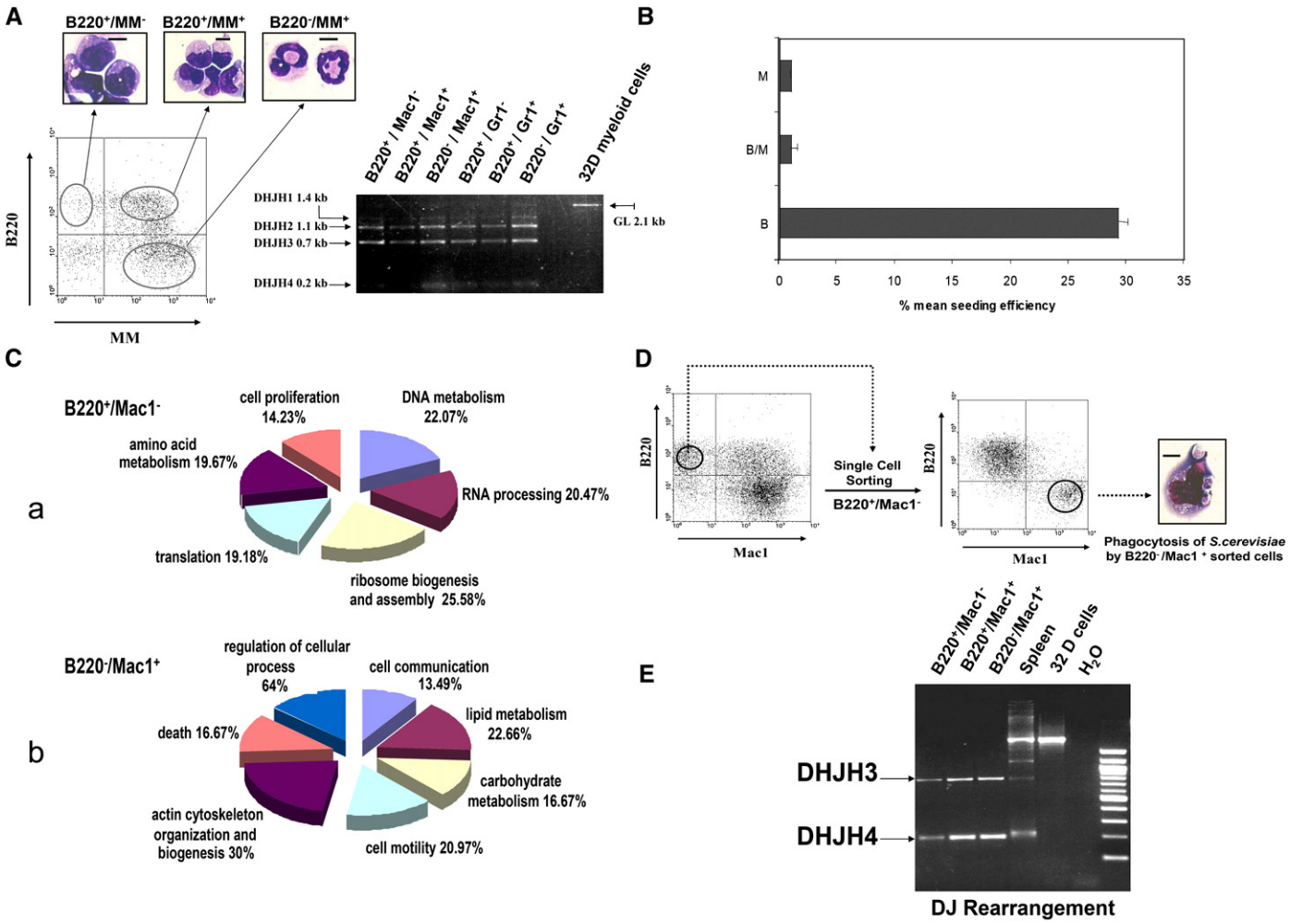

Figure 2. Transformed B220$^+$/MM$^-$ cells are IgH DH-JH positive and can generate IgH DH-JH rearranged myeloid cells at the single-cell level

A: Morphology and genomic DH-JH recombination of the immunoglobulin locus in different populations. Wright-Giemsa-stained cytospins of highly purified B220$^+$/MM$^-$, B220$^+$/MM$^+$, and B220$^-$/MM$^+$ cells and the genomic DH-JH status in different highly purified subpopulations from a representative leukemic *CALM/AF10* mouse. DH-JH status in B220$^+$/Mac1$^-$, B220$^+$/Mac1$^+$, B220$^-$/Mac1$^+$, B220$^+$/Gr1$^-$, B220$^+$/Gr1$^+$, and B220$^-$/Gr1$^+$ cells is indicated; the myeloid cell line 32D was used as a DH-JH naive germline control. GL, germline; MM, myeloid marker. Scale bar, 10 μm.

B: Seeding efficiency of the different populations. Single-cell sorting of the three subpopulations, B220$^+$/Mac1$^-$, B220$^+$/Mac1$^+$, and B220$^-$/Mac1$^+$, isolated from a leukemic bulk cell population was performed in 96-well plates, and single-cell growth was determined after culture for 4–5 weeks in IL3-supplemented medium. The mean seeding efficiency for each population is indicated (n = 3, plotted as mean values ± SD).

C: Distribution of gene categories significantly overrepresented in highly purified B220$^+$/Mac1$^-$ compared to B220$^-$/Mac1$^+$ cells (**Ca**) and in B220$^-$/Mac1$^+$ versus B220$^+$/Mac1$^-$ cells (**Cb**). Analysis was performed by DNA microarray-based expression profiling using a chip with 20,172 PCR-amplified, sequence-verified, gene-specific DNA fragments (LION Biosciences).

D: Phagocytosis by B220$^-$/Mac1$^+$ cells derived from a single-cell-sorted B220$^+$/Mac1$^-$ cell. Single-cell-sorted B220$^+$/Mac1$^-$ cells were expanded in vitro, and the B220$^-$/Mac1$^+$ cells generated from these cells were tested for phagocytosis of the yeast *S. cerevisiae*. A representative picture of a B220$^-$/Mac1$^+$ phagocytosing cell is shown. Scale bar, 5 μm.

E: Clonal DH-JH rearrangements in the three subpopulations. B220$^+$/Mac1$^-$, B220$^+$/Mac1$^+$, and B220$^-$/Mac1$^+$ cells generated from a single B220$^+$/Mac1$^-$ sorted cell all showed the identical clonal DH-JH3 and DH-JH4 biallelic rearrangements. Genomic DNA from splenic cells from a nontransplanted mouse and the myeloid cell line 32D were used as positive and negative controls for recombination, respectively. B, B220$^+$/Mac1$^-$; B/M, B220$^+$/Mac1$^+$; M, B220$^-$/Mac1$^+$.

transplanted initially with independently transduced bone marrow; input number 100–1000 cells/dish in both arms). Importantly, the B220$^-$/Gr1$^-$/Mac1$^-$ cells did not show leukemic engraftment into secondary recipients or induced leukemia, whereas as few as 25 B220$^+$/MM$^-$ cells caused leukemic engraftment of the same phenotype as described before (input number between 25 and 113 cells for the B220$^-$/Gr1$^-$/Mac1$^-$ cells [n = 5] and an equal number of cells per mouse for the B220$^+$/MM$^-$ population [n = 5]) (Table S3). Taken together, the high frequency of the leukemia-propagating cell in the B220$^+$/MM$^-$ population, together with its ability to proliferate and to give rise to a myeloid DJ rearranged cell population, demonstrated that the leukemia-propagating cell resided in the B220$^+$/Mac1$^-$ cell compartment in this murine model.

More detailed analysis of the cell surface phenotype of the B220$^+$/MM$^-$ cells characterized them as CD43$^+$/AA4.1$^+$/CD24$^{low\text{-}pos}$/FLT3^{med}/IL-7R$^{low\text{-}neg}$, c-Kit$^{low\text{-}neg}$, CD19$^-$, and Sca1$^-$ (Figures 4A and 4B). The cells did not express CD21, CD23, sIgM, λ5, Bp1, or Igβ (Figures S4A and S4B), or CD4 or NK1.1 (data not shown). Transcriptional profiling by RT-PCR

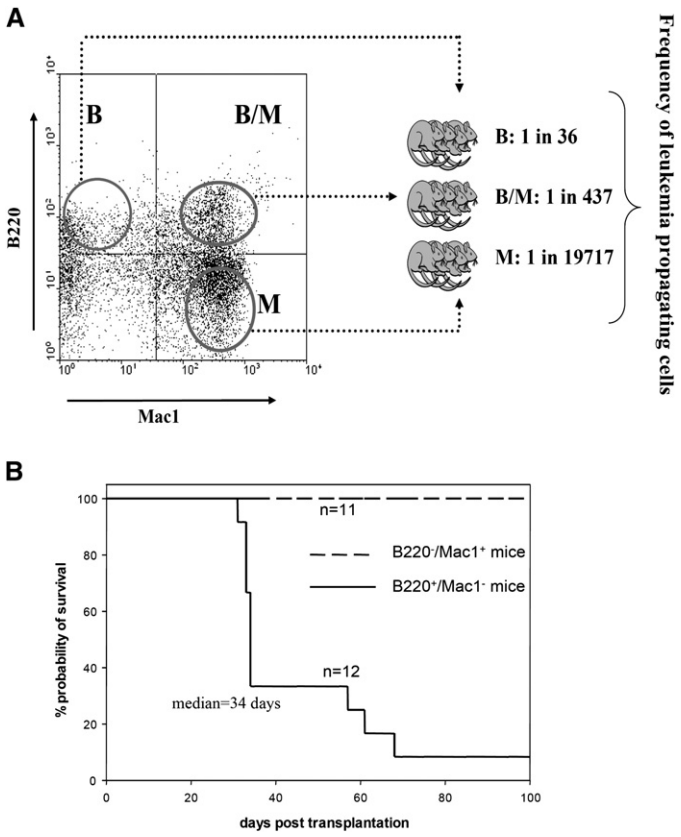

Figure 3. Frequency of leukemia-propagating cells

A: Determination of the frequency of leukemia-propagating cells. Cohorts of secondary mice were injected with highly purified B220$^+$/Mac1$^-$, B220$^+$/Mac1$^+$, and B220$^-$/Mac1$^+$ populations from primary leukemic mice in a limiting dilution assay. The frequency of leukemia-propagating cells in each population is indicated. Details of cell numbers, number of mice per arm, and the median latency of disease are described in Table S2.

B: Survival of mice transplanted with leukemic BM depleted of B220$^+$ cells (B220$^-$/Mac1$^+$cells, n = 11; 50 cells [n = 4], 500 cells [n = 4], and 5000 cells [n = 3] isolated from the primary leukemic population). In comparison the survival of mice (n = 12) transplanted with B220$^+$/Mac1$^-$ cells with the same range of cell numbers (50 [n = 4], 500 [n = 4]), and 5000 cells [n = 4]) is shown.

showed lineage-promiscuous expression of the lymphoid factors *EBF*, *VpreB*, and *Rag2* and the MM *MPO* (Figure 4C; Figure S4C). Importantly, there was no transcription of *Pax5*, which is compatible with the incomplete rearrangement status at the IgH locus (data not shown) and the CD19 negativity of the cells (Figure 4B). In the B220$^+$/Mac1$^+$ and in the B220$^-$/Mac1$^+$ cells, transcripts for the M-CSF receptor became detectable, whereas transcription for *EBF* was downregulated. There was no detectable transcription of *Gata3*, *Zfpn1a3* (*Aiolos*) (Figure 4C), or *mb1* and only low expression of *λ5* transcripts (Figure S4C). In addition, we could not detect rearrangements of the TCRγ receptor, specifically Vγ 1.1-Jγ4, Vγ 2/4-Jγ1, or Vγ 5/7-Jγ1 by PCR (data not shown). The surface marker expression as well as the transcription factor expression profile collectively defined the B220$^+$/MM$^-$ population as a lymphoid progenitor (Figure S5).

In an effort to determine whether an earlier B220-negative cell could be transformed by the *CALM/AF10* fusion gene, we next analyzed whether transduction of *CALM/AF10* into highly purified B220-negative cells with IgH germline configuration resulted in the induction of AML of the same phenotype as described for the transduction of unfractionated bone marrow: two of two animals tested developed acute myeloid leukemia after transplantation of 1–2 × 10^5 B220-negative cells proven to have IgH germline configuration by PCR before injection, indicating that early B220-negative progenitors with IgH germline configuration can acquire leukemogenic potential after *CALM/AF10* transduction. However, whereas one of the AML cases showed B220$^+$ cells with IgH DJ rearrangement as described before, the other case did not display a B220$^+$ subpopulation. In addition, the leukemic bulk had a germline IgH configuration, a phenotype not observed in the transplantation assays using 5-FU-mobilized unfractioned bone marrow for viral infection (Figure S3B and Table 1). In contrast to early B220$^-$ progenitors, murine cell populations comprising pro-B cells (B220+/CD43+/CD25−; input number 2 × 10^6 cells per mouse; transduction efficiency, 10%) and pre-B cells (B220+/CD43+/CD25+ cells; input number 2 × 10^5 cells per mouse; transduction efficiency, 2%) did not acquire in vivo repopulating activity with no short- or long-term engraftment in lethally irradiated mice 4 or 8 weeks posttransplantation, respectively (data not shown).

To examine whether our findings in the murine CALM/AF10 leukemia model parallel characteristics of human *CALM/AF10*-positive AML, patient samples were analyzed for *IG* DH-JH rearrangement status and the presence of a CD45RA (the human homolog to B220) population. In addition, we further characterized the CD45RA$^+$ population by performing CFU-blast colony assays in vitro and FISH analysis for the presence of the *CALM/AF10* fusion gene. Table S4 summarizes the characteristics of patients diagnosed with AML or in one case with acute undifferentiated leukemia (AUL); two of the nine patients were children, six of nine patients had additional genetic alterations to the *CALM/AF10* t(10;11) translocation. Treatment consisted mainly of chemotherapy with high-dose Ara-C and anthracyclines, and outcome was dismal in all the patients with longer follow-up. Multiplex PCR and clonality analysis by GeneScanning techniques showed that seven out of nine AML samples demonstrated clonal *IG* DH-JH rearrangements (Table 2 and Figure 5A). We could also detect immature TCRδ (Dδ2,Vδ2) and TCRβ (TCRβ DJ) as well as TCRγ (Vγ10) rearrangements in six out of six patients tested (Table 2).

In all three patients tested, a substantial proportion of CD45RA$^+$ cells could be detected, ranging from 50.6% to 99.8% of bone marrow cells. In two of the three patients, the CD45RA-positive population coexpressed CD34. In all the patients tested, the CD34$^+$/CD45RA$^+$ cells harbored the *CALM/AF10* fusion gene as detected by FISH analysis (Figure 5Bb) (Table 3). Furthermore, CD34$^+$/CD45RA$^+$/CD10$^+$ cells, corresponding to the stage of early human lymphoid progenitors (Haddad et al., 2004), were also positive for the fusion gene (data not shown). The involvement of the CD45RA population in the malignant transformation process was further supported by the observation that the CD45RA population generated myeloid CFU-blasts (Table 3) in vitro, which showed the identical *IG* DH-JH rearrangement status at a single-colony level as detected in the myeloid bulk population (Figure 5C). To test whether early CD34$^+$/CD45RA$^-$ cells could be positive for the CALM/AF10 fusion gene, we highly purified CD34$^+$/CD45RA$^-$/lineage marker (lin)-negative (lin: CD38$^-$/CD19$^-$/CD10$^-$) cells of one patient with *C/A*-positive AML. Notably, the fusion gene could be detected in the majority of cells (92%) in this primitive

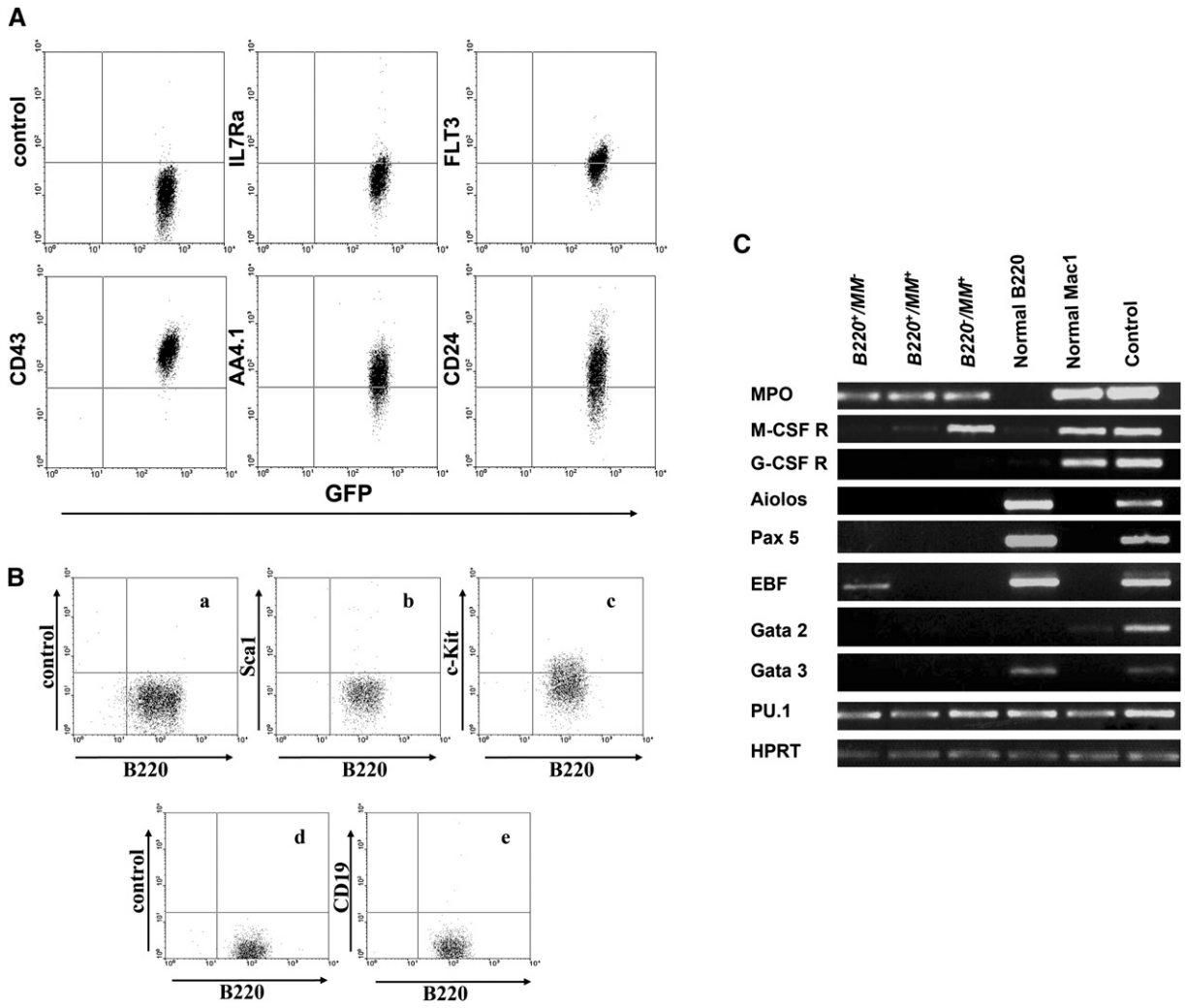

Figure 4. Leukemic B220$^+$/Mac1$^-$ cells express lymphoid markers

A: Expression of B cell-associated markers on leukemic B220$^+$/Mac1$^-$ cells: flow cytometric analysis after staining with various markers as indicated.
B: Expression of early and late markers on leukemic B220$^+$/Mac1$^-$ cells propagated in vitro for Sca1 (**Bb**) and c-Kit (**Bc**) or CD19 (**Be**); **Ba** and **Bd** are controls as indicated.
C: RT-PCR analysis of lineage associated genes. B220$^+$/MM$^-$, B220$^+$/MM$^+$, and B220$^-$/MM$^+$ cells clonally generated from a single B220$^+$/Mac1$^-$ cell were analyzed for the expression of genes associated with different hematopoietic lineages as indicated. B220$^+$ sorted cells from the spleen, Mac1$^+$ sorted cells from the bone marrow, and unsorted BM cells (all populations isolated from a nontransplanted control mouse) were used as controls for lymphoid and myeloid transcripts, respectively. MPO, myeloperoxidase; EBF, early B cell factor; HPRT, hypoxanthine phosphoribosyl transferase; *B220$^+$/MM$^-$*, B220$^+$/Mac1$^-$ cells; *B220$^+$/MM$^+$*, B220$^+$/Mac1$^+$ cells; and *B220$^-$/MM$^+$*, B220$^-$/Mac1$^+$ cells.

cell compartment (Figure 5Ba, patient number 9), indicating the involvement of early CD45RA-negative cells in the transformation process in this patient. In summary, these findings indicate that patients with *CALM/AF10*-positive AML are characterized by *IG* DH-JH rearrangements of their leukemic blasts and a CD45RA-positive population, which is positive for the leukemia-specific fusion gene and is able to generate myeloid blast colonies with the clonal *IG* DH-JH rearrangement ex vivo, reminiscent of several characteristics of murine CALM/AF10-induced AML in transplanted mice.

Discussion

Leukemias are considered to originate from a rare subset of transformed cells, which are able to initiate and maintain the disease. In particular, studies in patients with acute myeloid leukemia have shown that the transformation process involves early hematopoietic progenitor cells characterized by expression of CD34 and lack of CD38 and the different lineage markers (Blair et al., 1998; Dick, 2005). The concept that hematopoietic stem cells (HSCs) are a key target of leukemic transformation was further supported by murine models, which demonstrated that HSCs could acquire leukemic stem cell properties by forced expression of appropriate oncogenes, recurrently found in patients with AML (Huntly and Gilliland, 2005; Reya et al., 2001). Furthermore, inactivation of certain transcription factors such as JunB caused leukemia only when the targeted deletion took place in the HSC compartment and not in the more differentiated cell pool (Passegué et al., 2004). However, more recent data have provided in vivo evidence that also more

Table 2. IgH DJ and TCR rearrangements in CALM/AF10 AML patients

Patient no.	Type	IgH DJ rearrangements		TCR rearrangements		
		IgH DJ	IgH DJ sequences	TCRγ	TCRδ	TCRβ DJ
1	AML M0	monoclonal DH3	D39/ATTTTGACTGGTTATTATAAC*GT*CTGGTACTT CGATCTCTGGGGCCT/JH2	monoclonal Vγ10	Dδ2 biallelic	polyclonal
2	AML M2	monoclonal biallelic DH2 DH6	D2-15/TGGTAGCTGCTACTC*TT*TACGGTATGGAC GTCTGGGGCCA/JH6B D6-13/GGGTATAGCAG C*GGCTACAAGGGT*ACTACTGGGGCCA/JH4B	monoclonal Vγ10	Vδ2	monoclonal D1
3	AML M1	polyclonal DH1–7	—	polyclonal	Dδ2/Dδ3 biallelic	polyclonal
4	AUL	monoclonal DH1	DH1-26/TATAGTGGGAGCTACT*GTG*CTACTGG GGCCA/JH4B	monoclonal Vγ1-8 and Vγ10-11	Dδ2	monoclonal TCRβ DJ and TCRβ JA
5	AML M1	monoclonal DH7	ND	polyclonal	Dδ2 biallelic	polyclonal
6	AML M1	monoclonal DH7	ND	monoclonal Vγ10-11	Dδ2 biallelic	monoclonal TCRβ DJ
7	AML M1	monoclonal DH6	DH6-6/TATAGCAGCTCGT*TGT*ACTACTTTGACT ACTGGGGCCA/JH4B	ND	ND	ND
8	AML	monoclonal DH7	DH7-27/TAACCACTGGGGAC*CTCCCGGG* CTTTGACTACGGGGCCA/JH4B	ND	ND	ND
9	AML M5a	polyclonal DH1-7	—	ND	ND	ND

ND, not determined.

differentiated cells can acquire properties of leukemic stem cells: in a murine bone marrow transplantation model, retrovirally driven expression of the *MLL-GAS7* fusion gene induced acute leukemias with myeloid, lymphoid, or mixed phenotype. Immunophenotyping, transcriptional profiling, and the ability of the LSC to induce three distinct leukemia subtypes indicated

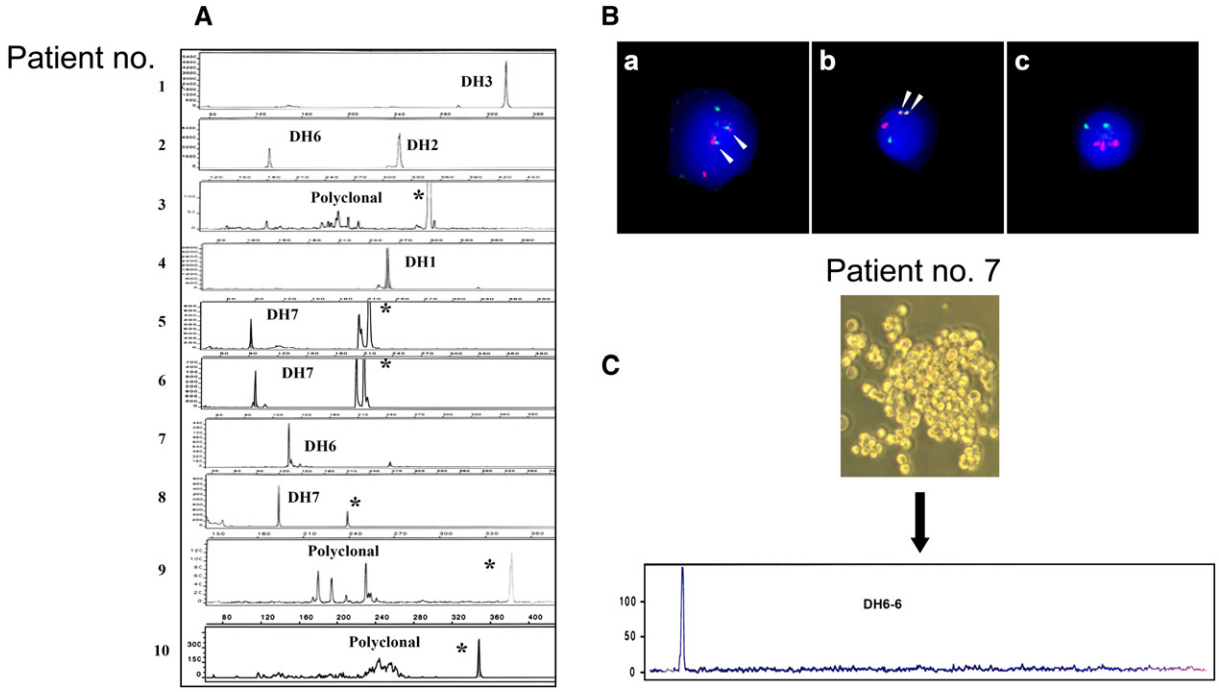

Figure 5. CALM/AF10-positive human AML samples show IgH DH-JH rearrangements and express CD45RA(B220)

A: GeneScanning analysis of IgH DH-JH rearrangements in nine cases of human CALM/AF10-positive AML using bone marrow of the leukemic patients with >80% myeloid blasts and polyclonal nonleukemic control cells. GeneScanning demonstrated a clonal IgH DH-JH rearrangement in seven out of nine cases. Unspecific background peaks resulting from annealing to nonrearranged alleles in the reactions are indicated with an asterisk.

B: Detection of the CALM/AF10 rearrangement in flow-sorted patient cells. **Ba:** A representative CD34+/CD45RA$^-$/lin$^-$ cell with the CALM/AF10 fusion, showing a normal AF10 (red) and a normal CALM (green) locus as well as two red/green signals, indicating the two reciprocal fusion genes (arrowheads) (92% of the cells were positive for the fusion gene; one representative CALM/AF10-negative cell of the same compartment is shown in **Bc**) (patient number 9). **Bb:** A representative CD34$^+$/CD45RA$^+$ cell carrying the CALM/AF10 fusions, showing the same signal pattern as in **Ba** (fusion signals are indicated by arrowheads) (patient number 7). **Bc:** A CD34$^+$/CD45RA$^-$/lin$^-$ cell without CALM/AF10 fusion showing two normal AF10 (red) and two normal CALM (green) signals (patient number 9).

C: Myeloid blast colony formation in methylcellulose of CD45RA$^+$ cells of a representative human AML patient (patient 7, magnification 100×). Lower panel shows the clonal IgH DJ rearrangement peak from a singly isolated myeloid blast colony analyzed by GeneScan. The rearrangement was identical to the rearrangements detected in the leukemic bulk of the patient (Figure 5A).

Table 3. Proportion of CD45RA-positive cells and CFU-blast frequency of C/A-positive AML patients

Patient no.	$CD34^+$/$CD45RA^+$	Overall $CD45RA^+$	CD34+/$CD45RA^-$/lin$^-$[b]	Positivity for CALM/AF10[c]		CFU-blast frequency[a]	IgH DJ of CFU-blast colonies
				$CD34^+/CD45RA^+$	$CD34^+/CD45RA^-$/lin$^-$		
3	94.52%	98.59%	0.13%	+	ND	92 ± 14	NA
7	96.21%	99.8%	0.01%	+	ND	12 ± 3	monoclonal DH6
9	1.68%	50.6%	33.07%	ND	+	ND	ND

ND, not determined; NA, not applicable.
[a]Per 10^6 $CD45RA^+$ bone marrow cells isolated from C/A AML patients (0.2–2 × 10^5 cells plated per dish).
[b]Lineage markers comprised CD38, CD19, and CD10.
[c]As determined by CALM- and AF10-specific FISH probes.

that the fusion gene targeted a multipotential progenitor in this murine model (So et al., 2003). In addition, retroviral expression of the *MLL-ENL* or *MOZ-TIF2* fusion gene in murine myeloid committed progenitor cells clearly demonstrated that committed progenitor cells can function as leukemic stem cells in these models and that transformation of HSC is not mandatory for the development and maintenance of acute leukemia (Cozzio et al., 2003; Huntly et al., 2004). The murine data presented here now provide evidence that a progenitor cell with lymphoid characteristics can propagate acute myeloid leukemia. Detailed characterization of the leukemic stem cell showed that the cells expressed B220, CD43, AA4.1, and CD24 but lacked expression of MMs as well as Sca1. Importantly, transcriptional profiling demonstrated a lineage-promiscuous expression of lymphoid factors such as *EBF*, *VpreB*, and *Rag2* (Busslinger et al., 2000) with progressive downregulation following differentiation into the $B220^+/Mac1^-$ and the $B220^-/Mac1^+$ cells together with the MM *MPO*. Of note, we did not detect transcription of *Pax5*, which is compatible with our finding that the $B220^+$ cells had an incomplete rearrangement status at the *IG* DH-JH locus and did not express CD19. Even though this progenitor showed characteristics of the early B lineage, the classification of this CALM/AF10 leukemia-propagating cell according to the different B cell classification systems remains difficult because of its leukemogenic characteristics and the potential impact of the fusion gene on its cell surface phenotype and transcriptional network. The phenotype we observed differed from the $B220^+/CD19^+$ cell stage, which is associated with *Pax5* positivity and the entire commitment to the B cell lineage (Hardy, 2003), but also from the profile of the earliest lymphoid progenitor, the common lymphoid progenitor (CLP), which lacks expression of B220 (Kondo et al., 1997).

In our model, a single transformed Pax5-negative progenitor with lymphoid characteristics was able to generate myeloid cells with IgH immunoglobulin rearrangements. Interestingly, $Pax5^{-/-}$ B cell progenitors show lineage-promiscuous transcription of B-lymphoid and myeloid genes, display a remarkable multilineage potential in vitro, and are able to be directed into the myeloid lineage (Heavey et al., 2003; Schaniel et al., 2002). In addition, the latent myeloid differentiation capacity of the CLP, which does not express *Pax5* yet, has become obvious due to the observation that it can be redirected to the myeloid lineage by retrovirally induced *IL-2Rβ* chain or *GM-CSF* receptor expression (Kondo et al., 2000). Thus, one intriguing possibility is that *CALM/AF10* instructed myeloid development of an early Pax5-negative lymphoid progenitor in our model. This commitment into the myeloid pathway was irreversible in the *C/A* model, as highly purified $B220^+/Mac1^-$ cells were not able to differentiate along the B lineage pathway in vitro on stromal OP9 feeders in lymphoid growth medium (data not shown).

The scenario that expression of *C/A* directs the lineage choice of *Pax5*-negative lymphoid progenitors is only one potential explanation for the myeloid phenotype of the leukemia. We cannot exclude that the fusion gene instructed myeloid lineage decision at the later stage of *Pax5*-positive cells, as it was recently shown that the myeloid transcription factors C/EBPα and C/EBPβ could convert *Pax5*-positive B cells into macrophages by downregulation of *Pax5* expression and upregulation of myeloid genes (Xie et al., 2004). However, we could not observe any significant downregulation of *Pax-5* expression following CALM/AF10 expression for 48 hr in the in vitro cultivated murine pro-B cell line Ba/F3 or primary murine fetal pre-B cell lines by real-time quantitative PCR and did not observe repopulating ability of murine pro-B or pre-B cells in lethally irradiated mice after transduction with CALM/AF10 (data not shown).

Another important scenario would be that the CALM/AF10 fusion gene targets a rare and early B220-negative progenitor with IgH germline configuration and activates lymphoid developmental programs in these cells, resulting in a $B220^+/MM^-$ IgH rearranged cell population with high leukemia-propagating potential as described in the murine model. Indeed, highly purified B220-negative progenitor cells with IgH germline configuration acquired leukemogenic properties in vivo in two independent experiments after infection with the CALM/AF10 retrovirus, indicating that an early progenitor cell can be transformed by the fusion gene. Interestingly, one of the mice developed an AML that lacked a $B220^+$ population and displayed an IgH germline configuration, which was never observed when unfractionated bone marrow was infected with the *CALM/AF10* retrovirus and transplanted into recipients. One explanation for this might be that C/A can target IgH rearranged $B220^+$ lymphoid progenitors, giving rise to AML with the consistent phenotype of a $B220^+$ transformed progenitor population, as well as early $B220^-$ progenitors with IgH germline configuration, resulting in AML with or without the $B220^+$ cell population.

Importantly, the experiments performed in this study do not rule out the other possibility, that the *CALM/AF10* fusion gene had an instructive effect on myeloid progenitors, initiating a lymphoid-specific program in these cells. In this scenario a myeloid cell would acquire lymphoid characteristics as a result of transformation by an appropriate oncogene. Another possibility is that *C/A* directly transformed a rare cell subset of B/macrophage progenitors, which was identified in fetal liver but also in adult bone marrow (Lacaud et al., 1998; Montecino-Rodriguez et al., 2001). However, this cell was described to be

CD19/*Pax5* positive and negative for CD45R/B220, a phenotype different than the phenotype of the LSC described here.

Of note, these different scenarios would result in the development of AML with a $B220^+$/MM-negative cell population with a very high frequency of leukemia repopulating cells, which would be accessible to an antibody-based B220 depletion. Indeed antibody-mediated depletion of the $B220^+/MM^-$ cells from leukemic transplants efficiently prevented leukemic development in mice, underlining the key role of this population for disease propagation. One implication of our findings is that in a subset of AML the leukemia-propagating cell might show a distinct cell surface and transcriptional phenotype, setting it apart from the leukemic myeloid bulk population, but also from the normal stem cell pool. In particular, the expression of lymphoid antigens would allow to discriminate this cell from the normal hematopoietic stem cells, which would facilitate the development of treatment strategies using the lymphoid surface antigens to target the leukemia-propagating cell but to spare the normal stem cell (Passegué et al., 2003). As illustrated in the murine CALM/AF10 leukemia model, such a strategy would have therapeutic potential. Depletion of the $B220^+$ transformed progenitor cells would fail to eradicate the malignant clone, if a rare leukemic B220-negative progenitor cell population existed, which gives rise to the $B220^+/MM^-$ population described. But even in this scenario, diminishing the B220-positive leukemia-propagating cells would promise clinical benefit, as mice transplanted with B220-depleted bone marrow failed to develop leukemia up to an observation time of 100 days, compared to rapid development of AML in mice transplanted with $B220^+$ transformed progenitors.

Recently, substantial progress has been made to characterize very early stages in human B cell development (Haddad et al., 2004; Hou et al., 2005; LeBien, 2000; Ryan et al., 1997). These reports have shown that similar to the murine system these early human progenitors express the B220 human homolog CD45RA, as well as CD34 and CD10, but lack CD19 and *Pax5* expression. In an effort to determine potential similarities between the murine CALM/AF10 AML and human disease, we analyzed nine patients with *CALM/AF10*-positive AML. Interestingly, the cases tested showed a CD45RA population with coexpression of CD34 in two of three patients. Furthermore, in seven out of nine patients tested, clonal IgH immunoglobulin rearrangements could be detected in the myeloid bulk. The leukemic nature of the CD45RA population in these cases was indicated by the presence of the fusion gene, its clonal IgH rearrangement, and its ability to form CFU-blast colonies ex vivo. Interestingly, in the $CD34^+/CD45RA^-/lin^-$ progenitor compartment of one patient we detected a mosaic of cells carrying the fusion gene or showing normal signal pattern by FISH, indicating that this cell compartment might be involved in the malignant transformation process.

In addition to IgH rearrangements, six of six patients were also positive for clonal rearrangements of the T cell receptor (TCR). These observations are in line with reports associating the *CALM/AF10* fusion gene with T-ALL, in particular with T-ALLs expressing the γ/δ TCR (Asnafi et al., 2003). In the murine model the constitutive expression of CALM/AF10 failed to induce T cell leukemia, and the observed myeloid leukemias did not show the TCRγ rearrangements that were analyzed (Vγ 1.1-Jγ4, Vγ 2/4-Jγ1, or Vγ 5/7-Jγ1). This could be attributable to various factors predisposing the murine model to leukemias of the myeloid lineage, such as the cell population initially used for retroviral infection; the in vitro culture conditions with IL3, IL6, and SCF stimulation before transplantation; or the level of expression of the fusion gene in the murine system compared to human disease. However, real-time PCR quantification of *CALM/AF10* transcripts showed low *CALM/AF10* expression in both the murine and human myeloid bulk (data not shown). Insertional mutagenesis was identified as an important factor in murine leukemogenesis (Akagi et al., 2004; Suzuki et al., 2002) and might explain the predisposition to AML development in the CALM/AF10 model: in an analysis of the proviral integration sites in leukemic mice, 10 of 18 detected sites were described before as common integration sites or transposon-tagged cancer genes according to the Retroviral Tagged Cancer Gene Database (RTCGD; http://RTCGD.ncifcrf.gov/) (Akagi et al., 2004). However, there were no recurrent insertion sites or a correlation of the integrations with the consistent phenotype of the leukemias in this model. As described for human *CALM/AF10*-positive T-ALLs (Dik et al., 2005; Soulier et al., 2005), the murine AML cases also displayed aberrant expression of *HoxA7* and *Meis1* (unpublished data); furthermore, we also observed deregulation of HOX genes in patients with *CALM/AF10*-positive AML (unpublished data). This indicates that deregulation of this transcription factor family is a common characteristic of CALM/AF10 leukemias independent of the phenotype.

In summary, this murine leukemia model demonstrates that a progenitor cell with lymphoid characteristics and a phenotype that differs from that of normal hematopoietic stem cells and the leukemic myeloid bulk, is able to propagate AML. These data provide a rationale for the development of therapeutic strategies targeting the leukemia-propagating stem cell without harming the normal stem cell pool and raise the hope that such innovative concepts may improve treatment outcome in a subgroup of patients with AML in the future.

Experimental procedures

Retroviral transduction of primary bone marrow cells and BM transplantation

Breeding and maintenance of the mice were conducted as described previously (Rawat et al., 2004). Production of high-titer helper-free retrovirus was carried out following standard procedures by using the ecotropic packaging cell line GP^+E86 (Schessl et al., 2005). Lethally irradiated (0.80 Gy) mice were transplanted with either highly purified $EGFP^+$ cells alone (4×10^5 cells per mouse) (FACSVantage, Becton Dickinson) or with a mixture of transduced and nontransduced cells (on average 1.76×10^5 transduced cells with 1.9×10^5 nontransduced cells per mouse). Lethally irradiated secondary and tertiary recipients were injected with 1×10^6 BM cells from a primary and secondary diseased mouse, respectively, with an equal number of nontransduced cells from a syngenic disease-free mouse bone marrow for radioprotection. Both animal and human studies were approved by the Ethics Committee of Ludwig Maximilians University and abided by the tenets of the revised World Medical Association Declaration of Helsinki (http://www.wma.net/e/policy/b3.htm).

In order to determine the frequency of leukemia-propagating cells, $B220^+/Mac1^-$, $B220^+/Mac1^+$, and $B220^-/Mac1^+$ cells were isolated and highly purified from the BM of a leukemic primary mouse. The sort purity of these cells was analyzed with the FACSCalibur and determined to be over 98%. In each cohort 10-fold serial dilutions of these cells were injected intravenously (50 cells to 5×10^5 cells per mouse cohort) into lethally irradiated secondary recipient mice. Carrier cells (1×10^6) (nontransduced BM from a syngenic disease-free mouse) were added to each sample for radioprotection. Diseased mice were sacrificed and assessed for leukemia development. Mice that did not develop disease within 20 weeks posttransplantation were sacrificed and

tested for engraftment. The frequency of leukemia-propagating cells was calculated using Poisson statistics using the L-Calc Limiting dilution analysis software (Version 1.1 StemSoft Inc., Vancouver, Canada) (Buske et al., 2002).

Patient samples

BM samples from adult patients diagnosed with AML were analyzed. The diagnosis of AML was performed according to the French-American-British criteria and the World Health Organization classification (Bennett et al., 1985; Harris et al., 1995). Cytomorphology, cytochemistry, cytogenetics, and molecular genetics were applied in all cases as described below. The clinical features of patients are provided in Table S4. The study abided by the rules of the local internal review board and the tenets of the revised Helsinki protocol (http://www.wma.net/e/policy/b3.htm).

Sorting of cells from human AML patient samples

Frozen mononuclear peripheral blood or bone marrow cells from patients with AML were rapidly thawed and were washed twice in IMDM with 10% FBS, resuspended in PBS, and stained with various antibodies. For lineage depletion experiments, immunostaining was done with FITC-labeled anti-human CD34 (Beckman Coulter, Marseille, France) and PE-labeled anti-human CD38, PE-labeled anti-human CD19, PE-labeled anti-human CD10, and PE-labeled anti-human CD45RA (all from BD Pharmingen, Heidelberg, Germany). Cells were incubated with appropriate antibodies for 20 min on ice and washed with cold PBS prior to sorting. The trial was approved by the responsible local ethics committees, and all patients gave written informed consent according to the Helsinki Declaration.

FISH

Dual Colour Dual Fusion (DCDF) probes were developed with bacterial artificial chromosome (BAC) clones RP11-418C1 for the 5′-AF10 region (Texas Red; red in Figure 5B), RP11-249M6 for the 3′-AF10 region (red), RP11-12D16 (FITC, green) for the 5′-CALM region, and RP11-90K17 (green) for the 3′-CALM region (kindly provided by Dr. Mariano Rocchi, Bari). BAC DNA preparation, labeling, and FISH were performed as described (Crescenzi et al., 2004). Normal nuclei display a two-red and two-green (2R2G) hybridization pattern, whereas nuclei carrying the translocation display a one-red, one-green, twored/green fusion (1R1G2F) pattern. Other hybridization patterns, e.g., 1R1G1F (found in 0.5%–2% of nuclei) or 1R1G3F (found in 0.5%–1% of nuclei), were interpreted as technical artifacts.

The cells were directly sorted onto aminoalkylsilane-coated slides (SilanePrep Slides, Sigma, Germany) with or without preloading of 15 μl 3% bovine serum albumin solution in PBS and fixed in 1:3 acetic acid-methanol fixative.

Supplemental data

The Supplemental Data include Supplemental Experimental Procedures, five supplemental figures, and five supplemental tables and can be found with this article online at http://www.cancercell.org/cgi/content/full/10/5/363/DC1/.

Acknowledgments

We thank Bianka Ksienzyk for her excellent technical assistance and the members of the GSF animal facility for the excellent breeding and maintenance of the animals. We want to thank Georg Bornkamm, Fritz Melchers, and Meinrad Busslinger for their valuable discussion of the manuscript. A.J.D. and F.A. and the work were supported by a grant of the Deutsche Krebshilfe (10-1838-Bu 2 to C.B., 70-2968-Fe I to M.F.-B.) by the Bundesministerium für Bildung und Forschung (NGFN2 grant 01GS0448 and DFG grant SFB684 to C.B., S.K.B., and M.F.-B. and NGFN2 grant 01GR0418 to P.L. and M.H.) and by a grant from the National Cancer Institute of Canada and funds from the Terry Fox Foundation (R.K.H.). C.M. was supported by AIRC (Associazione Italiana per la Ricerca su Cancro). H.R. is a scholar of the Deutsche José Carreras Leukämie-Stiftung e.v. (DJCLS F04/01).

Received: February 13, 2006
Revised: June 21, 2006
Accepted: August 24, 2006
Published: November 13, 2006

References

Akagi, K., Suzuki, T., Stephens, R.M., Jenkins, N.A., and Copeland, N.G. (2004). RTCGD: Retroviral tagged cancer gene database. Nucleic Acids Res. *32*, D523–D527.

Asnafi, V., Radford-Weiss, I., Dastugue, N., Bayle, C., Leboeuf, D., Charrin, C., Garand, R., Lafage-Pochitaloff, M., Delabesse, E., Buzyn, A., et al. (2003). CALM-AF10 is a common fusion transcript in T-ALL and is specific to the TCRγδ lineage. Blood *102*, 1000–1006.

Bennett, J.M., Catovsky, D., Daniel, M.T., Flandrin, G., Galton, D.A., Gralnick, H.R., and Sultan, C. (1985). Proposed revised criteria for the classification of acute myeloid leukemia. A report of the French-American-British Cooperative Group. Ann. Intern. Med. *103*, 620–625.

Blair, A., Hogge, D.E., Ailles, L.E., Lansdorp, P.M., and Sutherland, H.J. (1997). Lack of expression of Thy-1 (CD90) on acute myeloid leukemia cells with long-term proliferative ability in vitro and in vivo. Blood *89*, 3104–3112.

Blair, A., Hogge, D.E., and Sutherland, H.J. (1998). Most acute myeloid leukemia progenitor cells with long-term proliferative ability in vitro and in vivo have the phenotype CD34(+)/CD71(−)/HLA-DR. Blood *92*, 4325–4335.

Buske, C., Feuring-Buske, M., Abramovich, C., Spiekermann, K., Eaves, C.J., Coulombel, L., Sauvageau, G., Hogge, D.E., and Humphries, R.K. (2002). Deregulated expression of HOXB4 enhances the primitive growth activity of human hematopoietic cells. Blood *100*, 862–868.

Busslinger, M., Nutt, S.L., and Rolink, A.G. (2000). Lineage commitment in lymphopoiesis. Curr. Opin. Immunol. *12*, 151–158.

Cozzio, A., Passegue, E., Ayton, P.M., Karsunky, H., Cleary, M.L., and Weissman, I.L. (2003). Similar MLL-associated leukemias arising from self-renewing stem cells and short-lived myeloid progenitors. Genes Dev. *17*, 3029–3035.

Crescenzi, B., La Starza, R., Romoli, S., Beacci, D., Matteucci, C., Barba, G., Aventin, A., Marynen, P., Ciolli, S., Nozzoli, C., et al. (2004). Submicroscopic deletions in 5q-associated malignancies. Haematologica *89*, 281–285.

Dick, J.E. (2005). Complexity of the human acute myeloid leukemia stem cell compartment: Implications for therapy. Biol. Blood Marrow Transplant. *11*, 9–11.

Dik, W.A., Brahim, W., Braun, C., Asnafi, V., Dastugue, N., Bernard, O.A., van Dongen, J.J., Langerak, A.W., Macintyre, E.A., and Delabesse, E. (2005). CALM-AF10+ T-ALL expression profiles are characterized by overexpression of HOXA and BMI1 oncogenes. Leukemia *19*, 1948–1957.

Dreyling, M.H., Schrader, K., Fonatsch, C., Schlegelberger, B., Haase, D., Schoch, C., Ludwig, W., Loffler, H., Buchner, T., Wormann, B., et al. (1998). MLL and CALM are fused to AF10 in morphologically distinct subsets of acute leukemia with translocation t(10;11): Both rearrangements are associated with a poor prognosis. Blood *91*, 4662–4667.

Feuring-Buske, M., Haase, D., Buske, C., Hiddemann, W., and Wormann, B. (1999). Clonal chromosomal abnormalities in the stem cell compartment of patients with acute myeloid leukemia in morphological complete remission. Leukemia *13*, 386–392.

Feuring-Buske, M., Frankel, A.E., Alexander, R.L., Gerhard, B., and Hogge, D.E. (2002). A diphtheria toxin-interleukin 3 fusion protein is cytotoxic to primitive acute myeloid leukemia progenitors but spares normal progenitors. Cancer Res. *62*, 1730–1736.

Forsberg, E.C., Prohaska, S.S., Katzman, S., Heffner, G.C., Stuart, J.M., and Weissman, I.L. (2005). Differential expression of novel potential regulators in hematopoietic stem cells. PLoS Genet *1*, e28. 10.1371/journal.pgen.0010028.

Haddad, R., Guardiola, P., Izac, B., Thibault, C., Radich, J., Delezoide, A.L., Baillou, C., Lemoine, F.M., Gluckman, J.C., Pflumio, F., and Canque, B. (2004). Molecular characterization of early human T/NK and B-lymphoid progenitor cells in umbilical cord blood. Blood *104*, 3918–3926.

Hardy, R.R. (2003). B-cell commitment: Deciding on the players. Curr. Opin. Immunol. *15*, 158–165.

Harris, N.L., Jaffe, E.S., Stein, H., Banks, P.M., Chan, J.K., Cleary, M.L., Delsol, G., De Wolf-Peeters, C., Falini, B., Gatter, K.C., et al. (1995). Lymphoma classification proposal: Clarification. Blood *85*, 857–860.

Heavey, B., Charalambous, C., Cobaleda, C., and Busslinger, M. (2003). Myeloid lineage switch of Pax5 mutant but not wild-type B cell progenitors by C/EBPα and GATA factors. EMBO J. *22*, 3887–3897.

Hiddemann, W., Spiekermann, K., Buske, C., Feuring-Buske, M., Braess, J., Haferlach, T., Schoch, C., Kern, W., Schnittger, S., Berdel, W., et al. (2005). Towards a pathogenesis-oriented therapy of acute myeloid leukemia. Crit. Rev. Oncol. Hematol. *56*, 235–245.

Hope, K.J., Jin, L., and Dick, J.E. (2004). Acute myeloid leukemia originates from a hierarchy of leukemic stem cell classes that differ in self-renewal capacity. Nat. Immunol. *5*, 738–743.

Hou, Y.H., Srour, E.F., Ramsey, H., Dahl, R., Broxmeyer, H.E., and Hromas, R. (2005). Identification of a human B-cell/myeloid common progenitor by the absence of CXCR4. Blood *105*, 3488–3492.

Huntly, B.J., and Gilliland, D.G. (2005). Leukaemia stem cells and the evolution of cancer-stem-cell research. Nat. Rev. Cancer *5*, 311–321.

Huntly, B.J., Shigematsu, H., Deguchi, K., Lee, B.H., Mizuno, S., Duclos, N., Rowan, R., Amaral, S., Curley, D., Williams, I.R., et al. (2004). MOZ-TIF2, but not BCR-ABL, confers properties of leukemic stem cells to committed murine hematopoietic progenitors. Cancer Cell *6*, 587–596.

Jamieson, C.H., Weissman, I.L., and Passegue, E. (2004). Chronic versus acute myelogenous leukemia: A question of self-renewal. Cancer Cell *6*, 531–533.

Jordan, C.T., Upchurch, D., Szilvassy, S.J., Guzman, M.L., Howard, D.S., Pettigrew, A.L., Meyerrose, T., Rossi, R., Grimes, B., Rizzieri, D.A., et al. (2000). The interleukin-3 receptor α chain is a unique marker for human acute myelogenous leukemia stem cells. Leukemia *14*, 1777–1784.

Kogan, S.C., Ward, J.M., Anver, M.R., Berman, J.J., Brayton, C., Cardiff, R.D., Carter, J.S., de Coronado, S., Downing, J.R., Fredrickson, T.N., et al. (2002). Bethesda proposals for classification of nonlymphoid hematopoietic neoplasms in mice. Blood *100*, 238–245.

Kondo, M., Weissman, I.L., and Akashi, K. (1997). Identification of clonogenic common lymphoid progenitors in mouse bone marrow. Cell *91*, 661–672.

Kondo, M., Scherer, D.C., Miyamoto, T., King, A.G., Akashi, K., Sugamura, K., and Weissman, I.L. (2000). Cell-fate conversion of lymphoid-committed progenitors by instructive actions of cytokines. Nature *407*, 383–386.

Kroon, E., Krosl, J., Thorsteinsdottir, U., Baban, S., Buchberg, A.M., and Sauvageau, G. (1998). Hoxa9 transforms primary bone marrow cells through specific collaboration with Meis1a but not Pbx1b. EMBO J. *17*, 3714–3725.

Lacaud, G., Carlsson, L., and Keller, G. (1998). Identification of a fetal hematopoietic precursor with B cell, T cell, and macrophage potential. Immunity *9*, 827–838.

LeBien, T.W. (2000). Fates of human B-cell precursors. Blood *96*, 9–23.

Montecino-Rodriguez, E., Leathers, H., and Dorshkind, K. (2001). Bipotential B-macrophage progenitors are present in adult bone marrow. Nat. Immunol. *2*, 83–88.

Morrison, S.J., Wandycz, A.M., Hemmati, H.D., Wright, D.E., and Weissman, I.L. (1997). Identification of a lineage of multipotent hematopoietic progenitors. Development *124*, 1929–1939.

Morse, H.C., III, Anver, M.R., Fredrickson, T.N., Haines, D.C., Harris, A.W., Harris, N.L., Jaffe, E.S., Kogan, S.C., MacLennan, I.C., Pattengale, P.K., and Ward, J.M. (2002). Bethesda proposals for classification of lymphoid neoplasms in mice. Blood *100*, 246–258.

Passegué, E., Jamieson, C.H., Ailles, L.E., and Weissman, I.L. (2003). Normal and leukemic hematopoiesis: Are leukemias a stem cell disorder or a reacquisition of stem cell characteristics? Proc. Natl. Acad. Sci. USA *100* (*Suppl 1*), 11842–11849.

Passegué, E., Wagner, E.F., and Weissman, I.L. (2004). JunB deficiency leads to a myeloproliferative disorder arising from hematopoietic stem cells. Cell *119*, 431–443.

Rawat, V.P., Cusan, M., Deshpande, A., Hiddemann, W., Quintanilla-Martinez, L., Humphries, R.K., Bohlander, S.K., Feuring-Buske, M., and Buske, C. (2004). Ectopic expression of the homeobox gene Cdx2 is the transforming event in a mouse model of t(12;13)(p13;q12) acute myeloid leukemia. Proc. Natl. Acad. Sci. USA *101*, 817–822.

Reya, T., Morrison, S.J., Clarke, M.F., and Weissman, I.L. (2001). Stem cells, cancer, and cancer stem cells. Nature *414*, 105–111.

Ryan, D.H., Nuccie, B.L., Ritterman, I., Liesveld, J.L., Abboud, C.N., and Insel, R.A. (1997). Expression of interleukin-7 receptor by lineage-negative human bone marrow progenitors with enhanced lymphoid proliferative potential and B-lineage differentiation capacity. Blood *89*, 929–940.

Schaniel, C., Bruno, L., Melchers, F., and Rolink, A.G. (2002). Multiple hematopoietic cell lineages develop in vivo from transplanted Pax5-deficient pre-B I-cell clones. Blood *99*, 472–478.

Schessl, C., Rawat, V.P., Cusan, M., Deshpande, A., Kohl, T.M., Rosten, P.M., Spiekermann, K., Humphries, R.K., Schnittger, S., Kern, W., et al. (2005). The AML1-ETO fusion gene and the FLT3 length mutation collaborate in inducing acute leukemia in mice. J. Clin. Invest. *115*, 2159–2168.

So, C.W., Karsunky, H., Passegue, E., Cozzio, A., Weissman, I.L., and Cleary, M.L. (2003). MLL-GAS7 transforms multipotent hematopoietic progenitors and induces mixed lineage leukemias in mice. Cancer Cell *3*, 161–171.

Soulier, J., Clappier, E., Cayuela, J.M., Regnault, A., Garcia-Peydro, M., Dombret, H., Baruchel, A., Toribio, M.L., and Sigaux, F. (2005). HOXA genes are included in genetic and biologic networks defining human acute T-cell leukemia (T-ALL). Blood *106*, 274–286.

Suzuki, T., Shen, H., Akagi, K., Morse, H.C., Malley, J.D., Naiman, D.Q., Jenkins, N.A., and Copeland, N.G. (2002). New genes involved in cancer identified by retroviral tagging. Nat. Genet. *32*, 166–174.

Warner, J.K., Wang, J.C., Hope, K.J., Jin, L., and Dick, J.E. (2004). Concepts of human leukemic development. Oncogene *23*, 7164–7177.

Xie, H., Ye, M., Feng, R., and Graf, T. (2004). Stepwise reprogramming of B cells into macrophages. Cell *117*, 663–676.

Accession numbers

The microarray data in Figure 2C can be accessed from NCBI's Gene Expression Omnibus (GEO) with accession number GSE5030.